Foreword

The International Symposium Rock Slope Stability 2018, held in Chambéry (13-15 November 2018), takes place following the previous sessions organized in Paris (2010), Marrakech (2014) and Lyon (2016).

In the continuity of the previous sessions, RSS 2018 is an international forum which aims to bring together all actors of the academic and professional sectors over three days. The topics covered include, among others, site investigation and rockfall hazard modelling, monitoring techniques, rockfall trajectory analysis, risk management, protection structures and case studies. To affirm the strong connexion between researchers and practitioners, this edition includes, in addition to the regular sessions, a half-day fully dedicated to technical presentations and exhibitions, together with an excursion tour that will take place at the end of the Symposium to discover some of the prominent sites around Chambéry basin.

In the context of climate change, illustrated by frequent extreme climatic events, the international community must consider the risks related to rockfall and landslides with a new perspective. This is one of the major goals of the French national project C2ROP (Chutes de blocs, Risques Rocheux et Ouvrages de Protection), under the auspices of which the Symposium is placed. C2ROP demonstrates in an outstanding manner the necessity to bridge all the components related to the relevant topics, both in academic areas and industrial sectors, to make rapid progress and to benefit from knowledge developed in related fields.

Among the various Sponsors, we would like to thank specially IREX (Institut pour la recherche appliquée et l'expérimentation en génie civil), INDURA (Infrastructures durables Rhône-Alpes) and the Université Savoie Mont-Blanc.

We are also very grateful to the five invited Lecturers, who highly and diligently contribute to the success of the Conference.

The Organizing Committee will find here also our warm gratitude: M. Bernard (INDURA), M-A. Chanut (CEREMA), D. Fabre (CNAM), M. Gasc (CEREMA), S. Lambert (IRSTEA), J. Martin (EGIS), P. Plotto (IMS-RN), and N. Villard (NGE Fondations). Special and warm thanks to A. Hardouin (IREX) for making possible this event!

With over 60 communications and 150 attendees, the Organizing Committee hopes to make this workshop a memorable event to bring together engineers and scientists from all over the world on a number of topics, to promote informal discussions, and to give rise to promising collaborations in the future.

Welcome to Chambéry!

François Nicot, Chair of RSS 2018
Félix Darve, Chair of the Scientific Board of RSS 2018

International Symposium Rock Slope Stability
13-15 November, 2018, Chambéry (France)

The Symposium RSS (Rock Slope Stability) 2018 takes place in Chambéry (France) from 13 to 15 November 2018, after Paris session (2010), Marrakech session (2014) and Lyon session (2016).

This 2018 session is organized in the framework of the National Project C2ROP (blocks falls, rocky risks, and protection works). This conference is also an international forum permitting to gather all actors of the academic and professional sector during three days.

Topics covered during the Symposium:

- Site investigation and rockfall hazard modelling,
- Monitoring techniques,
- Rockfall trajectory analysis,
- Risk management,
- Protection structures
- Case studies.

C2ROP

Chutes de Blocs
Risques **R**ocheux
Ouvrages de **P**rotection

In a sustainable and proven climate change context, an increase in rockfall events, landslides, rock falls is feared.

Therefore, it has become urgent to bring together all stakeholders in the field of rock risks, to propose a collaborative research framework and a platform of integrated operational resources

C2ROP aims to build a coordinated toolchain (hazard – risk – protection), to bring out a repository of risk and its acceptable cost, organize and develop the community, to provide a structured results from digital and experimental equipment tools, and finally position the French expertise internationally. Started in 2015, this collaborative project will bring the products of research available to those who need them, especially the owners and infrastructures managers.

www.c2rop.fr
Projet National C2ROP
Institut pour la Recherche appliquée et l'Expérimentation en Génie Civil
9 rue de Berri
75008 PARIS
+ 33 1 44 13 32 79 – contact@c2rop.fr

Summary

Keynote speakers

Keynote speakers 1
Pierre Azémard 2
The RN1 in Reunion Island: Rock Hazard Management: circulation management, protections works and new route 3
Tom Badger 6
Perceptions of risk in response to geologic hazards 7
Anna Giacomini 8
Rockfall in mining: mitigation measures design and hazard assessment 9
Fabien Hobléa 12
1248-2018: the chronic instability of Mont Granier in Chartreuse (Isère/Savoie, French Alps): a review 13
Michel Jaboyedoff 16
About the “rockfall” failure hazard assessment 17

Extended abstracts

Extended abstracts 21
Comparative analysis of different climate predictions in a temperate zone in France and their impact on slope stability 23
Rock reinforcement monitoring using passive seismics: a first case study 25
Impacts of land-use and land-cover changes on the quantitative analysis of rockfall risk: The case study of the village of Crolles 27
Thermal conditions of an unstable permafrost-affected rock ridge below a refuge: the Cosmiques case (Mont Blanc massif) 29
On the role of forest in rockfall hazards mitigation – A perspective from the numerical modelling of non-spherical rock-tree interaction using non-smooth mechanics 31
Flexible rockfall mitigation design for varying site conditions 33
Quantification of 3D displacements for landslides by photogrammetry and image correlation 35
Using a simplified model to assess the ability of a protection barrier to mitigate rockfall hazard 37
The tree, an indicator of rock landslide hazards owing to dendro- geomorphology 39
Protection against the rockfall hazards in the area of the former quarry Carriere de Michelau, Luxembourg 41
Effect of dynamics on the Soil-geosynthetic interfaces used in reinforced rockfall embankments 43
New rockfall protection barriers in Formentor (Mallorca) 45
Rayleigh waves in seismic signals of rockfalls 47
Sensitivity analysis of rockfall trajectory simulations to material properties 49
Real scale impact experiments on Bloc Armé® as facing of rockfall protection embankment 51
Testing of UAV to inspect rockfall fences over railways 53
Rockfall Attenuators – a design approach 55
Slope stability analysis of a rock-cliff subjected to climate actions 57
Rockfall dynamics inferred from seismic signals and thermal camera: a controlled block release experiment 59
Evaluation of mechanical proprieties and lifespan of rockfall nets according to ISO standards 61
Surface motion detection at the Chambon landslide with terrestrial optical imaging 63
An automated processing pipeline for the photogrammetric analysis of high frequency terrestrial optical images: application to unstable slopes 65
Rock fall analysis of instable wedges potentially impacting a concrete dam 67
Combined rockfall modelling and protective dam simulation 69

On four frictional mechanisms in rockfall analysis: ground deformation, surface roughness, vegetation drag and basal sliding with rebound....71
Landslide displacement tracking using radio-frequency identification....73
Using InSAR to map slope instability over the French territory....75
Influence of block shapes and sizes on the variability of DEM trajectories....77
Benchmark of trajectory analysis models....79
Applications of 3D laser scan data for slope characterization and stability analysis....81
Rockfall release frequency for different rock wall types....83
Quantitative assessment of rockfall impact frequency....85
Debris flow flexible fence: barrier/flow interaction model....87
Numerical investigation of rockfall barrier under realistic on-site impacts....89
An advanced method for designing rockfall fences by surrogate modelling....91
Comparison of two DEM modeling of flexible rockfall fences under dynamic impact....93
The 2016 rock falls sequence at Mont Granier (1933 m a.s.l., Chartreuse massif, France) characterized by seismology and photogrammetry....95
Coupling 3D rockfall propagation to the spatio-temporal frequency for a realistic rockfall hazard mapping....97
Effect of rockfall fragmentation on exposure and subsequent risk analysis....99
Run-out of rockfall: towards objective assistance in determining the angles of the energy line method 101
Multiscale testing of geogrids used for rockfall protection.... 103
Bloc Armé© –Landslides passive protective structure.... 105
Falling of C40 rock at Livet Gavet 107
Innovative prefabricated rockfall gallery using a polymer geosynthetic mesh 109
Failure mechanisms within unreinforced concrete wall under rockfall impact loading.... 111
Study of rebound mechanisms using a Material Point Method (MPM) – Discrete Element Method (DEM) coupling113
Erosion of the right lateral moraine of the Mer de Glace (France) surveyed by airborne and terrestrial LiDAR 115
Lessons learned from Degotalls rock wall monitoring in the Montserrat Massif (Catalonia, NE Spain).... 117
Extended experimental analysis of friction energy dissipating device aging.... 119
Automatic monitoring of landslide displacements using total station.... 121
Evolution of quarry exploitation plan as a suitable countermeasure against rock instability phenomena 123
A new method of dating rockfalls in the Mont Blanc massif using reflectance spectroscopy 125
Robust sub-mm displacement measurements with interferometric radar technology applied to early warning systems.... 127
Bioengineering in rockfall mitigation : innovative high-energy barriers anchored on trees (case study).... 129
On the interest of reduced models for the design of soft rockfall barriers.... 131
Scale effect on roughness estimation by non-contact survey 133

Part 1
Keynote speakers

Pierre Azémard

Engineer geologist from ENSG (1986) my professional career begins with a stay of 3.5 years on the island of La Réunion where I am successively in charge of water research studies and landslides risks (BRGM) then flood hydrology (DDE974). From 1990, I work at regional laboratory of Aix en Provence at the CETE Méditerranée (now Cerema Méditerranée) in charge of infrastructure projects reconnaissance (A75, TGV Med, Tamarins Route) in south of France ; mainly specialized on rock massifs. Gradually from 1994 my activity turns towards landslides risks (hazards and protection) and more particularly the rockfalls which constitute now the essence of my work.

The RN1 in Reunion Island: Rock Hazard Management: circulation management, protections works and new route

Pierre AZEMARD (corresponding author)[1]

Keywords: Rockfall, protective structure, rock hazard management, risk management, RN1, Reunion Island

RN1 on Reunion Island is a strategic road infrastructure linking the port to the departmental headquarters; over 12 km long it is dominated by a cliff almost 200 m high. Supporting a traffic of 60,000 vehicles / day, it is also subject to significant daily traffic jams on arrival at St Denis, which lead to long wait times under the cliff. Securing this route is a major concern for its successive managers.

1 THE CURRENT RN1, SEARCH FOR OPTIMIZED SECURITY

1.1 ROCKS FALLS AND CONSEQUENCES

Opened in 1976 about 25 m from the foot of the cliff, the 2x2 lane road is highly exposed to this risk. Between 1976 and 2012 rock falls caused 23 dead and 62 wounded. The manager's findings indicate an average of 108 falls per year, 28 of which reach sea-side lanes, for a cumulative weight of 73 tonnes. In addition, there are some majors events in bulk of cliffs whose volumes exceed 10,000 m3 (1980, 1988, 2006)

The exploitation of the rock falls statements allowed the establishment of a law of distribution of the landslides:

$$\mathbf{N}(\text{fall/year}) = \mathbf{4{,}23 * V}(m^3)^{-0.40}$$ (1976-2003 period, before implementation of protections)

Between 1996 and 2008, the traffic was cut 2.6 days per year and switched to sea side lanes 56 days per year, causing significant disruption in the local economy.

1.2 PROTECTIVE WORK

The first work carried out is the laying of ASM nets on the Pointe du Gouffre in 1987. In 1995 and 2002-2003 the first 3 km are protected by ASM nets hanging on posts which is one of the first applications of this technique. These devices are designed to hold a 50 tonne landslide including a larger 5 ton block. Given the efficiency observed (see Figure 1 below), these devices are generalized over all 12 km between 2006 and 2008. In total, on the basis of a statistical study of rock falls and trajectory studies, 767,000 m² of nets were laid on nearly 44% of the surface of the cliff, supplemented by a 4 m height gabion screen over the entire linear.

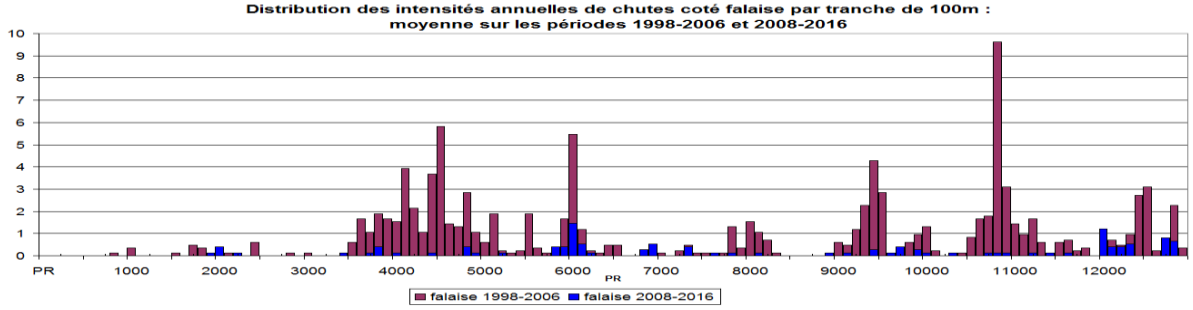

Figure 1: Comparison of rock fall intensities before (1998-2006) and after protection work (2008-2016)

Over all 12 km, this work has reduced the average exposure to block falls by 83% (93% in areas protected by nets and gabions). Additions are gradually added to the areas that remain the most active.

The post-event inspection reports analysis (figure 2) confirmed the good performance of the deflection nets: out of 85 events only 11% had an impact on the RN1 and especially 81% of the events exceeding, on 1 of the 2 criteria, the dimensioning values were retained (Azemard, 2017).

[1] AZEMARD Pierre, Cerema, Direction Méditeranée, Av A. Einstein, F-13593 Aix en Provence, FRANCE, pierre.azemard@cerema.fr

1.3 TRAFFIC MANAGEMENT MEASURES

From the first years traffic is cut off during rainy episodes. Offered in 1983, the first rule of tipping traffic on sea side lanes was formalized in 1989. Subsequent statistical studies (Batista, 2003) make it possible in 2004 to move to a more efficient rule differentiating the changeover time according to the cumulative rainfall. In 2008, after the completion of the protective works, the rule is adjusted again by raising the thresholds and decreasing the switching time. Optimization considerations are still in progress (Batista, 2016) for assess the impact of delaying the switchover after of the trafic peak.

Year of implementation	Cumulative rain in 24 h	Tipping time	Tipping
1989	15 mm	72 h	58,6 d / y
2004	15 mm	24 h	
	30 mm	72 h	
2009	30 mm	24 h	24,7 d / y
	50 mm	48 h	

2 A ENTIRELY SECURE NEW ROAD

In order to completely secure the route a new route has been studied since 1996. The solution at sea was finally preferred to the options going up on the La Montagne massif or in tunnel. The alignment of the route required taking into account the propagation of the landslides in various configurations, and in particular after a landslide in large mass.

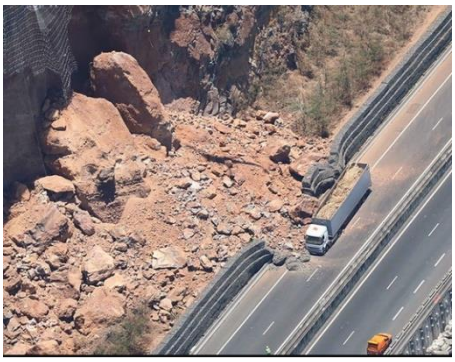

Figure 2: November 2016 Cliff fall

Figure 3: Viaduct under construction in 201

3 CONCLUSION

The risk management strategy put in place, based on a combination of traffic management rules and protection works, limits the exposure of users and the economic effects. This is quantified through regular records by the managing department.

The new road under construction will be completely sheltered from the rocks falls.

4 REFERENCES

Alfonsi, P., Durville, J.-L.(1999), Estimation of a minimum risk criterion on Route 1 of Reunion Island, *Proceedings of the twelfth european conference on soils mechanics and geotechnical engineering,* Amsterdam

Azemard, P. (2017) Feedback on the efficiency of the deflector nets set up on the RN1 in Réunion, *Journées Aléas Gravitaires,* Besançon

Batista, D (2003) Statistical analysis of the rock fall phenomenon and study of the modification of the tipping rules, *Rapport CETE Méditerranée*

Batista, D (2016) Feedback and analysis of the residual risk after securing; optimization of failover rules», *Rapport CETE Méditerranée*

Rat, M (2006) Optimization of coastal road management in Reunion with respect to the rock fall risk, *Bulletin de Liaison des Laboratoires des Ponts et Chaussées.*

Tom Badger

Tom Badger received a BS in geology in 1983 and an MS in geological engineering in 2002. He worked for the Washington State Department of Transportation for 32 years, the last five serving as Chief Engineering Geologist, before retiring in 2016. In this role, he was responsible for managing design, construction and maintenance aspects pertaining to soil and rock engineering, blasting, and rockfall and landslide hazards. He has authored numerous publications on these topics, and presently consults on geologic hazards and risk management for transportation infrastructure.

Perceptions of risk in response to geologic hazards

Thomas C. BADGER[1]

Keywords: risk management, risk tolerance

Examples abound of neglect or diminished importance given to planning and response decisions regarding exposure to geologic hazards. There are many reasons for these decisions of apparent disregard, some of which are well founded and informed – for instance, limited alternatives or resources for mitigation, no regulatory or uncertain jurisdictional authority, liability concerns, and insufficient understanding of the hazard. Action/inaction to manage exposure (risk) to a geohazard(s) is also commonly motivated by one's perception of the likelihood of occurrence and severity of consequences. These latter parameters are well known to geoscientists as often being difficult to characterize even for failures that appear imminent.

Geoscientists are often challenged to effectively communicate technical aspects of hazard and risk to others not professionally or regularly engaged in these topics. Geoscientists are trained to envision subsurface conditions and geologic complexity, and those regularly engaged with geologic hazards are familiar with typical triggering mechanisms, the range of failure modes, potential mobility, and uncertainty. The consideration of these topics informs geoscientists' perceptions about hazard and risk and guides their response.

These topics are typically unfamiliar to individuals not regularly engaged with geologic hazards. More often they rely on different bases for perceiving and decision-making. Unfamiliarity with scientific concepts and complexity are obvious impediments to initial understanding. Apparent frequency/infrequency is commonly cited as a basis for action/inaction. The likelihood and potential range of severity is commonly a judgment based more on personal experiences. Competing priorities are often distractions and draw attention and resources elsewhere. Additionally, time passed dilutes one's initial sense of importance. There are cultural influences, as well, for risk tolerance, which greatly influence our response to hazards. For example within the United States, there are notable regional and urban v. rural differences in risk tolerance.

An effective management response to a specific geologic hazard relies upon a well-founded characterization of the problem, understanding potential consequences and imminence of occurrence, as well as the identification of uncertainties. Such a response places considerable burden and expectations on the geoscientist to concisely frame the problem and to clearly communicate recommendations and uncertainties. When managing response for many hazards, a means is also needed to prioritize resources.

Management responses to geologic hazards and their associated impacts can range from proactive to reactive approaches. Motivation for implementing a proactive program has often historically occurred in reaction to a catastrophic event (Badger, 2017). In Western North America, most sectors of publicly and privately managed infrastructure that regularly experience landslide and/or rockfall damage or would experience severe societal consequences from a significant landslide/rockfall event have leading organizations/companies with relatively mature management programs in place. Public awareness and interest in geologic hazards is also heightened in this region because of the frequency and severity of events. As a result, risks associated with these hazards are increasingly and more effectively being addressed.

1 REFERENCES

Badger, T.C. (2017), Managing for landslide risk: a perspective from Western North America, in *Proceedings of Third North American Symposium on Landslides*, pp. 61-70.

[1] BADGER, Thomas C., Badger Geotechnics, Olympia, U.S.A.(2), badgergeotechnics@gmail.com

Anna Giacomini

Associate Professor Giacomini is committed to the deployment of innovative procedures to promote and improve safety in civil and mining environments. She received her PhD in 2003 from the University of Parma, Italy, and joined the University of Newcastle in 2005. She is currently Associate Professor in the Priority Research Centre of Geotechnical Science in Engineering and Higher Degree Research Director for the School of Engineering in the Faculty of Engineering and Built Environment of the University of Newcastle, Australia.

Associate Professor Giacomini has worked in the area of Rock Mechanics for more than 15 years. Adapting to the new Australian Environment, she has extended her rich background and extensive research experience in rockfall analysis and rock mechanics from civil engineering to mining. She is leading six major research projects through the Australian Coal Association Research Program (ACARP) on rockfall hazard and mitigation. Associate Professor Giacomini was the principal researcher of an Australian Research Council Linkage Project devoted to developing new designs for engineered barriers to protect valuable infrastructure, such as roads and railways, from rock fall hazards, and she is currently leading a recently funded Australian Research Council Linkage Project for the development of new innovating monitoring methodologies of rock slopes.

Rockfall in mining: mitigation measures design and hazard assessment

Anna GIACOMINI (corresponding author)[1], Klaus THOENI (others)[2], Federica FERRARI[3], Cedric LAMBERT[4]

Keywords: rockfall, hazard, mining, mitigation measures

Rockfall risk is most of the time considered and managed in the context of civil infrastructure, such as road or railway corridors. Rockfall is less frequently analysed in the context of mining environments, yet it threatens human lives, machinery and portal structures for underground entry located at the toe of highwalls. Safety of workers in all mine areas affected by rockfall has to be rigorously managed and appropriate mitigation measures become necessary to reduce the risk to an acceptable level. In addition, rockfall hazard can have significant financial consequences as it stops production until the pit is again deemed to be safe. Millions of dollars are lost annually due to rockfall.

1 ROCKFALL IN SURFACE MINING

Australia is one of the world's largest exporters of minerals and is a leading country in the production and exportation of coal. The stratiform deposits of the New South Wales and Queensland coalfield basins are often mined using open cast configurations. Highwalls are quite steep (between 60° and 80°) and characterised by good quality rock mass made of sequences of interbedded sedimentary layers. Portal entries located at the base of the highwalls are designed to ensure continuity of mining operations to and from the underground mining activities. Rockfall protection measures are commonly used to prevent the detachment of rocks from the highwalls, control the trajectories of the falling blocks and dissipate the rockfall energy at impact at the bottom of steep rock surfaces. Drapery systems combined with rock bolting, embankments of waste rock material located at various distances from the toe of the highwalls and muckpiles of waste rock material located on top of the concrete portals, are within the most common rockfall mitigation measures applied in Australian open-cut mines. Even though an increasing number of mines have started to document rockfall event occurrence as a part of their reporting procedures, it is still not common practice, and mine practitioners and engineers highlighted the need of more rigorous guidance on rockfall protection management strategies and hazard assessment for a saver working environment.

1.1 RECENT DESIGNS AND ASSESSMENT STRATEGIES

Over the last 10 years, in collaboration with the Australian mining industry and experienced practitioners in the field, the University of Newcastle has been conducting a series of research with the objective to provide more confidence in the application and design of various rockfall protection measures in surface mining. The team conducted experimental and numerical studies to investigate the efficiency of rockfall drapery meshes and to assess the residual energy associated with such solutions (Fig. 1). In fact, it was observed that blocks can still fall under the net and land on top of the portals and/or in their vicinity and a clear estimate of the associated energy is fundamental to protect highly-worked areas located at the bottom of the rock surfaces. The study combined 3D digital photogrammetry, discrete fracture network modelling, kinematic analysis and discrete element modelling to obtain accurate predictions of trajectories and velocities for blocks which are representative of a highwall. The efficiency of the rockfall protection measures was investigated by large scale field testing (Giacomini et al., 2012) and advanced tridimensional discrete element models (Thoeni et al. 2014). The study evidenced that drapery systems are efficient solutions in reducing the velocity and bouncing height for most cases, especially for small blocks whereas big blocks need to be pinned. Rockfalls under restraining nets resulted in impact velocities on top of the portals reduced by about 50%, with impact zones reduced by more than 60% (Fig. 2). However, it

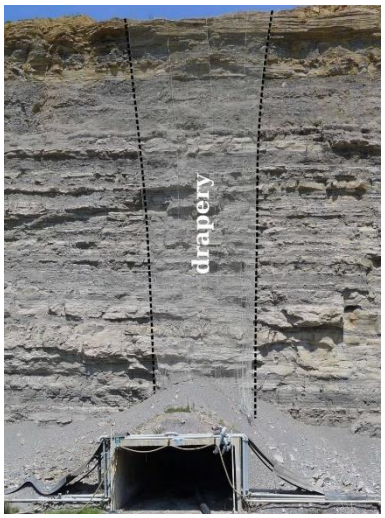

[1] GIACOMINI Anna, University of Newcastle, Callaghan, Australia (ISO 3166-2:AU), Anna.Giacomini@newcastle.edu.au

[2] THOENI Klaus, University of Newcastle, Callaghan, Australia (ISO 3166-2:AU), Klaus.Thoeni@newcastle.edu.au

[3] FERRARI Federica, University of Newcastle, Callaghan, Australia (ISO 3166-2:AU), federica.ferrari1984@gmail.com

[4] LAMBERT Cedric, Grenoble, France (ISO 3166-2:FR), cedric.lambert@outlook.co.nz

was observed that some scenarios currently used for the design of underground portals tend to overestimate the frictional resistance of the rockfall mesh. Results showed a significant dependence of the block trajectories on the highwall geometry/roughness (presence of ledges and channels) and the essential role of muckpiles of waste rock material on top of the portals. The findings of the initial phase of the research were therefore used to numerically investigate the energy absorption capacity of rockfall protection solutions such as muckpiles and dumping modules filled by granular material (Effeindzourou et al., 2017a,b).

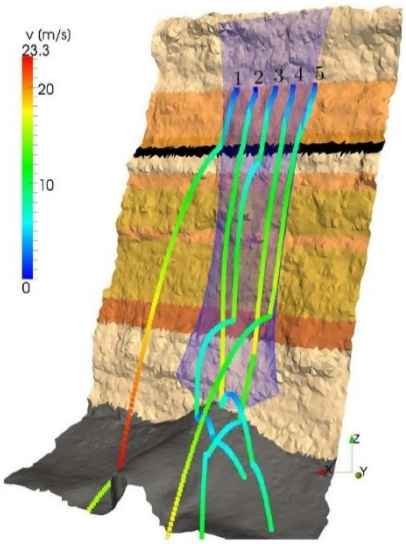

Figure 2: Modellig of 3D rockfall trajectories using the open source DEM code YADE

Rockfall protective measures typically deployed in mining environments, however, do not completely eliminate the rockfall hazard. Given the constant evolution of the worked areas to respond to the mine activity plans, an effective rockfall hazard zoning should entail a rapid identification of different hazard levels at the bottom of highwalls that can be easily updated according to the highwall changes. For this purpose, the research team proposed to the Australian coal mining environment, a new qualitative Evolving Rockfall Hazard Assessment (ERHA) methodology that involves a first qualitative assessment for the identification of the most hazardous areas where a second more robust quantitative analysis is required (Ferrari et al., 2016, 2017).

Inspired by the Swiss guidelines, ERHA applies a state of activity–intensity matrix (Fig. 3) to identify the rockfall hazard level and the required standoff distance at the base of a highwall from simple in-situ observations. The method rapidly estimate the predisposition of a highwall to be affected by rockfall and the level of intensity of the event according to the vulnerable elements at the base of the highwall. The proneness of a rock wall to rockfall is evaluated by means of a rating approach that accounts for the geological structure of the highwall, the potential for instability mechanisms, the slope performance and the evidence of signs of previous rock detachments.

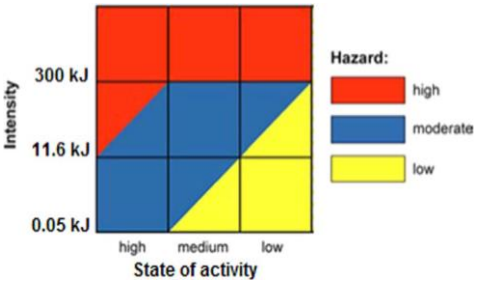

Figure 3: ERHA Adapted hazard matrix

2 CONCLUSION

The study focuses on rockfall hazard and its impact in surface mining. Recent innovative techniques for the investigation of the efficiency of rockfall protection measures are presented and the development of a rigorous guidance on rockfall management strategies are discussed. The research was developed in an Australian context but is applicable to a broader international context, both in civil and mining environments.

3 ACKNOWLEDGEMENTS

The support of the Australian Coal Association Research Program and the Priority Research Centre for Geotechnical Science and Engineering is gratefully acknowledged by the Newcastle authors. We would also like to thank Prof S. Fityus, Prof M. Jaboyedoff, Dr J. Abbruzzese, Dr R. Seedsmann and Dr J. Simmons for their valuable advises.

4 REFERENCES

Effeindzourou, A., Thoeni, K., Giacomini, A. and Wendeler, C. (2017a). Efficient discrete modelling of composite structures for rockfall protection. *Computers and Geotechnics*, 87, 99-114.

Effeindzourou, A., Giacomini, A., Thoeni, K. and Sloan, S.W. (2017b). Numerical Investigation of Rockfall Impacts on Muckpiles for Underground Portals. *Rock Mechanics and Rock Engineering*, 50, 1569–1583

Ferrari F, Thoeni K, Giacomini A, and Lambert C. (2016) A rapid approach to estimate the rockfall energies and distances at the base of rock cliffs. *Georisk: Assess Manag Risk Eng Syst Geohazards*, 10(3):179–199.

Ferrari F., Giacomini A., Thoeni K. and Lambert C. (2017) A qualitative rockfall hazard assessment tool for open-pit highwalls. *Int J Rock Mech Min Sci*, 98C:88-101

Giacomini A, Thoeni K, Lambert C, Booth S and Sloan S.W. (2012) Experimental study on rockfall drapery systems for open pit highwalls. *Int J Rock Mech Min Sci.* 2012; 56:171–181.

Thoeni, K., Giacomini, A., Lambert, C., Sloan, S.W. and Carter, J.P. (2014). A 3D discrete element modelling approach for rockfall analysis with drapery systems. *International Journal of Rock Mechanics and Mining Sciences*, 68, 107-119.

Fabien Hobléa

Dr. Fabien Hobléa is senior lecturer and geomorphologist member of the laboratory EDYTEM (Environments, Dynamics and Territories of Mountain areas) at University Savoie Mont Blanc (Chambéry, France). He is involved in several scientific councils of mountain protected areas and Geoparks; he is also co-chairman of the Working Group on Geomorphosites of the International Association od Geomorphologists. He works on calcareous and karstic mountains, aiming to study the interactions between the different dynamics shaping these type of mountains, especially karst processes and mass movements. This approach has been developped since his PhD defended in 1999, based on the case study of the Mont Granier in the French subalpine massif of Chartreuse, nearby Chambéry.

1248-2018: the chronic instability of Mont Granier in Chartreuse (Isère/Savoie, French Alps): a review

Fabien HOBLEA[1]

Keywords: Mont Granier, Chartreuse Massif, landslide, rockslide, rockfall, debris-flow, monitoring, hazard cascading.

Located in the French Alps at the northeastern end of the Chartreuse Massif in the nature reserve of Hauts de Chartreuse, the Mont Granier is a half perched syncline of alternating strata of limestone and marls, eastward tilted and very karstified. This mountain, overhanging the valley and the city of Chambéry (Savoie), is famous since the Middle Age because of the 1248 major landslide that affected its north face, which is known as one of the major historical collapse events in Europe. The Mont Granier instability continues nowadays, with several large rocksfalls observed during the 20th Century, and a recent impressive sequence of collapses and debris-flows during the winter and spring 2016. These last events induced a renewed interest for the study and the monitoring of the instability of this iconic mountain in order both to prevent risks and to increase scientific knowledge on mass-movement processes. This paper summarizes the main events and modalities of the Mont Granier rock slope instability and presents the collaborative and participatory monitoring device set up after the 2016 instability crisis.

1 A FAMOUS INSTABILITY FOR MORE THAN SEVEN CENTURIES

1.1 THE MAJOR EVENT OF 1248

On the night of November 24, 1248 AD, the whole rocky cliff of the north face of Mont Granier collapsed. By destabilizing the marly lands at the foot of the wall, this collapse of about 5 x 10^6 m^3 of limestone rocks led to a huge landslide estimated at 5 x 10^8 m^3 (Goguel & Pachoud, 1972), the largest of the historical period in the Alps. The event was reported and its memory perpetuated throughout medieval Europe by monastic chronicles which announced 5000 deaths, reduced to a thousand by current geographers and historians. At the end of the twentieth century, new field data, acquired through geological studies prior to major railway developments, made it possible to specify the characteristics and spatial influence of the event of 1248 which spread on 32 km^2, over a distance of more than 11 km).

1.2 A CONTINUOUS INSTABILITY

Since the major event of 1248, the instability of Mont Granier has continued sporadically and more modestly. This instability is not only characterized by rock collapses (the biggest of the twentieth century occurred the 26th of June 1953) but also by debris-flows that affect the scree and rock falls deposits accumulated at the foot of the north face, at least since 1755. Very recent events have revealed the relationships between rock collapses and debris flows.

2 LESSONS FROM THE EVENTS OF WINTER-SPRING 2016

2.1 TWO BIG ROCK COLLAPSES IN FIVE MONTHS

The 9 January 2016 early morning, the northwest pillar of Mont Granier collapsed. The collapsed volume was calculated at about 10^5 m^3 by 3D analysis (photogrammetry) (Ravanel et al., 2016).
A second serie of rock falls and rock collapses occurred at the end of April and the beginning of May 2016 (major event the 7th of May), totalizing also about 10^5 m^3, but this time in the northeast corner of the mountain, where cavers exploring the Granier karst underground network had already long time ago spotted signs of instability.
This two sequences of rock collapses are supposed to have been induced by similar meteorological conditions characterized by both wet and thermally-contrasted conditions occurred during abnormal sweet winter and cold spring.

2.2 THE CONSECUTIVE MUDFLOWS AND DEBRIS FLOWS.

The rockfalls and collapses of April-May 2016 were ducted by a subvertical gully forming a dihedron in the northeast angle of the mountain, opening at the foot of wall on a marly slope where the debris were massively accumulated, building

[1] HOBLEA Fabien, Univ. Grenoble Alpes, Univ. Savoie Mont Blanc, CNRS, MCC, EDYTEM, Chambéry, FR, fabien.hoblea@univ-smb.fr

an imposing debris fan. As we had assumed, the first heavy rainfall, which occurred a week later, caused a series of debris flows from May 13, 2016 (fig. 4). If the collapses did not cause much damage (except to some mountain trails and paths), the debris-flows have blocked a road which was closed for several months.
The debris flows are clearly due to the conjunction between large amount of intense rainfall and presence of a big volume of instable debris consecutive to the rock collapses of April-May 2016. This sequence of connected events can be considered as an example of hazard cascading (Gill & Malamud, 2016).

2.3 A PARTICIPATORY AND COLLABORATING MONITORING DEVICE.

These events had strong media impact and induced the constitution of a cluster of scientists and managers for studying and assessing the processes and the risk of disaster within a multi-method approach summerized as following (Hobléa *et al.*, 2018):

- Detection, monitoring and quantification of the current and recent rockfalls and movements by crossing classic methods of extensometry, coupled with innovative methods of seismic signal analysis and 3D reconstruction by photogrammetry and laser scanning (LS). Drones and auto-gyre were used for safe and complete photogrammetry data acquisition in very steep, high rock walls, compared and crossed with long range terrestrial and aerial LS surveys. Joined seismometry and photogrammetry provided accurate data about both occurrence time, volume, shape and tectonic guideline network of the successive rockfalls.
- Diachronic characterization of the present and past detachment and deposit zones, morphological changes in cliffs and slopes, as well as damages to forest, by photocomparison methods (monoplotting), 3D morphological mapping and dendromorphology. Aerial LS and drone surveys were also useful, as well as research of old textual or iconographic documents and testimonials allowing to date the past events and study their frequency.
- Diachronic study of the dynamics and processes of the debris-flows and their relationships with collapses events affecting the cliffs.

Local inhabitants were associated to the observation device and a participatory and collaborative observatory of the Granier risks has been designed.

3 CONCLUSION: THE MONT GRANIER AS A HOTSPOT OF ROCK SLOPE INSTABILITY?

The Mont Granier shows for centuries an active and recurrent instability whose frequency and intensity merits to be studied as well as its environmental and social consequences.
After the spectacular, but not so dangerous, events of 2016, active slopes of Mont Granier should so become a reference test site for crossing and correlating various methods for observing, reconstructing and studying current and past landslides and “hazard cascades” as well as to manage a local “risk scene” in a participatory and collaborative approach, in accordance with the Integrated Risk Management principles.

4 ACKNOWLEDGEMENTS

this paper presents a nutshell of years of collaborative research gathering scientists, advanced students, risk and nature reserve managers, as well as non-academic partners (especially cavers, local inhabitants and elective representatives) who are all warmly thanked hereby. The author would like to cite more particularly the colleagues forming the academic part of the collaborative research team on the Granier, from University Grenoble-Alpes (ISTerre: D. Amitrano, D. Hantz, A. Helmstetter, M. Langlais, G. Le Roy, J. Weiss), University Savoie Mont-Blanc (EDYTEM: L. Astrade, P. Deline, X. Gallach, E. Malet, L. Ravanel) and University of Lausanne (Antoine Guérin). As well as the Master students who have completed their research internship on hazards and risks related to Granier: Thibaut Cardinal, Enzo Cavalier, Suzon Lejeune.

5 REFERENCES

Gill J.C., Malamud B.D., (2016) Hazard interactions and interactions networks (cascades) within multi-hazard methodologies. *Earth Syst. Dynam.*, 7, 659–679.

Goguel J. & Pachoud A. (1972) Géologie et dynamique de l'écroulement du Mont Granier en novembre 1248. *Bull. BRGM*, section 3, 1, 29-38.

Hobléa F., Amitrano D., Astrade L., Barnave S., Buffle A., Cardinal T., Cavalier E., Cayla N., Deline P., Gallach X., Guerin A., Hantz D., Helmstetter A., Laïly B., Langlais M., Lejeune S., Le Roy G., Malet E., Ravanel L., Saint-Bézar B., Weiss J. (2018) Multi-method diachronic approach of the rockfalls and landslides at Mont Granier (1933 m a.s.l., Chartreuse Massif, French Alps). *Geophysical Research Abstracts*, 20: 10006.

Ravanel L., Amitrano D., Deline P., Gallach X., Helmstetter A., Hobléa F., Le Roy G., Ployon E. (2016). The small rock avalanche of January 9, 2016 from the calcareous NW pillar of the iconic Mont Granier (1933 m a.s.l., French Alps). *Geophysical Research Abstracts*, 18: 13535.

Michel Jaboyedoff

Michel Jaboyedoff is a geologist and has a degree in physics and a PhD degree in clay mineralogy. During his PhD, he started doing research on natural hazards, especially on rockfall. In 2017, he received the DPRI Award. Since 2005, he is a full professor at the University of Lausanne, focusing his research on natural hazards and related risks. He is working on integrated risk analysis and he is involved in several risk management projects around the world (Argentina, Canada, Nepal, Norway, Switzerland …), and is part of several European Projects FP7 (Mountain Risks, Safeland, CHANGES) and Swiss National Science Foundation. Many studies are related to remote sensing technique such as Lidar. One of his focuses is the development of software for hazard and risk analysis. Especially about rockfall hazard rating. He also the president of the Quanterra foundation and co-founder of a spin-off of the University of Lausanne (terr@num).

About the "rockfall" failure hazard assessment

Michel Jaboyedoff[1], Cécile D'Almeida[2], Marc-Henri Derron[3], François Noël[4], Antoine Guerin[5]

Keywords: Rockfall hazard, rockfall sources, structural setting, infrared thermal imaging.

Usually rockfall hazard assessment is mainly based on rockfall modelling statistics, and on inventories of observed fallen blocks. Only few studies include source hazards assessment by varying the failure frequency depending on the source areas. Such assessment is mainly performed when large volumes can fall (Hantz et al., 2003), but it is not dedicated to zones with diffuse hazard. The rockfall hazard (H) has two components, the frequency of failure (λ) and the probability of propagation (P_p):

$$H = I \times P_p$$

Some approaches mixed the evaluation of both terms, including risks such as Rockfall Hazard Rating System (RHRS) (Pierson, 1990). Here we deal with the assessment of λ. An approach is to use a susceptibility scale and to calibrate it to reach a frequency, when a rockfall inventory is available. The parameters that control the stability can be subdivided in two groups: the internal characteristics which are the rock type, the structures, permeability, friction angle, cohesion, etc. and that are evolving under the action of external factors such as, temperature, rain, ice, groundwater, earthquakes, etc.

1 INTERNAL CHARACTERISTICS

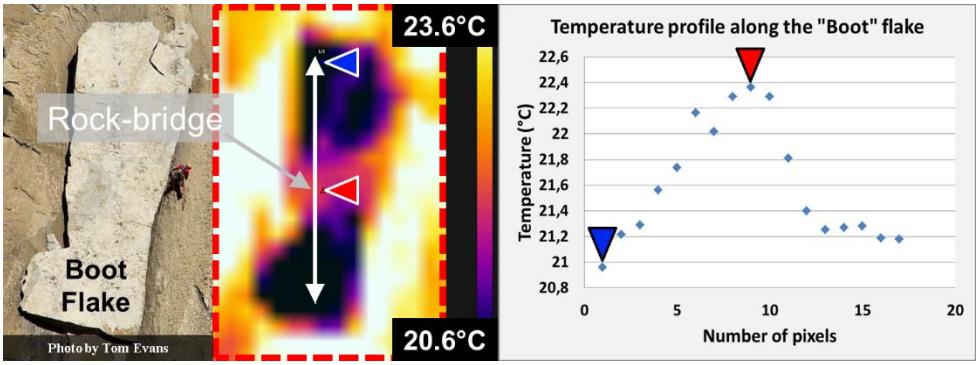

Figure 1: Left: Infrared thermogram showing a warmer thermal anomaly at the centre of the Boot Flake (8 October 2015, 17h45). Right: Longitudinal profile indicating a temperature difference of about + 1.5 °C at the rock bridge level. (modified after Guerin et al., in prep.).

It is obvious that discontinuities are controlling stabilities of a rock face. Nevertheless, there exist two more important variables controlling stability which are the spatial frequency of structures and their persistence. The probability to find structures can be characterized by the average density of discontinuities at surface which qualifies indirectly the probability to find a hazardous structure (Dershowitz, and Herda, 1992). Some attempts were made to include some geomechanical parameters which lead to a 3D rock failure susceptibility (Matasci et al., in press). The above approach may integrate the probability of the continuity of structures which is equivalent to the evaluation of the presence of rock bridges. This represents a weighing factor. Nowadays the infrared thermal imaging allows to probably identify where are located the rock bridges by indicating warmer areas that may correspond to the link to the rock mass (Figure 1; Guerin et al., in prep.).

[1] JABOYEDOFF Michel, Risk Analysis Group, Institute of Earth Sciences, University of Lausanne, Lausanne, Switzerland (CH), (michel.jaboyedoff@unil.ch)

[2] D'ALMEIDA Cécile, Risk Analysis Group, Institute of Earth Sciences, University of Lausanne, Lausanne, Switzerland (CH), (d.almeidacecile@gmail.com)

[3] DERRON Marc-Henri, Risk Analysis Group, Institute of Earth Sciences, University of Lausanne, Lausanne, Switzerland (CH), (marc-henri.derron@unil.ch)

[4] NOËL François, Risk Analysis Group, Institute of Earth Sciences, University of Lausanne, Lausanne, Switzerland (CH), (francois.noel@unil.ch)

[5] GUERIN Antoine, Risk Analysis Group, Institute of Earth Sciences, University of Lausanne, Lausanne, Switzerland (CH), (antoine.guerin@unil.ch)

2 EXTERNAL FACTORS

The external factors are usually degrading the rock mass quality or stability, by mechanical fatigue, weathering, increase of pore water pressure, etc.

Temperature variations induce expansion and contraction of rock faces which leads to degradation or to rockfall triggering. This is now well documented in Yosemite National Park (Collins and Stock, 2016), where exfoliation sheets were deforming daily by more than 1 cm over 10-m long. Yearly cyclic deformation can be induced by water flow within a cliff, the cliff expanding by several millimetres when water level changes (Preisig et al., 2016; Rouyet et al., 2016). These slight changes have to be accommodated and lead progressively to increase the size of pre-existing discontinuities.

Meteorological factors are obvious in particular freezing and thawing cycles are promoting rockfalls (Matsuoka and Sakai, 1999). The permafrost melting is nowadays, in high altitude, a real security concerns (Ravanel et al., 2010), even if it often not the direct triggering factor, but a complex play between melting freezing and pore water pressure rise by melting snow and ice. The importance of water is highlighted by the results obtained by D'Amato et al. (2016), indicating that rainfall can be assumed as a major triggering factor in limestones rock. The origin of this effect can be thermal shock or change in apparent cohesion of the infilling material of joints because it occurs also with normal rainfall intensity.

3 CONCLUSION

The frequency (λ) of failure prior to rockfalls are one of problems that have to be solved in order to improve the rockfall hazard assessment (H). The propagation is nowadays rather well studied (P_p). The above elements that affect the failure prior to rockfalls pushed us to better understand rock mass fatigue caused mainly by direct or indirect thermal effects and weathering but also to improve the “geometrical” characterization of the discontinuities including rock bridges. A first attempt to couple λ and P_p is presented here by D’Almeida et al. (2018), who differentiates the sources frequency depending on an inventory providing rockfall volume frequency distribution and sources spatial distribution.

4 REFERENCES

Collins, B.D., Stock, G.M. (2016) Rockfall triggering by cyclic thermal stressing of exfoliation fractures. *Nature Geoscience* 9, 395–400.

D’Almeida, C., Noël, F., Guerin, A., Jaboyedoff, M., Hantz, D., Derron, M.-H. (2018) Coupling 3D rockfall propagation to the spatio-temporal frequency for a realistic rockfall hazard mapping. *4th RSS Rock Slope Stability Symposium*, Chambéry 2018

D'Amato, J., Hantz, D., Guerin, A., Jaboyedoff, M., Baillet, L., and Mariscal, A. (2016) Influence of meteorological factors on rockfall occurrence in a middle mountain limestone cliff, *Nat. Hazards Earth Syst. Sci.*, 16, 719-735, https://doi.org/10.5194/nhess-16-719-2016.

Dershowitz, W., and Herda, H.H., (1992) Interpretation of Fracture Spacing and Intensity. Proceedings of the 33rd U.S. Symposium on Rock Mechanics, Santa Fe, NM. p. 757.

Guerin, A., Derron, M.-H., Jaboyedoff, M., Boesiger, M., Lefeuvre, C., Stock, G.M., Collins, B. D., Matasci, B. and Podladchikov, Y. (in prep.) Detection of potential rock bridges with infrared thermal imaging: examples from El Capitan, Yosemite Valley.

Hantz, D., Vengeon, J. M., and Dussauge-Peisser, C. (2003) An historical, geomechanical and probabilistic approach to rock-fall hazard assessment, *Nat. Hazards Earth Syst. Sci.*, 3, 693-701, https://doi.org/10.5194/nhess-3-693-2003.

Matasci, B., Stock, G.M., Jaboyedoff, M., Carrea, D., Collins, B.D., Guerin A., Matasci, G., Ravanel, L. (in press): Assessing rockfall susceptibility in steep and overhanging slopes using three-dimensional analysis of failure mechanisms. Landslides. DOI 10.1007/s10346-017-0911-y

Matsuoka, N. &Sakai, H. (1999) Rockfall activity from an alpine cliff during thawing periods. *Geomorphology*, 28:309–328.

Pierson, L., Davis, S. A. and Van Vickle, R. (1990) The Rock Fall Hazard Rating System, *Implementation Manual. Technical Report #FHWA-OR-EG-90-01*, Washington, DC.

Preisig G., Eberhardt E., Smithyman M., Preh A., Bonzanigo L. (2016) Hydromechanical Rock Mass Fatigue in Deep-Seated Landslides Accompanying Seasonal Variations in Pore Pressures. *Rock Mechanics and Rock Engineering*, Volume 49, Issue 6, pp 2333–2351.

Ravanel, L., Allignol, F., Deline, P., Gruber, S., Ravello, M. (2010) Rock falls in the Mont Blanc Massif in 2007 and 2008. *Landslides* 7: 493-501.

Rouyet, L., Kristensen, L., Derron, M.-H., Michoud, C., Blikra, L., Jaboyedoff, M., Lauknes ,T. (2016) Evidence of rock slope breathing using ground-based InSAR. *Geomorphology*. doi.org/10.1016/j.geomorph.2016.07.005.

Part 2
Extended abstracts

Comparative analysis of different climate predictions in a temperate zone in France and their impact on slope stability

Alain THORAVAL (corresponding author)[1], Augustin COLETTE[2], Auxane CHERKAOUI[2], Jean-Marc WATELET[2], Christian FRANCK[2]

Keywords: slope, climate change, temperate zone, climate scenarios, modeling, UDEC

Many studies (Cherkaoui, 2015) highlight that climate change impacts the stability of the slopes on the national territory through climatic factors and site factors. Depending on the climatic environment in which the slope is located (mountain zone, coastal zone, temperate zone), these factors do not play the same role and do not have the same influence. We wished to characterize the impact of climate change on the stability of rocky slopes in a temperate zone. The study was conducted in 2 stages: first we evaluate the impact of climate change on pluviometry of 2 sectors located in a temperate zone in France, then we assess the impact of pluviometry changes on slope stability.

1 EVALUATION OF THE IMPACT OF CLIMATE CHANGE ON PLUVIOMETRY

First of all, we chose 2 sectors (Mendes and Montsoreau) for which we had rainfall flows for the last 60 years (reference case) and for the next 100 years under the IPCC scenarios described in (van Vuuren & al., 2011). The two scenarios selected for this study are the median scenario (RCP4.5 - Representative Concentration Pathway followed by a figure corresponding to the radiative forcing in W/m^2) and the strong global warming scenario (RCP8.5). Those scenarios have been simulated with the model WRF Regional Climate Program as part of the EuroCordex program (Jacob & Colette & al., 2013). The results show that the climatic effects modify only slightly the average rainfall flow (± 10%, depending on the site), but increases the number of days of heavy rain without the maximum intensity of rain being significantly modified (Table 1).

Table 1: Layout of the proceedings

	Number of days where the indicated rainfall threshold is exceeded (days/year)				
Montsoreau	**> 1 mm**	**> 4 mm**	**> 10 mm**	**> 20 mm**	**> 40 mm**
HIST (1951-2005)	169	78	20,1	3,2	0,20
RCP4.5 (2007-2100)	168	78,7	22,9	4,2	0,31
RCP4.5 (2050-2010)	169	79,8	24,1	4,6	0,24
RCP8.5 (2007-2100)	168	79,3	24,6	5,1	0,37
RCP8 ;5 (2050-2100)	168,4	82,2	26,7	5,6	0,30
Mende	**> 1 mm**	**> 4 mm**	**> 10 mm**	**> 20 mm**	**> 40 mm**
HIST (1951-2005)	170	97	39,3	8,8	0,67
RCP4.5 (2007-2100)	159	91,3	37,8	9,2	0,95
RCP4.5 (2050-2010)	162	92,8	39,0	9,7	0,96
RCP8.5 (2007-2100)	158	89,3	36,4	9,6	1,04
RCP8.5 (2050-2100)	156	87,5	36,4	10,1	1,30

2 IMPACT OF PLUVIOMETRY CHANGES ON SLOPE STABILITY

The hydromechanical behavior of a typical 30 m high slope at the stability limit was then evaluated and compared when subjected to reference case rainfalls or RCP4.5 and RCP8.5 scenarios. For this purpose, we used the UDEC code (Itasca, 2006) which is a 2D numerical modeling program based on the distinct elements method. The fractured slope is represented by blocks that can move and rotate relative to each other. The rock-mass is crossed by two families of fractures whose orientations are chosen so that the slope is close to its limit of stability. Over-fracturing, simulating rock-mass degradation, is added in an area 12 m wide along the slope. The model simulates the gradual degradation of fractures subjected to a shear force from an initial angle to a residual angle (the progressive "scrubbing" of the asperities of the fracture plane). It also simulates the fluid flow through the fracture network (the blocks are assumed to be impermeable), as well as the impact of the fluid pressure on the mechanical behavior of the slope.

The results show that the effect of an increase in the average infiltration rate has no impact on slope stability. This is explained by the fact that the pressures induced by average rainfall flow rates remain very low (<1 Pa) compared with normal stress values on fractures (> 100 Pa). If a sufficiently high infiltration rate is imposed, a mechanical impact may appear for a slope initially "in

[1] THORAVAL Alain, INERIS, 54000 Nancy, FRANCE, alain.thoraval@ineris.fr

[2] INERIS, 60550 Verneuil en Halatte, FRANCE (firsname.lastname@ineris.fr)

limit of stability" (Figures 1), without this necessarily resulting in additional instabilities. Given the increase in the number of rainy days for RCP4.5 and RCP8.5, we conclude that climate change may impact rocky slopes in temperate zone.

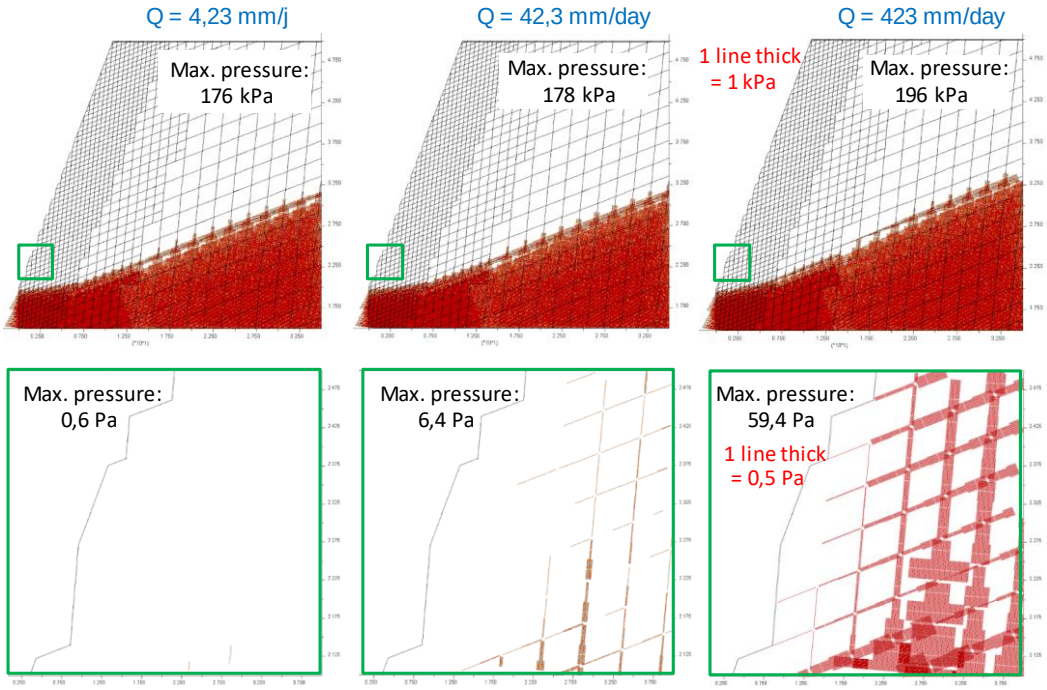

Figure 1: Water pressure in fractures according to rainfall: (a) 4.23 mm / day; (b) 42.3 mm / day; (c) 423 mm / day (The 3 bottom outputs are a zoom located at the base of the slope (green square). The 3 top outputs (respectively the 3 bottom outputs) were made considering the same pressure scale. The maximum pressure is the maximum pressure computed inside the window considered)

3 CONCLUSION

Given the increase in the number of rainy days for RCP4.5 and RCP8.5, we conclude that climate change may impact rocky slopes in temperate zone. To go further, we plan to evaluate the impact of the fracture network geometry / connectivity on the evolution of the slope foot pressures and the effect of this evolution on the mechanical stability of the slope. We also plan to take better account of transient effects and the change over time of the hydromechanical characteristics of fractures to simulate leaching of the filling of initially clogged fractures.

4 ACKNOWLEDGEMENTS

This work was supported by the MTES (Ministère de la Transition Ecologique et Solidaire).

5 REFERENCES

Cherkaoui, A. (2015) Impact du changement climatique sur la stabilité des versants : hiérarchisation des facteurs prépondérants influençant la stabilité selon les milieux climatiques. *INERIS report DRS-15-149572-12884A*.

van Vuuren, D. et al. (2011) The representative concentration pathways: an overview. *Climatic Change*. 109, 5-31.

Jacob, D., Colette, A. et al. (2013) EURO-CORDEX: new high-resolution climate change projections for European impact research. *Regional Environmental Change*. 1-16.

Itasca Consulting Group Inc. (2006) Universal Distinct Element Code. *User's guide*.

Rock reinforcement monitoring using passive seismics: a first case study

Pierre BOTTELIN (corresponding author)[1], Laurent BAILLET[2], Eric LAROSE[3], Denis JONGMANS[4], Didier HANTZ[5], Ombeline BRENGUIER[6], Héloïse CADET[7], Agnès HELMSTETTER[8]

Keywords: Rock bolting; Ambient vibrations; Resonance frequency; Monitoring; Passive seismics

Coeur The D518 road carved through the narrow Bourne gorges (Vercors massif, France) is particularly subject to rockfalls and benefits from a risk mitigation plan for about 10 years. This study focuses on one rock block stabilized with untensioned steel bolts to provide additional shear and tensile strength technique. The efficacy of such rock bolting works is rarely assessed (Cao et al., 2013), even though its performance greatly depends on the bolting design, the care taken during the fieldwork and the presence of local rock heterogeneities and discontinuities.

In this study, we used passive seismics to track changes in unstable rock compartment's dynamic parameters (i.e. its resonance frequencies) throughout the bolting works. Such methods proved their ability to monitor various unstable rock slopes (Burjánek et al., 2010, 2012; Galea et al. 2014) and detect precursory patterns before failure (Lévy et al., 2010; Mainsant et al. 2012).

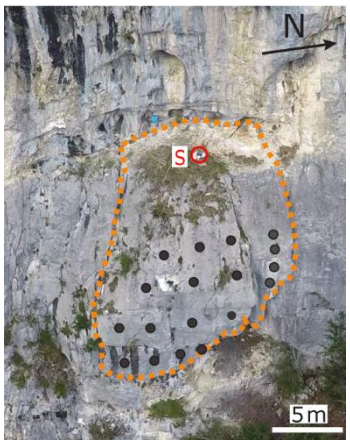

Figure 1: Front view of the unstable compartment (delineated with dashed orange line) with the passive seismic sensor on top (S, red circle). Bolt location is shown by the grey

1 EXPERIMENTAL SETTINGS

1.1 STUDY SITE

The unstable compartment studied lies about 130 m above the D518 road. It is made of massive limestones and measures ~5 m in thickness, ~10 m in width and ~15 m in height, for a volume of ~760 m^3 (Figure 1). It is separated from the rock mass by a widely opened rear fracture (about 0.5 m) at surface, its continuity at depth remaining poorly constrained (orange dashed line, Figure 1).

The reinforcement works consist in bolting the unstable compartment with ø43 mm steel rebar rods grouted over their whole length (grey dots, Figure 1). Major grout leak was observed at the rock column's toe due to rear fracture opening, making the rock-bolt bonding surface (i.e. strength) uncertain (Zou, 2004).

1.2 METHODS

Passive seismic measurements were acquired before (BW), during (DW) and after (AW) the bolting works on top of the unstable compartment (S, Figure 1). Seismic Power Spectral Density (PSD) was computed using Welch's method (Welch, 1967). Air temperature was recorded simultaneously on-site using a Testo 174 T data logger with 10 min sampling interval.

2 SEISMIC NOISE SPECTRAL ANALYSIS

The seismic noise on top of the unstable compartment shows clear spectral peaks (Figure 2, see also similar observations in Burjánek et al., 2010, 2012; Moore et al., 2011; Bottelin et al., 2013a), corresponding to its resonance frequencies (noted f_x). We selected the f_0, f_3 and f_5 for monitoring because they showed distinct and high-amplitude peaks. We observe resonance frequency wandering related to temperature variations during BW, DW and AW periods (Figure 2, see also Bottelin et al., 2013b; Starr et al., 2015). A clear rise in f_x was spotted during the grouting phase (black double headed arrow, DW period), with a +8 %, +17 % and +1 % increase for f_0, f_3 and f_5 after correction from the air temperature influence.

[1] BOTTELIN Pierre, ADRGT, Gières, France (FRA), p.bottelin@adrgt.org

[2] BAILLET Laurent, ISTerre, Grenoble, France (FRA), laurent.baillet@univ-grenoble-alpes.fr

[3] LAROSE Eric, ISTerre, Grenoble, France (FRA), eric.larose@univ-grenoble-alpes.fr

[4] JONGMANS Denis, ISTerre, Grenoble, France (FRA), denis.jongmans@univ-grenoble-alpes.fr

[5] HANTZ Didier, ISTerre, Grenoble, France (FRA), didier.hantz@univ-grenoble-alpes.fr

[6] BRENGUIER Ombeline, ADRGT, Gières, France (FRA), o.brenguier@adrgt.org

[7] CADET Héloïse, ADRGT, Gières, France (FRA), h.cadet@adrgt.org

[8] HELMSTETTER Agnès, ISTerre, Grenoble, France (FRA), agnes.helmstetter@univ-grenoble-alpes.fr

Three dimensional numerical simulations using a finite element model (FEM) of the rock column were carried out to interpret these rises in resonance frequencies. The numerical model was first calibrated on the experimental resonance frequencies values. Then, tensile and shear stiffness was added at 18 points on the compartment's backside to simulate the bolting, assuming a full bound between the rock mass and the steel bolts (i.e. effective bolt grouting). Rises of +5.5 %, +16 % and +17 % were observed for f_0, f_3 and f_5, respectively. These values are of same order of magnitude as the experimental observations.

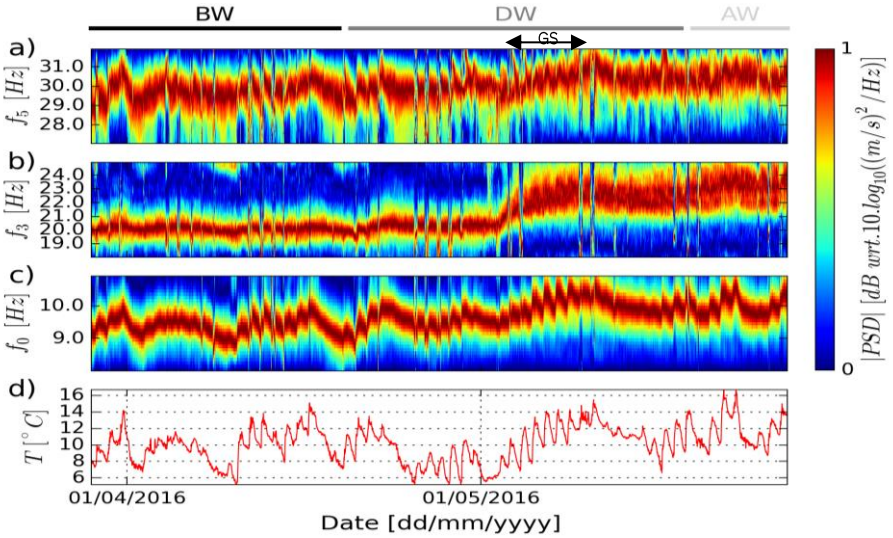

Figure 2: Normalized PSD of seismic noise versus on top of the unstable compartment. Frequency bands a, b, c show variations in f0, [illegible]nd f5 resonance frequencies, respectively. d) Air temperature recorded on site. Before bolting work (BW), during bolting work (DW) and after bolting work (AW) periods are shown at the top. Grouting stage (GS) is shown as black double-headed arrow.

3 CONCLUSION

This innovative monitoring of rock reinforcement works using passive seismics showed that significant changes occur in the rock compartment's dynamic properties (~ +8 % mean rise in resonance frequencies) due to the bolting. Such changes were successfully simulated in a 3D FEM via introduction of additional stiffness at 18 locations on the compartment's backside. This suggests that the bolts were appropriately bounded with the rock mass, despite the major grout leaks observed during the works.

This new kind of observational parameter may be used to assess the coupling between the bolts and adjacent rock masses, and adapt the bolting design if necessary.

4 ACKNOLEDGEMENTS

This work was funded by C2ROP and VOR programs (IREX-INDURA and Univ. Grenoble-Alpes). Thanks to Hydrokarst company and CG38 for granting access to the site, providing details on bolting design and the high-resolution DEM of the area. This work could not have been accomplished without the help of many colleagues at ISTerre. ISTerre is part of Labex OSUG@2020 (ANR10-LABX56).

5 REFERENCES

Bottelin, P., et al., (2013a). Spectral analysis of prone-to-fall rock compartments using ambient vibrations. J. Environ. Eng. Geophys. 18, 205–217. http://dx.doi.org/10.2113/JEEG18.4.205.

Bottelin, P., et al., (2013b). Modal and thermal analysis of Les Arches unstable rock column (Vercors massif, French Alps). Geophys. J. Int. 194, 849–858. http://dx.doi.org/10.1093/gji/ggt046.

Burjánek, J. et al., (2010). Ambient vibration analysis of an unstable mountain slope. Geophys. J. Int. 180, 820–828.

Burjánek, J., et al., (2012). Instrumental evidence of normal mode rock slope vibration. Geophys. J. Int. 188, 559–569.

Cao, C et al., (2013). A study of rock bolting failure modes. Int. J. Min. Sci. Technol. 23, 79–88.

Galea, P., et al. (2014). Dynamic characteristics of an active coastal spreading area using ambient noise measurements—Anchor Bay, Malta, *Geophysical Journal International*, Volume 199, Issue 2, 1 November 2014, Pages 1166–1175, https://doi.org/10.1093/gji/ggu318

Lévy, C. et al., (2010). Dynamic response of the Chamousset rock column (Western Alps, France). J. Geophys. Res. Earth Surf. 115, F04043. http://dx.

doi.org/10.1029/2009JF001606

Mainsant, G., et al. (2012). Ambient Seismic Noise Monitoring of a Clay Landslide: Toward Failure Prediction.

Moore, J.R., Gischig, V., Burjanek, J., et al., 2011. Site effects in unstable rock slopes: dynamic behavior of the Randa instability (Switzerland). Bull. Seismol. Soc. Am. 101, 3110–3116.

Starr, A.M., Moore, J.R., Thorne, M.S., 2015. Ambient resonance of Mesa Arch, Canyonlands National Park, Utah. Geophys. Res. Lett. 42http://dx.doi.org/10.1002/2015GL064917. (2015GL064917).

Welch, P.D., 1967. The Use of Fast Fourier Transform for the Estimation of Power Spectra: A Method Based on Time Averaging Over Short, Modified Periodograms. IEEE Trans. Audio Electroacoust. 15, 70–73.

Impacts of land-use and land-cover changes on the quantitative analysis of rockfall risk: The case study of the village of Crolles

Manon FARVACQUE[1], Jérôme LOPEZ-SAEZ[2], Christophe CORONA[3], Franck BOURRIER[4], David TOE[5], Nicolas ECKERT[6]

Keywords: Rockfall hazard, Quantitative-Risk-Assessment, Land-use/land-cover changes

1 INTRODUCTION

Rockfall phenomenon is defined as a rock block detachment from a vertical or sub-vertical cliff, travelling down the slope by rapid motions. Some rockfalls have enough energy to reach urbanized areas, causing damages to structure or injuring people. Thus, rockfall risk assessment is essential for land use planning and mitigation measures.

Risk analysis can be envisaged following two methods: a qualitative one, known as "Rockfall Hazard Rating System" (RHRS) and a quantitative one, called "Quantitative Risk Assessment" (QRA). Both methods consider the same risk definition, which is the combination of hazard, elements at risk, exposure and damages. RHRS approaches build the assessment using qualitative descriptors, such as ranking matrices and classifications, scoring schemes or weighted indices. QRA approaches define each term of the risk components as probabilities and, by including the cost of the different issues, set the risk as an annual damage in monetary value. The choice between these two procedures will mostly depend of the input data, their availabilities and the nature of the elements at risk. The subjectivity introduced in RHRS approaches is a major limit to compare the different risks while the quantitative character of QRA approaches favors inter-comparisons and cost-benefit analyses.

Given the potential of the latter approach, the aim of this study is (i) to propose a quantitative analysis that combines rockfall models with physical vulnerability curves to calculate risk, and (ii) to demonstrate the impacts of land-use and land-cover (LULC) changes on rockfall risk at the urban front of the village of Crolles.

2 STUDY SITE

The village of Crolles (45°17′09″N, 5°53′01″E) is located in the Grenoble conurbation on the southeastern slopes of the Chartreuse Massif (French Alps). Since the 1950s, land-use and land-cover on these concave talus slopes (250–600 m a.s.l.) have changed substantially in a way which can be considered typical for south-facing slopes in the French Prealps. Covered with vineyard since the mid-19th century, these slopes have experienced a rapid agropastoral decline during the interwar period, followed by intense afforestation.

The village of Crolles has constantly faced rockfall hazard as reflected in toponymy, since the Latin root of Crolles, *corrotulare*, means "to roll a block". Crolles site is dominated by a 300 m-high sub-vertical cliff made of thick-bedded limestones and marls from the upper Jurassic period. Archival records report numerous rockfall events since 1900 with rockfall fragments varying from clasts with edge lengths of only a few decimeters to blocks with volumes > 30 m^3. Fresh blocks, recent impact craters on the ground and visible growth disturbances (i.e. scars, decapitated trees) on the forest stand confirm ongoing intense rockfall activity during the last decades.

3 METHODOLOGY

The vast majority of risk studies consider only one or several specific scenarios that generally reproduce historical rockfall events. In this study, we developed a quantitative analysis of rockfall risk for the Crolles urban plan, by considering block volumes between 1 and 20 m^3 sorted in 19 equal volume classes. Thus, the total risk for a specific element at risk z is the summation of the risk corresponding to the different volume classes, as:

$$R_z = q(z_w) \times z_w \times \sum_{i=1}^{l} f\left(V_{CL_i}\right) \times p_z\left(V_{CL_i}\right) \times \overline{D}_z\left(V_{CL_i}\right)$$

[1]Université Grenoble Alpes, Irstea, UR ETNA, Grenoble, FR manon.farvacque@irstea.fr

[2]Université Grenoble Alpes, Irstea, UR EMGR, Grenoble, FR jerome.lopez@irstea.fr

[3]Centre National de la Recherche Scientifique CNRS, UMR 6042, GEOLAB, Clermont-Ferrand, FR christophe.corona@univ-bpclermont.fr

[4]Université Grenoble Alpes, Irstea, UR EMGR, Grenoble, FR franck.bourrier@irstea.fr

[5]Université Grenoble Alpes, Irstea, UR EMGR, Grenoble, FR david.toe@irstea.fr

[6]Université Grenoble Alpes, Irstea, UR ETNA, Grenoble, FR nicolas.eckert@irstea.fr

where R_z is the annual monetary risk-averaged of the element at risk z, which is characterized by a monetary value z_w and an exposure factor $q(z_w)$.

The frequency $f(V_{CLi})$ of each volume class is derived from a volume-frequency relationship constructed through an asymptotic model of the Generalized Pareto family (extreme value theory) and based on the survey of rockfall volumes in a representative slope section of Crolles site. The reach probabilities $p_z(V_{CLi})$ (see Figure 1) result from numerical propagations of rockfalls, performed using the simulation model Rockyfor3D (Dorren, 2015) and a Digital Elevation Model with 5 m resolution covering the whole Crolles village and the surrounding slopes. The mean structural damage $\overline{D}_z(V_{CLi})$ resulting from the impact on an element at risk z is characterized from the empirical assessment introduced by Agliardi et al. (2009).

The sum of individual risks R_z provides the total risk for the whole system of Crolles.

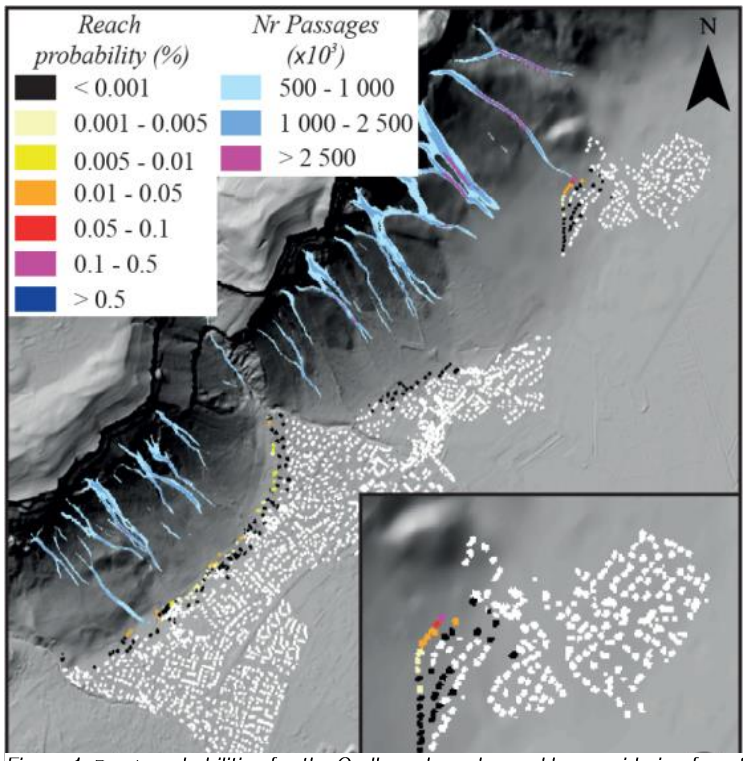

Figure 1: Reach probabilities for the Crolles urban plan and by considering forest cover landscape scenario.

4 RESULTS

The methodology for risk calculation, as shown above, has been applied through four land-use and land-cover patterns deduced from the diachronic landscape analysis performed in Lopez-Saez et al. (2016). Results clearly show the influence of LULC on risk results, and its reduction since afforestation process on talus slopes. For example, forest cover contributes to a 54% reduction of the risk value compared to a landscape covered with vineyard.

5 CONCLUSION

This study demonstrates the practicability of risk analysis in its quantitative form, and its potential for risk interpretations. The analysis through four landscape scenarios shows the importance to consider land-use and land-cover changes on risk values, and the protective function of a forest against rockfall. Finally, "case by case" risk study for a given configuration allows a better assessment of areas highly subjected to risk and thus an optimized planning of protection measures.

6 REFERENCES

Agliardi F., Crosta G.B., Frattini P. (2009). Integrating rockfall risk assessment and countermeasure design by 3D modelling techniques. Nat. Hazards Earth Syst. Sci., Volume 9, pp. 1059-1073.

Dorren, L. (2015). Rockyfor3d (v5.2) revealed - transparent description of the complete 3D rockfall model. Technical report, ecorisQ (www.ecorisq.org).

Lopez-Saez J., Corona C., Eckert N., Stoffel M., Bourrier F., Berger F. (2016). Impacts of land-use and land-cover changes on rockfall propagation: insights from the Grenoble conurbation. Science of the Total Environment, 547, 345-355.

Thermal conditions of an unstable permafrost-affected rock ridge below a refuge: the Cosmiques case (Mont Blanc massif)

Pierre-Allain DUVILLARD[1], Florence MAGNIN[2], Ludovic RAVANEL[3], Jean-Yves JOSNIN[4]

Keywords: rock ridge stability, mountain infrastructure, permafrost, temperature modelling, Mont Blanc massif

1 INTRODUCTION

The thermal state of steep permafrost rock faces is crucial to assess the safety and reliability of mountain infrastructures because permafrost degradation affects rock slope stability in high mountains. In the Mont Blanc massif, 23 infrastructures are built on rockwall permafrost with 13 of them characterized by a high risk of destabilization (Duvillard *et al.*, 2015).

So far, the main event happened below the Cosmiques refuge (3613 m a.s.l., Chamonix, France) on the 22st of August 1998. A 600 m^3 rockfall occurred in the SE face of the lower Cosmiques ridge and damaged the refuge that had to be closed for 8 months (Fig. A-B).

In order to better assess the role of permafrost in this destabilization and to gain insight on possible future geomorphic activity, we conducted studies based on three different methods : (1) a stability survey between 1998 and 2017, (2) a characterization of the current permafrost conditions with Electrical Tomography Resistivity (ERT) and rock surface temperature loggers, and (3) a thermal modelling of the rock wall permafrost degradation from 1998 to the end of the 21st century.

2 BACKGOUND

The lower Cosmiques ridge underwent an important rockfall activity on its SE face with 16 events (20 to 600 m^3) documented between 1998 and 2011 with direct observations and Terrestrial Laser Scanning surveys (Ravanel *et al*, 2013). The first important collapse occurred in August 1998, immediately below the refuge with destabilisation of the hut foundations (600 m^3; see above).

Since 2009, TLS surveys are conducted annually from the Midi pass (except in 2012 and 2013). 5 rockfall events happened directly under the hut foundations between 2011-2014 and 2015-2016 (1.24 to 2.7 m^3). It was probably mechanical readjustments of the 1998 rockfall, given their location into the scar.

3 THERMAL CONDITIONS

A first diagnosis of permafrost occurrence was made using two rock surface temperature loggers between 2011 and 2012 at 3, 30 and 55 cm in depth. To characterise the distribution of the permafrost, an ERT survey was carried out under the hut in October 2016 covering the steep NW and the SE rock faces (two surveys in Wenner 32 in both face and one in Wenner 64; Fig. A-C). Three rock surface temperature loggers were also installed at 10 cm depth in July 2016 in the SE and NW faces and directly under the refuge. The relationship between electrical resistivity of the granite tested in the laboratory (Magnin *et al.*, 2015b) has been used to adapt the colour scale of the ERT transect.

At this stage, we observed that SE face no longer allows the presence of permafrost conditions at the surface, although permafrost is still present at depth under the effect of the - still relatively - cold north face. The hut also induces a local cooling effect as indicated by the data from the sensors installed near the foundations.

4 TEMPERATURE MODELLINGS (1998, CURRENT STATE AND 2099)

The long-term evolution of permafrost on the Cosmiques ridge between LIA (Little Ice Age) to the end of 21st century was simulated following the approach from Magnin et al. (2017) used for simulations on three rock walls in the Mont-Blanc. The simulations uses air temperature time series, including two contrasted air temperature scenarios for the 21st century representing possible lower and upper boundaries of future climate change according to the most recent models and climate change scenarios. The 2-D finite element model accounts for heat conduction and latent heat transfers, and the outputs for the current period (2010-2017) are evaluated using borehole temperature measurements of the Aiguille du Midi, located very close to the Cosmiques refuge.

[1] DUVILLARD & Pierre-Allain, IMSRN, Montbonnot, France / EDYTEM Lab., Univ. Savoie - CNRS, Le Bourget-Du-Lac, France, pierre-allain.duvillard@univ-smb.fr

[2] MAGNIN& Florence, Department of Geosciences, University of Oslo, 0316 Oslo, Norway, florence.magnin@geo.uio.no

[3] RAVANEL & Ludovic, EDYTEM Lab., Univ. Savoie - CNRS, Le Bourget-Du-Lac, France, ludovic.ravanel@univ-smb.fr

[4] JOSNIN & Jean-Yves, EDYTEM Lab., Univ. Savoie - CNRS, Le Bourget-Du-Lac, France, jean-yves.josnin@univ-savoie.fr

The simulation showed that between 1998 and 2016, cold permafrost has disappeared in the north face and that the active layer has deepened in both faces (Fig. D). For simulating until 2099, we used a moderately optimistic scenario (IPCC RCP4.5) corresponding to air temperature increase of +3°C for the end of the 21st century, and suggesting that the permafrost will completely disappear in the ridge.

5 CONCLUSION

Constructing, operating and maintaining infrastructure in mountain permafrost terrain is an engineering challenge in the present context of temperature rise. The present study of the Cosmiques refuge with multi methods and analysis (geomorphologic characterization, thermal condition and temperature modelling) is a good example of how to support the assessment of permafrost thermal state and the possible damages of infrastructures in high mountain in the context of the ongoing climate change.

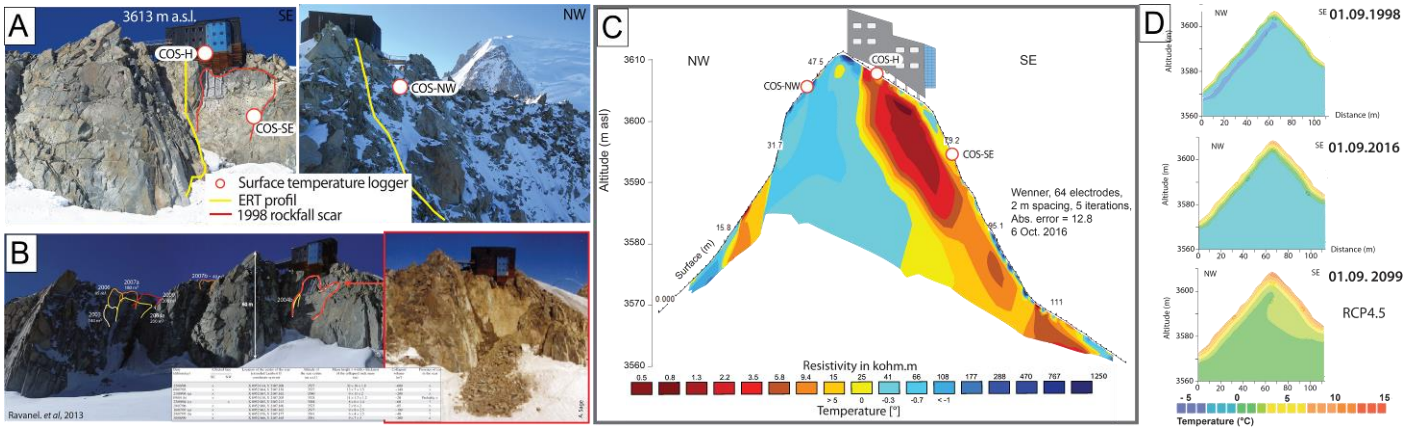

Figure: Cosmiques refuge site (Mont Blanc massif) and methods used.

6 ACKNOWLEDGEMENTS.

Pierre-Allain Duvillard's PhD fellowship was supported by a grant from Ingénierie des Mouvements du Sol et des Risques Naturels (IMSRN) and the Association Nationale de la Recherche et de la Technologie (ANRt).We also thank E. Malet, M. Marcer, C. Mörtl, J. Mourey and G. Guillet for their help with equipment installation and data acquisition. This work was supported by the EU ALCOTRA *PrévRisk Haute Montagne* project.

7 REFERENCES

Duvillard, P.-A., Ravanel, L., and Deline, P. (2015). Risk assessment of infrastructure destabilisation due to global warming in the high French Alps. J. Alp. Res. doi:10.4000/rga.2896.

Magnin, F., Brenning, A., Bodin, X., Deline, P., and Ravanel, L. (2015a). Statistical modelling of rock wall permafrost distribution: application to the Mont Blanc massif, Geomorphologie, 21, 145–162, doi:10.4000/geomorphologie.10965.

Magnin, F., Krautblatter, M., Deline, P., Ravanel, L., Malet, E., and Bevington, A. (2015b). Determination of warm, sensitive permafrost areas in near-vertical rockwalls and evaluation of distributed models by electrical resistivity tomography. J. Geophys. Res. Earth Surf. 120, 745–762. doi:10.1002/2014JF003351.

Magnin, F., Josnin, J.-Y., Ravanel, L., Pergaud, J., Pohl, B., and Deline, P. (2017). Modelling rock wall permafrost degradation in the Mont Blanc massif from the LIA to the end of the 21st century. The Cryosphere, 1813–1834. doi:10.5194/tc-11-1813-2017.

Ravanel, L., Deline, P., Lambiel, C., and Vincent, C. (2013). Instability of a high alpine rock ridge: the lower arête des cosmiques, mont blanc massif, france. Geogr. Ann. Ser. Phys. Geogr. 95, 51–66. doi:10.1111/geoa.12000.

On the role of forest in rockfall hazards mitigation – A perspective from the numerical modelling of non-spherical rock-tree interaction using non-smooth mechanics

Guang LU[1], Andrin CAVIEZEL[1], Marc CHRISTEN[1], Yves BÜHLER[1], **Perry BARTELT (corresponding author)**[1]

Keywords: natural hazards, rockfall dynamics, forest, non-spherical, numerical modelling, non-smooth mechanics

Rockfall hazard has increasingly become a major natural threat to human lives and public facilities in the mountainous regions. A fundamental understanding of rockfall dynamics, e.g. modes of rock motion and run-out zones, plays a key role in the prevention of potential damages (Crosta et al., 2015; Volkwein et al., 2011). To this end, WSL Institute for Snow and Avalanche Research SLF in Switzerland has developed a rockfall simulation software using non-smooth mechanics modelling method, aiming to accurately reproduce and predict falling rock trajectories (Leine et al., 2014). The numerical modelling of rockfall processes has exhibited some unique advantages over experimental investigations as the dynamics of the rock are readily obtained on different kinematic levels. This work extends the existing software module to the simulation of rock-tree interactions, and particularly investigates the role of forest in rockfall hazards mitigation. Here one of the major interests is how rock-tree interactions lead to a reduced speed, jump height and run-out for the rock (Toe et al., 2017a, 2017b).

1 MATHEMATICAL FOUNDATION FOR THE ROCK-TREE CONTACT MODEL

The first part of the presentation introduces the mathematical foundation for the rock-tree contact model. The rock is represented as a three-dimensional, convex, polyhedral rigid-body, with its boundary being constructed via finding the convex hull of a given point cloud. The tree geometry is simplified as a truncated cone (Figure 1), with the mechanical parameters e.g. tree's position, height, diameter, friction coefficient, restitution coefficient, and energy threshold being input by user. We employ non-smooth mechanics coupled with hard contact laws to model rock-tree and rock-terrain impacts. The equation of rock motion can be written as:

$$M\mathrm{d}u - h(q, u, t) = W(q)\lambda \qquad (1)$$

where M is a diagonal matrix containing the rock mass m and the moment of inertia θ, $\mathrm{d}u$ is the variation of the rock's translational velocity v and rotational velocity Ω within a given time step $\mathrm{d}t$, and $h(q, u, t)$ is the external forcing terms composed of gravitational force F_g, damping force F_d, and gyroscopic force $-\Omega \times \theta\Omega$. $W(q)$ is the matrix of generalized force directions, which transmits the forces λ (a vector which contains rock-ground impact/contact forces λ_{ground} and/or rock-tree impact/contact forces λ_{tree}) applied on the boundary of a rock to its centre of mass. Note that in the framework of our hard contact model equation (1) needs to be solved iteratively using time-stepping schemes. One major advantage of this model compared to the existing discrete element model (Lu et al., 2015) is that the former does not require using many mechanical parameters to calculate rock-ground/tree contact forces. Therefore, some potential difficulties can be precluded regarding system calibration and extraction of the leading parameters that govern rock dynamics after impacts. To detect the contact between rock and tree, the well-known Separating Axis Test (SAT) model (Gottschalk et al., 1996) is tailored considering the specific tree geometry.

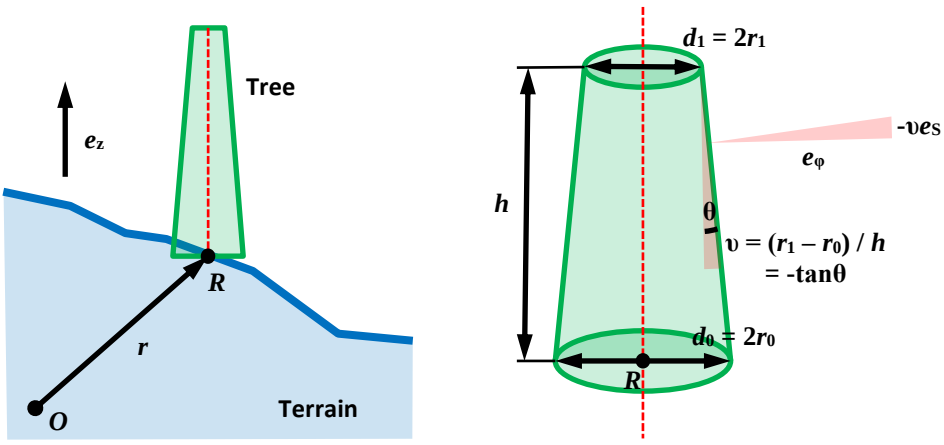

Figure 1: Geometrical modelling of a tree (along the direction e_z) as a truncated cone. The main parameters controlling the shape of a tree are: height h, bottom circle diameter d_0 and top circle diameter d_1. The tree can be also represented in the coordinate frame spanned by e_φ and e_S.

[1] LU Guang, CAVIEZEL Andrin, CHRISTEN Marc, BÜHLER Yves, **BARTELT Perry**, WSL Institute for Snow and Avalanche Research SLF, Davos Dorf, Switzerland (ISO 3166-2:CH), **bartelt@slf.ch**

2 SIMULATION OF ROCK-TREE AND ROCK-FOREST INTERACTIONS

The second part of the presentation studies rock-tree and rock-forest interactions. It is crucial to understand how the kinetic energy of rock can be dissipated when it collides with tree stands. Firstly, we perform impact tests between a non-spherical rock (e.g. EOTA-shaped, flattened, and elongated) and a single tree. Initially, a translational and a rotational velocity are provided to the rock, allowing it to collide with the tree trunk at random positons with random impact orientations. The mechanical parameters of the rock and the tree are varied identifying the leading factors governing a rock-tree interacting process. Secondly, we perform rockfall simulations letting the above simulated rocks pass through a 'virtual' forest, with the trees being randomly generated on an inclined plane (Figure 2). The role of forest in rockfall hazards mitigation is highlighted by comparing the run-out distances measured for the rock under the condition with/without forest. On one hand, this aids us to verify the function of the leading factors that we have found in governing a rock's kinetic energy dissipation after impacting with a tree. On the other hand, the influence of rock shape on the hazard reduction function of the forest can be quantified. Finally, the information of trees measured in Surava, Switzerland is employed to simulate a real rockfall event in forest, and the numerically obtained deposition points of the EOTA-shaped rock is compared with those acquired from experimental measurements. This demonstrates the effectiveness of the non-smooth approach to capture rock-forest interactions.

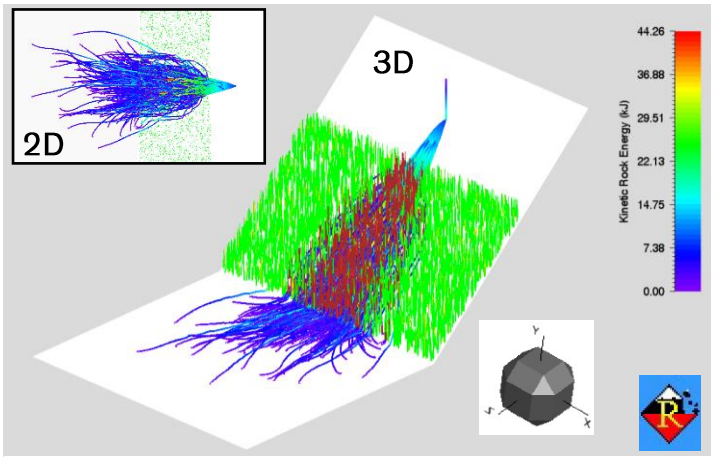

Figure 2: Simulation of an Eota-shaped rock falling along an inclined plane (40°) and passing through a forest (3451 trees). In total 500 simulations are performed with initially random rock orientations. The trees are modelled as truncated cones and are distributed randomly on the inclined ground. Trees that are collided by the rock are highlighted in red.

3 CONCLUSION

A rock-tree contact model has been implemented using non-smooth mechanics coupled with hard contact laws, allowing us to study rock-forest interactions. The simulation software developed in this work provides a powerful solution to daily geo-technical applications, where engineers need a tool in natural hazards assessment e.g. rockfall mitigation or adaptation. In the next development step, an obstacle-interaction module will be realized, enriching the applications in which the safety of protective measures (dams, barriers) need to be evaluated against potential rockfalls.

4 REFERENCES

Crosta, G.B., Agliardi, F., Frattini, P. & Lari, S. (2015) Key issues in rock fall modelling, hazard and risk assessment for rockfall protection. In G. Lollino et al. (eds), Engineering Geology for Society and Territory – Volume 2: 43-58. Cham: Springer.

Gottschalk, S., Lin, M.C. & Manocha, D. (1996) OBBTree: a hierarchical structure for rapid interference detection. Proceedings of the 23rd annual conference on computer graphics and interactive techniques. ACM New York, NY, USA.

Leine, R.I., Schweizer, A., Christen, M., Glover, J., Bartelt, P. & Gerber, W. (2014) Simulation of rockfall trajectories with consideration of rock shape. Multibody System Dynamics 32: 241-271.

Lu, G., Third, J.R. & Müller, C.R. (2015) Discrete element models for non-spherical particle systems: From theoretical developments to applications. Chemical Engineering Science 127: 425-465.

Toe, D., Bourrier, F., Olmedo, I., Monnet, J.-M. & Berger, F. (2017a) Analysis of the effect of trees on block propagation using a DEM model: implications for rockfall modelling. Landslides 14: 1603-1614.

Toe, D., Bourrier, F., Dorren, L. & Berger, F. (2017b) A novel DEM approach to simulate block propagation on forested slopes. Rock Mechanics and Rock Engineering https://doi.org/10.1007/s00603-017-1348-2.

Volkwein, A., Schellenberg, K., Labiouse, V., Agliardi, F., Berger, F., Bourrier, F., Dorren, L.K.A., Gerber, W. & Jaboyedoff, M. (2011) Rockfall characterisation and structural protection – a review. Natural Hazards and Earth System Sciences 11: 2617-2651.

Flexible rockfall mitigation design for varying site conditions

Laura Coiffe (corresponding author)[1], Mallory Jones & William Kane (others)[2]

Keywords: Rockfall hazards, scaling, stain-steel wire mesh

1 ROCKFALL MITIGATION AND SLOPE STABILIZATION SYSTEMS

1.1 INTRODUCTION

As populations increase, development in areas susceptible to geohazards increases. In addition to the construction of homes, highways have been widened exposing travellers to the risk of rockfall. Because the highway danger zones can cover significant distances, flexibility and variation in the treatment of rockfall hazards is necessary.

1.2 ROCKFALL MITIGATION IN THE UNITED STATES

Geobrugg Protection Systems began as part of a wire-rope manufacturing firm, Fatzer A.G., of Romanshorn, Switzerland. Early on, Brugg, as it was called then, began fabricating nets made from wire rope to use as snow nets for avalanche protection in the Swiss Alps. During spring net maintenance, the nets were often full of rock from rockfall events. As a result, Brugg began to manufacture barriers made of wire rope nets exclusively for rockfall protection.

Unlike the French and European experiences (Villard and McHugh, 2013), rockfall protection in the United States is a young engineering practice. In 1989, Brugg opened its first North American factory in Santa Fe, New Mexico to manufacture wire rope net rockfall barriers. In the early 1990s, the California Department of Transportation began using the rockfall barriers with a high degree of success. Since then rockfall barriers have been commonly used on American highways in mountainous areas.

Subsequent technical advances led to the development of high strength steel wire. This wire was used in rings as a replacement for the wire rope nets in the barriers. In addition, the wire also was fabricated into high strength chain link mesh. The mesh is used for rockfall draperies or tensioned slope stabilization systems. This material has proven to be easier to install and more durable than the hexagonal mesh product that has been used on slopes over the years.

2 U.S. HIGHWAY 11 ROCKFALL MITIGATION PROJECT

2.1 BACKGROUND

Perry County, Pennsylvania is the location of the longest stone masonry arch railroad viaduct in the world. To provide sandstone blocks needed for bridge construction, quarries were developed near by. A road was later constructed at the base of quarry highwalls in the 1930s. This later became U.S. Route 11, a heavily-travelled commuter highway.

At the time of highway construction, rockfall mitigation on the highly fractured, sandstone highwall was not considered. Soon after highway opening, rockfall hazards developed. As a result in 2014 the Pennsylvania Department of Transportation retained a local geotechnical engineering company to perform an initial site investigation, analyses, and preliminary rockfall mitigation design (GEO-Technical Services, Inc., 2014).

Project constraints required that all preliminary work had to be done without clearing the slopes, which were heavily vegetated (Pennsylvania Department of Transportation, 2015). This resulted in a preliminary design using large, massive rockfall barriers along the roadway.
However, following the project bid award, the contractor was required to retain a consultant engineer specializing in rockfall mitigation. The consultant engineer's responsibility was to finalize the preliminary mitigation design once the slope was cleared of the vegetation and loose rock was scaled. It was determined that the large, high rockfall barriers originally thought necessary were not needed. The consultant engineer determined that many of the rockfall barriers were unnecessary and could be

[1] COIFFE, Laura Y., KANE GeoTech, Inc., Stockton, California, US, laura.coiffe@kanegeotech.com
[2] JONES, Mallory A., KANE GeoTech, Inc. Stockton, California, US, mallory.jones@kanegeotech.com
KANE, William F., KANE GeoTech, Inc. Stockton, California, US, william.kane@kanegeotech.com

replaced with a combination of high-strength steel tensioned mesh and mesh draperies, Figure 1. Rock dowels were also utilized in the final design to create buttresses at the base of the slopes.

The consultant engineer was required to provide daily construction oversight. This assured conformance with the design and allowed design modifications, if necessary, to be made quickly and efficiently.

2.2 CONSTRUCTION

Due to the heavy traffic along U.S. Route 11, a maximum time of 50 days for complete highway closure was put in place. Some roadside work was able to be done utilizing traffic control prior to complete road closure. This enabled construction to be completed within the allowed time frame. A team of 20 contractor personnel worked 12 hours a day, six days a week to meet the deadline. The team was divided in two main crews working in each of two areas.

Figure 1: High-strength steel wire mesh can replace rockfall barriers with a smaller environmental and visual impact. It also requires less maintenance.

TaTable 1

Area Designation	Area Surface (m^2)
Area 1 Drape	17.550 m^2
Area 1 Spider Mesh	2.360 m^2
Area 3 Drape	2.680 m^2
Area 3 Spider Mesh	1.150 m^2

During construction, rockfall mitigation designs were modified to fit the actual field conditions. This required that rapid calculations and drawings be produced as not to delay the construction schedule. At this time, it was determined that the large rockfall barriers, originally assumed to be necessary, could be replaced with tensioned or draped high strength mesh systems. Clearing the slopes took approximately 11 days: 4 days to clear the vegetation and 7 days of scaling operation. Simultaneously, contractors started drilling anchors. The road was closed 23 days after work began. It took 58 days to complete the work. A total of 23,740-m^2 of high strength steel wire mesh was required, Table 1. Figure 1 shows the difference in the visual impact between the two mitigation methods.

3 CONCLUSION

Rockfall mitigation strategies have now become more sophisticated than in the early days of “one size fits all” rockfall barriers. New materials and engineering advances have provided more tools to solve problems especially when combined with properly staged investigations and proactive design-build strategies.

4 REFERENCES

GEO-Technical Services, Inc. (2014). U.S. Routes 11 and 15 Rock Slope Protection Project, Cumberland and Perry Counties, Pennsylvania. GTS #10032-2. November 26, 2014.

Pennsylvania Department of Transportation. (2015). Proposal Report 69796, District 08, County: Perry. December 17, 2015.

Villard, N. and McHugh, N. (2013). Rockfall protection systems – the French approach. Proceedings, 19th NZGS Geotechnical Symposium, Ed. C. Y. Chin, Queenstown.

Quantification of 3D displacements for landslides by photogrammetry and image correlation

Jean-Paul DURANTHON[1], Marie-Aurélie CHANUT[1], Johan KASPERSKI[2]

Keywords: landslides, photogrammetry, image correlation, point clouds, 3D displacements

Remote sensing technologies based on satellite images, radar or laser scan provide surface descriptions with a very fine precision (Abellan et al, 2010, Jaillet et al, 2011). Concerning landslides studies, it requires new tools to get a better analysis of the movements (Eltner et al, 2016, Stumpf et al, 2014). Simple tools such as distance between point clouds or sections are not good enough. Real displacements have to be known to better understand slope mechanisms. This is the main goal of the method we developed called Photogrammetry-based method for Landslide Study (PLaS method). In this article, we will present our innovative method and show the results on two landslides studies as an example.

1 THE PHOTOGRAMMETRY-BASED METHOD FOR LANDSLIDE STUDY (PLAS METHOD)

The photogrammetry-based method for landslide study is based on the photogrammetric process used both to generate point clouds and calculate 3D displacements (Chanut et al, 2017). Point clouds of landslide surfaces are generated from terrestrial images, every campaign, by photogrammetry (Egels et al, 2001). Then, a correlation image process is developed to register point clouds in the same reference. 3D displacements of the surface are inferred by taking advantage of the properties of photogrammetry which allow deducing the 3D coordinates of the points from their image coordinates (Figure 1).

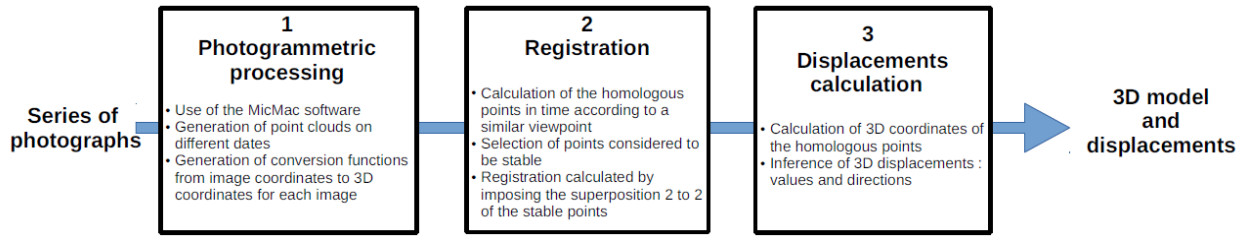

Figure 1: The three steps of the PLas Method

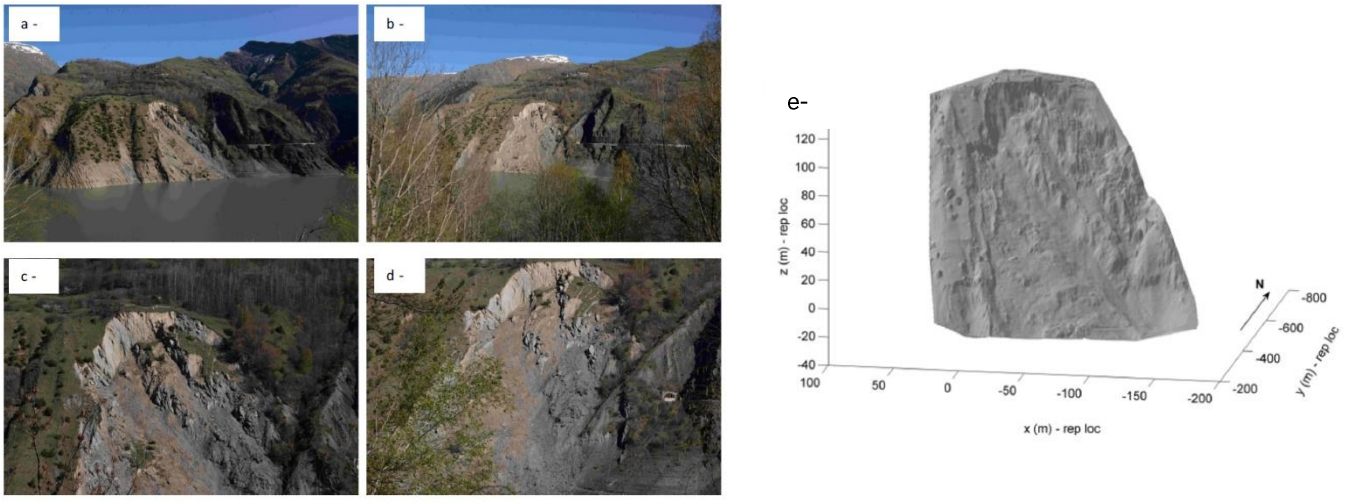

Figure 2: Campaign of 19/04/16– examples of images of the Chambon landslide taken from the opposite slope with a focal length of 28 mm (a and b) and 105 mm (c and d), shaded DTM modelling the surface (e).

[1] Cerema Centre-Est, 25 avenue François Mitterand, CS 92803, 69674 Bron Cedex, France, jean-paul.duranthon@cerema.fr,marie-aurelie.chanut@cerema.fr

[2] CETU, 25 avenue François Mitterand, 69674 Bron Cedex, France, johan.kasperki@developpement-durable.gouv.fr

2 APPLICATIONS ON TWO LANDSLIDES LOCATED IN THE ALPS: SECHILIENNE AND CHAMBON SITES

In this communication, we implement this approach to identify and monitor two landslides in the Alps along the departmental road RD 1091 (Séchilienne and Chambon landslides). The first step consists in using photographs taken on sites during several campaigns (Figure 2), carrying out the PLaS method and analyzing directions and values of displacements to identify moving areas and quantify 3D displacements (Figure 3). The second step consists in comparing calculation results with the different measures available for the two sites. It shows the possibility of this innovative method to identify the zones in motion with respect to the stable zones and to provide an order of magnitude of the 3D displacements and access a kinematics of the two moving slopes.

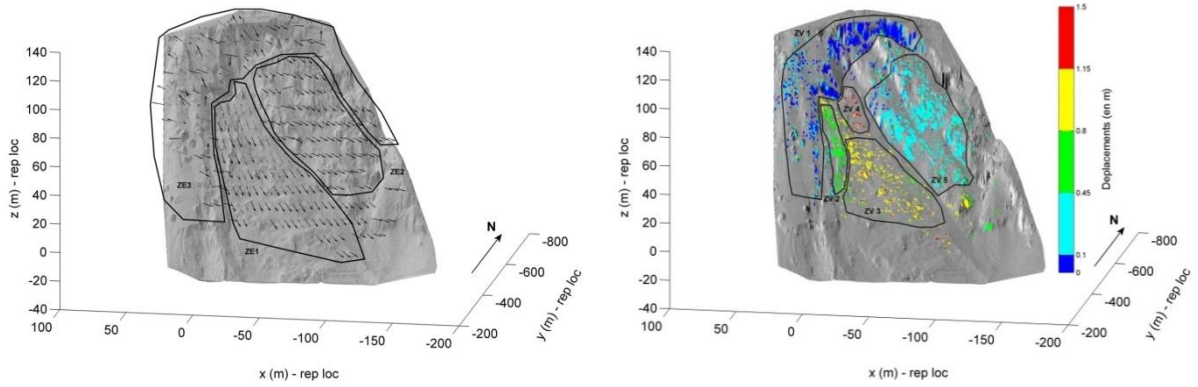

Figure 3: Chambon landslide: value (a) and normalized direction (b) of the displacements represented on the shaded DTM, the gray arrows indicate a direction of displacement under the surface of the DTM

3 CONCLUSION

The PLaS method to quantify displacements by photogrammetry not only allows identifying stable and unstable zones, but also provides values and directions of the 3D displacements. Comparisons have been done that confirm displacement inferred from the method with real measured values. Therefore, PLaS method makes it possible to access low-cost data over large areas at the scale of studied areas (stable or moving). This can be a first approach to the study of a site or can come in addition to a more localised instrumentation.

4 REFERENCES

Abellán A, Calvet J, Vilaplana JM, Blanchard J. (2010). Detection and spatial prediction of rockfalls by means of terrestrial laser scanner monitoring. *Geomorphology* 119: 162–171.

Chanut M.-A., Kasperski J., Dubois L., Dauphin S., Duranthon J.-P., (2017), Quantification des déplacements par la méthode PLaS – application au glissement du Chambon, *Revue Française de Geotechnique*.

Egels Y., Easser M., (2001). Photogrammétrie numérique. *Hermes Science publications*, 379 p.

Eltner A., Kaiser A., Castillo C., Rock G., Neugirg F., Abellán A., (2016), Image-based surface reconstruction in geomorphometry – merits, limits and developments, *Earth Surf. Dyn.*, 4, 359-389

Jaillet S, Ployon E, Villemin T. (2011). Images et modèles 3D en milieux naturels. *Collection Edytem*, n 12, 978–2–918435–04–4.

Stumpf A, Malet J-P, Allemand P, Ulrich P. (2014). Surface reconstruction and landslide displacement measurements with Pleiades satellite images. *ISPRS J Photogramm Remote Sens* 95:1–12.

Using a simplified model to assess the ability of a protection barrier to mitigate rockfall hazard

David TOE[1], Alessio MENTANI[2], Stéphane LAMBERT[3], Laura GOVONI[4], Guido GOTTARDI[5], Franck BOURRIER[6]

Keywords: rockfall mitigation, barrier, meta-model

1 INTRODUCTION

Various types of rockfall countermeasures can be used to intercept falling blocks such as barriers, nets and dams. There is a growing interest to fully consider the effect of these protection structures in rockfall trajectory simulation tools. Thus, there is a strong need for developing tools and methods that can integrate the protective effect of these structures in both rockfall trajectory simulations and risk assessment methods.

In practice, the design of a barrier for a given site is done by comparing a statistical descriptor of the block kinematic energy and the barrier reference capacity. The barrier reference capacity could be calculated following the European guideline (ETAG 027: Guideline for European Technical Approval of falling Rock Protection Kits (2013)). However this method does not account for the varaibility of the block kinematic parameters (translational velocity, rotational velocity, impact angle, impact position) which can lead to inefficient design. Quantifying the response of the barrier for different loading conditions requires complex and time consuming modelling approaches (Finite Element Method (FEM) or Discrete Element Method (DEM) which cannot be directly coupled with classical rockfall trajectory analysis models. To overcome this problem, meta-models, that mimic the behaviour of complex models for reduced computational effort, can be created.

This study is dedicated to the development and evaluation of a new approach dedicated to integrate realistic impact loading conditions into the design of barriers. A low-energy barrier, for which a FEM model is available, is considered. First, a meta-model is created based on the FEM model simulation results. Then, the meta-model is used to evaluate the efficacy of the barrier for two real rockfall scenarios. Finally, the advantages and limitations of the approach are discussed and compared with current practices in protection structure design.

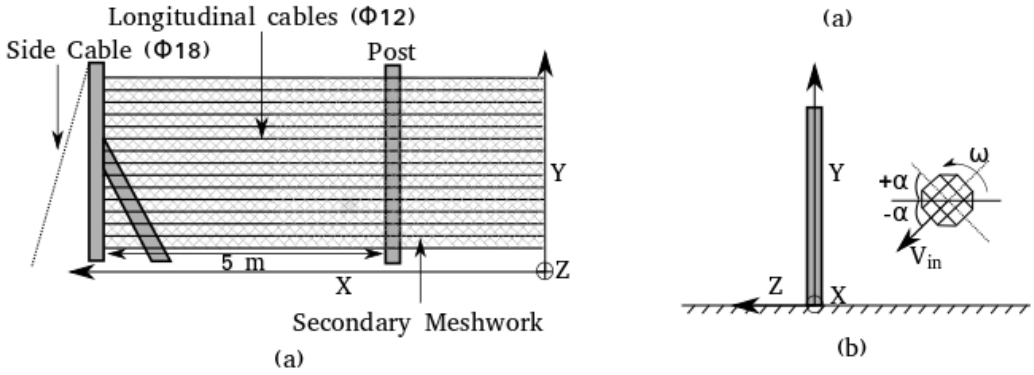

Fig. 2: Geometry and impact conditions for the cable-net protection barrier: a) back view and b) side view.

1 TOE David, Irstea, Saint-Martin-d'Hères, France, david.toe@irstea.fr
2 MENTANI Alessio, Università di Bologna, Bologna, Italy, alessio.mentani2@unibo.it
3 LAMBERT Stéphane, Irstea, Saint-Martin-d'Hères, France, stephane.lambert@irstea.fr
4 GOVONI Laura, Università di Bologna, Bologna, Italy, l.govoni@unibo.it
5 GOTTARDI Guido, Università di Bologna, Bologna, Italy, guido.gottardi2@unibo.it
6 BOURRIER Franck, Irstea, Saint-Martin-d'Hères, France, franck.bourrier@irstea.fr

2 BARRIER

The study addresses the response of a low-energy barrier widely spread in the Italian Alps. The barrier was model using the Finite Element (FE) method and calibrated using experimental results. The barrier is made of steel post fixed at its base, transverse cables evenly spaced and a hexagonal mesh-work (Fig. 1). Side cables connect the outer most post to the ground. The barrier is 3.2 m in height and has 15 evenly spaced longitudinal cables of 12 mm diameter. Side cables were 18 mm. Three spans are considered, with a 5m inter-posts spacing.

3 META-MODEL CREATION

Based on 280 simulations of the FE model, a meta-model which can predict the success or the failure of the barrier to stop the block is created using the Support Vector Machine (SVM) method. 6 input parameters related with the block trajectory are considered: the block translational velocity, the block rotational velocity, the block volume, the block impact position along the horizontal and vertical axes, the incidence impact angle.

4 PRACTICAL EVALUATION OF THE BARRIER EFFICIENCY

The ability of the barrier to mitigate rockfall hazard was evaluated for two scenarios following current practices and using the meta-modelling approach. The rockfall scenarios were selected to test the influence of the loading conditions on the barrier efficacy. For each scenario, the blocks reach the barrier with a maximum translational kinetic energy below the reference capacity of the barrier. 10 000 blocks were released for each scenario. In the numerical model, two measurement screens were defined at the location of the rockfall barriers in order to register the blocks kinematic parameters. The meta-model was then used considering these records to evaluate the barrier efficacy.

5 CONCLUSION

This study was dedicated to assess the effectiveness of a cable net barrier through the development and the application of a meta-model.

The results of 280 FE simulations showed that the barrier efficacy is not only controlled by the block volume and its translational velocity but also by other parameters related with the block trajectory. As a consequence, quantifying the barrier efficacy without accounting for their influence may lead to unconservative design.
A meta-model which is able to predict the ability of the barrier to arrest the block has been developed based on the results of the 280 FE. The meta-model hasbeen shown to provide an accurate prediction of the barrier response. In particular, the unconservative error associated to the ability in arresting the block is less than 5 %, compared with 40 % following a classical design approach.
The meta-model was then coupled to a rockfall trajectory simulations tool to estimate the barrier effectiveness for two rockfall scenarios. This coupling approach allows accounting for the real distributions of the various parameters describing the possible block trajectories. It was shown that, depending on the scenarios studied, the barrier effectiveness can be highly overestimated by using only the reference capacity of the barrier instead using the meta-model.

One perspective would be to use the meta-model developed to help in the optimization of the design of rockfall barriers, allowing for the identification of detrimental mechanisms leading to structure failure. In this case, parameters related to the design of the **structures may be considered, such as the position and initial tension of the cables, post spacing, position of energy dissipating device.**

The tree, an indicator of rock landslide hazards owing to dendro-geomorphology

Rémy MARTIN (ONF-RTM)[1], Frédéric BERGER (Irstea)[2]

Keywords: rock landslide, emergency, dendro-geomorphology

Since 1995, a landslide, named « La Ravine », on the territory of the municipality of Taninges (Haute Savoie, France), regularly disrupts the traffic on the departmental road : RD n°328. Several mudslides and rock falls, some of which have reached one thousand cubic meters, have led to the closing of the road. (see figure 1)

In 2016, Geolithe (engineering office), in charge of the survey of the site and of the design of a protection solution for the "Conseil Départemental de la Haute-Savoie – CD74" (manager of the departmental roads), discovered the signs of a large landslide in the slopes directly above the site "La Ravine". This landslide affects the rock substratum and includes the site where the protection works are planned.

The CD74 commissioned the ONF-RTM to specify the potential impact of this discovery on the protection project, and to assess the emergency situation. To complete the geological and geomorphological approaches, the IRSTEA was asked for a dendro-geomorphology study. This technique uses the tree as a bio-indicator of the past activity of natural hazards through the study of the tree's growth rings. The disturbances which can impact on the tree, like rock falls, avalanche or ground movements, above a certain threshold, can cause changes in the radial tree growth.

On a sample of trees chosen within the limit of the landslide, 72 cases of disturbances were found and dated. They enabled to distinguish six phases of active movements on the slopes: 1894, 1914, 1972, 1999, 2010 and 2016. They also showed that the active areas had not always been the same.

The information collected by the dendro-geomorphology study, helped to understand the mechanisms of the landslides, and put into perspective the emergency of the situation.

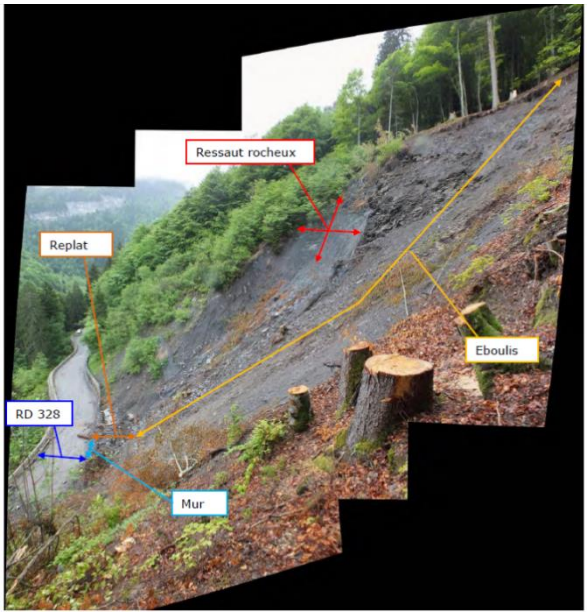

Figure 1: Active area of the "Ravine" landslide (source: Geolithe)

[1] ONF-RTM : Office national des Forêts – service de restauration des terrains en Montagne, remy.martin-02@onf.fr

[2] Irstea : Institut national de recherche en sciences et technologies pour l'environnement et l'agriculture, Frederic.berger@irstea.fr

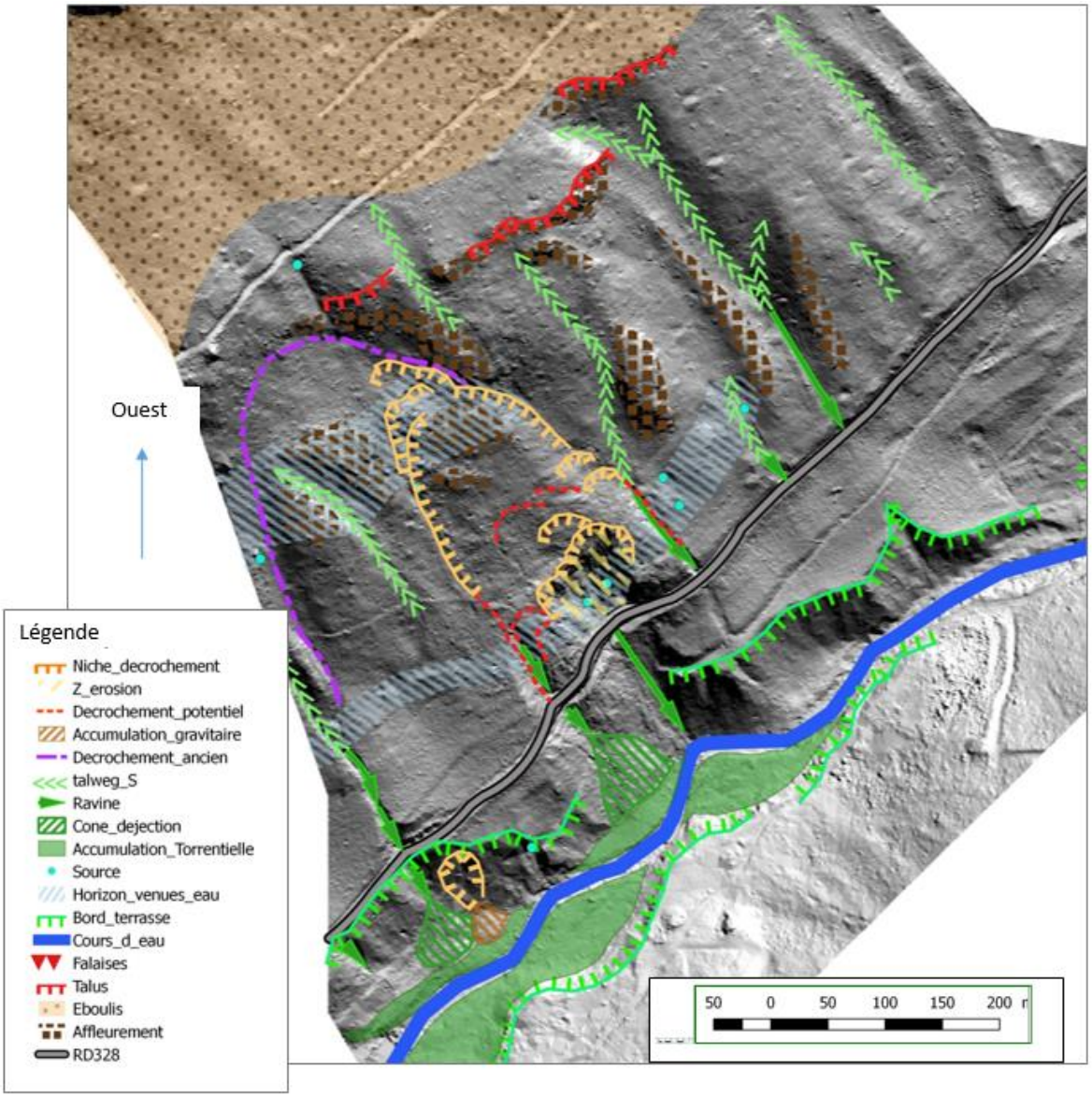

Carte géomorphologique sur fond lidar

Protection against the rockfall hazards in the area of the former quarry Carriere de Michelau, Luxembourg

Christian SPANG[1], Berit SYHRE[2], Ger EENENS[3]

Keywords: Rockfall hazards, stone-impact protection, rock bolts, high-tensile rockfall protection mesh

1 ABSTRACT

On the RN 27 between Michelau and Erpeldange in the Diekirch district in Luxembourg, in the years 1997 and 2005, rockfalls occurred in a former quarry located north of the national road N27 in an order of approximately 5.000 m³ and 1.000 m³, respectively. Since the event of the 7th July 1997, the underlying part of the road has been completely closed and relocated to the other side of the river "La sure" via two pre-fabricated Bailey bridges. The quarry pit is delimited by a steep rock slope in the middle and two areas with up to 17 m thick scree heaps to the sides of it. The steep quarry face is up to 104 m high and has a slope dip of approx. 70° to 90° partly overhanging due to lack of abutment of up to 2 m thick layer packages. The pre-existing stone dam which was located on the sideroad could only protect against smaller stones or block strokes (see Figure 1). Based on the geotechnical assessment and the preliminary planning of the Ministère du Développement durable et des Infrastructures des Ponts et Chaussées, Luxembourg, a study was carried out to prepare the preferred protection measures.

Figure 1: Overview of the former quarry Carriere de Michelau

The planned measures included stone-impact protection fences as well as an upscaling of the existing stone dam which was additionally secured with a high-tensile rockfall protection mesh (see Figure 2). The planning adapted to the numerous necessary points, such as the tight time constraints for construction and the consideration of the concerns of nature conservation. The former quarry is a cliff of the Sûre valley and is located in the Natura 2000 area "Vallées de la Sûre, de la Wiltz, de la Clerve et du Lellgerbaach". The stone-impact protection software of Dr. Spang GmbH ROCKFALL V 7.1 was used for the analysis of the stone impact protection fences. This software can be used to simulate physically exact rockfall paths. The input parameters for the simulation are, the profile of the terrain morphology, surface parameters, the dimension of the decisive stone, as well as the highest possible tripping zone. The resulting impact energies and bounce heights were then used to design and locate the protection fences (two RXI-500 and one GBE-100A-R, both systems of Geobrugg AG). Necessary criteria for

[1] SPANG Christian, Dr. Spang GmbH, Witten, Germany (DE), zentrale@dr-spang.de

[2] SYHRE Berit, Dr. Spang GmbH, Witten, Germany (DE), zentrale@dr-spang.de[3] EENENS Ger, GEO Hazards BV., Horn, The Netherlands (NL), info@geohazards.eu

choosing the right the location are in addition to the distance to road N 27, taking into account the deflection of the protective fences in case of an event, the most economical design, i.e. the lowest possible energy class and structure height as well as the feasibility and the safety of the construction. The simulations resulted impact energy levels of 5,000 kJ and building heights of 5,5 m and 7 m respectively. The RXI-500 fences had to be anchored with up to 20,5 m long rock bolts and up to 25 m long spiral rope anchors in the up to 17 m mighty scree heap. In addition to the rockfall simulations with ROCKFALL V 7.1, the GGU-STABILITY software was used to design the upscaled stone wall. The anchors used to fasten the high-tensile steel wire mesh system TECCO G65/3 from Geobrugg AG were considered to be the reinforcement of the dam. Additionally to the GGU design analysis, a proof with the RUVOLUM Software of Geobrugg AG, Romanshorn, Switzerland was carried out.

Figure 2: Overview of the measures against the rockfall hazards at the former quarry Carriere de Michelau

During the construction phase an acoustic hazard warning system was installed to prevent accidents and to secure the construction site. The Rock wall monitoring system (self-contained CR800 data logger with GPRS modem by GEO Hazards BV., Horn, The Netherlands) served to alert persons to clear the danger zone in case of an rockfall event.

Effect of dynamics on the Soil-geosynthetic interfaces used in reinforced rockfall embankments

Ismail BENESSALAH[1], Stéphane LAMBERT[2], Pascal VILLARD[3], Ahmed ARAB[4]

Keywords: Numerical modelling, discrete elements method, rockfall embankment, pull-out test

Among the various passive protection structures, embankments reinforced with horizontal inclusions are one of those capable of containing the blocks with the highest kinetic energies, e.g. exceeding 5000 kJ (Descoeudres, 1997). The design of such structures requires consideration of parameters related to the soil-geosynthetic interfaces during the impact by the block on the embankment. In spite of recent technological developments, the response of soil-geosynthetic interfaces under dynamic loading of impact type remains largely unknown. This issue is tentatively addressed using a numerical study of the dynamic pull-out behaviour of a geotextile sheet embedded into soil, as in rockfall protection embankments.

1 NUMERICAL MODELS

A 3D coupling DEM-FEM code (Villard et al., 2009) was used to determine the relationship between the extraction force and displacements at the soil/geotextile interface during a pull-out test considering application to protection barriers. Thin triangular finite elements were used to describe the mechanical behaviour of the geosynthetic sheet while clumps of spheres were used to restore the soil behaviour. Specific interaction laws are used at the interface between the soil particles and the triangular finite elements. For comparison with analytical solution formulated under static conditions, the numerical tool was first tested considering low extraction velocity.

The analytical approach of the extraction behaviour of geotextile layer anchored in soil is established assuming that the normal stress acting on the sheet remains constant during the test (stress related to the thickness of soil above the geotextile sheet) and that the movements of the soil are negligible compared to the movements of the sheet. The extensibility of the sheet is taken into consideration as well as the friction forces on the two interfaces of the sheet.

The shear stress that can be mobilized by friction on both lower and upper interfaces is defined using classical friction law as shown in Fig. 1a. The displacement at each point x of the sheet is obtained by summation of each segment of length Δx included between the rear of the sheet and the position x.

2 GEOMETRY OF THE EXPERIMENTAL DEVISE

The dimensions of the numerical model are similar to those of an experimental pull-out device (Jenck et al., 2014) shown on Fig 1b, namely a test tank of 1.00 m in length, 0.50 m in width and 0.80 m in height. Rigid rubbing walls were used at the base of the model and on its periphery to simulate the internal walls of the tank which are made of steel. The numerical soil samples consist of 45 000 clusters of two imbricated spheres of diameter D and maximum length 1.2 D. The micromechanical characteristics of the numerical soil are defined experimentally in order to mimic the behaviour of an average dense sand with a 33.75° friction angle. The bulk density of the soil is 13.4kN/m^3. The geosynthetic sheet consists of a set of 288 triangles with three nodes. The geosynthetic sheet was positioned at 0.25 m from the bottom of the tank (Fig 1b).

3 RESULTS

First, low extraction velocity was used considering different values of the interface friction angle. In terms of the pull-out force as a function of the head displacement (Fig 2a), a good fit is observed between the numerical model and the analytical approach including the extraction force peak value (Soil/Gtx = 31.8°). The observed differences are attributed to simplifying assumptions made in the analytical model. In particular a perfectly plastic behaviour of the soil is considered in the analytical model while the numerical model takes into account a slightly softening behaviour of the soil. Moreover, it can be deduced from Fig 1c that the vertical stresses acting on the geotextile increases during the pull-out test, particularly in the rear part. Fig 2a and 2b compares the results of the DEM simulations in terms of pull-out force and rear displacement of the geotextile sheet versus the head displacement of the sheet. The influence of the soil-geotextile friction angle is noticeable on the value of the

[1] BENESSALAH Ismail, Univ. UHBC of Chlef, LsmE Lab, 02091 Chlef, Algeria, i.benessalah@univ-chlef.dz

[2] LAMBERT Stéphane, Univ. Grenoble Alpes, Irstea - UR ETGR, Saint Martin d'Hères, France, stephane.lambert@irstea.fr

[3] VILLARD Pascal, Univ. Grenoble Alpes, CNRS, Grenoble INP, 3SR, Grenoble, France, pascal.villard@3sr-grenoble.fr

[4] ARAB Ahmed, Univ. UHBC of Chlef, LsmE Lab, 02091 Chlef, Algeria, ah_arab@yahoo.fr

maximal pull-out force but also onto the extraction mechanism (mobilization of the soil areas located on either side of the geosynthetic sheet and on the front wall).

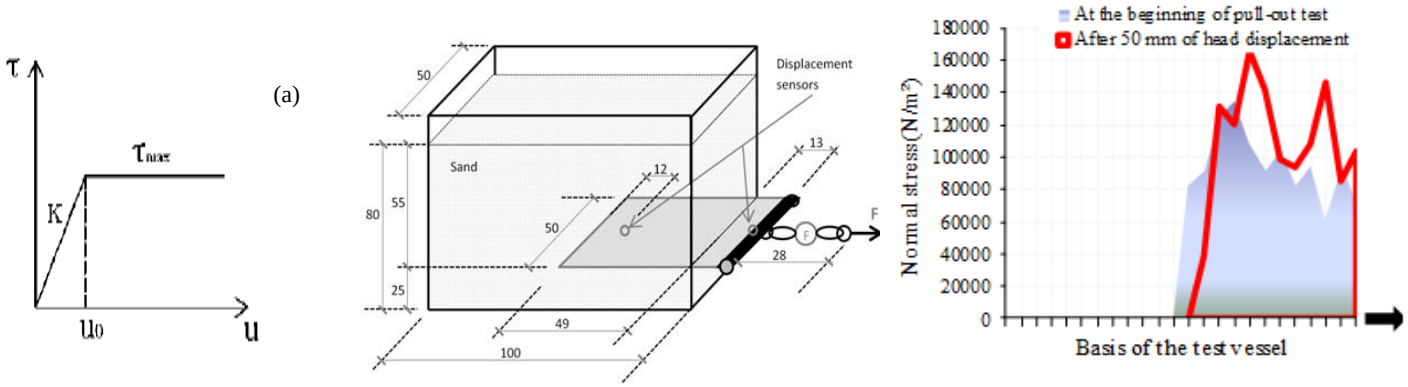

Figure 1: Constitutive law of soil/geotextile interface (a), Geometry of the pull-out tank (b), Normal stress on the geotextile sheet (c)

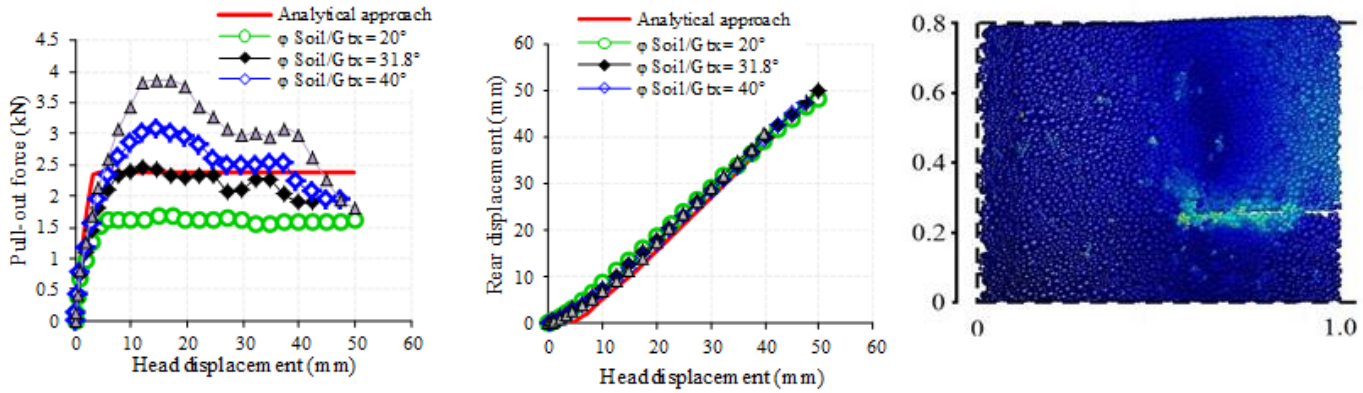

Figure 2: Pull-out force versus head displacement (a), Rear displacement versus head displacement (b), Movement of the soil particles during the pull-out test (c).

Fig 2c presents the evolution of the displacements of the soil particles during a pull-out test. It can be seen in this Figure that the displacements of soil particles are essentially concentrated around the geotextile sheet, in particular at the point where the sheet has been extracted. There is also a slight raising of the soil particles above the geotextile sheet, and in particular at the soil layer surface close to the wall, which is linked to the abutment effect. Introduction to high extraction velocity lead to an increase of the extraction forces that it is difficult to connect to experimental data due to the lack of results in this field.

4 CONCLUSION

A DEM model for simulating the pull-out behaviour a geotextile sheet embedded in soil has been developed and validated in quasi static condition. The influence of friction between the geotextile sheet and the soil particles has been addressed, providing strong conclusions to highlight the influence of each parameter and to determine those that have a major influence on the extraction force. The modelling of dynamic tests, considering high extraction rates, can easily be achieved but the experimental data that can support this work are currently lacking. On the face of it, we can nevertheless think that the numerical model can be validated on dynamic experimental tests and that it will lead to a more realistic dimensioning of the soil/reinforcement interaction.

5 REFERENCES

Descoeudres F., (1997) Aspects géomécaniques des instabilités de falaises rocheuses et des chutes de blocs. *Publication de la société Suisse de mécanique des sols et des roches*, vol 135, pp 3-11, 1997.

Jenck O., Lambert S., Aprialdi D., (2014) Experimental characterization of the soil-geotextile interaction when subjected to a dynamic load of impact type, *10th International Conference on Geosynthetics (10ICG), Berlin,* 2014.

Villard P., Chevalier B., Le Hello B., Combe G., (2009) Coupling between finite and discrete element methods for the modelling of earth structures reinforced by Geosynthetic, *Computers and Geotechnics* 36 (2009) 709–717.

New rockfall protection barriers in Formentor (Mallorca)

Joan M RIUS[1], Raül AGUILÓ[2]

Keywords: rockfall, dynamic barriers, rockfall modelling

Tramuntana mountain range in Mallorca is a prone area to landslides and rockfall events. The main triggering factor is high intensity rainfall events. The specially wet winter of 2017 affected several areas all over Tramuntana with rockfall events of different magnitudes up to hundreds of cubic meters damaging roads and some of their facilities. The rockfall event of January 30th, 2017 affected an area where the Ma-2210 road in Formentor crosses a cliff and talus slope in a specially threatened area severely damaging the dynamic barriers installed. A new stability analysis with rockfall simulation and considering data from field investigations like fragmentation or impact energy of rock blocks was performed to update the protection systems (dynamic barriers) using new standards and design parameters. An emergency action was undertaken and by the end of April 2017 new dynamic barriers were installed.

1 THE FORMENTOR ROCKFALL IN MALLORCA

The main mountain range of Mallorca island, Tramuntana, located on the northwest side of the island has complex geological characteristics, composed of a set of superimposed folds of Jurassic and Cretaceous ages, sliding upon Triassic materials. The alternative presence of weak rocks (marls and claystones) and hard but fractured rocks (dolomites and limestones), in addition to its typical Mediterranean climate, make it a very prone area to landslides and rockfall events. The local authorities have carried out several actions to protect the roads and villages from a long time. Thus, different protective measures, like dynamic barriers and other structures have been implemented in recent years.

One of the most active areas is the Formentor peninsula, located in the northern part of Tramuntana. Its main road, Ma-2210, is systematically affected by rockfall events and, thus, some rockfall protection systems were installed more than 20 years ago. The specially wet winter of 2017 affected several areas all over Tramuntana with rockfall events of different magnitudes up to hundreds of cubic meters damaging roads and some of their facilities. The rockfall event of January 30th 2017 affected an area where the Ma-2210 road crosses a cliff and talus slope in a specially threatened area severely damaging the dynamic barriers installed (figure 1).

2 ANALYSIS OF ON-SITE FIELD INVESTIGATIONS

A new stability analysis with rockfall simulation was performed to update the protection systems using new standards and design parameters. A previous work with on-site investigation of rockfall event conditions like geological characteristics of detaching area, rock volumes mobilized, and fragmentation or impact energy of rock blocks was also carried out to determine actual dimension parameters to a new design of rockfall protection systems. Finally, an emergency executive project was developed to install new dynamic barriers.

Not much previous data of events that have taken place in this area are available. Several rockfall events occurred and in January 1994 an executive project was developed to install 3 m height dynamic barrier with low protection energy (150 kJ). In December 1995 a rockfall event overcome the installed barrier and impacted on the road. Several blocks had been retained during 2 years from installation. No additional action was undertaken. During more than 20 years a lot of blocks have been retained (maximum measured block volume of 0.8 m^3) until January 30th 2017 when a 12 m^3 volume rockfall event with several blocks and a maximum block volume of 3 m^3 occurred (figure 1).

Figure 1: Formentor rockfall of 30th January 2017

1 Rius, Joan M, Consell de Mallorca, Palma, Spain (ISO Code), jmrius@conselldemallorca.net
2 Aguiló, Raül, Consell de Mallorca, Palma, Spain (ISO Code), raguilo@conselldemallorca.net

Additional investigations were performed to acquire more information about the detaching mass conditions for a better understanding of rockfall process (Corominas, 2017). The whole detached mass of the event was about 14 m^3. From a structural analysis of discontinuities, it was shown that the mass was composed of at least two big blocks of about 7 and 5 m^3 and some other ones of less than 1 m^3 volumes. From the detected trajectory of blocks, it was also shown that a free height of only 12 m (from detachment area to first impact area) triggers a considerable block fragmentation of the involved mass. A rock fragmentation model applied and impact kinetic energy considerations leaded to the conclusion that rock fragmentation plays an important role in this cliff area. Also, it was concluded that most of future rockfall events that will take place from higher parts of the cliff will be affected by important block fragmentation. Unless the whole rockfall volume expected for a maximum design rockfall event is about 15 m^3, no blocks of more that 3 m^3 are expected. Therefore, two main different scenarios have been selected for dimensioning of protection systems purposes considering European standards of ETAG 027.

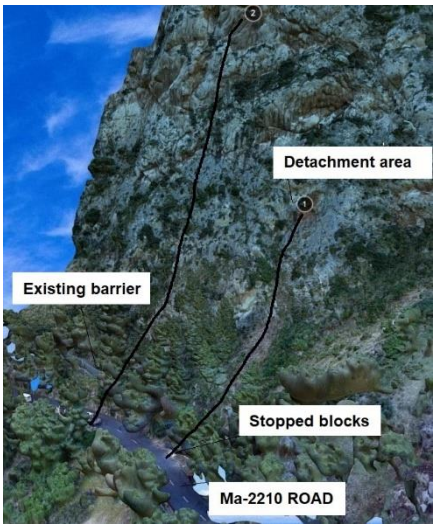

Figure 2: Cross sections scenarios analysed in image DEM

3 ROCKFALL PROTECTION SYSTEM MODELLING

The first scenario is a rockfall from the lower part of the cliff (10 to 20 m height) with a maximum rock volume of about 4-5 m^3 as dimensioning of Maximum Energy Level (MEL) with low occurrence probability. The second scenario, which is more likely to occur, is a rockfall from all over the cliff with a maximum volume of 1 m^3 as dimensioning of Service Energy Level (SEL). Different cross sections, extracted from the digital elevation model (DEM) (figure 2), have been modeled by means of 2D rockfall simulation program. The input parameter values have been selected and adapted from previous references of modelling approaches in Tramuntana range (Mateos et al, 2015). The worst ones in terms of velocities and rebound height of blocks that reach the road area (cross sections 1 and 2) have been selected for dimensioning purposes.

Dimension values from simulation program are shown in table 1. Statistical values have been obtained as considered in the Standard ONR24810 (2013). The final design of new rockfall protection system has been performed considering aspects as damage classification, selected CC2 (medium consequence for loss of human life or economic, social or environmental consequences considerable, secondary roads) or event frequency, selected EF2 (1event/year – 1event/30years). Corresponding safety factors (SF) were applied and final design parameters are shown in table 1. They were uniformed to a 4 m high barrier of 210 m long and protection energy of 3000 kJ (MEL).

Table 1: Dimension values from simulation and final design parameters

Scenario	Cross section	volume (m^3)	Calculated Energy (kJ)	Calculated Height (m)	Design energy (kJ)	Design Height (m)
MEL	1	4.7	2250	2.8	2362.5	3.08
MEL	2	0.5	1470	3	1543.5	3.3
SEL	1	0.8	445	2.5	467.25	2.75
SEL	2	0.18	515	3.2	540.75	3.63

4 CONCLUSION

An emergency action had to be undertaken after a rockfall event on January 30th, 2017 along the Formentor road in Tramuntana range in Mallorca, which severely damaged existing dynamic barriers. Previous analyses on rockfall event conditions including rock fragmentation, impact energy and detaching area characteristics were performed along with rockfall simulation. New dynamic barriers were executed updating their design to current European Standards.

5 REFERENCES

Corominas J. (2017) Rockfall occurrence and fragmentation. *4th World Landslide Forum (4WLF), 29 May- 2 June 2017.* Ljubljana (Slovenia).

Mateos, R.M; Garcia-Moreno, I; Reichenbach, P; Herera, G; Sarro, R; Rius, J; Aguiló, R; Fiorucci, F. (2015) Calibration and validation of rockfall modelling at regional scale: application along a roadway in Mallorca (Spain) and organization of its management. *Landslides. DOI 10.1007/s10346-015-0602-5.* Springer-Verlag Berlin Heidelberg (Germany).

Rayleigh waves in seismic signals of rockfalls

Clara LEVY[1], Agnès Helmstetter[2], David Amitrano[3], Gaëlle Le Roy[4], Fabrice Guyoton[5]

Keywords: rockfall impacts, Rayleigh waves, signal processing, S-transform

Seismic signals of rockfalls are usually very complex, as they are the result of superimposed arrivals of wave trains generated by successive impacts and have a low signal-to-noise ratio (SNR). Thus, retrieving information from these signals is usually challenging. Our objective was to apply the signal processing method proposed by Meza-Fajardo et al. (2015) in order to isolate Rayleigh waves from the rest of the signals. We expect to retrieve: 1) a simplified output signal as only Rayleigh waves trains are extracted, 2) the azimuth of incoming Rayleigh waves (e.g., information on the rockfall localisation), 3) an output signal with a better SNR than the original signal as the decrease of energy due to geometrical attenuation is proportional to 1/r (with r the distance of propagation) for Rayleigh waves, and is proportional to $1/r^2$ for body waves. Our work confirms the large presence of surface waves for this type of signals (a fact widely accepted in the literature, without ever being really discussed). Future studies will determine whether the use of Rayleigh waves (rather than the entire seismic signal) improves the localization of rockfalls, especially when using a method specific for surface waves (the Fast Marching Method).

1 IDENTIFICATION OF RAYLEIGH WAVES IN ROCKFALL SEISMIC SIGNALS

We used signals of 17 rockfalls recorded by four large band 3-components stations between 2013 and 2015 at the limestone cliff of St Eynard, France. The event volumes were deduced using photogrammetry and range from 1.2 m^3 to 1546 m^3. The distances stations-events range from 0.4 km to 2.9 km. The strong attenuation of the signal with distance, as well as the decrease of SNR with distance are illustrated by a 20m^3 rockfall signal in Figure 1 (left).

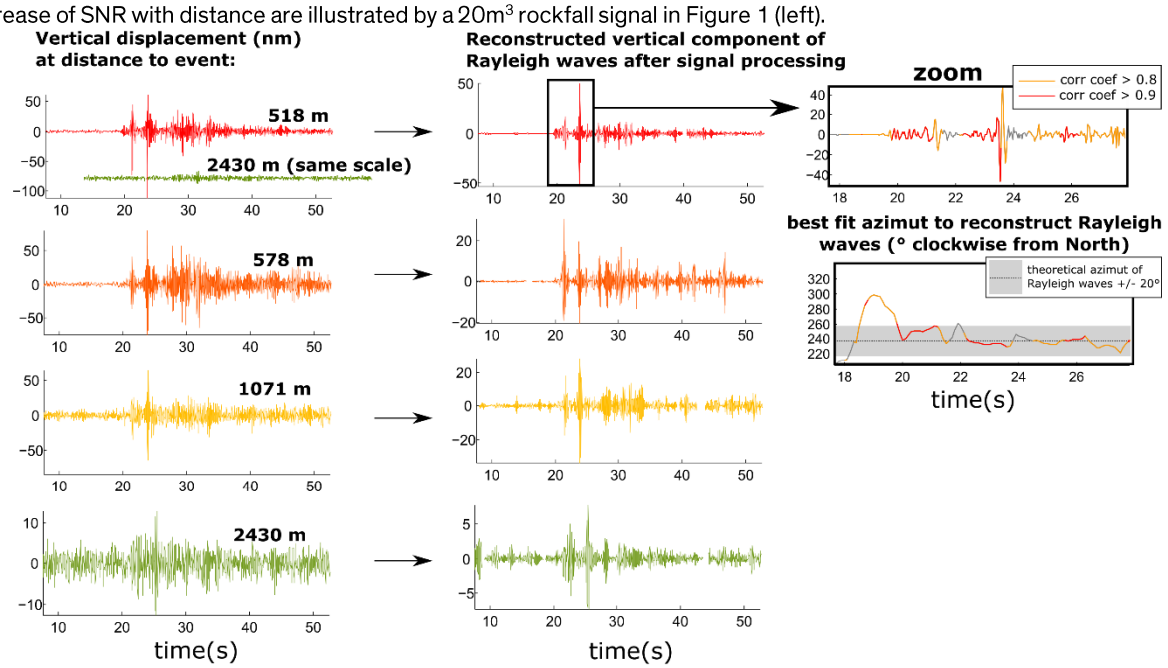

Figure 1: Seismic signals of a 20m3 rockfall at the limestone cliff of St Eynard (France), recorded by four large band stations at distances from 0.5 to 2.4 km (left). Signals are filtered between 2 and 15 Hz. The furthest is the station; the lowest is the Signal to Noise Ratio (SNR). Signal attenuation is evidenced by the representation of the most distant signal (green) on the same scale as the nearest signal (red). The Rayleigh waves of each signal were reconstructed using shifting windows (middle), showing an increase of the SNR. The zoom of the left plot shows the value of the quality criterion (corr coef) for the signal processing used to reconstruct Rayleigh waves: when this criterion is less than 0.8, we consider that we do not satisfactorily reconstruct Rayleigh waves (hence the presence of holes in the reconstructed signals). The bottom plot shows the best fit azimuth of the reconstructed Rayleigh waves which can be compared to the theoretical azimuth (dotted black line).

[1] LEVY Clara, BRGM, Orléans, France (FR), c.levy@brgm.fr

[2] Helmstetter Agnès, ISTerre, Grenoble, Orléans, France (FR), agnes.helmstetter@univ-grenoble-alpes.fr

[3] AMITRANO David, ISTerre, Grenoble, France (FR), david.amitrano@univ-grenoble-alpes.fr

[4] LE ROY Gaëlle, ISTerre et Géolithe, Grenoble, France (FR), gaelle.le-roy@univ-grenoble-alpes.fr

[5] GUYOTON Fabrice, Géolithe, Grenoble, France (FR), fabrice.guyoton@geolithe.com

We applied the signal processing method proposed by Meza-Fajardo et al. (2015) in order to isolate Rayleigh waves from the rest of the seismic signals. This method uses the time-frequency signal characteristics deduced from Stockwell transforms (ellipticity, etc.) to construct a time-frequency filter and was originally developed to analyse earthquake signals. Rayleigh waves were extracted using sliding windows of 1.5 s every 0.1 s for a filtered signal between 2 and 15 Hz. The obtained signals show, as expected, an increase of SNR and an overall simplification of the signal (Figure 1 middle).
The particle movement of Rayleigh waves is elliptical, e.g. the signal in the horizontal direction is similar to the signal in the vertical direction by a phase shift of 90°. Therefore, the quality of the filtering process can be verified by estimating the correlation coefficient between these two components. When this coefficient is less than 0.8, we consider that we do not reconstruct an elliptical wave, and therefore, that we do not satisfactorily reconstruct Rayleigh waves. As a result, the obtained signals can present holes (Figure 1 middle). Figure 1 (left) shows the evolution of this quality criterion with time for one signal, together with the best fit azimuth of the reconstructed Rayleigh waves. For this example, the best fit azimuth is more of less very close to the theoretical azimuth (Figure 1 left).

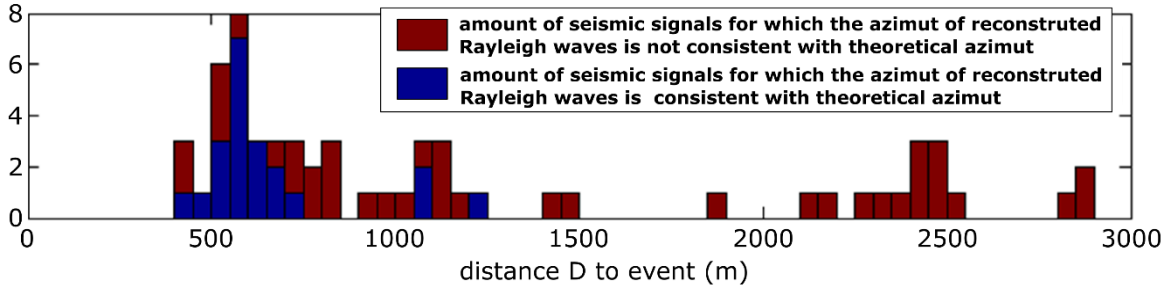

Figure 2: The best fit azimuth of the reconstructed Rayleigh waves was compared to the theoretical azimuth of Rayleigh waves for 17 rockfalls recorded by four large band stations at the limestone cliff of St Eynard, France. The event volumes range from 1.2 m3 to 1546 m3 and the distances stations-events range from 0.4 km to 2.9 km.

The best fit azimuth of the reconstructed Rayleigh waves (of the first 2 s of signal) were compared to the theoretical azimuth of Rayleigh waves for the 17 rockfalls (Figure 2). Results show that the best fit azimuth of Rayleigh waves is generally not consistent with the theoretical azimuth, except when: 1) the distance event-station is less than 800 m, 2) the reconstructed signal has a quality criterion greater than or equal to 0.9, 3) the station is located on top of sound rock rather than on scree. The origin of the differences between theoretical azimuth and estimated azimuth has not yet been investigated. At first sight, it seems reasonable to imagine that the wave path is complex for a cliff with scree. Site effects, whether due to topography (cliff) or geology (scree), are likely to influence the propagation azimuth of Rayleigh waves. The greater the distance to the seismic source, the more likely are these effects.

2 CONCLUSION

The presence of a majority of surface waves in rockfall seismic signals is widely accepted in the literature, without ever being really discussed. This work confirms the large presence of surface waves for this type of signals. For all signals we were able to extract, at least partially, Rayleigh waves (only retrograde waves were obtained). The retrieved signals are simplified (as only Rayleigh waves trains are extracted) and have a better SNR than the original signals. All in all, the proposed method has both advantages and inconvenient to improve the localization of rockfalls with seismic data. On one hand, 1) we obtain a simplified signal with a better SNR, 2) we obtain information on the source-station azimuth when the distance event-station is less than 800 m, 3) we focus the analysis on waves that propagate at slow speeds (a favourable situation to find perceptible arrival-time delays between stations). On the other hand, 1) the proposed method is expensive in computation time and 2) requires knowing *a priori* the position of the source relative to the station at an opening angle of 180 °. In addition, Rayleigh waves are dispersive waves, and it is therefore more difficult to identify the same wave train on different recordings. Further analysis of rockfall seismic signals will be performed using data of a controlled block release experiment that took place in a quarry of Authume (France) in October 2017 (see the paper of Le Roy et al. submitted at RSS 2018 for a description of the experiment).

3 ACKNOWLEDGEMENTS

This work was partially funded by the French National project C2ROP.

4 REFERENCES

Meza-Fajardo, K. C., Papageorgiou, A. S., & Semblat, J. F. (2015). Identification and Extraction of Surface Waves from Three-Component Seismograms Based on the Normalized Inner Product. *Bulletin of the Seismological Society of America*, 105(1), 210-229.

Sensitivity analysis of rockfall trajectory simulations to material properties

Clara LEVY[1], Jérémy ROHMER[2], Bastien COLAS[3], Anthony REY[4]

Keywords: rockfall trajectory simulations, sensitivity analysis, Kolmogorov smirnov, road

Many tools have been developed to manage rockfall risk. In particular, many softwares are designed to simulate rockfall trajectories. These softwares require the definition of many parameters, especially those describing the mechanical properties of soils (rigidity, roughness, etc.). Choosing appropriate values for these parameters remains a difficult task and will depend on the expert know-how. Here, we propose a simple method that can be used routinely to evaluate the relative influence of these parameters (about 50 parameters for the examples below) on the simulation results. The objective is 1) to identify the parameters that are playing a key or predominant role in the simulations and that require additional characterization efforts, 2) to estimate the uncertainty that exists on the simulation results. The application cases for this sensitivity analysis are two busy roads on Reunion island (France) when considering the residual rockfall risk after a major rockfall event.

1 SIMULATION OF THE RESIDUAL ROCKFALL RISK AT TWO SITES ON REUNION ISLAND

The residual rockfall risk after a major rockfall event is studied for two busy roads on Reunion island (France): the national roads RN1 and RN5 (upper part of Figure 1). A probable residual rockfall volume of 0.2m^3 is considered for RN1 and of 6.4m^3 for RN5. Both slopes are mostly constituted of volcanic rocks. However, their topographies are very different: the slope at RN1 (landmark PR12+800) is almost vertical while the slope at RN5 (landmark PR10+960) is of moderate declivity. Thus, rockfall trajectory simulations at these two slopes show typical characteristics: mostly free flight for RN1 and mostly rolling/sliding for RN5 (upper part of Figure 1).

Rockfall trajectory simulations are carried out using the 2D Pierre-98 stochastic rock fall dynamics simulation program (co-developed by BRGM and university of british Columbia, Mellal et al., 1998). The materials along the profiles are described using mechanical parameters (Table 1) that we consider variable. Thus, a simulation corresponds to 1000 realizations of trajectories for which these properties are randomly drawn in the parameter space (according to predefined probability distributions), while the size of the falling blocks remains constant.

Table 1: List of parameters defined for each material to perform rockfall trajectory simulations

Parameter	Description
Rf	dynamic friction coefficient for rolling/sliding
Rd (m)	maximum rolling/sliding distance before rebound
S (m)	roughness
Cf	static friction coefficient
En, Et	normal and tangential restitution coefficients
F0 (kN)	limit beyond which there is reduction of the restitution coefficients under impact
C1 (kN/m)	soil stiffness for impacts where F <F0
Rn, Rt	coefficient of reduction of normal and lateral rigidity under strong impact

2 SENSITIVITY ANALYSIS ON THE SIMULATION RESULTS

The probability of the road to be damaged by a falling block correspond to the percentage of simulated blocks that reached it and which can be deduced from the Cumulated Distribution Function (CDF) of the maximum runout distances. In order to estimate the relative influence of each parameter on the simulation results, we will thus quantify the changes of the maximum runout CDF when removing the uncertainty about one material property following the approach named PAWN developed by Pianosi and Wagener (2015) (e.g. the targeted material property remains constant while all others vary). The central insert of Figure 1 shows the evolution of the maximum runout CDF when the parameter S of the parent rock is successively fixed at $0+n\times0.1$ m with $n=[0,1,2,3,4]$.

[1] LEVY Clara, BRGM, Orléans, France (FR), c.levy@brgm.fr

[2] ROHMER Jérémy, BRGM, Orléans, France (FR), j.rohmer@brgm.fr

[3] COLAS Bastien, BRGM, Montpellier, France (FR), b.colas@brgm.fr

[4] REY Anthony, BRGM, Réunion, France (FR), a.rey@brgm.fr

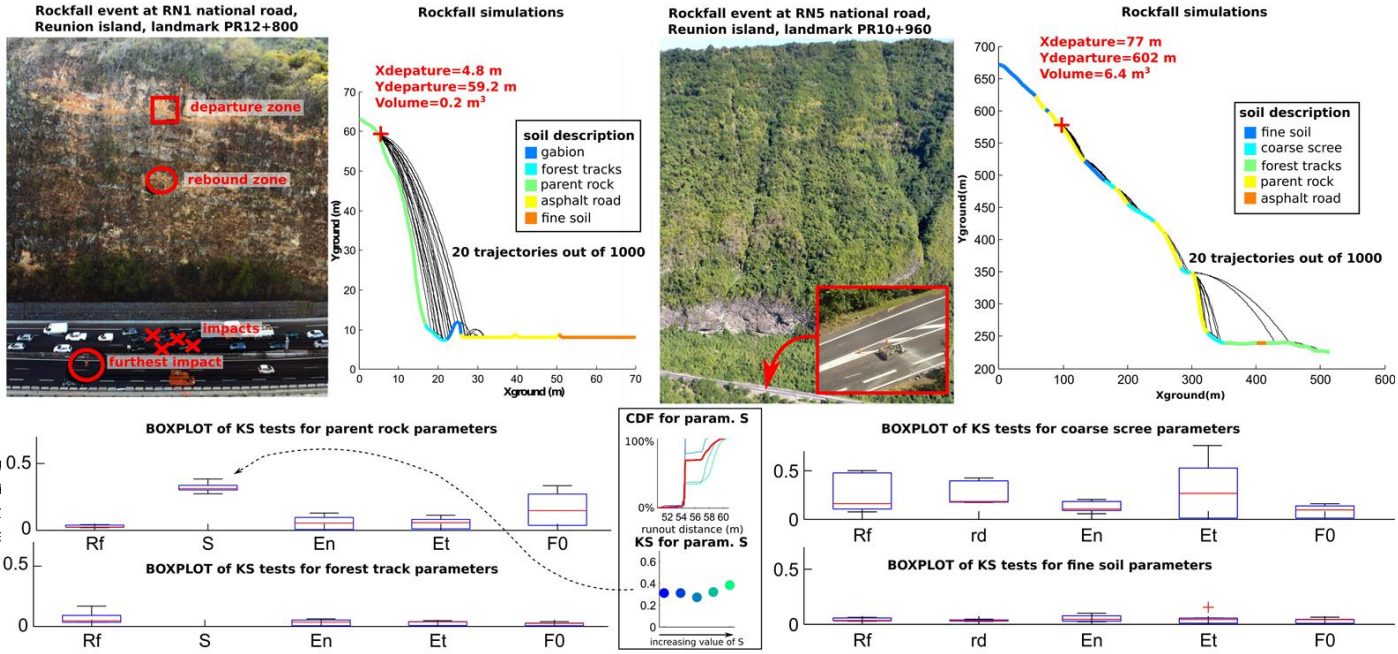

Figure 1: Photographs of two sites exposed to rockfall risk at Reunion island together with corresponding 2D simulations (upper part). Boxplots of the Kolmogorov Smirnov (KS) statistics on several parameters used in the simulations summarizing their relative influence on the distribution of runout distances (lower part). Bottom and top of the boxplots are the 25th and 75th percentile of the obtained KS values, red line is the median and the whiskers are the minimum and maximum KS values. The central insert illustrates how KS values are obtained from Cumulative Distribution Functions (CDF) of the maximum runout distances: the upper plot shows the CDF of the reference simulation in red (e.g. 1000 random realizations of trajectories where all inputs vary simultaneously) together with 5 CDFs corresponding to simulations where all inputs vary except S, which successively takes 5 fixed values (blue lines), the lower plot shows the obtained values for the KS statistics that quantifies the distance between the reference (or unconditional) CDF and each of the other CDFs.

Figure 2 shows the roughness of the parent rock (basalt) at the RN1 site, translated by the expert by a variation of parameter S between 0 and 0.1 m. The variation of the maximum runout CDF compared to a simulation for which all the parameters vary simultaneously is estimated using the Kolmogorov smirnov statistic (denoted KS distance), which can vary between 0 and 1. The larger the KS distance, the larger the importance of the studied parameter on the simulation results (central insert of Figure 1). For all parameters, we study the variation of the maximum runout CDF using 5 different fixed values of the parameter and by calculating the corresponding KS distances. The distribution of the obtained KS distances is represented using boxplots in Figure 1 (lower part). For the RN1 site, we observe that parameters S and F0 of the parent rock play a dominant role on the simulation results when compared to other parameters (whether they are other parameters describing the parent rock or parameters describing the forest tracks). This result is very consistent with the characteristics of the trajectories on this profile (free flight). Indeed, these two parameters play a key role on the characteristics of the initial collision and the following rebound. On the other hand, we observe that it is parameters Rf, rd and Et of the coarse scree (see Table 1) that play a dominant role on the simulation results at RN5 site. This result is also consistent with the characteristics of the trajectories on this profile (rolling/sliding), because these parameters are involved in the modelling of rolling/sliding. Interestingly, coarse screes constitute only a small proportion of the RN5-profile where rolling/sliding occurs, nonetheless this material is by far the most heterogeneous material of the profile and it plays a major influence on the block trajectories.

Figure 2: Detail of the outcrop at RN1 site, showing the roughness of the parent rock (basalt).

3 CONCLUSION

We propose a simple method that can be used routinely to evaluate the relative influence of parameters used in simulations of rockfall trajectories. The above examples show that out of a large number of initial parameters (about 50), only 2 or 3 influence considerably the results. This information can be quickly integrated by the expert to estimate the uncertainty of the probability of the road to be damaged by a falling block.

4 REFERENCES

Pianosi, F., & Wagener, T. (2015) A simple and efficient method for global sensitivity analysis based on cumulative distribution functions. Environmental Modelling & Software, 67, 1-11.

Mellal A., Hungr O., Evans S. G. (1998) An advanced stochastic lumped-mass analysis of rock fall dynamics.

Real scale impact experiments on Bloc Armé® as facing of rockfall protection embankment

Agathe FURET[1,2,3], Stéphane LAMBERT[2], Pascal VILLARD[3], Jean-Philippe JARRIN[1], Julien LORENTZ[4], Lucas MEIGNAN[1]

Keywords: rockfall, protection structure, impact, real scale experiments, Bloc Armé®

This article presents real-scale experiments aiming to improve the understanding of protection structure facing's response when subjected to dynamic loading. Here, we focus on the presentation of the test conditions and measurement methods and we introduce first experimental results.

1 INTRODUCTION

Rockfall protection embankments protect humans and infrastructures from high energies rockfall (Lambert and Bourrier, 2013). The national project C2ROP is currently conducted to develop tools and methods concerning rockfall hazard, risk management and protection. In this framework, part of the ongoing researches aims at (1) developing technological solutions with limited footprint and (2) improving rockfall protection embankment dimensioning methods. Experiments on innovative facing, including impacts from 200 kJ to 2000 kJ, were conducted on the Ifsttar's testing site of Montagnole in order to provide (1) a better understanding of the dynamic response of the Bloc Armé® structure and (2) a calibration dataset for numerical models.

2 EXPERIMENTAL METHODS

2.1 LAYOUT AND EQUIPMENT

The experimental layout (Figure 1) consists of the tested facing layed on a 2-m thick granular layer, acting as support platform. This platform is made of rolled gravel 20 to 40 mm in grain size. This material was chosen because it permits displacement while keeping mechanical characteristics rather constant after successive impacts (low sensitivity to compaction).

The facing is composed of concrete blocks joined together with continued metallic frames (Bloc Armé® patent). 19 blocks are positioned in staggered rows forming a bi-pyramid shaped facing which is 4-m large, 8-m long and 0.8-m thick (Figure 1).

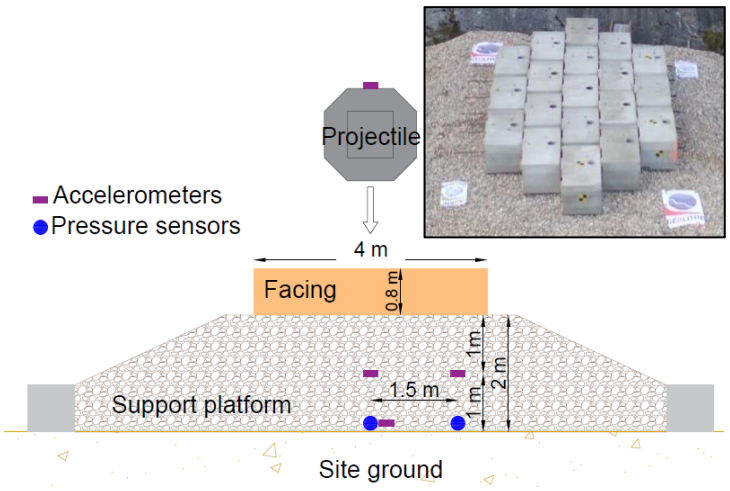

Figure 2: Cross-section of the experimental layout and facing tested

2.2 IMPACT TESTS

The experiment included three successive impacts series on: (i) the site ground, (ii) the granular platform and (iii) the facing layed on the support platform. The 2 first series aimed to characterize the platform and the soil underlying the tested structures under dynamic loading.

Impacts were performed dropping ETAG27-type reinforced concrete projectiles of varying mass (2580 to 12 490 kg) from various heights (0.83 to 16.54 m.). Most of the impacts concerned the facing center.

2.3 MEASUREMENTS

Measurements were taken to evaluate the impact response of the tested structures, in the different stages:

- In order to evaluate displacement and load transfer in the support platform, acceleration and vertical stress were recorded in different locations within the platform. (Figure 1).

[1] GEOLITHE, 181 rue des Bécasses, 38920 Crolles, France, agathe.furet@geolithe.com

[2] Univ. Grenoble Alpes, Irstea, UR ETGR, F-38402 St-Martin-d'Hères, France

[3] Univ. Grenoble Alpes, 3SR, F-38402 St-Martin-d'Hères, France

[4] GEOLITHE INNOV, 181 rue des Bécasses, 38920 Crolles, France

- The projectile's acceleration is measured by:
  - 3-axis accelerometer placed on top of the projectile.
  - Two high-speed cameras recording images at 500 frames per second in two perpendicular axes at the impact height.
- Three dimensions and one-dimension geophones systems were used to measure ground vibration with the aim to estimate the energy transferred to the ground soil.
- A topographic survey was conducted during all the experiments based on sets of pictures taken by a drone to measure the deformation of the structures.
- In addition, a thermic camera showed heating and point out some element displacements during impact.

3 PRELIMINARY RESULTS

The tests permit to observe the dynamic response and to compare the whole impacted system response on behavior with or without the facing structures. Measuring devices in the granular support platform showed acceleration at the layer mid-height and stress increment at its bottom (Figure 2).

CONCLUSION

The significant measurement dataset provided by the global experimental campaign will be used to investigate carefully the dynamical response of the facing-support platform system and to calibrate some

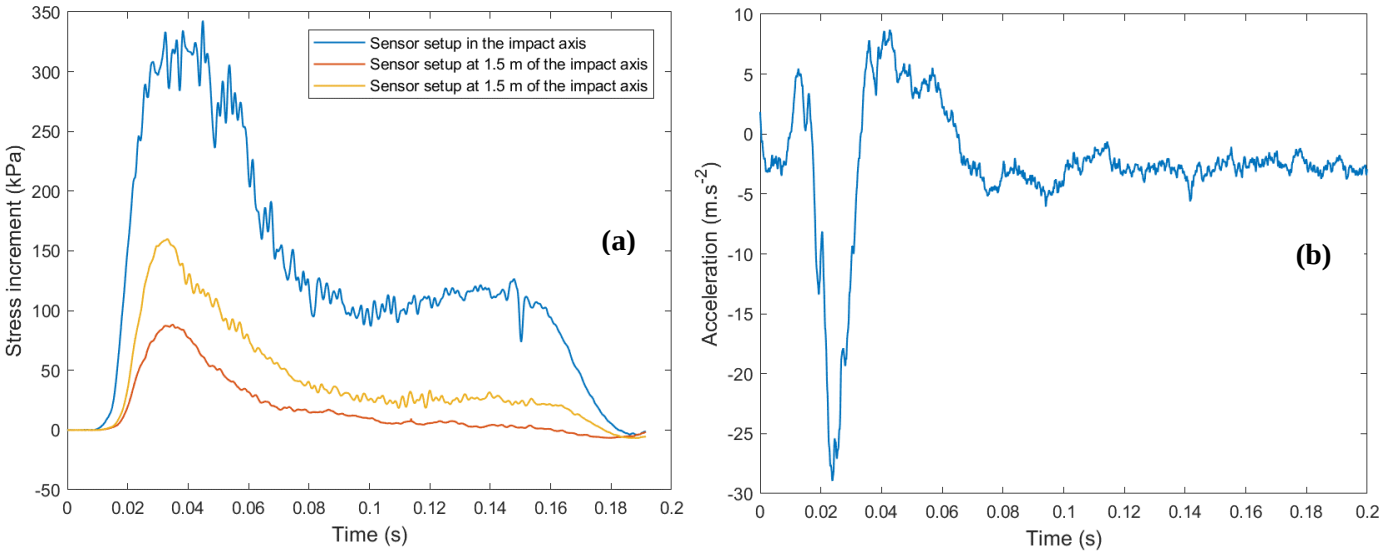

Figure 2: Measured data a) Stress increment in the pressure sensors for a 200-kJ impact test on the support platform b) Acceleration in the granular support platform for a 200-kJ impact test on the facing structure

future numerical models. Data will be analyzed in order to investigate the efficiency of the facing structure in reducing deformation under impact and distribute the loads in the support platform.

AKNOWLEDGEMENTS

The authors would like to thanks Ifsttar and Céréma for their assistance in conducting the experiments.

4 REFERENCES

Lambert, S, and Bourrier, F (2013): Design of rockfall protection embankments: a review. Engineering geology 154 (28), 77-88.

Testing of UAV to inspect rockfall fences over railways

Cécile SAINT-MARC (corresponding author)[1], Stéphane MARTINEZ[2], Pierre ASSALI[3], Jean-Luc BOYER[4]

Keywords: UAV, inspection, 3D modelling, boulders, natural risk, infrastructure

Rockfall is a major hazard for the safety of railway operations (Pollet 2012). Rocks falling may damage infrastructure components and create a collision risk. Rockfall fences are one of the protection barriers to ensure the safety of railway operations. The monitoring of these components is time consuming and dangerous for railway agents, because of their locations in areas which are difficult to access. Since 2016, SNCF Réseau led experiments about the use of UAVs to optimize annual inspection visits of rockfall fences (Assali et al. 2016), in cooperation with the UAV operator ALTAMETRIS. This article deals with the results of UAV experiments of the last two years.

1 CONTEXT AND AIMS

About 4.000 sites in France, representing more than 2.300 km of rock outcrop along railways, require a specific monitoring and a regular maintenance (Assali et al. 2016). Rockfall fences are one of the « protection » barriers (Mihailovitch et al. 2014) against rock falling near railways (Figure 1).

Annual inspection visits are organized to detect potential stress and damages that could affect the functionning of rockfall fences. During these visits, experts decide if maintenance actions should be planned to guarantee fences nominal resistance. The two main issues are that these inspection visits are very time-consuming and that they threaten agents' safety. As a consequence, UAV figured to be a possible solution to remotely inspect rockfall fences, with an optical sensor (in-board camera).

UAV may be used for two purposes:

- to detect the presence of objects stressing rockfall fences (lower storage capacity, geometric deformation, or other issues which may affect their resistance in kJ),
- to estimate boulders volume and so their weight and energy, in order to prioritize maintenance operations.

In these aims, several acquisition modes were tested on 5 sites in France, in Jura and Massif central mountains.

Figure 3. Rockfall fences

2 DATA COLLECTION

2.1 MATERIAL AND METHODS

The experimental scenario was to collect images by UAV, for the experts to inspect back in his office. Each experimental session was conducted in cooperation between a telepilot and a railway expert. The expert watched the image return coming from the UAV camera in real-time and gave guidelines about the flight to the telepilot. UAV flights were led in S1 (150m max distance) and S2 (1000m max distance) regulatory scenarios.

Several experimental variables were tested:

- Test of several multirotor UAVs (Astec Falcon 8 with Sony NEX7 24Mpx camera, DJI Phantom 4 PRO with its 20 Mpx camera, DJI Mavic PRO with its 12.35 Mpx, DJI Spark with its 12 Mpx camera),
- Test of several video return in real-time: virtual reality glasses (Fatshark or DJI) or 7'' tablet,
- Test of several capture angles: nadir-viewing (vertical direction) or oblique with yaw, to capture both sides of fences (several capture angles were tested).

2.2 RESULTS

All the tested vectors seemed to be pertinent to inspect rockfall fences, with good signal reception and resistance to electromagnetic disturbances. However, the quality of real-time video varied. The final resolution which appeared to be the most adapted for experts was a 1080p video. The tablet is preferred by experts compared with virtual reality glasses, because immersive glasses raise safety issues in a railway or near-road context.

[1] SAINT-MARC Cécile, ALTAMETRIS, Paris, FRA, cecile.saint-marc@altametris.com

[2] MARTINEZ Stéphane, SNCF Réseau - Ingénierie & Projets - PRI Lyon, Lyon, FRA, stephane.martinez@reseau.sncf.fr

[3] ASSALI Pierre, ALTAMETRIS, Lyon, FRA, pierre.assali@altametris.com

[4] BOYER Jean-Luc, ALTAMETRIS, Lyon, FRA, jean-luc.boyer@altametris.com

The difficult configuration of sites, with mountains stopping the GPS reception from time to time and many obstacles, such as electric power lines, do not allow the use of an automated flight plan. The presence of a professional telepilot on-site is thus required.

Figure 4. Nadir photograph of a rockfall fence

Even if the first aim was to capture images for delayed inspection in the office, it appeared that real-time inspection was also of great interest for experts. As a consequence, two inspection modes appeared to be pertinent:

- Real-time inspection, with a collaboration between a confirmed telepilot and a domain expert. The advantages of this method are:
    - the agility of UAV to answer the expert needs: change of camera angle, zoom, etc.
    - no need to physically go on fences sites: increased safety and diminished inspection time. Once the agents are on the take-off site, 30 minutes are needed for the inspection, whereas the usual inspection requires two people for two hours.

  However, real-time inspection by UAV make it difficult to precisely identify and quantify damages to fences caused by a rock impact. Dense vegetation or snow on the ground may also be an obstacle to the quality of pictures.
- Images inspection in the office: for delayed inspection, the best collection mode is to combine nadir photographs with an oblique + yaw one, with a 45° angle. The first capture mode better detects geometric deformations of the fences and the second better detects objects stressing them (see Figure 2). The energy measurements associated with stressing objects may be compiled and stored to be used in diachronic analyses. At the same time, collected images may be used to build a 3D model and to calculate boulders volume.

2.3 BOULDERS VOLUME CALCULATION

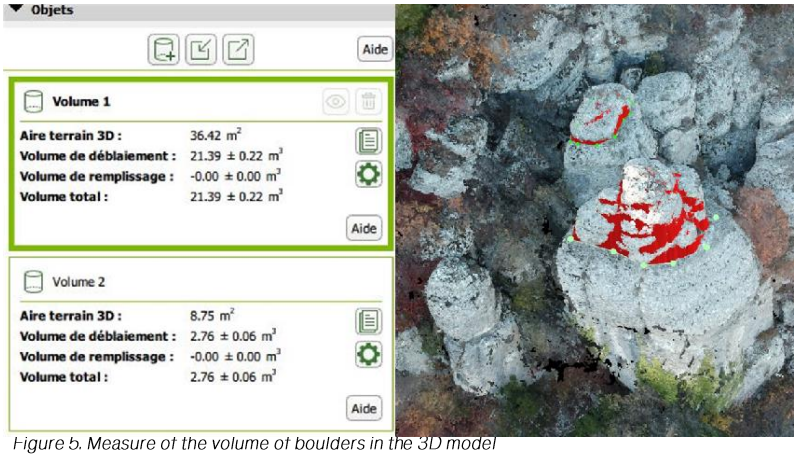

Figure 5. Measure of the volume of boulders in the 3D model

Oblique UAV photos with a recovery rate of 80% may be used to reconstruct a 3D model of the site thanks to photogrammetry, using commercial softwares (Pix4D® or Agisoft Photoscan®). Then, the expert can select portions of the model to automatically calculate boulders volume (see Figure 3). This semi-automatic method allows the assessment of the energy of objects stressing the fences, more accurately than visual estimations currently used by experts.

The combination of precise volume assessments and the quick inspection by UAVs allows to conduct more efficient maintenance operations at lower costs.

3 CONCLUSION

As a conclusion, UAV seems to be a useful tool to inspect rockfall fences. The paired nadir and oblique + yaw acquisition, coupled with a partnership between the expert and the telepilot on-site enables the capture of high quality footage. The images, after being computer processed, enable the creation of 3D models of rockfall fences environment, that may be used to estimate boulders volume.

The repetition of measures in time will make possible to automatically detect which rockfall fences are the most often stressed. This analysis will make possible to concentrate maintenance costs on the most active areas, leading to a more sustainable maintenance. This analysis may also lead to set up more preventive measures in the most impacted areas. In this scope, UAV appears to be a way to prioritize, optimize and adapt maintenance on rockfall fences.

4 REFERENCES

Assali, P., Fivel, A., Pollet, N., and F. Viguier (2016). UAV systems for linear outcrop inspection. *Proceedings of 3rd RSS Rock Slope Stability conference*. Lyon (France).

Mihailovitch, F., Narcy, A., Pollet, N., and J-M. Terpereau (2014). Natural hazard management integrated within the railway system. *Proceedings of 19th Congrès de Maîtrise des Risques et Sûreté de Fonctionnement*. 21-23 octobre 2014, Dijon (France).

Pollet, N. (2012). Risk management of rockfall hazards on the French railway network. *Revue Générale des Chemins de Fer*, mai 2012.

Rockfall Attenuators – a design approach

Hélène HOFMANN (corresponding author)[1], James GLOVER[2], Duncan WYLLIE[3]

Keywords: rockfall, attenuators, impulse, rotational component, RAMMS::ROCKFALL

Attenuators are a passive rockfall protection solution combining a flexible rockfall barrier prolonged with drape. To date there is no formal solutions to their design. In comparison to classical flexible rockfall barriers where only translational kinetic energy is considered; attenuators present a design challenge wherein both the rotational and translational component of rockfall must be considered. In order to develop a dimensioning concept that addresses these dynamics, it is important to fully understand the attenuation process. Addressing the need for a formal dimensioning concept, Wyllie & Norrish Rock Engineers (Canada), Geobrugg North America LLC and Geobrugg AG Switzerland conducted extensive real scale field testing of attenuator systems in the province of British Columbia, in Canada. In the past three years over 200 concrete blocks and natural rocks were rolled into an attenuator, recording the forces in the systems with load cells and the rockfall trajectory with high-speed cameras.

1 ATTENUATOR PRINCIPLE

The principle of an attenuator is to intercept a rockfall's trajectory and guide it, between the mesh and the slope, to a designated collection zone for easy, rapid and cost effective maintenance. See Figure 1 for a typical setup. Attenuators are a protection solution applicable in different settings complementing flexible rockfall barriers. Wherever frequency, access or space is an issue concerning high maintenance costs, an attenuator could be an alternative. A setting where it is easier to guide the rocks to a designated catchment area rather than servicing a barrier illustrates an ideal setting.

2 FIELD TESTING AND RESULTS

Field testing was conducted in 2015, 2016 and 2017. The results of 2017 are currently being analysed and will be presented. During the most recent test series, 101 rocks were rolled into an attenuator, wherein three different meshes were tested: TECCO G65/3, TECCO G80/4 and SPIDER S4/130.

2.1 INSTRUMENTATION

Instrumentation of the test site consisted of load cells in all ropes, camera views from the front, the side and the top, high speed cameras from the side. Rock motion sensors with three gyroscopes and three accelerometers were incorporated in custom-made concrete blocks.

2.2 LOAD CELLS

First analysis of the load cell data captures well the classical behaviour of attenuator systems. The first peak corresponds to the initial impact of the block with the mesh and the second peak corresponds to the torque peak generated as the friction between the attenuator netting and the rock causes a reversal of the rocks rotational direction while rolling along the mesh (see Figure 3). Both the translational impulse and rotational impulse of the rock interacting with the attenuator system form the principal load cases attenuators should be designed for and are the basis of the proposed attenuator design concept conserving momentum (Wyllie et al., 2017). These two load cases seem to correspond to the boundary conditions of the mesh. Maximum translational impulse presents a puncturing risk trough the mesh whereas a high rotational component of rockfall can shear the mesh open while being contained behind it. Additionally, the load cell readings have allowed us to identify these load cases which is forming the basis of one of the design principles for attenuators.

2.3 HIGH-SPEED VIDEO ANALYSIS

Velocity and rotation are analysed by video analysis with the open source software Kinovea (Glover et al., 2012). Trajectory tracking fore and after impact plot the rock's x and y coordinates over time (see Figure 4). Scaling the video images for the depth of field, it is possible to obtain velocity and acceleration. These data are then compared to measurements obtained by the rock motion sensors. Impact angle is always measured as it plays a key role in the effective force applied to the net. Rotation is measured both with the gyroscopes of the rock motion sensor and by video tracking every 90 degree rotation of the block with its associated time.

[1] HOFMANN, Hélène, Geobrugg AG, Romanshorn, Switzerland (CH), helene.hofmann@geobrugg.com

[2] GLOVER, James, Mountain Geohazards, Davos, Switzerland (CH), jmh.glover@gmail.com

[3] WLLIE, Duncan, Wyllie and Norrish Rock Engineers, Vancouver, Canada (CA), dwyllie@wnrockeng.com

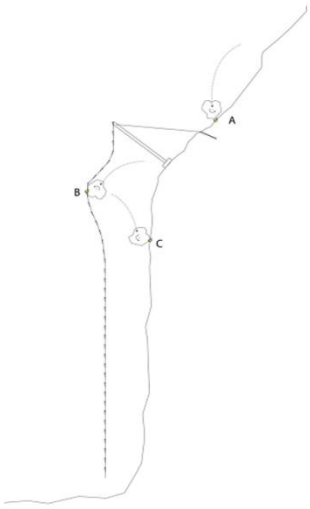

Figure 7 (left): geometry of an attenuator, freely hanging from the slope.

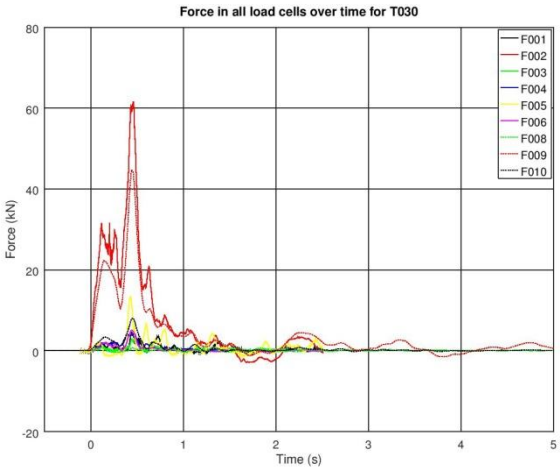

Figure 6 (right): two peaks recorded with load cells (F002 and F009 correspond to the top rope), t=0 corresponds to the time of impact.

3 ROCKFALL MODELLING

Rockfall simulation was performed with RAMMS::ROCKFALL (Leine et al., 2014) in order to optimise the location of the rockfall attenuator in the test slope. Calibration of the rockfall model for the test site was completed in a separate study (MSc Thesis Hofmann, 2017, unpublished). By constructing a wall in the terrain model to represent the location of the attenuator netting, the possible rockfall hit rate for the testing series could be estimated; optimising the test site setup. The full range of possible impact angles (Figure 3) could be predicted with the rockfall simulations (Figure 4), whereby the impact angle of the rock with the netting has been identified as key to defining the maximum loading on attenuator systems. Finally the simulations provided detailed insights into the rotational dynamics of rockfall impacting attenuators, which could be corroborated with both the video and rock motion sensor measurements.

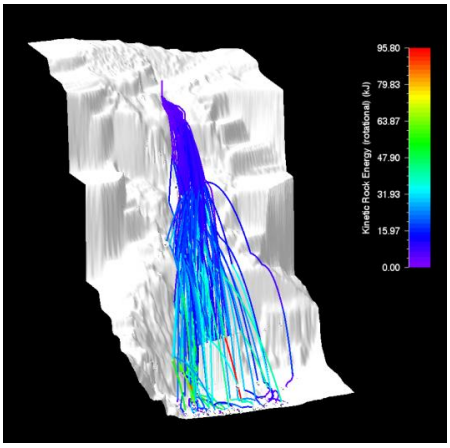

Figure 8 (left): High speed velocity analysis by tracking the block's trajectory through time

Figure 9 (right): 100 rockfall trajectories modelled for the test site with RAMMS::ROCKFALL. An artificial elevation of the terrain model was created in the DEM to simulate the presence of the attenuator, visible on the figure, where most trajectories stop behind it.

4 CONCLUSION

The proof of concept and advantages of attenuators have long been known, now the concept for a design approach is being assembled with these latest results, in order to build standardized systems. The necessity of high tensile steel to cope with shearing load because of rotation is evident from additional single component testing. Attenuators are an interesting addition to flexible protection structures for rockfall hazard and a formal design procedure is important.

5 REFERENCES

Glover, J., Denk, M., Bourrier, F., Volkwein, A., Gerber, W.; 2012:Measuring the kinetic energy dissipation effects of rockfall attenuating systems with video analysis- Conference Proceedings, Interpraevent, 2012.

Hofmann, H., 2017: Rockfall trajectories and dynamics analysis from 1:1 real rockfall tests. MSc Thesis, University of Portsmouth, unpublished.

Leine, R. I.; Schweizer, A.; Christen, M.; Glover, J.; Bartelt, P. and Gerber, W., 2014: Simulation of rockfall trajectories with consideration of rock shape. Multibody System Dynamics 32, 2: 241 – 271.

Wyllie, D., Shevlin, T., Glover, J., Wendeler, C., 2017: Development of design method for rockfall attenuators. Proceedings of the 68th Highway Geology Symposium.

Slope stability analysis of a rock-cliff subjected to climate actions

Sergio SAMAT[1]

Keywords: solar radiation, internal energy, entropy, plastic hinge, failure mechanism

A slope stability analysis of a rock block which is part of a cliff located in the area on La Roque Gageac-France is performed. The analysis is based on the Bernoulli beam theory and compare the threshold envelope obtained assuming a failure criterion based on Drucker proposal (Bezukhov referenced by Jirásek 2002) susceptible to soften under temperature increments in the rocky medium. The studied cliff is subjected to weathering actions which causes a slow and continuous degradation of the material integrity. The first and observable proof of this degradation is the spalling of the cliff face. However, the presence of a progressive crack development that starts at a corner of the troglodyte cavern roof supports the analysed rock block, Fig. 1b. The report issued by the Centre dÉtudes Techniques de lÉquipement du Sud-Ouest responsible for controlling and monitoring the massif highlighted the atmosphere heat in general and the radiation in particular as the main external actions that compromise both the material integrity and the crack progress. Figure 1a shows the geometry of the rock cliff section used in the numerical analysis of the coupled thermo-mechanical (TM) problem with atmospheric boundary condition. The study required the development and the implementation in a finite element scenario of the atmospheric condition as a boundary of the IBVP. The condition encompasses fluxes of fluids and heat given by the gas, vapour and temperature gradients between the atmosphere and the soil in addition to precipitation, solar radiation, and atmospheric radiation (Samat 2016). Although only heat flux entering or leaving the rock cliff is considered in this case.

1 NUMERICAL MODELLING OF THE ROCK CLIFF AND STABILITY OF THE BLOC

The cliff is located in the Dorgdone area. In winter it undergoes mountain weather influences due to its proximity to the Central Massif while, in summer, the weather can be subjected to streams of hot air from the Mediterranean. The annual maximum temperature in the village range between 27 °C and 32 °C and the minimum between -10 °C and -15 °C. Initial temperature To at the exposed upper cliff face was selected equal to the mean temperature in summer, while the geothermal gradient was used to initialize To within the rock mass. The thermo-mechanical problem is governed by the system of Eq. 1. The upper expression represents the local form of energy balance in the medium (1st Law of thermodynamics) and the expression at the bottom states the local form of the entropy inequality (2nd Law of thermodynamics):

$$\frac{\partial(\mathrm{E_s}\rho)}{\partial t} + \mathbf{j}_{\mathbf{E_s},i} + f^{Q} = \boldsymbol{\sigma}:\dot{\boldsymbol{\varepsilon}} - \mathbf{i}_{\mathbf{c},i} \qquad (1)$$

$$\frac{\partial(\mathcal{S}_\mathrm{s}\rho)}{\partial t} + \mathbf{j}_{\boldsymbol{\mathcal{S}}_\mathbf{s},i} \geq \frac{\partial(\mathcal{S}_\mathrm{s}^{r}\rho)}{\partial t} + \mathbf{j}_{\boldsymbol{\mathcal{S}}^{r}_{\mathbf{s}},i} \equiv \left(\frac{\mathbf{i}_\mathbf{c}}{\mathrm{T}}\right)_{,i}$$

where $\mathbf{E_s}$ and $\boldsymbol{\mathcal{S}}_\mathbf{s}$ are the internal energy and entropy of the solid skeleton, $\mathbf{j}_{\mathbf{E_s}}$ and $\mathbf{j}_{\boldsymbol{\mathcal{S}}_\mathbf{s}}$ are the net fluxes of heat and entropy, $\mathbf{i_c}$ is the conductive flux of energy, $\boldsymbol{\rho}$ is the dry density and $\boldsymbol{\sigma}, \boldsymbol{\varepsilon}$ are conjugated stress and strain tensors. From system Eq. 1 the state equations defining the constitutive relations and the momentum balance can be easily derived leading to a clear comprehension of the problem. Because the conditions reported emphasize radiation as the main actor (R.E.G.G. 2011), the massif has been considered in dry state with negligible actions of precipitation and wind. Thus the main contribution to the flow of heat is the radiation given by the expression of the net radiation [Eq. 2]; where $\mathrm{R_n}$ is the net radiation reaching the Cliff Surface, $\mathrm{A_l}$ is the surface albedo, ϵ_a and ϵ_t are the atmosphere and terrestrial emissivities and ϑ is the Stefan-Boltzman constant.

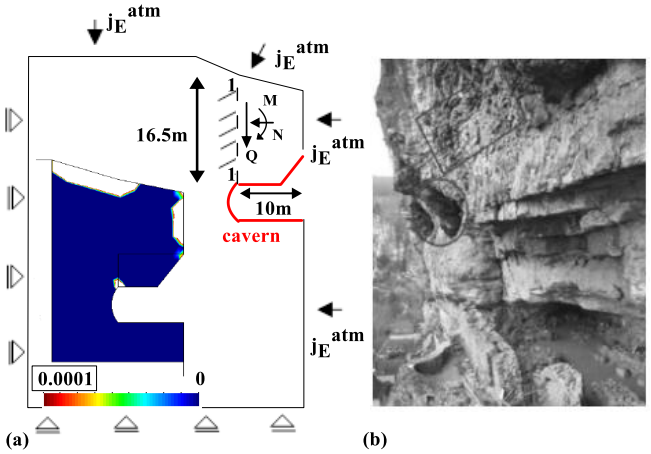

Figure 1 1: Modelling section and a view of the cliff.

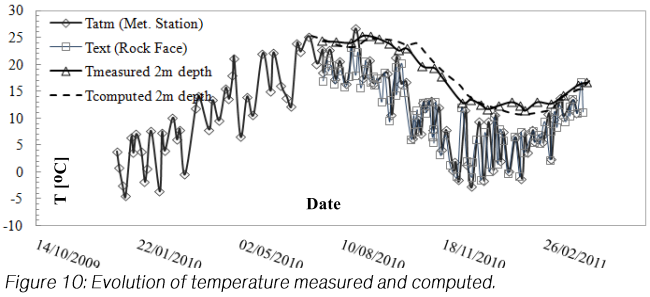

Figure 10: Evolution of temperature measured and computed.

$$\mathrm{R_n}\left[\frac{\mathrm{J}}{\mathrm{m^2 s}}\right] = (1-\mathrm{A_l})\mathrm{R_g} + \epsilon_\mathrm{a}\mathrm{R_a} - \epsilon_\mathrm{t}\vartheta\mathrm{T}^4 \qquad (2)$$

[1] SAMAT Sergio, Laboratoire Navier, UMR 8205, Ecole des Ponts, IFSTTAR, CNRS, UPE. Paris, France (FR), sergio-luis.samat@enpc.fr

Fig. 2 shows evolution of temperature at the weather station, at the cliff face and those measure and computed in an upper point of the rock block at 2m depths from the cliff face. Comparison of the last two validates the model and allows determining accurate thermal stresses at section 1-1.

The intuitive a priori critical character of section 1-1 in the block stability and the failure mechanism of plastic hinge type are confirmed by the computed isochrones of plastic multiplier (Fig. 1a). Figure 3 depicts the computed evolutions of normal force, shear force, momentum and curvature at section 1-1 due to the applied radiation. According to the framework proposed by Bezukov the rectangular section 1-1 is divided in two: (a) a core where the material remains elastic and (b) plastic regions. In the core the moment capacity is evaluated according to the stress distributions (σ_n, τ) proposed by Bezukov which are based on the foundations of beam elasticity. Moreover these stresses must satisfy the plastic admissibility condition by the Drucker yield surface leading to the failure envelope criterion:

$$|Q| \leq bd\left(\underbrace{r_c^o - \gamma_T(T - T_o)}_{r_c(T)}\right) a(c') \sqrt{\frac{4}{3}\left(1 - \frac{M}{M_o}\right)} \qquad (3)$$

where b and d are the dimensions of the section, $r_c(T)$ is the thermal softening law considered of the generalized Drucker-Prager criterion that includes (a) r_c^o the value of the thermal degradation parameter r_c at $T = T_o$ and (b) γ_T the rate of thermal degradation (enhancing), $a(c')$ is a cohesion dependent function, M and M_o are the bending moment and the fully plastic moment which depends on the yielding tensile strength of the rock and Q is the shear force. Eq. 3 defines the maximum allowable shear force such that (σ_n, τ) remains plastically admissible within the elastic core. Outside it is fulfilled by imposition of the yield locus. Figure 4 compares the computed shear-moment pairs as result of the applied radiation at the cliff and the determined failure envelope. The comparison reveals that the stability of the block is still far from being compromised. The plastic regions should develop even more reducing the elastic core and therefore the resistant area.

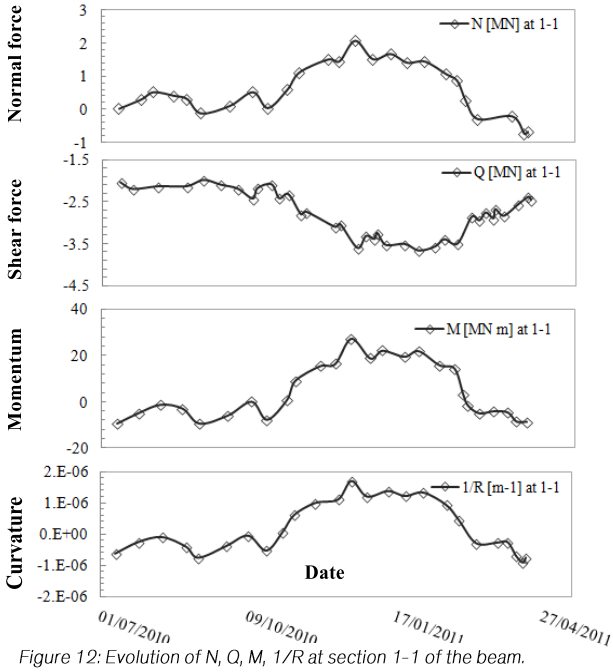

Figure 12: Evolution of N, Q, M, 1/R at section 1-1 of the beam.

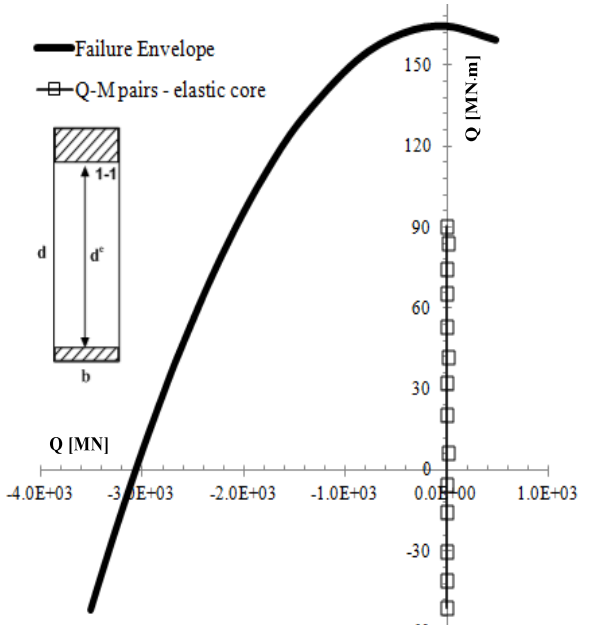

Figure 13: Interior envelope of the plastic limit M-Q and shear-moment pairs obtained with the numerical model.

2 CONCLUSION

The implementation and calibration of the atmospheric boundary condition in a finite element scenario have allowed analysing the stability of a block of rock, belonging to a cliff, subjected to the action of solar radiation. Further studies of the massif considering material anisotropy and damage are planned.

3 REFERENCES

Jirasek, M. & Bazant Z.P. (2002) Inelastic analysis of structures. John Wiley & Sons. London, England.

Samat, S. (2016) Thermomechanical modelling of ground response under environmental actions. PhD. Thesis, Technical University of Catalonia UPC - BarcelonaTECH, Barcelona, Spain.

R.E.G.G., (2011) Project DOSMS "La Roque Gageac - Damage to a Rock under Climate Cycles" Report 1. Centre dÉtudes Techniques de lÉquipement du Sud-Ouest. Toulouse, France.

Rockfall dynamics inferred from seismic signals and thermal camera: a controlled block release experiment

Gaëlle LE ROY[1,2], Agnès HELMSTETTER[1], David AMITRANO[1], Fabrice GUYOTON[2], Romain LE ROUX-MALLOUF[2]

Keywords: trajectography, seismology, thermal camera, rockfall

As part of the C2ROP (Chutes de Blocs Risques Rocheux Ouvrages de Protection) actions, a trajectography benchmark study was organized in October 2017, in Authume's limestone quarry (Jura, France). We took opportunity of this experiment to implement a seismological network and a thermal camera in order to develop and improve rockfall's detection and characterization methods.

1 ROCKFALL DETECTION AND CHARACTERISATION

Rockfalls are responsible for lot of damages, especially in heavily urbanized areas but also in remote areas. It is important to be able to detect and characterize them to assess the actions that need to be done depending on their inherent hazard. Various methods have been developed to detect rockfalls using relief measurement (LiDAR,etc.), seismology, etc.

Seismic detection is an efficient and reliable method to detect remote gravitational hazard. More than the detection of these events, it is possible to characterize their dynamics from the seismic waves they generate (Deparis et al., 2007, Ekström and Stark, 2013). However, most of the studies focused on large events (>1000m^3), which constitute only a small fraction of the damaging events. Only a few studies have investigated small events (Vilajosana et al, 2008; Hibert et al, 2017). A scaling law has been proposed between the potential energy loss, the kinetic energy and the energy of the seismic radiation generated by the impacts. However high uncertainties persist and these relations must be refined.

A trajectography benchmark was a good opportunity to enhance and develop rockfalls detection methods as the trials were well calibrated and monitoring methods, such as fast cameras or relief measurement, were already planned.

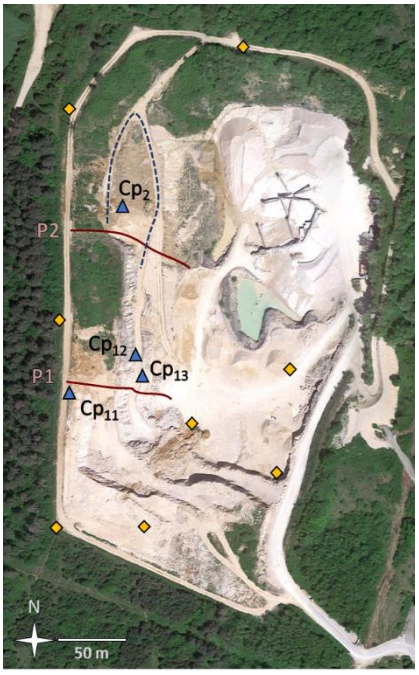

Figure 1: Aerial image of the quarry with the red lines showing the trial profiles, diamonds the seismic sensors and triangles the various locations of the thermal camera.

2 EXPERIMENTAL PROCEDURE

This benchmark study aimed to compare the different approaches of trajectography analysis compared with the results of field trials. This experiment consisted in dropping calibrated boulders into a slope in order to measure their trajectory, bouncing height, stopping points, etc. Trials were conducted on two different slopes (P1 and P2 in Figure 1). Over fifty boulders, with volumes approaching 1m^3, were dropped for each slope.

Several cameras recorded the trajectory of the boulders. Numerous parameters can be extracted from these recording such as boulders' trajectory and velocity, bouncing height, time of occurrence and the localization of the different impacts on the slope. These observations has been then compared to the results obtained from trajectography analyses in order to assess the reliability of these analyses.

3 SEISMOLOGICAL DETECTION

A network of 8 seismic stations has been also installed in order to record the seismic signals produced during the propagation of the boulders. This network allowed to monitor the vibrations produced by the boulders' impacts on the slope. As the distance between the rebounds and the seismic sensors for each impact was known, it is possible to determine the associated seismic signal amplitude corrected from propagation and attenuation effects.

The velocity, loss of potential energy, and kinetic energy of the block at each impact has been linked to the corrected amplitude and energy of the seismic signal in order to draw relations between these parameters.

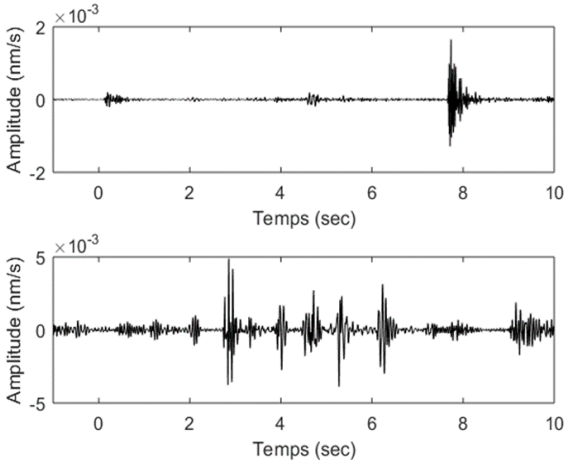

Figure 2: Examples of recorded seismic signals of a boulder dropped in P1 (top) and P2 (bottom)

[1] Institut des Sciences de la Terre, Université Grenoble Alpes, CNRS, Grenoble, France, gaelle.le-roy@univ-grenoble-alpes.fr

[2] Géolithe, Crolles, France

4 THERMOGRAPHY OF ROCKFALLS

A thermal imaging camera was also deployed to record the movements of the blocks using infrared radiations. This camera was used to detect changes in temperature during the propagation of the blocks.
It has been possible to detect the movement of the boulders but also their interaction with the slope during the impacts. Each impact produced small environment deformations, which can be observed through the increase of the environment temperature. Moreover, during their propagation, blocks remodeled the slope. This produced changes of temperature due to the reorganization of the environment. The use of thermography enabled a precise localization of the impacts and allowed us to distinguish the type of impact (bouncing, rolling, or sliding).

Figure 2: Propagation of a block (white circles) recorded with a thermal camera. Left: illustration of the augmentation of temperature due to rock impacts (white arrows). Right: difference between a bouncing (white arrow) and sliding (grey arrow) impact.

5 CONCLUSIONS

This controlled block release experiment enabled us to collect a significant quantity of information on rockfall dynamics recorded by different instruments. By implementing a seismic network and a thermal imaging monitoring, we aim to develop and refine rockfall's detection and characterization methods. Rockfall impacts produce seismic waves, whose amplitude depends on the kinetic energy of the block. Part of the energy is also released by thermal energy, and can be recorded by the thermal camera. Analyzing this large dataset should allow us to characterize quantitatively rockfall dynamics and trajectory from seismic signals and thermal camera. The next steps will be to apply these methods to natural rockfalls.

ACKNOWLEDGEMENTS

This work was partially funded by the French National project C2ROP. We thank Franck Bourrier (IRSTEA) for organizing this benchmark.

6 REFERENCES

Deparis, J., Jongmans D., Cotton F., Baillet L., Thouvenot F., and Hantz D. (2007), Analysis of rock-fall seismograms in the western Alps, *Bull. Seismol. Soc. Am.*, 98, 1781–1796.

Ekström, G. and Stark, C. P. (2013), Simple scaling of catastrophic landslide dynamics, *Science*, 339, 1416–1419

Hibert, C., Malet J-P., Bourrier F., Provost F., Berger F., Bornemann P., Tardif P., Mermin E. (2017), Single-Block Rockfall Dynamics Inferred from Seismic Signal Analysis. *Earth Surface Dynamics,* 1–15.

Vilajosana, I., Suriñach E., Abellan A., Khazaradze G., Garcia D., and Llosa J. (2008), Rockfall induced seismic signals: Case study in Montserrat, Catalonia, *Nat. Hazards Earth Syst. Sci.*, 8(4), 805–812

Evaluation of mechanical proprieties and lifespan of rockfall nets according to ISO standards

Alberto Grimod[1], Giorgio Giacchetti[2]

Keywords: rockfall nets, ISO standard, tests, lifespan, tensile strength, punch load capacity

Secured and simple drapery systems using steel wire meshes are worldwide used as rockfall mitigation protections. For both solutions, the design of these nets must take into consideration their mechanical properties, such as the longitudinal tensile strength and the ultimate punch load, as well as their lifespan according to the site environment. In order to characterize the resistances (tensile strength and punching) of the nets, laboratory tests must be carried out. Since 2012, the Italian norm UNI 11437 standardized the test procedures to define the tensile strength and the load bearing capacity of rockfall meshes and panels (ring net or cable net). Moreover, in September 2016 the Italian procedures were adopted in two new ISO standards respectively published for ring nets and cable nets: ISO 17745 and ISO 17746. The innovation of these two standards was the introduction of the concept of lifespan. Following the Annex A of the EN 10223-3 standard, the assumed working life of the nets can be defined according to the type of environment (ISO 9223) as well as the type of coating applied on the steel wire. In this way, designers, producers, contractors and owners are able to estimate the design life of a specific rockfall net. UNI 11437, ISO 17745 and ISO 17746 give to designers the possibility to compare the mechanical proprieties of different nets produced by the same or by several manufacturing companies.

1 MECHANICAL PROPRIETIES

1.1 TENSILE STRENGTH

The International Standard ISO 17745:2016 [1] and ISO 17746:2016 [2] describe the test procedure for determining the tensile strength (resistance and elongation) of steel wire ring panels and steel wire rope net panels and rolls.
This mechanical property is defined by testing a specimen connected to a metal frame equipped with load cells in order to acquire the load applied and the overall side reaction (longitudinal and transversal reactions). The sample has to be not less than 1,000 mm wide, with a minimum area of 1.0 m^2. It has to be fixed to the frame through lateral coupling devices, such as shackles or turnbuckles. The side coupling device is also free to slide along the longitudinal beams (see Fig. 1). The tensile strength reported at the end of the test is usually identified in kN/m.

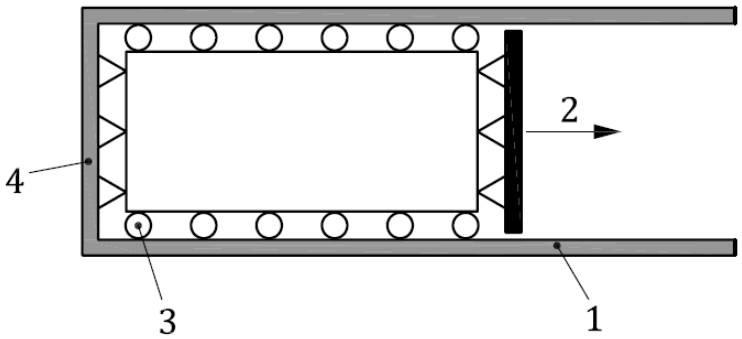

Figure 1 - Example of frame configuration for the tensile strength test. Legend: 1) Fixed frame; 2) Movable beam; 3) Lateral constraint; 4) Side connection device.

1.2 PUNCH LOAD CAPACITY

The punch test is carried out on a sample having a size of 3.0 x 3.0 m ±20%, restrained into a large steel frame and loaded by mean of punching device with a diameter of 1.0 m (see Fig. 2).
The knowledge of the deformation is very important during the design of a secured drapery system, because of the following main reasons:

- When the deformation reaches the design limit, it means that the maintenance (cleaning) of the secured drapery is needed before that further displacements induce the mesh rupture. A simple visual monitoring let the owner plans the maintenance interventions.

[1] Alberto Grimod, Maccaferri France, Valence, France (FRA), alberto.grimod@maccaferri.fr

[2] Giorgio Giacchetti, Officine Maccaferri SpA, Zola Predosa, Italy (ITA), g.giacchetti-cons@maccaferri.com

- Too much deformed mesh implicates easy stripping on the anchors and lower durability of the intervention. The designer must be aware of this and he has foreseen the right mesh type accordingly.
- Since the meshes are largely deformable, the facing of the secured drapery could interfere with close infrastructures or vehicles.

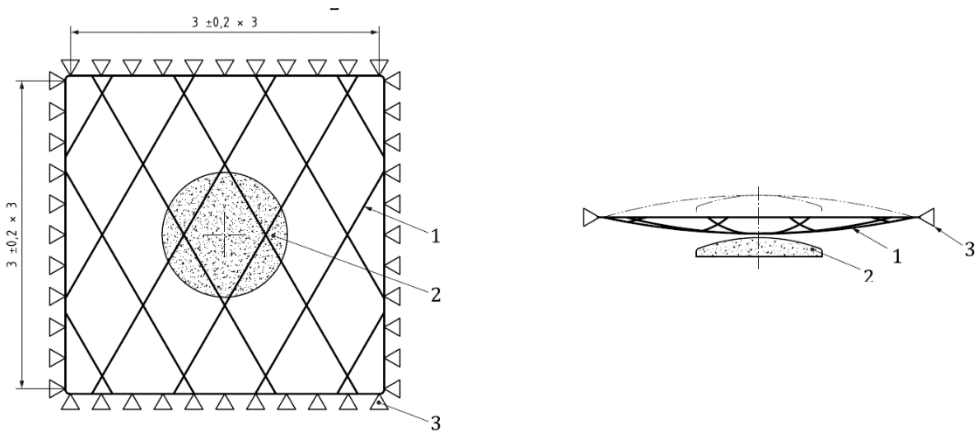

Figure 2 - Example of set up for punching test according to ISO 17745 and ISO 17746. Legend: 1) Tested mesh sample; 2) hemispherical shaped load sharing device (1.0 m in diameter); 3) Perimeter constraint between the mesh and the frame.

1.3 WORKING LIFE OF THE PRODUCT

The two new ISO standards define the estimated working life of the nets depending on the type of coating applied on the steel wire (i.e. Zinc, Zinc + Aluminium alloy or Advanced Metallic Coating) and on the site environmental level, defined according to the ISO 9223:2012 [3] (i.e. environment C2, C3, C4 etc).

2 CONCLUSIONS

The design of steel wire nets, used as rockfall mitigation systems, requires the knowledge of the mechanical properties, as well as the expected lifespan of the nets.

Considering that there is a large number of nets available on the market, the ISO 17745:2016 and ISO 17746:2016 where introduced to impose to producers a standardized procedure to test the tensile strength and the load punch capacity of ring nets and cables panels. In this way, the mechanical proprieties of different nets produced by the same or by several manufacturing company can be easily compared between each other.

These two standards set also the lifespan for rockfall netting based on the type of environment and steel wire coating.

3 REFERENCES

[1] ISO 17745:2016 (2016): Steel wire ring net panels - Definitions and specifications.

[2] ISO 17746:2016 (2016): Steel wire rope net panels and rolls - Definitions and specifications.

[3] ISO 9223:2012 (2012): Corrosion of metals and alloys - Corrosivity of atmospheres - Classification, determination and estimation.

Surface motion detection at the Chambon landslide with terrestrial optical imaging

Mathilde DESRUES[1,2], Ombeline BRENGUIER[1], Jean-Philippe MALET[2], André STUMPF[2], Lionel LORIER[1]

Keywords: photogrammetry, monoscopic terrestrial images, Photoscan, MicMac, LiDAR, Tunnel of Chambon

Several image analysis methods are used to determine surface displacements and generate 3D surface models (DSM) from multiview photogrammetric techniques. In our case, we focused on the contribution of different softwares to generate 3D models fom multiview images and document the surface motion from a fixed monoscopic camera. The methods are presented in the case of the Chambon landslide (Isère, France).

1 STUDIED SITE

1.1 LOCATION

The landslide is located upstream from the departmental road RD1091, a major road giving access to Grenoble (Isère, France) and Briançon (Hautes-Alpes, France). The tunnel situated close to the Chambon lake (Fig. 1) underwent several damages since its construction (e.g. two successive rockfalls happened in 1977 and 1978). Nevertheless, no correlation between those damages and a possible surface motion was detected. The tunnel closed in April 2015 due to surface fissure openings; then, due to a major crisis starting in July 2015, the major part of the unstable masses movements started to accelerate.

1.2 GEOLOGICAL AND GEOMORPHOLOGICAL CONTEXT

The slope is part of sedimentary rocks dated from the Lias. The bedrock is principally composed of shales. From a geomorphological point of view, two thalwegs limit the extension of the unstable slope to the West and the East. The upper limit is characterized by a 1-m thick fracture at the surface; the lower limit could not be determined because of the water level of the lake.

1.3 FIELD MONITORING DURING THE CRISIS

The site was instrumented during the main crisis by the SAGE society and included topographic measurements by automated total station and geophysical surveys. From the topographic displacements and measures by extensometers, it was possible to predict the time of the rupture. The main crisis was predicted at the beginning of July 2015.

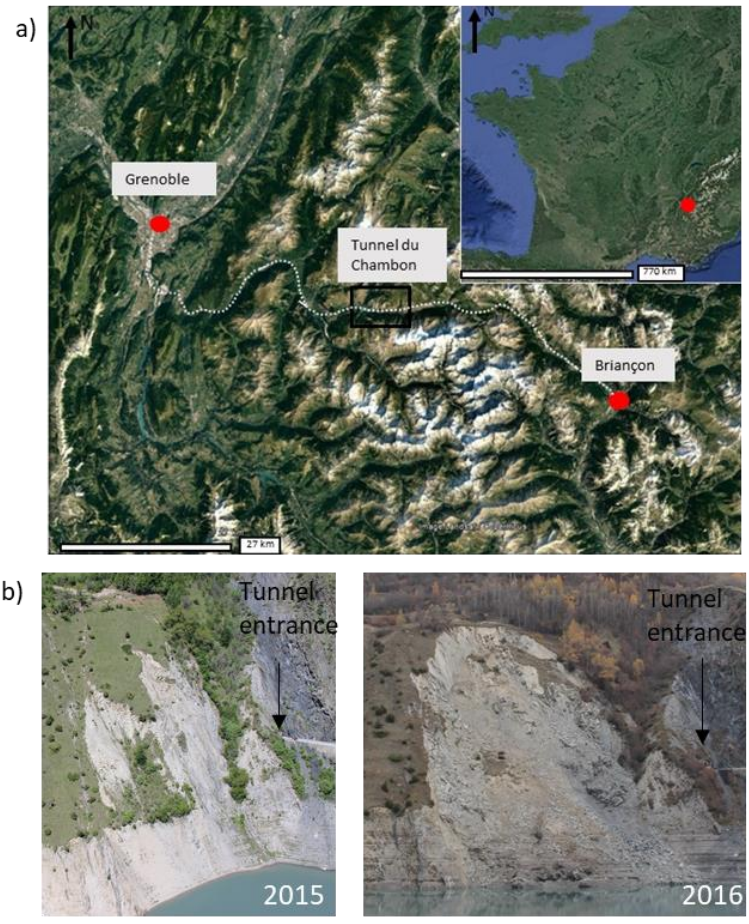

Figure 1: Location of the Chambon landslide (Isère, France). a) Location of the landslide in the Alps. b) Images of the landslide before the main crisis (April 2015) and after (December 2016).

[1] SAGE Ingénierie, 2 rue de la condamine 38610 Gières, France. o.brenguie@sage-ingenierie.com

[2] Institut de Physique du Globe de Strasbourg, CNRS UMR 7516, EOST/Université de Strasbourg, 5 rue René Descartes, Strasbourg, France, mathilde.desrues@unistra.fr

2 DATA AND METHODS

2.1 TERRESTRIAL OPTICAL IMAGING

After the crisis, several photogrammetric surveys were carried out to detect the still active zones and characterize their evolution in terms of amplitude. Images were acquired with a CANON EOS 600D using a lens with a focal length of 35mm (SIGMA). Later, a fixed CANON EOS 100D camera with a lens with a focal length of 50 mm was installed in front of the landslide. Images were acquired hourly.
A classical approach is used for analysis of the two populations of images. For the multi-view images, the workflow consisted in (1) point cloud generation, (2) georeferencing, (3) correlation to estimate the surface displacement fields. For the monoscopic images, the workflow consisted in (1) pre-processing of images (correction of camera movement), and (2) correlation to estimate the surface displacement fields.

2.2 COMPARISON BETWEEN METHODS

A comparison between the results obtained with the commercial Photoscan Agisoft software and the MicMac open source library (IGN) was realized. A DSM generated at high spatial resolution with a Terrestrial Laser Scanner (Riegl VZ2000) were used as reference.

2.3 MOTION DETECTION

The surface displacement fields were generated from the multi-view acquisitions and from the monoscopic camera time series. The dataset derived concerned motions for the period June 2016 to May 2017. Displacements were compared to in-situ measurements (topographic targets) to determine the performance of the photogrammetric methods.

3 CONCLUSIONS

Methods based on terrestrial optical images provide several information for a space and time characterization of the landslide surface motion. Such information is necessary for a better understanding of the geometry and dynamics of the main movement.

4 ACKNOWLEDGMENTS

These works were part of a CIFRE / ANRT agreement between IPGS/CNRS UMR7516 and the SAGE society.

An automated processing pipeline for the photogrammetric analysis of high frequency terrestrial optical images: application to unstable slopes

Mathilde DESRUES[1,2], Jean-Philippe MALET[2], André STUMPF[2], Ombeline BRENGUIER[1], Lionel LORIER[1]

Keywords: terrestrial optical images, image processing, slope stability problems

The objective of this work is to design, test and implement an automated image processing pipeline for the quantification of surface motion from monoscopic and/or stereoscopic image time series acquired with fixed terrestrial optical cameras.

1 ACQUISITION SYSTEM

Passive remote sensing sensors (i.e., sensors operating in the visible light spectrum such as Single Lens Reflex -SLR- cameras) are increasingly being used for geohazards monitoring (ice glaciers, volcano flanks, landslides) partly because of their low cost compared to expensive active sensors (i.e., terrestrial laser scanner –TLS- or radar imaging -GB-InSAR-). Indeed, due to the large consumer market, for digital cameras, sensor spatial resolution is upgrading rapidly; for example, inexpensive 15 megapixel cameras are available allowing arrays of cameras to be set up in the field. Here, we used a SLR CANON 100D and a PENTAX K200D. Both are connected to acquisition systems (LNS/Paratronics, and/or DigiSnap/Harbrotonics). Photographs are acquired at a time frequency depending on the slope movement kinematics.

2 IMAGE PROCESSING PIPELINE

The processing pipeline is based on the open-source photogrammetric library MicMac. It associates modules for the selection and creation of the image sequence, tools for image stack registration and correction of the camera movement, and tools for time series motion detection.

2.1 SELECTION OF THE IMAGES AND CREATION OF THE SEQUENCES

The first step of the pipeline consists in selecting the optimal images to analyse according to weather conditions. Indeed, because of mist, rain or shadow, images are degraded (Fig. 1). The selection is based on the statistical comparison of the radiometric properties of the images according to a master image. The method aggregates all radiometric (red, green, blue) bands; however, for most use cases, the red band is the most discriminant.

Figure 14 : Photographs of the Sanières landslide at different time (Alpes-de-Haute-Provence, Ubaye valley, France).

2.2 2.2. IMAGES CO-REGISTRATION

Cameras installed in the field can be affected by spurious movements linked to temperature variations, wind effects and soil movement (*Gance et al. 2014*). To correct the camera movement, several methods based on specific points are used such as the Harris or SIFT detection methods (*Gance et al. 2014*, *Lowe et al. 2004*). Here, we implemented the co-registration method COREGIS which is based on the evaluation of the movement of the whole image and which has been initially used for the co-registration of satellite image stacks (*Stumpf et al. 2018*).

2.3 MOTION DETECTION

For slope stability problems, recent research has focused on the development of image correlation techniques to determine the average spatial shift by maximizing cross-correlation functions between at least a pair of stereo-images. This technique has proven its performance for estimating the displacement fields of ice glaciers and slow-moving landslides at sub-pixel accuracy

[1] SAGE Ingénierie, 2 rue de la Condamine, Gières, France,

[2] Institut de Physique du Globe de Strasbourg, CNRS UMR 7516, EOST/Université de Strasbourg, 5 rue René Descartes, Strasbourg, France, mathilde.desrues@unistra.fr

(1/10th pixels) and generates a pseudo-continuous map of the deformation (*Travelletti et al. 2012*). The correlation technique used is implemented in MicMac (*Rosu et al. 2015*) and change detection is determined directly from the co-registered image stacks by estimating robust statistics.

3 RESULTS

The automated processing pipeline is presented and its performance will be evaluated for three use cases, respectively a rockslide (Sanières), and two soft-rock landslides (Montgombert, Aiguilles-Pas de l'Ours). Results are compared to in-situ sensors measurements and to terrestrial laser scanning or multi-view photogrammetry surface models.

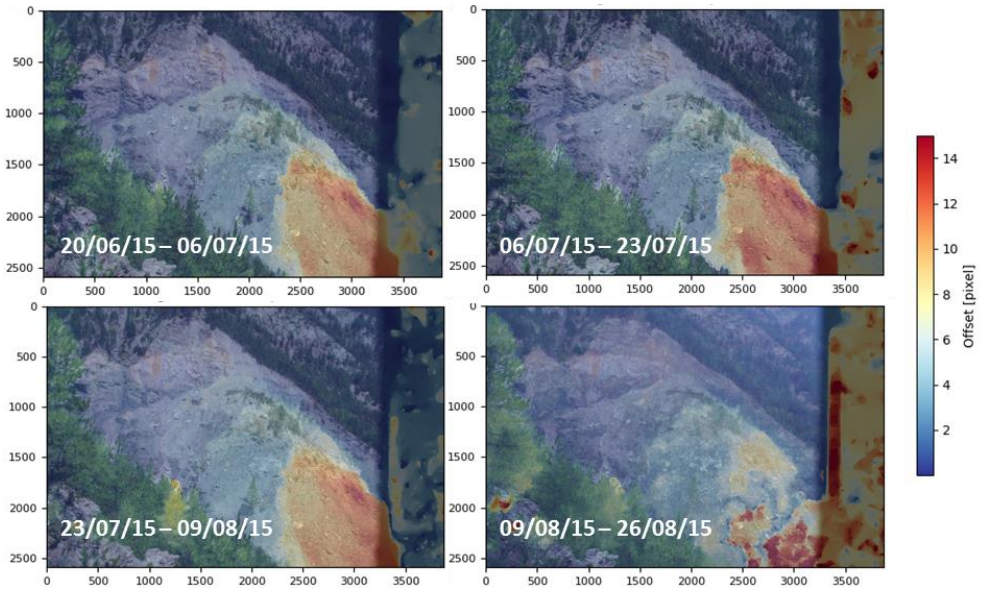

Figure 15 : Displacement fields in pixels on the Sanières landslides (Alpes-de-Haute-Provence, Ubaye, France) at different times.

4 CONCLUSION

Passive optical sensors provide both qualitative (identification of changes in the surface morphology, presence and location of snow cover and water discharges) and quantitative (velocity field, tracking of changes of the surface states) information on the dynamics of slope movements. The developed processing pipeline has the objective to facilitate the automatic analysis of stacks of terrestrial photographs for the estimation of advanced properties of the unstable slopes.

5 REFERENCES

Gance, J., Malet, J.-P., Dewez, T., & Travelletti, J. (2014). Target Detection and Tracking of moving objects for characterizing landslide displacements from time-lapse terrestrial optical images. Engineering Geology, 172, 26-40.

Lowe, D. G. (2004). Distinctive image features from scale-invariant keypoints. International journal of computer vision, 60(2), 91-110.

Rosu, A. M., Pierrot-Deseilligny, M., Delorme, A., Binet, R., & Klinger, Y. (2015). Measurement of ground displacement from optical satellite image correlation using the free open-source software MicMac. ISPRS Journal of Photogrammetry and Remote Sensing, 100, 48-59.

Stumpf, A., Michéa, D., & Malet, J.-P. (2018). Improved Co-Registration of Sentinel-2 and Landsat-8 Imagery for Earth Surface Motion Measurements. Remote Sensing, 10(2), 160.

Travelletti, J., Delacourt, C., Allemand, P., Malet, J.-P., Schmittbuhl, J., Toussaint, R., & Bastard, M. (2012). Correlation of multi-temporal ground-based optical images for landslide monitoring: Application, potential and limitations. ISPRS Journal of Photogrammetry and Remote Sensing, 70, 39-55.

6 ACKNOWLEDGMENTS

This work is part of a CIFRE / ANRT agreement between IPGS/CNRS UMR7516 and the SAGE society.

Rock fall analysis of instable wedges potentially impacting a concrete dam

Aïssa MELLAL[1]

Keywords: dam abutment, rock fall, trajectory, impact, damage, concrete dam

In the framework of the stability assessment of an arch dam's abutments, a rock fall analysis of potentially instable wedges has been carried out. The purpose of the study was to determine the plausible trajectories of detaching rock masses identified as potentially instable and to evaluate the consequences of an eventual impact on the dam.

1 DAM ABUTMENT STABILITY

The right bank abutment of the dam under study is characterized by unfavorable geological conditions with a system of discontinuities consisting of five faults (A, B, C, D) and bedding (E) sets in the limestone foundation (Figure 1). Moreover, prevailing uplift pressures and potential release of existing prestressed anchors contribute to weaken the stability of the dam abutment.

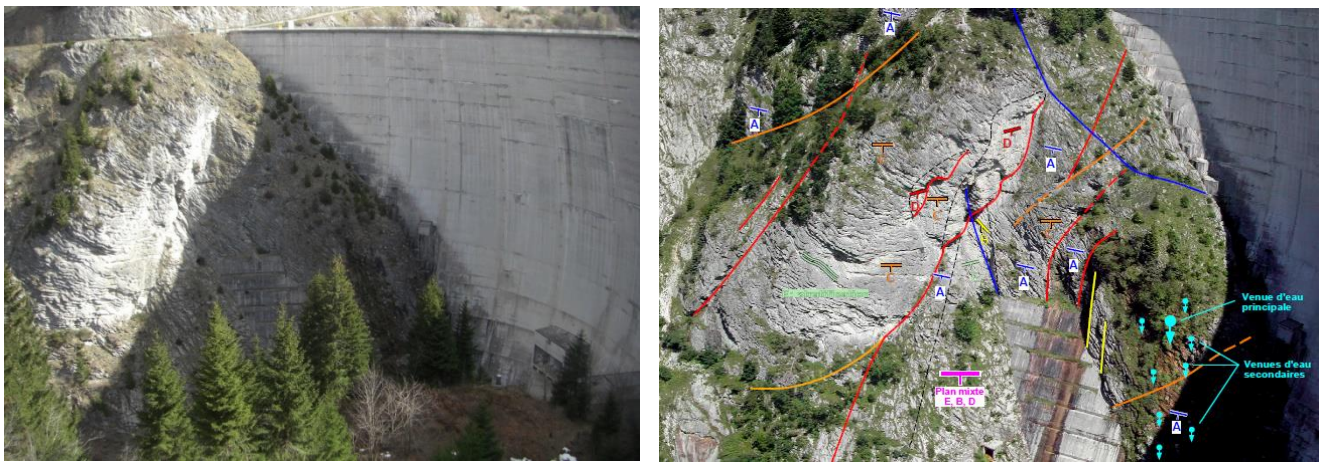

Figure 1: Right abutment of the concrete arch dam and main geological discontinuities

A stability analysis of the abutment zone by means of a 3D joints model including the discontinuities, bedding and local hydromechanical conditions has allowed identifying the main potentially instable wedges and corresponding factors of safety. It was found that the failure mode is a sliding mechanism along the bedding planes E, with detachment on the other joints. Average spacing of strata (plane E) was taken as 3 m.

Figure 2 shows the topographic profile along the steepest slope of plane E and crossing the unstable zone of the abutment. In this zone, the fault C which is a detachment plane, intercepts the bedding plane E and forms wedges.

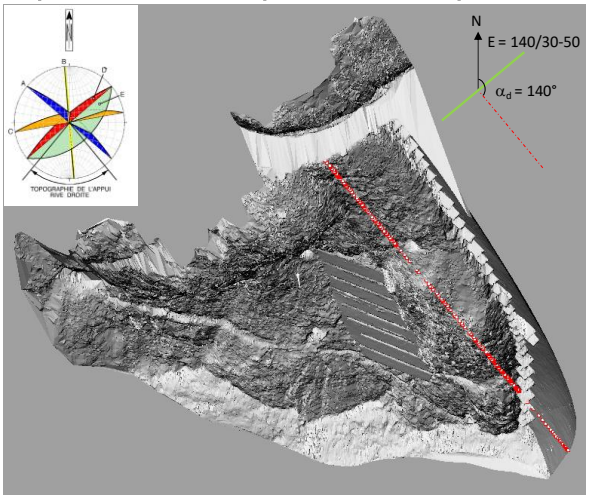

Figure 2: Sliding path of wedges formed by bedding plane E and fault plane C

Figure 3: scenarios of sliding wedges

[1] MELLAL Aïssa, STUCKY Ltd., Renens, Switzerland (CH), amellal@stucky.ch

2 ROCK FALL ANALYSIS OF DETACHING WEDGES

The rock fall analysis of the wedges is carried out considering that a portion of the potentially instable zone detaches from the rock mass and moves along the steepest slope of the bedding plane. It is considered that blocks with trajectories occurring out of this direction and heading towards the dam would have a lower impact energy due to a shorter travel distance and a lower velocity. The trajectories are calculated in one direction in a vertical plane (2D).

The analysis is carried out using the rock fall software PIERRE© (Mellal & Hungr, 1998). In addition to considering different movement modes (free flight, rolling/sliding, impact), the program handles uncertainties on parameters by means of intervals or probability density functions. Table 1 lists the input parameters (mean and standard deviation).

In order to evaluate the effect of the spacing between joints and therefore of the mass of the block that can potentially detach and move, the trajectories of the rock masses are determined for three scenarios (Figure 3): wedge with one strata (3 m thickness), two strata (6 m thickness) and five strata (15 m thickness).

For each scenario, the rock fall analysis of the corresponding wedge is realized by performing 1000 simulations of trajectories that may follow the wedge depending on the values of parameters (friction, restitution coefficient) within their interval of variation. Output results are given in the form runout histograms, bounce height and velocity envelopes. Figure 4 shows the trajectories and runout histograms for the 3 considered scenarios: after a few meters of sliding, the lightest wedges (scenario 1) are characterized by long jumps and most of them hits the dam. On the other hand, the heaviest wedges (scenario 3) are characterized essentially by a sliding movement, followed by a short parabolic jump before immobilizing near the dam toe. This is due to the significant weight of the wedge which promotes the friction on the bedding surface and maintains the wedge in sliding mode with a relatively low velocity.

Table 1: Model input parameters

Parameter	Mean (std.-dev.)
Rock density	2.7 t/m^3
Friction angle (joint E)	38° (1°)
Rolling/sliding friction coefficient	0.78 (0.03)
Normal restitution coefficient	0.50 (0.05)
Tangential restitution coefficient	0.70 (0.05)

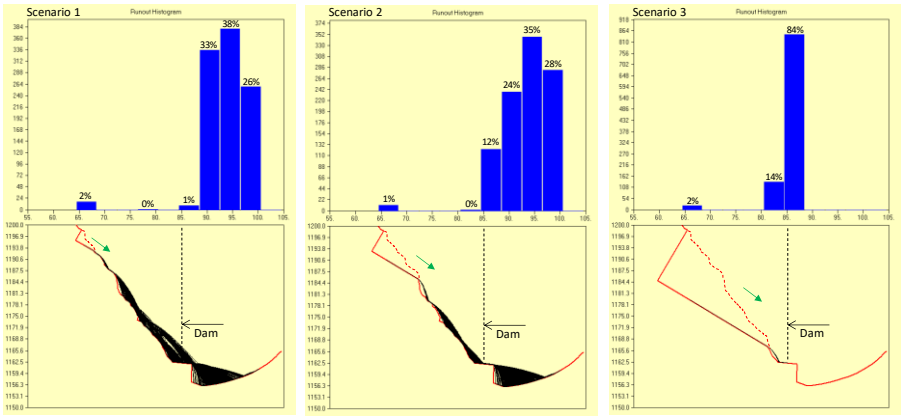

Figure 4: Trajectories of sliding wedges for the 3 scenarios

3 IMPACT RISK AND POTENTIAL DAMAGE ON THE DAM

The detailed analysis of the results of each scenario suggests that the wedges with one or two strata would most likely hit the dam, whereas larger wedges (five strata) would probably not reach the dam toe. In all cases the bounce height is below 5 m from the ground and therefore well below the gate chamber located 15 m above the dam toe.

The penetration depth in case of impact was estimated according to the NDRC method (Maurel, 2011) between 3 cm (scenario 3) and 12 cm (scenarios 1 and 2) which is “superficial” compared to the 20 m dam thickness.

4 CONCLUSION

The trajectory analysis of unstable wedges has shown a high risk of impact at the dam toe. However, the calculated bounce height and penetration depth in concrete may induce very limited and superficial damage on the dam toe. To avoid any impact on the dam, protecting structures as merlons or reinforced dykes are suitable to dissipate the impact energy of the wedges (Descoeudres, 1997).

5 REFERENCES

Mellal, A. & Hungr, O. (1998) PIERRE© – An interactive software for computer-aided rock fall analyses, University of British Columbia, UBC, Vancouver, Canada.

Maurel, Ph. (2011) Impact sur structure béton – Calcul de perforation de dalle en béton soumise à l’impact d’un projectile

Descoeudres, F. (1997) Aspects géomécaniques des instabilités de falaises rocheuses et des chutes de blocs. Société Suisse de Mécanique des Sols et des Roches, no. 135, pp.3-11.

Combined rockfall modelling and protective dam simulation

Pierre Dalban [1], Robert Pfeifer [2]

Keywords: rockfall modelling, protective embankments, dam design

1 INTRODUCTION

The rockfall simulation models currently available provide inputs about energy and rebound heights of falling blocs. In this respect, they represent very helpful tools for the dimensioning of the height, the retention capacity and the positioning of protective measures as well as to verify the protective effect they offer at a given location along the modelling profile. In the case of dams, dimensions have to be specifically defined according to the terrain specificities in order to stop the impacting bloc and to maintain the structural integrity during and after the impact. More particularly, the absorption of the impact energy by the structure as well as its propensity to be damaged or destroyed are key parameters, which can be now simulated with a new module in the modelling software ROFMOD5.

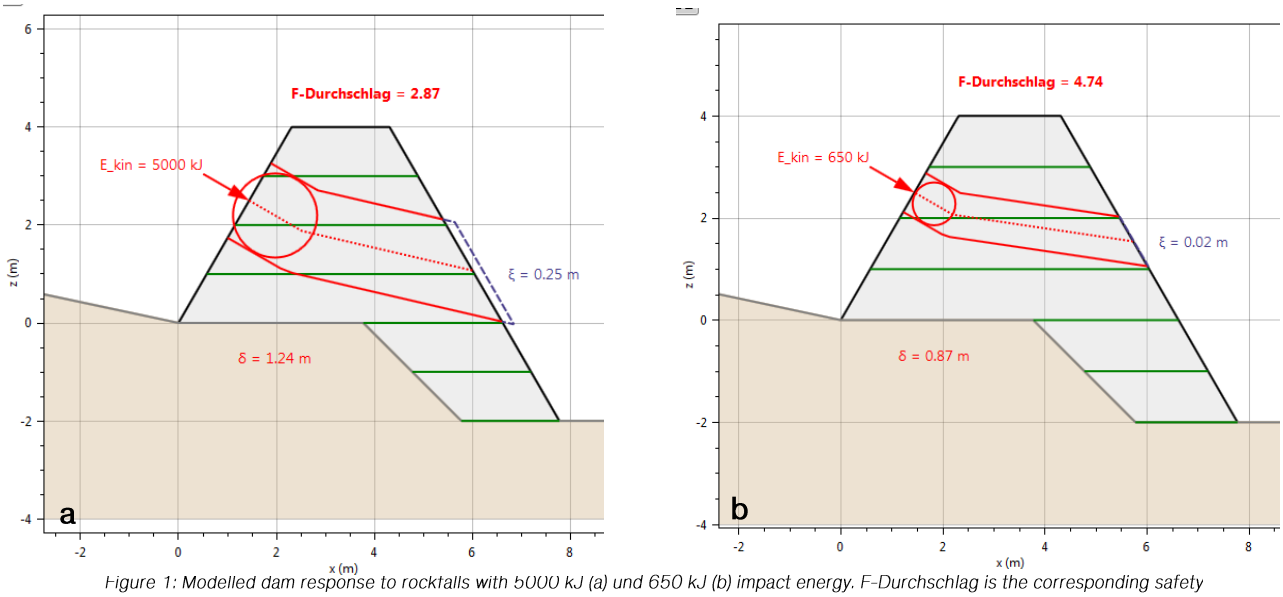

Figure 1: Modelled dam response to rockfalls with 5000 kJ (a) und 650 kJ (b) impact energy. F-Durchschlag is the corresponding safety factor and ξ the downstream deformation.

2 THE ROFMOD5 SOFTWARE

ROFMOD (Zinggeler and Pfeifer, 2009) allows to model rockfall along 2D profiles. This software has been successfully in use for over 20 years for numerous projects with very demanding modelling works. It is distinguished by an intuitive setting-up of the underground parameters (roughness and attenuation values) and enables to take into account the forest cover in a very realistic way. The latest version ROFMOD5 includes a module allowing to easily implement protective dams along the modelling profile and to directly simulate their response to the impact. The results of the simulation are given in the form of annotated diagrams with deformations values and general safety coefficients easy to interpret (see figure 1), which significantly make it easier to decide concerning the sizing and the relevance of an envisioned dam.

3 MODELLING PRINCIPLE

Among the numerous methods existing for the dimensioning of protective dams, only few allow to properly take into account the load-bearing capacity of the structure during the impact. The procedures used in practice are mostly based on static geotechnical assumptions (Hofmann and Mölk (2012)), which confine the response of the dam to a static behaviour and do not take into account damping effects due to plastic deformation. As a result, the built structures are generally characterized by very large section, which tends to contradict feedbacks from field experience as well as the results of full-scale experiments (Ronco et al, 2009). Indeed, observations of impacted dams show that structures with modest dimensions were capable to

[1] DALBAN Pierre, GEOTEST, 3052 Zollikofen, Switzerland, pierre.dalban@geotest.ch

[2] PFEIFER Robert, GEOTEST, 3052 Zollikofen, Switzerland, robert.pfeifer@geotest.ch

retain huge amount of energy. Furthermore, building smaller structures is financially advantageous and requires less space. The Dam-module implemented in ROFMOD5 is based on a rheological impact model (Kretz, 2016, Kister and Fontana, 2012). This model was designed, calibrated and validated based on full-scale experimental and natural rockfall events. It locally simulates the penetration depth by means of a viscoplastic damper and determines the downstream deformation of the dam body by taking into account the internal friction of the dam material (see figure 2). The module allows considering rockfall events involving blocks with size up to 3 x 3 x 3 m. It permits to easily set the characteristic dimensions of the envisioned protective dam and to rapidly verify their reliability with help of a safety factor.

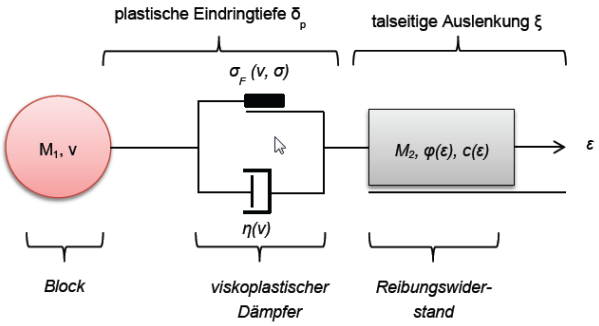

Figure 2: Description of the implemented rheological model. δ_p is the penetration depth and ξ is the downstream deformation (Source: Kretz, 2016).

4 USE OF ROFMOD5 ON CONCRETE CASES

The new Dam-module is successfully used in practice for the design of protective dams on demanding terrains, in the Swiss Alps and abroad. It allows for rapid decisions to be made and to promptly react when modifications of the envisioned dam are required. The advantages and the limitations of the model will be illustrated during the contribution through several case studies.

5 CONCLUSION

The new dam-module implemented in ROFMOD5 brings new insights for the dimensioning of protective dams and offers arguments for the size-optimization of these structures, often showed to be oversized. Practically, it allows a rapid design of protective concepts with a great flexibility in the choice of the key parameters. In the current context of growing need for construction standards, the modelling results also represent innovative inputs for discussion with the stakeholders of the sector.

6 REFERENCES

Hofmann R., Mölk M. (2012): Bemessungsvorschlag für Steinschlagschutzdämme. *Geotechnik 35, Heft 1*, Verlag Ernst & Sohn.

Kister B., Fontana O. (2012): Zu den Unsicherheiten bei der Bestimmung der Eingangsparameter für die Bemessung von Steinschlagschutzdämmen. *8. Kolloquium Bauen in Boden und Fels*. Technische Akademie Esslingen, 17. und 18. Januar 2012.

Kretz A. (2016): Bemessungsmöglichkeiten von Steinschlagschutzdämmen. Zertifikatsarbeit CAS, Berner Fachhochschule.

Zinggeler A., Pfeifer R. (2009): GEOTEST+Zinggeler rockfall modelling. Outline of the model. Zollikofen.

Ronco C., Oggeri C., Peila D. (2009): Design of reinforced ground embankments used for rockfall protection, Natural Hazards and Earth System Sciences

On four frictional mechanisms in rockfall analysis: ground deformation, surface roughness, vegetation drag and basal sliding with rebound

Andrin CAVIEZEL[1], Marc CHRISTEN[1], Guang LU[1], Werner GERBER, Yves BÜHLER[1], **Perry BARTELT (corresponding author)**[1]

Keywords: rockfall dynamics, trajectory modelling, braking mechanisms, non-smooth mechanics, friction

Real scale rockfall experiments have identified four different frictional mechanisms that are responsible for rock stopping (Caviezel et al., 2017). These mechanisms are: (1) plastic ground deformation (scarring), (2) surface roughness, (3) vegetation drag including tree stem impact and (4) basal sliding with impulsive rebound. Although each mechanism involves contact between the rock and ground (or forest), each process is governed by a unique operating principle. Terrain parameterization for rockfall modelling therefore consists in linking the observed geomorphological terrain features (and vegetation cover) to the appropriate frictional mechanism. Although this modelling step appears obvious, it is complicated by the fact that rock size plays a key role in deciding which mechanism is acting, and therefore controlling runout and dispersion. For example, the onset of plastic deformation in soil layers is largely controlled by rock size; roughness layers operate on smaller rock sizes. In this presentation, we discuss how we model rock-ground interaction within the framework of non-smooth mechanics using physically consistent constitutive models that can be verified using newly obtained experimental data.

1 NON SMOOTH MECHANICAL MODEL FOR ROCK-GROUND INTERACTION

The first part of the presentation introduces the overall physical/mathematical foundation of the RAMMS::ROCKFALL model with special emphasis on the rock-ground interaction algorithm. The ground surface in RAMMS is defined by a three-dimensional digital elevation model (DEM) with coordinates [X,Y,Z]. At each location [X,Y] we define a local Z-coordinate measured relative to the elevation Z. The DEM therefore defines the $z = 0$ surface where we define terrain properties governing rock-ground interaction. Four different frictional layers can be specified relative to the z = 0 surface: 1) the *roughness* layer, 2) the *scarring or plastic deformation* layer, 3) the *forest* layer including both the canopy drag layer and discrete tree stem and finally 4) the *hard contact* layer or *rebound* layer (Figure 1). The roughness and forest layers are located *above* the digital elevation model $z > 0$, while the scarring and rebound layers are located below the DEM, $z < 0$. Because the rock is represented as a three-dimensional, convex, polyhedral rigid-body (see Leine et al., 2014), the z-location of the rock is either defined by the location of the rock's center-of-mass z_r or the location of the rigid-body surface.

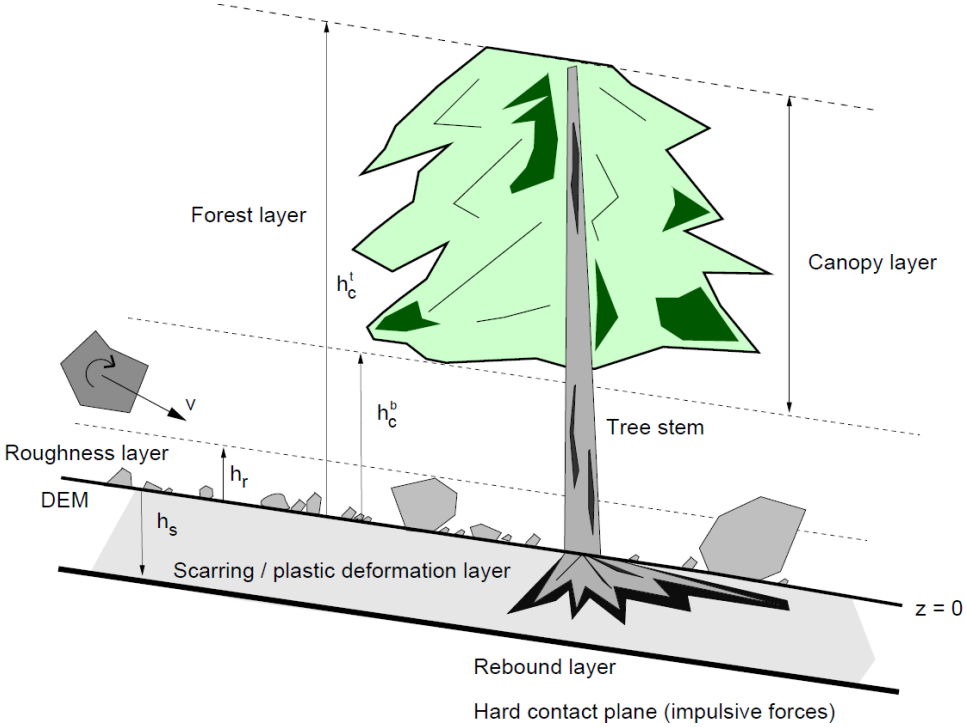

Figure 16: The three-dimensional DEM surface defines the local z=0 coordinate system which we use to define frictional parameters. Four layers are defined: 1) the roughness *layer, 2) the* scarring or plastic deformation *layer, 3) the* forest *layer including both the canopy drag layer and discrete tree stem and finally 4) the* hard contact *layer or* rebound *layer.*

[1] CAVIEZEL Andrin , CHRISTEN Marc, LU Guang, GERBER Werner, BÜHLER Yves, BARTELT Perry, WSL Institute for Snow and Avalanche Research SLF, Davos Dorf, Switzerland (ISO 3166-2:CH), bartelt@slf.ch

2 ROUGHNESS LAYER AND GROUND SCARRING

The roughness and scarring layers are defined by the two layer heights, h_r and h_s (Figure 2). When the rock's center-of-mass z_r enters either the roughness layer ($z_r > 0$ and $z_r < h_r$) or the scarring layer ($z_r < 0$ and $z_r > -h_s$), a rigid-body drag D operates on the rock. For example, for the roughness layer we have

$$D_r^T = d_r^T \cdot v \cdot \|v\| \text{ and } D_r^R = d_r^R \cdot \Omega \cdot \|\Omega\| \qquad (1)$$

where v is the total translational velocity and Ω the total rotational velocity of the rock. The coefficients (d_r^T, d_r^R) parameterize the drag forces. The same velocity squared dependent drag terms are used for the scaring layer, but with different drag coefficients. The roughness and scarring layers do not change the direction of the rock, but only serve to reduce the translational and rotational velocity of the rock.

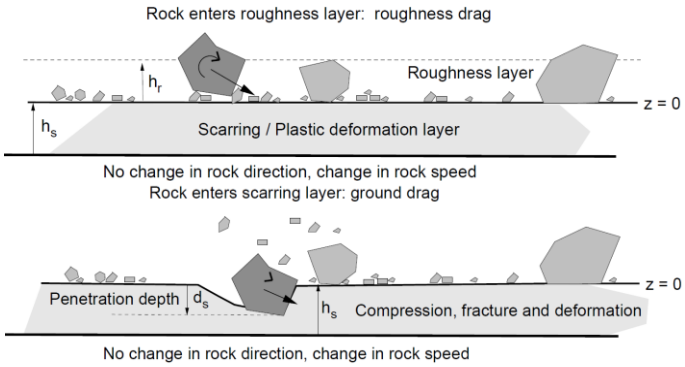

Figure 2: Definition of roughness and scarring layers. These layers serve to reduce the translational and rotational speed of the rock, not change the rock's direction.

3 BASAL SLIDING WITH REBOUND

At the distance h_s the ground layer can no longer deform and the rock can no longer continue to move in the same direction. The rock experiences a hard boundary and begins to rebound. The rebound process is governed by contact forces applied to the rock surface. During the rebound process (change in direction) it is possible that the rock slides on the rebounding surface. Frictional resistance is provided by a Coloumb-type law (Leine et al., 2014). The sliding distance s (Figure 3) governs the increase in sliding friction $\mu(s)$:

$$\mu(s) = \mu_{\min} + \frac{2}{\pi}(\mu_{\max} - \mu_{\min})\arctan(\kappa \cdot s) \quad \dot{s} = \begin{cases} \|v_s\| \\ -\beta s \end{cases} \qquad (2)$$

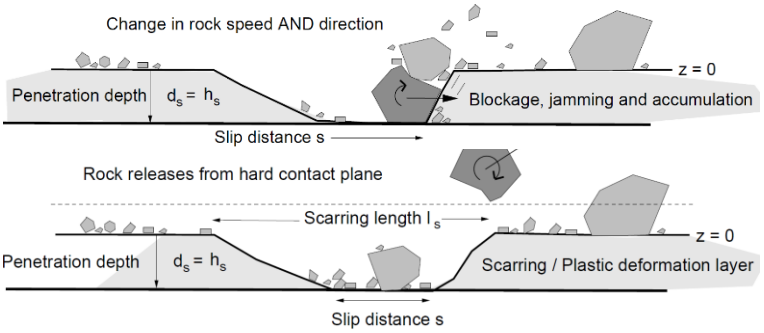

Figure 17: At the distance hs below the DEM surface there exists a hard rebound plane. This plane is created when ground material can no longer deform. As the rock is rebounding (changing direction) sliding frictional forces act on the rock.

The parameters κ and β control the change in friction from $\mu_{\min}$ to $\mu_{\max}$ and thus define the jamming properties of the soil scar.

4 CONCLUSION

The surface complexities of natural slopes require rockfall models that account for different frictional mechanisms: roughness, ground deformation and basal sliding. These mechanisms introduce scaling effects (rock size, rock shape) into the rockfall problem that cannot be adequately treated with simple rebound models. Although we have presented a general model that can be used to parameterize a wide range of terrain types, extensive experimentation is still required.

5 REFERENCES

Caviezel, A., Schaffner, M., Cavigelli, L., Niklaus P., Bühler, Y., Bartelt, P., Magno, M. & Benini, L. (2017). Design and evaluation of a low-power sensor device for induced rockfall experiments. IEEE Transactions on Instrumentation and Measurement PP(99): 1-13.

Leine, R.I., Schweizer, A., Christen, M., Glover, J., Bartelt, P. & Gerber, W. (2014) Simulation of rockfall trajectories with consideration of rock shape. *Multibody System Dynamics* 32: 241-271.

Landslide displacement tracking using radio-frequency identification

Mathieu LE BRETON[1,2], Laurent Baillet[1], Eric Larose[1], Etienne Rey[1,2], Philippe Benech[3], Denis Jongmans[1], Fabrice Guyoton[2]

Keywords: landslide, RFID, monitoring, displacements, velocity

Structures prone to slow motions, such as landslides, volcanoes, and civil infrastructures often need to be monitored to track their stability. Those structures typically move from a few centimeters to a few meters over a year, requiring an accuracy of ten centimeters or less per year. There are already solutions available to track this motion, such as wire extensometers (Angeli *et al.*, 2000), differential GPS (Gili *et al.*, 2000), optical laser (Travelletti *et al.*, 2012), lidar (Abellàn *et al.*, 2009), radar interferometers (Herrera *et al.*, 2009), or radar nodes (Kennedy *et al.*, 2009). However, passive RFID tags localization (Miesen *et al.*, 2011, Nikitin *et al.* 2010) offers a lower-cost alternative in terms of installation and maintenance. Moreover, real-time monitoring of tag grids can provide dense data, both in space and time, at reasonable cost.

1 MATERIAL AND METHODS

1.1 INSTRUMENTATION OF PONT-BOURQUIN LANDSLIDE

The material used in the experiments is presented in Figure 1. We used an off-the-shelf, monostatic interrogator with four channels, controlled by a custom software, running on an embedded computer. The interrogator used 865-868-MHz carrier frequencies, and was connected to a radome-protected panel antenna through a phase-stable coaxial cable. It acquired the RSSI and the phase shift while identifying the tags. Each embedded tag consisted of a quarter-wavelength patch antenna, connected to a battery-assisted chip, protected by a hard-plastic casing. The tags are deployed on the moving area of the landslide and are supported by 0.9-m-high fiber-glass stakes. The radome-protected panel antenna is attached on a tree located on the right stable bank of the landslide (Fig. 1). This system was designed to reduce the phase drift from meteorological factors, based on guidelines from (Le Breton *et al.*, 2017).

The position of the tags and base antenna was measured at 3 different dates with an infrared laser theodolite with millimetric precision, and a wire extensometer, extendend by a 10-m kevlar wire, attached within 1 meter of the RFID instruments.

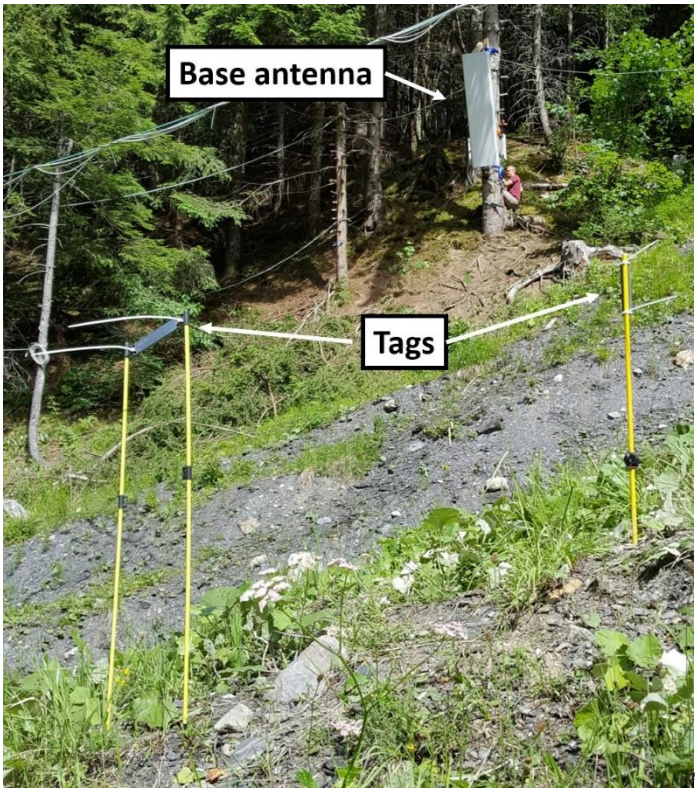

tags are on the landslide.

1.2 PRINCIPLES OF PHASE-BASED DISPLACEMENT TRACKING

In free space, the phase shift (Nikitin *et al.* 2010) related to the direct propagation of a two-way backscattered wave is given by

$$\varphi_{air} = -\frac{4\pi f}{v} d \quad (1), \text{ where :}$$

φ_{air}	phase resulting from the propagation in the air;
d	distance between the base and the tag;
v	RF wave velocity in the medium;
f	carrier frequency.

The relative variations of the phase across time, measured by the base station, is converted as a relative displacement of the tag.

[1] ISTerre, Université Grenoble Alpes, CNRS, France (38000), firstname.lastname@univ-grenoble-alpes.fr

[2] Géolithe, Crolles, France (38920), firstname.lastname@geolithe.com

[3] IMEP-LAHC, Université Grenoble Alpes, Grenoble, France (38016), fisrstname.lastname@minatec.grenoble-inp.fr

2 RESULTS

2.1 VALIDATION WITH OPTICAL AND MECHANICAL TECHNIQUES

In order to validate the technique of RFID displacement tracking, it is compared on a real landslide over 5 months, with a mechanical automatic extensometer, and theodolite topographic levees. The sample period of the two curves is one hour (averaged) for the wire extensometer and RFID, and about two months for laser theodolite. The results are presented on Fig. 2, which shows that extensometric, optical and RFID displacement measurements are coherent. The extensometer progressively cumulates a negative offset of up to 5 centimetres, due to a small differential effective motion between the stakes supporting the tag and the extensometer (identified by theodolite levees).

The RFID tracking shows a better continuity and accuracy of values in time, compared to the wire extensometer.

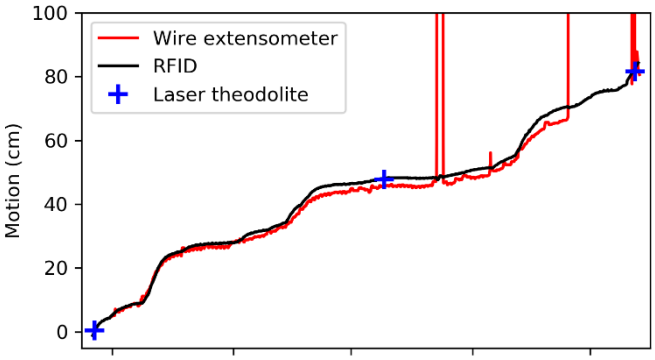

Fig. 2. Cumulative displacement of Pont-Bourquin landslide, measured for five months by a Radio-Identification tag, a wire extensometer, and a laser theodolite.

2.2 ENVIRONMENTAL EFFECTS ON VELOCITY MEASUREMENTS

MeteoSuisse acquisitions provided the daily fall of fresh snow (Diablerets village, 1-km away), the rainfall and atmospheric parameters (Col des Mosses, 6-km away). Figure 3 correlates the velocity motion (derived from figure 2) of the tag with extensometer velocity and rain fall or snow height.

The better continuity and accuracy of the RFID method is especially significative during the snow periods where the wire of the extensometer is grounded by the weight of the snow, and therefore useless (see around 20th october or end of november/beginning of december period).

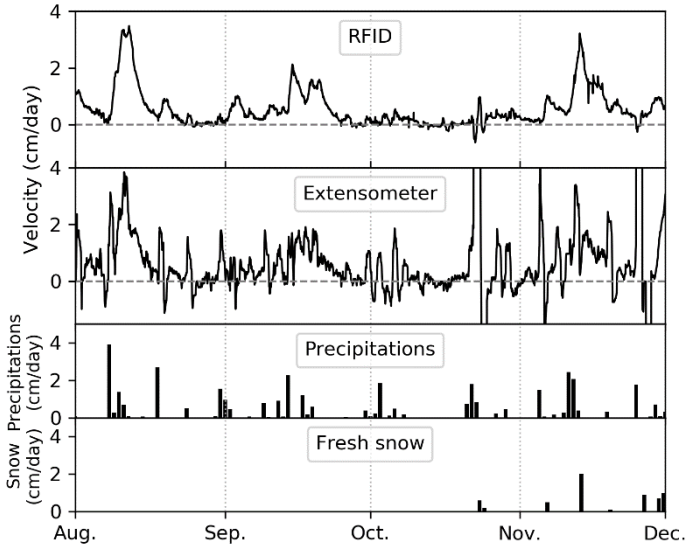

Fig. 3. Comparison of velocities, after filtering daily variations, between RFID and extensometer, along with rainfall, and snow height.

3 CONCLUSION

RFID displacement tracking provides an interesting alternative for the monitoring of slow motion structures, such as landslides, volcanoes or civil infrastructures, at a reasonable cost. It appears less sensitive to environmental conditions such as snow falls compared to classic wire extensometers or optical methods (laser, lidar, photogrammetry).

4 AKNOWLEDGEMENT

The authors want to thank Géolithe, the ANRT, the Labex OSUG@2020, the VOR program from Univ. Grenoble-Alpes, and Tagsys, for their support.

5 REFERENCES

Abellán, A., Jaboyedoff, M., Oppikofer, T. & Vilaplana, J. M. (2009) Detection of millimetric deformation using a terrestrial laser scanner: experiment and application to a rockfall event. Nat. Hazards Earth Syst. Sci. 9, 365–372.

Angeli, M.-G., Pasuto, A. & Silvano, S. (2000) A critical review of landslide monitoring experiences. Engineering Geology 55, 133–147.

Gili, J. A., Corominas, J. & Rius, J. (2000) Using Global Positioning System techniques in landslide monitoring. Engineering Geology 55, 167–192.

Herrera, G. et al. (2009) A landslide forecasting model using ground based SAR data: The Portalet case study. Engineering Geology 105, 220–230.

Kenney, J. D. et al. (2009) Precise positioning with wireless sensor nodes: Monitoring natural hazards in all terrains. in IEEE Int. Conf. Systems, Man and Cybernetics 722–727.

Le Breton, M. et al. (in press) Outdoor UHF RFID : Phase Stabilization for Real-World Applications. Journal of Radio-Frequency Identification.

Miesen, R. et al. (2011) Where is the Tag? IEEE Microwave Magazine 12, S49–S63.

Nikitin, P. V. et al. (2010) Phase based spatial identification of UHF RFID tags. in IEEE Int. Conf. RFID 102–109.

Travelletti, J. et al. (2012) Correlation of multi-temporal ground-based optical images for landslide monitoring: Application, potential and limitations. ISPRS Journal of Photogrammetry and Remote Sensing 70, 39–55.

Using InSAR to map slope instability over the French territory

Fifamè KOUDOGBO (corresponding author) [1], Anne URDIROZ [2], Frédéric ADRAGNA [3], Philippe DURAND [4], Marie-Aurélie CHANUT [5], Alessandro FERRETTI [6], Fabrizio NOVALI [7]

Keywords: Ground motion measurement, SAR Interferometry, slope instability, SqueeSAR™

1 INTRODUCTION

With the launch by European Space Agency of the Sentinel-1 mission, which offers free access to satellite data, initiatives are emerging in order to propose ground motion measurement based on InSAR (SAR Interferometry) advanced technique known as the Persistent Scatterer Interferometry (or PSI) into the Copernicus service portfolio. Overall transnational collaborations are considered on the bases of experiences led at the national level, in Italy, in Germany or in Norway for example.

It is in this framework that the development of a European ground motion service was officially proposed. The service, initially called Supra-National Ground Motion Service, was presented for the first time in November 2016 in BGR (Federal Institute for Geosciences and Natural Resources) Hanover. It consists in providing consistent, regular, standardized, harmonized and reliable information regarding natural and anthropogenic ground motion phenomena over Europe and across national borders. The main objective is to measure, with millimetre accuracy, ground displacements, including slope instabilities. The ground motion measurement is derived from time series analyses of Copernicus Sentinel-1 data using advanced radar interferometry approach called Persistent Scatterer Interferometry, together with Global Navigation Satellite Systems (GNSS) and other in-situ observations. The ground motion service will also provide tools for visualization, interactive data exploration and user uptake elements (protocols and best practice examples) for further ground investigations, implemented through related-application tools and downstream services.

As a precursor of such a service, the French Space Agency CNES - Centre National d'Etudes Spatiales - launched a pilot project over the whole metropolitan French Territory. The company TRE ALTAMIRA was appointed to process 3-year ascending and descending Sentinel-1 data; the results show the motion of hundreds of millions of stable scatterers distributed over the considered area of 551 500 km².

2 INSAR FOR SLOPE STABILITY MONITORING

InSAR data are now commonly used for a variety of purposes, such as landslide detection and mapping (Herrera et al. 2011; Cigna et al., 2013), monitoring and modelling, hazard and risk assessment (Lu et al. 2014) and, through time series analysis, for the identification of changes in deformation rates and seasonal trends. So far, the long revisiting time and the limited access to satellite radar data suitable for interferometric analyses have been the main limitations to the use of SAR sensors as a tool for monitoring ground deformations over wide areas. Over the last decade, with the launch of new constellations of satellites, the acquisition frequency increased to the point of making satellite InSAR suitable for displacement monitoring. This is particularly useful in the case of risks associated to slope instabilities where the detected motion can also be used for early warning purposes. To this end, ESA Sentinel-1A and B satellites can be considered a breakthrough. They allow for large-scale mapping, with short revisiting times (6 days, when both sensors are active over the same area) and quite good spatial resolution (Geudtner et al. 2014). The enhanced temporal resolution of Sentinel-1 compared to all previous ESA (European Space Agency) missions and the regularity of the acquisitions are now paving the way to the use of InSAR data for early detection of movements in places where ground-based monitoring is sometimes inapplicable.

Ground displacement measurement is based on the use of the SqueeSAR™ technique. SqueeSAR™ is the proprietary multi-interferogram technique patented by TRE ALTAMIRA, the largest InSAR group worldwide and part of the Collecte Localisation Satellite (CLS) Group. The methods belong to the persistent scatterer interferometry (PSI) family and is based on the processing of long temporal series of co-registered SAR images, acquired over the same target area from the same acquisition geometry. The SqueeSAR technique allows for the measurement of surface displacements by exploiting both point-wise coherent scatterers (i.e., the persistent scatterers - PS) and partially coherent distributed scatterers (DS) (Ferretti et al. 2001). This

[1] KOUDOGBO Fifamè, TRE ALTAMIRA S.L., Barcelona, Spain (ES), fifame.koudogbo@tre-altamira.com

[2] URDIROZ Anne, TRE ALTAMIRA S.L., Barcelona, Spain (ES), anne.urdiroz@tre-altamira.com

[3] ADRAGNA Frédéric, CNES, Toulouse, France (FR), frederic.adragna@cnes.fr

[4] DURAND Philippe, CNES, Toulouse, France (FR), philippe.durand@cnes.fr

[5] CHANUT Marie-Aurélie, Cerema Centre-Est, Bron, France (FR), marie-aurelie.chanut@cerema.fr

[6] FERRETTI Alessandro, TRE ALTAMIRA s.r.l., Milan, Italy (IT), alessandro.ferretti@tre-altamira.com

[7] NOVALI Fabrizio, TRE ALTAMIRA s.r.l., Milan, Italy (IT), fabrizio.novali@tre-altamira.com

approach provided a significant increase in spatial density of the total Measurement Points (MPs), with respect to the traditional PSI techniques, especially in the case of vegetated scenarios, enabling a much better understanding of possible ground deformation over a specific area of interest.
The results are displayed in the form of a deformation map showing the magnitude of the movement, which is measured in the Line of Sight (LOS) direction. Information on deformation velocity is given in mm per year from a scale varying from red to blue, depending on the orientation and intensity of the movement. Displacement time series (TS) representing the evolution of the MP's displacement for each acquisition date are also provided.

3 THE RESULTS OF THE ANALYSIS

Overall, about 7600 Sentinel-1 images acquired from October 2014 to October 2017 are processed in order to generate information on ground motion over the whole French Territory. Satellite image acquisitions in ascending and descending modes are moreover considered in order to guarantee the maximum visibility in mountainous areas providing an unprecedent ground motion cartography at national scale level (Figure 18). The presentation will focus on a landslide identified close to Saint-Jean-de-Maurienne sector and will involve Cerema Centre-Est for useful contextual information.

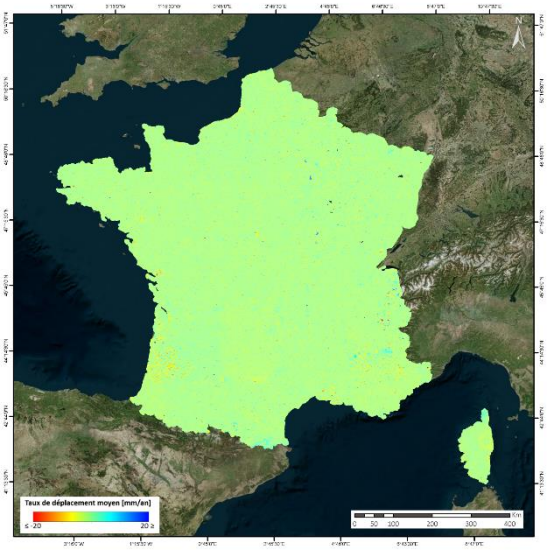

Figure 18: Ground motion map extracted from the SqueeSAR™ processing of the Sentinel-1 data acquired in ascending mode from October 2014 to October 2017.

4 PERSPECTIVES

The results obtained will allow for the assessment of the benefit of implementing a European Ground Motion Service. Key players from the institutional and private sector will be involved to compare results with existing ground motion information obtained by classical in-situ auscultation and to propose valuable recommendations for the service definition.

5 REFERENCES

Cigna F, Bianchini S, Casagli N (2013). How to assess landslide activity and intensity with persistent scatterer interferometry (PSI): the PSI-based matrix approach. *Landslides* 10(3): 267–283.

Ferretti A, Fumagalli A, Novali F, Prati C, Rocca F, Rucci A (2011). A new algorithm for processing interferometric data-stacks: SqueeSAR. *IEEE Trans Geosci Remote Sens* 49(9):3460–3470.https://doi.org/10.1109/TGRS.2011.2124465.

Geudtner D, Torres R, Snoeij P, Davidson M, Rommen B (2014). Sentinel-1 system capabilities and applications. *Proceedings of the In Geoscience and remote sensing symposium (IGARSS)*. IEEE International, Quebec, pp. 1457–1460.

Herrera G, Notti D, García-Davalillo JC, Mora O, Cooksley G, Sanchez M, Arnaud A, Crosetto M (2011). Landslides analysis with C- and X-band satellite SAR data: the Portalet landslide area. *Landslides* 8: 195–206.

Lu P, Catani F, Tofani V, Casagli N (2014). Quantitative hazard and risk assessment for slow-moving landslides from Persistent Scatterer Interferometry. *Landslides* 11(4): 685-696.

Influence of block shapes and sizes on the variability of DEM trajectories

Bruna GARCIA[1,2], Dominique DAUDON[2], Pascal VILLARD[2], Vincent RICHEFEU[2], Julien BAROTH[2]

Keywords: Discrete Element Model, Block Shape, Block Size, Trajectory, Variability.

1 INTRODUCTION

The correct design of protective structures and prediction of run-out of rock masses is crucial to ensure safety of highways, rail roads and populated areas that are affected by gravity hazards, in particular rock avalanches and rockfalls. The design of protective structures can be optimized if the main characteristics of a predicted event (*e.g.*, block trajectories and impact energies) are improved. The shape of an isolated boulder has a major influence on its trajectory, but it is not always explicitly taken into account in usual trajectory-analysis tools. Generally, the codes used in engineering offices consider variability in the rebound parameters and still make an extensive use of calculations based on the free-flight equations of a lumped mass (in other words, a point with a mass) (Bourrier et al., 2009; Cuervo, 2015). As a consequence, these works generally introduce a Monte-Carlo type approach in which the impact parameters are varying. The main interest of the discrete elements method (DEM) is to include the actual shape of boulders and therefore the variability is somehow naturally introduced at each rebound, considering the multiples possibilities of interaction between the hilly slope and the complex shape of the boulder. This work intends to evaluate the ability of the DEM to predict the variability in trajectory of a single boulder by considering various block shapes and sizes.

2 NUMERICAL TOOL

The numerical tool used is a three-dimensional discrete element code that takes into account frictional and collisional dissipation mechanisms. A block is modeled by a spheropolyhedron that is the shape resulting from the sweeping of a sphere onto the surface of a polyhedron. This allows us to employ realistic shapes and to optimize the contact detection algorithm (Richefeu & Villard, 2016). The same type of discretization was used to define the digital terrain model (DTM). The interaction laws are specific and they have been thought in order to make the physical parameters easily assessable by optimizing an inverse problem applied to experimentally measured 3D-trajectories. Also, the number of parameters was purposely limited for the sake of simplicity, and because the role of the block shapes was intuited to be great. The main parameters involved in a collision are the normal, tangential and rolling elastic-stiffnesses k_n, k_t and k_r, respectively, and the associated dissipation coefficients, namely: (*i*) the kinetic energy restitution e_n^2 in the normal direction, (*ii*) the tangential dissipation coefficient μ that relates to the friction and/or to the plasticity of the soil, and (*iii*) the rolling dissipation coefficient μ_r that acts analogously to μ but for the rolling movements. Notice that, since e_n^2 reflects the amount of energy restored in the perpendicular direction to the contact plane at each bounce, it can be thought of as the ratio of trajectory heights for vertical drop of a block on a horizontal plane (Mollon et al., 2012; Chau et al. 2002). These parameters can be obtained either by *in-situ* or laboratory bounce tests. In any case, the optimization criteria is based on the comparison of the experimental and the numerical output velocities (in translation and rotation obtained using cameras and numerical computation, respectively (Garcia et al., 2017).Table 1 gives the two sets of parameters estimated, using a single camera, in the field using a concrete-made boulder of 15 kg and considering two types of soil (soft and hard). Considering that the mass of the boulders are smaller than real ones and that was not possible to reconstruct the 3D-trajectories, the parameters obtained in Table 1 are only used to obtain qualitative results.

Table 1: Parameters deduced using the calibration process

	k_n (N/m)	k_t (N/m)	k_r (Nm/rad)	e_n^2	μ	μ_r
(Soft soil - dark grey)	10^7 3.6×10^7	10^7	0.01	0.70	0.18	
(Hard soil - light grey)	10^7	10^8	10^8	0.11	0.30	0.00

3 APPLICATION TO A REAL CASE

To appreciate the variability in trajectory of a boulder launched from quite similar positions, various numerical simulations were performed for two blocks of different shape and size. The hillside geometry of an open-mine pit has been reconstructed by LiDAR scanning (Bourrier et al., 2017) to obtain a DTM with a precision of about 0.5 m. The similar 3D-reconstruction method

[1] IMSRN (Ingénierie des Mouvements de sol et des Risques Naturels), bruna.garcia@imsrn.com

[2] Univ. Grenoble Alpes, 3SR, CNRS UMR 5521, Grenoble, France.

was employed to obtain the numerical shapes (3D mesh surfaces) of the two blocks (100 L and 500 L) from the stereo-correlation of a number of photographs. Two areas of different natures were considered in the DTM: dark grey areas are mainly soft soil, presenting rather important rolling resistance, while light grey represents a harder soil presenting a slightly higher restitution coefficient. The parameters used as a first attempt were those of Table 1. Results were plotted and analyzed in order to study the deviation and the variability of each trajectory while changing the size and the shape of blocks (and as a consequence the initial potential energy) before the real-size tests were performed in the framework of the National Project

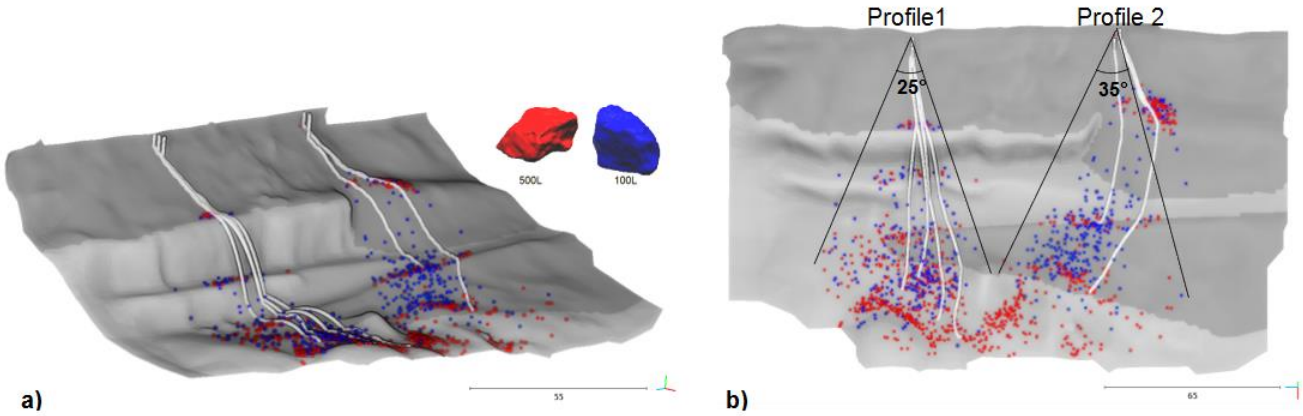

Figure 1: Top view (a) and 3D view (b) of the stop positions of the blocks: the smallest ones (100 L) are displayed in blue and the biggest ones (500 L) are colored in red. The white curves are some selected trajectories. The 3D view highlights that the blocks mainly roll over the soft terrain (dark gray); they are more prone to bounce in a harder soil (light gray).

C2ROP.

4 RESULTS AND CONCLUSIONS

Using the same set of parameters, trajectories of the two scanned blocks were computed on the DTM. As shown in Figure 1, the variability in the trajectories of the blocks is rather marked although no randomness has been introduced in the collision. A large deviation of run-out paths and distances were observed in the field and it appears narrower for the small blocks. It is noticed that for the same release point and block shape, changing the release orientation of the block has a great influence in the variability of the trajectories. The same is observed if we only change block position and keep orientation and shape unchanged. Coupling both cases of changing position and orientation leads to a deviation of the trajectory of about 20°±5° for the Profile 1 and 30°±5° for the Profile 2.

Further studies are being conducted to enlighten the process of energy dissipation of the block and to demonstrate that boulder rotations play a major role in real rockfall events.

REFERENCES

Bourrier, F. Dorren L., Nicot F., Berger F., 2009. Toward objective rockfall trajectory simulation using a stochastic impact model. Geomorphology Volume 110, Issues 3- 4, 15 September 2009, pp. 68-79.

Chau KT, Wong R.H.C., Wu J.J., 2002. Coefficient of restitution and rotational motions of rockfall impacts; International Journal of Rock Mechanics & Mining Sciences 39 (2002), pp. 69-77.

Cuervo, Y.-S., 2015. Modélisation des éboulements rocheux par la méthode des éléments discrets: application aux évènements réels. PhD thesis, 2015, University of Grenoble Alpes.

Garcia B. ,Villard P., Richefeu R., Daudon D, 2017. Experimental and DEM analysis of the dissipation involved in the collision of a boulder with a substratum EPJ Web Conf. 140 16010 (2017) DOI: 10.1051/epjconf/201714016010.

Mollon G., Richefeu V., Villard P., Daudon D., 2015. Discrete modelling of rock avalanches: sensitivity to block and slope geometries. Granular Matter.

Benchmark of trajectory analysis models

Consortium of task A3 "Benchmark analyse trajectographique" of C2ROP project[1]

Keywords: propagation, trajectory analysis, benchmark, experiments

A benchmark of trajectory analysis methodologies was held in the project C2ROP. The benchmark protocol, built from a collaborative approach, was dedicated to assess the capacity of trajectory analysis methodologies to design efficient structures for the protection of linear stakes. The objective is to identify general recommendations for the improvement of simulation works and for the assessment of the accuracy of these works.
In a study site, located in a quarry, predictive simulations of block propagation have been performed. Block release experiments were then held for the comparative analysis of the distributions of the block velocities, passing heights and passing percentages obtained in the simulations and in the experiments.

1 INTRODUCTION

Block propagation simulations are classically used for rockfall hazard zonation or protection structures design. The results from these simulations are potentially sensitive to the type of block propagation models used, on the expertise of the operator, and on the data available in the study site. As a consequence, it can be highly difficult for the decision makers to evaluate the relevance of the simulations works they receive.
In the project C2ROP, a benchmark of several trajectory models and methodologies was held to provide helpful information to the decision makers and the practitioners for the assessment of the quality of simulations works. This benchmark was also dedicated to make a critical comparative analysis between the existing tools and methodologies in order to identify general recommendations to improve simulation practices. The development of the benchmark protocol was based on a collaborative approach that consisted in the joint definition, by the members of the benchmark operation, of common objectives, study site specifications, and protocols for the experiments, simulations and comparative analysis.
The members decided that the general objective of the benchmark was to evaluate and compare the capacity of different trajectory analysis methodologies to design efficient structures for linear stakes protection. For that purpose, a study site was first identified to emphasize classical difficulties encountered by block propagation models, e.g. 3D effects and large slope changes. The members of the operation provided predictive simulations of block propagation in the study site. After all simulation results were provided, block release experiments have been done in the study site to perform a comparative analysis between the numerical and experimental results.

2 STUDY SITE

A study site with significant topographical complexity, slope changes and 3D effects in particular, and with linear stakes in the downhill part was chosen. As the aim of the study is the design of protection structures, the simulation results and experimental measurements focused on the assessment of the block passing percentages and distributions of blocks trajectories on specific locations of the site.

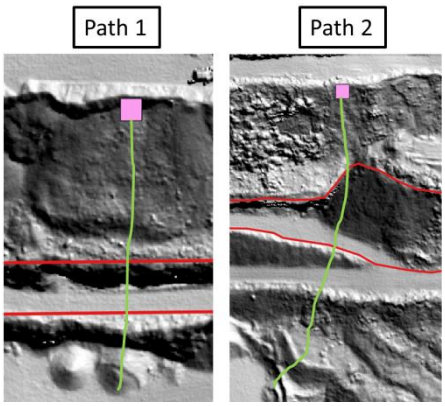

Figure 1: Top view of the propagation paths. The pink squares correspond to the block release zones, the red lines to the block trajectory assessment zones and the green lines to typical block trajectories.

[1] Corresponding author : Franck Bourrier, Irstea Grenoble, franck.bourrier@irstea.fr

The study site is a quarry located in Authume (39 - France). Two propagation paths were chosen. The first path is characterized by uphill slope of 32° overhanging two successive rock walls separated by a flat track. The difficulty in the prediction of block propagation along this path is related with the potential variability of block trajectories when passing over the two rock walls. The second path is characterized by an uphill slope of 32° that overhangs a narrowing area between a rockwall and a talus slope. The bottom part of this path is made of two successive slightly sloping tracks. This path was chosen because of potentially substantial 3D effects due to the narrowing and to the presence of two successive sloping tracks.
100 rocks, with weights ranging from 180kg to 1750kg, were selected for the block release experiments.

3 TRAJECTORY ANALYSIS

A digital terrain model (DTM), built using photogrammetry techniques with resolution of 0.2m, GIS data, that characterize the block release zones and block trajectory assessment zones, and pictures of all the released blocks were provided to the members of the operation.
The expected output were the detailed description of the trajectory analysis model and methodology, the predictive results of the percentages of passing blocks and distributions of the block trajectories (velocity and passing heights) at specific trajectory assessment zones. A design of protection solutions from the simulations results with the aim to protect the linear stakes, i.e. the downhill tracks, was also expected.
17 block trajectory analyses have been collected. A large range of block propagation models were used: 2D models (11 studies) and 3D models (5 studies) based on modelling of the block as a material point, a 3D model based on a Discrete Element Method (1 study).

4 EXPERIMENTS

The experimental protocol consisted in the release of 50 blocks on each propagation path. The successive releases from fixed release heights were filmed by two video cameras and all stopping points were measured. The analysis of the picture extracted from the videos and their projection on the DTM allowed measuring the 3D velocities and passing heights of each block in the block trajectory assessment zones.
The results from the experiments are thus the percentages of passing blocks and the distributions of the block velocities and passing heights in the block trajectory assessment zones.

5 PERSPECTIVES

The comparative analysis between the predictive simulations and the experimental results will allow evaluating the accuracy of the different trajectory analysis models and methodologies with the objective to identify general recommendations for the improvement of simulation works.
A second phase of the benchmark will consist in providing part of the experimental results, i.e. results from 5 to 10 block releases on each propagation paths, to the members of the operation so that they can update their simulation results. This second phase will allow analyzing the accuracy of simulation results in a more realistic context where a limited number of rockfall events is known.
A third phase will aim to discuss the sensitivity of simulations results to uncertain input parameters. Finally, general recommendations will be proposed, in connection with the other partners of C2ROP project.

Applications of 3D laser scan data for slope characterization and stability analysis

Thomas Richard (INERIS) [1], Marwan Al Heib [2] (INERIS), Stella Coccia [3] (INERIS)

Keywords: TLS, landslide, stability analysis, numerical modelling, open pit mine

In the framework of the RFCS (Research Fund for Coal and Steel) European Project SLOPES (Smarter Lignite Open Pit Engineering Solutions) INERIS used short-range laser scan (FARO Focus3D X330, 0.6-330 m range with ranging error is ± 2 mm) to scan instabilities in a small abandoned French coal mine. One of the main objectives of this project was to evaluate the capacity of terrestrial laser scan (TLS) for slope stability analysis within a lignite mine. The INERIS results of laser scan were also integrated to carry out a 3D numerical modelling. Results of the numerical modelling and laser scan were compared to existing displacement measurements.

1 TEST SITE AND OBJECTIVES

The French coal open-pit mine "Fosse Padène" is one of the latest open pit coal mine located in the city of Graissessac (about 80 km west of Montpellier, Figure 19). This mine was excavated between 1960's and 1990's. The open pit is now over the underground mine and is divided into two faces: North and East. The cliffs were not traced and the pit was not backfilled. In addition, the dump of coal materials has a high slope angle. Consequently, this open pit has several types of instability: rock falls at cliff level, deep or superficial slides in the coal deposits and coal deposits erosion. INERIS choses this abandoned mine to evaluate TLS regarding four points of interest: Backfills, East face, North face and one landslide (located in open pit deposits).

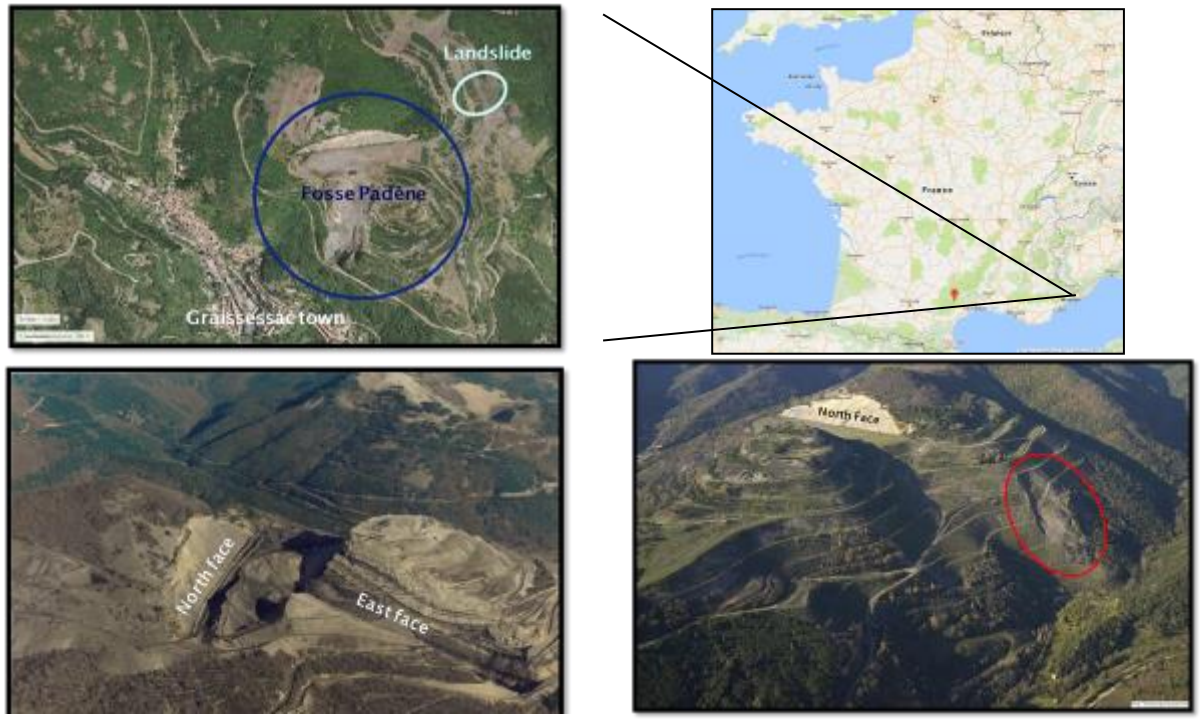

Figure 19 : Location of "Fosse Padène", North-East of Graissessac town

The objectives of using 3D laser scanner technology are to collect geometric and geotechnical data related to the fracturing of rocky slopes and mass displacement for coal mine deposits. 10 measurement stations were positioned into the pit and they were located from 50 m to 200 m from the fronts. Then, dataset was integrated into a numerical model to analyse instabilities.

2 RESULTS

For the 1st point of interest (East face) TLS application: structural geological framework realisation

On the field, this face is the most impressive because each coal layers could be directly observed. For this reason, a geological interpretation was directly performed from the 3D points cloud, and the pseudo-colour interpretation helped to determine geological layers. The result of this data processing was a structural geological framework.

[1] Thomas RICHARD, INERIS, Verneuil-en-Halatte, France, thomas.richard@ineris.fr

[2] Marwan AL HEIB, INERIS, Nancy, France, marwan.alheib@ineris.fr

[3] Stella COCCIA, INERIS, Nancy, France, stella.coccia@ineris.fr

For the 2nd point of interest (North face) TLS application: discontinuity identification

This face is characterized by several faults analysed thanks to the 3D dataset. Some dip measurements were noted, in a non-man-accessible area, directly form the points cloud. This last data allowed to build a stereogram and to identify discontinuities families. Three families were identified.

For the 3rd point of interest (Dump) TLS application: dip identification

No degradation was observed in the upper part of the dump while, in the lower part, several ravines were observed. Moreover, the Fosse Padène geometry forms a bowl that concentrate all the rainwater. Using the 3D dataset backfills, slopes were analysed to understand the active erosion in the lower part. It appears that the slopes are from 30° to 40° dip at the bottom of the dump, whereas they are about 20° to 30° at the top.

4th point of interest (landslide) TLS application: integration of 3D dataset in a numerical model

The landslide is in the north east of the Fosse Padène (Figure 19). It occurred in the upper part 2 years after the dump building. This landslide is composed of argillite and sandstone and it is built with several 10 m height benches. Its 3D dataset was used to make a numerical model (Figure 20) for stability analysis.

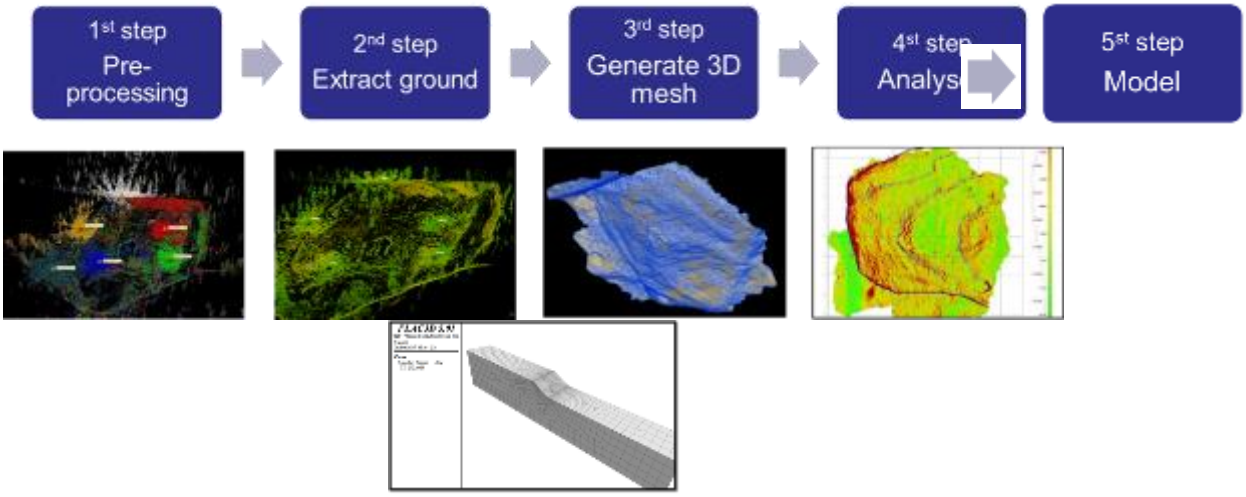

Figure 20 : Slopes analysis methodology based on laser scan and numerical modelling tools

A basic 3D elasto-plastic numerical model using FLAC3D was carried out, the method of strength reduction was employed to determine the safety factor of the slope. The upper layer of the slope is mainly characterized by the friction angle and the cohesion of the soil (phi= 31° and c=8.2 kPa). The deep layer is competent limestone layer, what was considered as elastic layer. Shear and plastic deformation were analysed and compared to the displacement observations. The safety factor after the first instability is equal to 1.2. The local safety factor is smaller. Figure 21 presents the total shear strain. The maximum shear strain is located in the centre of the unstable zone. The thickness of instable zone is about few meters and similar to the in-situ observations and measurements.

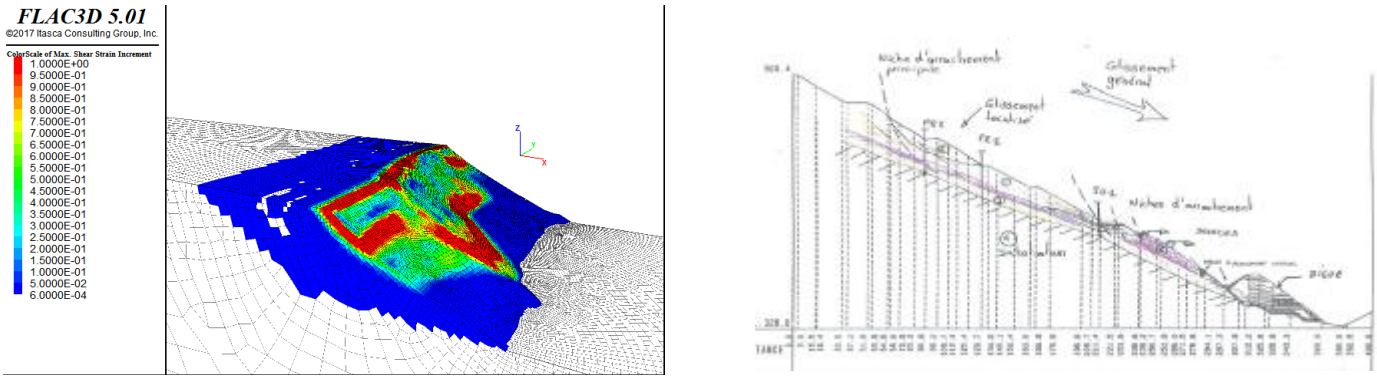

Figure 21: Numerical modelling results (left) of the slope and in-situ observations (right)

3 CONCLUSION

Terrestrial laser scanner technology appears as a very useful tool to characterize and analyse the stability of the inaccessible slopes with very reasonable costs comparing to classical displacement surveys. 3D datasets were also used to carry out a slope assessment and generate a numerical model. This innovative methodology, based on crossing and combination of 3D datasets, numerical modelling and in-situ observation, was successfully used for a real case study.

4 ACKNOWLEDGEMENTS

This work was supported by the RFCS-SLOPES project and the French Ministry of Environnent (MTES, Ministère de la Transition Ecologique et Solidaire).

Rockfall release frequency for different rock wall types

Didier HANTZ[1], Antoine GUILLEMOT[1], Charlotte EPINAT[1], Julie D'AMATO[1], Antoine GUERIN[2], Michel JABOYEDOFF[2], Simone ALBER[2], Antonio ABELLAN[2,3]

Keywords: rockfall, hazard, frequency

Quantitative hazard assessment of diffuse rockfall requires knowing: (a) the release frequency of rockfalls, (b) the frequency of the individual blocks that propagate on the slope, and (c) the probability that a block reaches an element at risk (Hantz et al., 2016, 2017). The release frequency (rockfall frequency) of 11 rock walls located in the French Alps at elevations between 300 m and 2000 m a.s.l., was determined from diachronic comparison of digital rock surface models obtained either by terrestrial laser scanning or photogrammetry (Guerin et al. 2014; Alber, 2016; Epinat, 2016; Guillemot, 2017). Ten limestone cliffs and one gneissic wall were investigated. The limestone cliffs are anaclinal slopes (bedding dips inside the slope), characteristic of the Subalpine Chains. According to the site, the minimal volume considered in the analysis varies between 0.01 and 0.1 m^3. The maximal observed volume was 4000 m^3.

The volume-frequency relation has been fitted by a power law with two parameters:

$$F = A\ V^{-B} \qquad (1)$$

Where F is the spatial-temporal frequency of the rockfalls (number of events per year per hm^2), V is the volume in m^3, A is an "activity" parameter (number of events bigger than 1 m^3, per year per hm^2) and B is a "structure" parameter (which reflects the decrease of the frequency when the volume increases).

Figure 1 shows the activity parameter (A) for the investigated rock walls. It varies by several orders of magnitude according to the rock mass structure. The first six walls are made of massive rock (limestone and gneiss, layer thickness usually bigger than 2 m); Five out of six have an activity parameter between 0.01 and 0.1. The bigger value obtained for the Granier cliff can be explained by a particular morphodynamic context: This Urgonian cliff is underlained by unusually steep and active Hauterivian and Valanginian walls, due to the famous Granier landslide in 1248. The three other Urgonian cliffs show an activity parameter increasing with the elevation. The last five walls in Figure 1 are made of bedded limestone (layer thickness usually between 0.2 and 0.6 m). Their activity parameter is between 0.1 and 2. The lower activity parameter corresponds to the lower elevation.

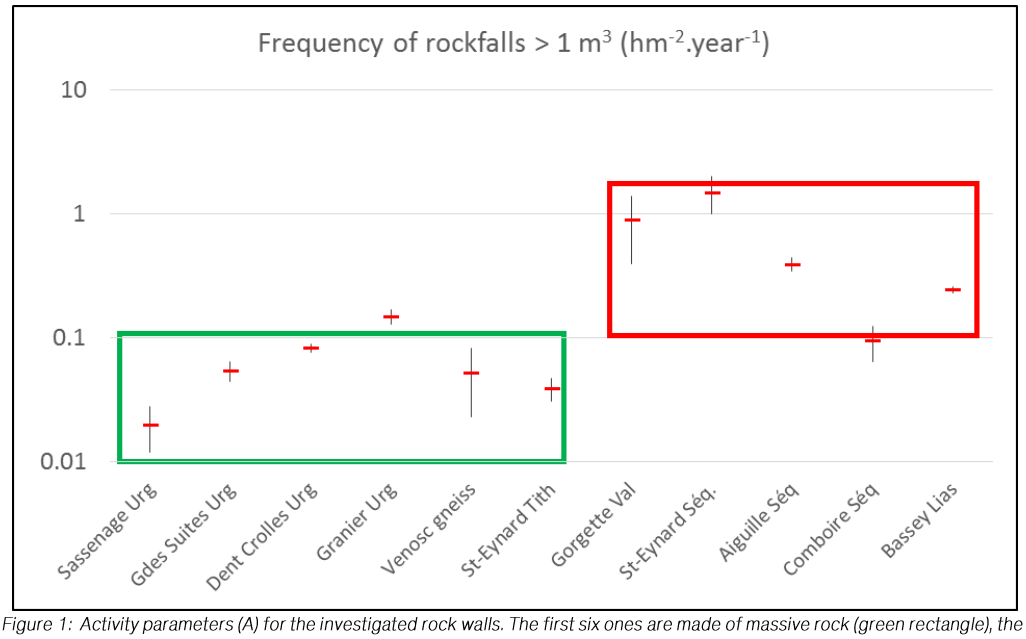

Figure 1: Activity parameters (A) for the investigated rock walls. The first six ones are made of massive rock (green rectangle), the last five ones of bedded limestone (red rectangle).

[1] Univ. Grenoble Alpes, ISTerre, 38000 Grenoble, France, didier.hantz@univ-grenoble-alpes.fr

[2] University of Lausanne, Center for Research on Terrestrial Environment (CRET), michel.jaboyedoff@unil.ch

[3] University of Cambridge, Scott Polar Research Institute, aa962@cam.ac.uk

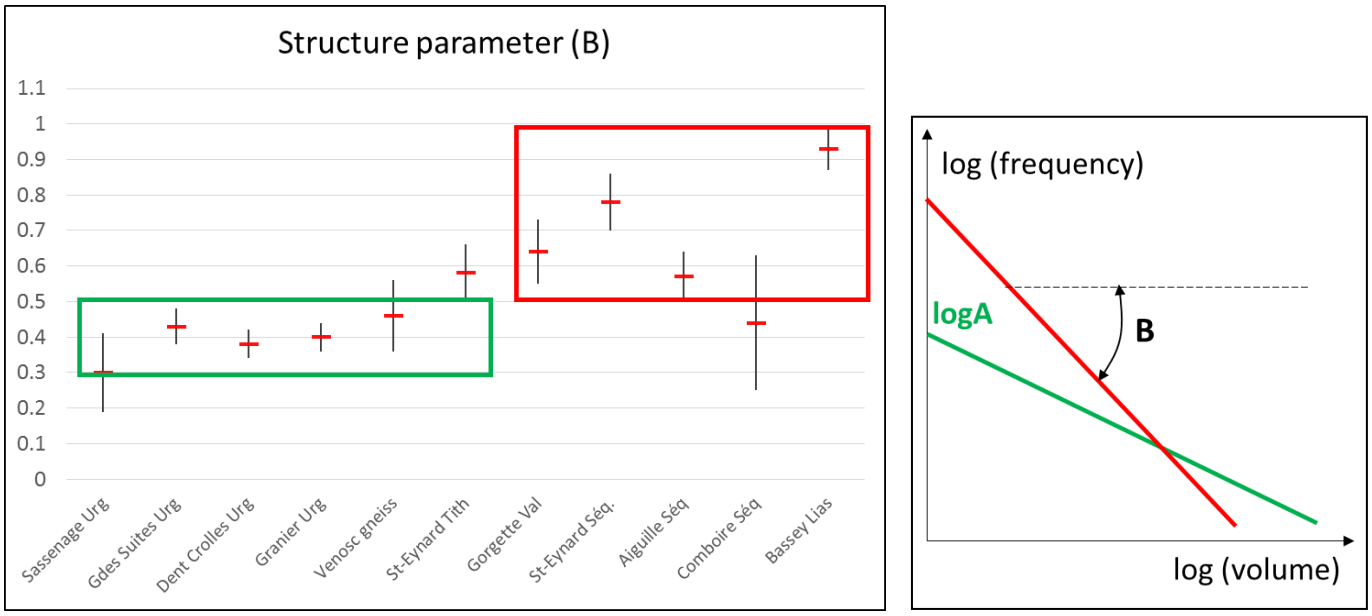

Figure 2: Left: Structure parameter (B) for the investigated rock walls; While the first six slopes are made of massive rock (green rectangle), the last five cliffs correspond to bedded limestone (red rectangle). Right: Volume-frequency relations for different B-values.

Figure 2 shows the structure parameter (B) for the different rock walls. Walls made of massive rocks show lower B-values than walls made of bedded rocks, with B-value ranging between 0.3 and 0.5, and 0.5 and 1.0, respectively.
Remark (1): The frequency of rockfalls bigger than 1 m^3 appears to be higher for bedded walls than for massive ones, but this pattern is reversed for rockfalls bigger than a certain volume (of the order of 10^3 m^3), as can be seen in Figure 2.
Remark (2): As the volume of a rockfall must necessarily be limited (Hantz et al., 2003; Corominas et al., 2017), the power law must be truncated at the maximal possible volume, which mainly depends of the possible failure mechanisms and the height of the rock wall.

1 CONCLUSION

It appears from the investigated rock walls that the rockfall frequency (characterized by A and B parameters) mainly depends on the rock wall structure, and secondarily of the climatic context (elevation) and the morphodynamic context (erosion of the underlying slope).

Acknowledgements. The authors thank the national project C2ROP and the Federation VOR for fundings.

2 REFERENCES

Alber S. (2016) Change detection combining SfM and LiDAR techniques: Application to the study of rockfalls using archival photographs. Master Thesis, Université de Lausanne, Faculté des Géosciences et de l'Environnement.

Epinat C. (2016) Evaluation quantitative de l'aléa d'éboulement rocheux par acquisitions Lidar sur 4 falaises de la région grenobloise. Master Thesis, Université Grenoble-Alpes, ISTerre.

Guillemot A. (2017) Évaluation quantitative de l'aléa de départ des éboulements rocheux. Master Thesis, Ecole Polytechnique Fédérale de Lausanne, ISTerre.

Guerin A., D'Amato J., Hantz D., Rossetti J-P., Jaboyedoff M. (2014) Investigating rock fall frequency using Terrestrial Laser Scanner. *Vertical Geology Conference, Lausanne, Switzerland, p.251-254.*

Hantz D., Dussauge-Peisser C., Jeannin M., Vengeon J-M. (2003) Rock fall hazard assessment: from qualitative to quantitative failure probability. *Int. conf. Fast Slope Movements, Naples, May 2003,* pp. 263-267.

Hantz D., Ventroux Q., Rossetti J-P., Berger F. (2016) A new approach of diffuse rockfall hazard. In: *Landslides and Engineered Slopes - Aversa et al. (Eds).* Associazione Geotecnica Italiana, Rome, Italy, ISBN 978-1-138-02988-0, 1063-1067.

Hantz D., Rossetti J-P., Valette D., Bourrier F. (2017) Quantitative rockfall hazard assessment at the Mont Saint-Eynard (French Alps). *6th Interdisciplinary Workshop on Rockfall Protection*, May 22–24, 2017, Barcelona, Spain.

Corominas J., Mavrouli O., Ruiz-Carulla R. (2017). Magnitude and frequency relations: are there geological constraints to the rockfall size?. *Landslides*, 1-17. DOI: 10.1007/s10346-017-0910-z.

Quantitative assessment of rockfall impact frequency

Jean-Pierre ROSSETTI[1], Didier HANTZ[2], Damien VALETTE[2], Quentin VENTROUX[2], Frédéric BERGER[3], Frank BOURRIER[3]

Keywords: rockfall, hazard, impact frequency

The rockfall impact frequency on a slope under a rock cliff results from the failure (or release) frequency of rockfalls in the cliff and of the probability of propagation of the blocks from the release point to the considered point. A new approach is proposed, based on the volumetric retreat rate of the cliff, the distribution of the block volumes and the simulation of the block trajectories. The method has been applied to the Mont Saint Eynard cliff, located in the Grenoble urban area. This 250 m high cliff is made of bedded limestone of Upper Oxfordian stage.

1 VOLUMETRIC RETREAT RATE OF THE CLIFF

The volumetric retreat rate of a cliff can be estimated by integrating the volume-frequency relation for the rockfalls occurring yearly in the cliff (Hantz et al., 2003). The volume-frequency relation can be obtained either from the photogrammetric or TLS (Terrestrial Laser Scanner) survey of the cliff during some years, or using a classification of the rock cliffs based on their geological, geomorphological and climatic context (Hantz et al., 2018). It is described by a power law (Figure 1) with a scaling exponent (B) varying from 0.3 (for the more massive rocks) to 0.9 (for the more fractured rocks):

$$F = A\,V^{-B} \qquad (1)$$

Where F is the frequency of rockfalls bigger than V and A the frequency of rockfalls bigger than 1 m^3. For the integration, a maximal possible rockfall volume V_{max} must be fixed, which can be bigger than the maximal observed volume (Corominas et al., 2017). The volumetric retreat rate is:

$$W = V_{max}^{(1-B)}\,A/(1-B) \qquad (2)$$

2 DISTRIBUTION OF THE BLOCK VOLUMES

The distribution of the volumes of the blocks released when a rock compartment falls from a rock cliff has been rarely analyzed. It can be obtained by measuring the volumes of the blocks deposited during a recent rockfall. Hantz et al. (2014, 2016) and Ruiz et al. (2015) have shown that it is well fitted by a power law (Figure 2) with a scaling exponent (b) varying from 0.6 to 1.3:

$$n = a\,v^{-b} \qquad (3)$$

Where n is the number of blocks with volume bigger than v and a is the number of blocks bigger than 1 m^3. Assuming this scaling exponent depends only on the rock mass structure, the value obtained from a single rockfall can be considered representative of the whole homogenous cliff and Equation (3) represents also the volume distribution of all the blocks falling yearly from the cliff. The volumetric retreat rate (W) can then be derived by integrating the volume in Equation (3):

$$W = v_{max}^{(1-b)}\,a_y/(1-b) \qquad (4)$$

Where a_y is the number of blocks bigger than 1 m^3 falling yearly from the cliff and v_{max} is the maximal possible volume of a block. It has to be estimated from the observation of the rock cliff. Knowing W, v_{max} and b, a_y can be derived from Equation (4). Hence the distribution of the volumes of the blocks which fall yearly is known (Figure 2).

3 SIMULATION OF THE BLOCK TRAJECTORIES

From the distribution obtained above, the trajectories of all the blocks which fall during a chosen time length can be simulated to determine the impact frequency on each pixel of the slope. Figure 3 shows the trajectories of the blocks falling during 1000 years from the Mont Saint Eynard, which overhangs a part of the Grenoble urban area (Hantz et al., 2016). A probabilistic modelling has been used with the software Rockyfor3D (Dorren, 2015). The length of the simulated period has been chosen so that a sufficient number of blocks start from each pixel of the DEM. The annual impact frequency can then be drawn, as shown in Figure 4.

[1] Alp'géorisques, Domène, F, jeanpierre.rossetti@alpgeorisques.com

[2] ISTerre, Univ. Grenoble-Alpes, F, didier.hantz@univ-grenoble-alpes.fr

[3] IRSTEA, Grenoble, F, Frank.Bourrier@irstea.fr

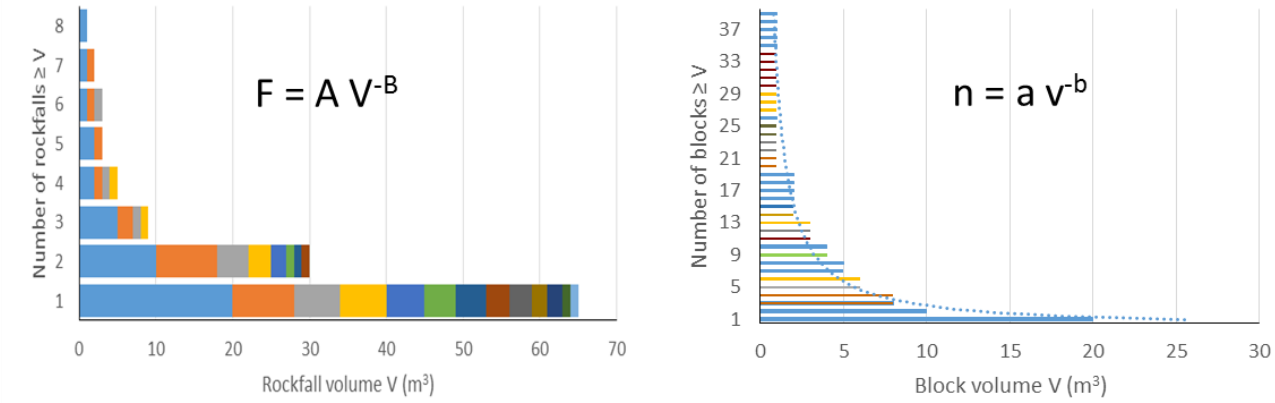

Figure 1: Distribution function of the rockfall volume.

Figure 3: Trajectories of the blocks bigger than 1 m3 falling during a period of 1000 years (simulated with Rockyfor3D).

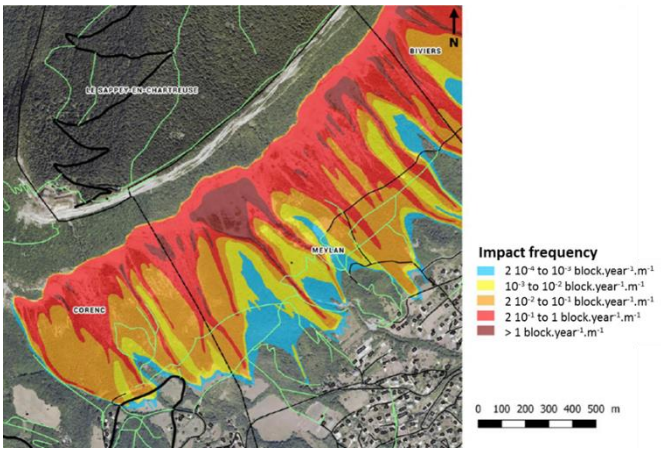

Figure 4: Annual impact frequency (block.year-1.m-2 or per meter parallel to the cliff) under the Mont Saint-Eynard for volume > 0.1 m3

4 CONCLUSION

Quantitative assessment of rockfall impact frequency becomes possible, but more rockfall inventories are needed, as well as more analyses of the block volume distribution. It makes it possible to quantify the natural risk, and the residual risk after mitigation measures have been taken.

Acknowledgements. The authors thank the national project C2ROP and the Federation VOR for fundings.

5 REFERENCES

Figure 2: Distribution function of the block volume

Corominas J., Mavrouli O., Ruiz-Carulla R. (2017). Magnitude and frequency relations: are there geological constraints to the rockfall size?. Landslides, 1-17. DOI: 10.1007/s10346-017-0910-z.

Dorren L. (2015) Rockyfor3D (5.2) revealed-Transparent description of the complete 3D rockfall model. www.ecorisq.org.

Hantz D., Dussauge-Peisser C., Jeannin M., Vengeon J-M. (2003) Rock fall hazard assessment: from qualitative to quantitative failure probability. Int. conf. on Fast Slope Movements, Naples, 11-13 May 2003, pp. 263-267.

Hantz D., Ventroux Q., Rossetti J-P., Berger F. (2016) A new approach of diffuse rockfall hazard. 12th Int. Symp. On Landslides, Napoli.

Ruiz-Carulla R., Corominas J., Mavrouli O. (2015) A methodology to obtain the block size distribution of fragmental rockfall deposits. Landslides, 12, 815-825.

Debris flow flexible fence: barrier/flow interaction model

Stéphane Lambert[1], Franck Bourrier[2], Ignacio Olmedo[3], Philippe Robit[4]

Keywords: debris-flow, flexible fence, DEM model

This article deals with the use of flexible barriers for catching gravity driven flows occurring in mountainous areas: debris and mud flows, snow avalanches, floating woods, etc. It particularly focuses on the interaction between a debris flow and a specific structure manufactured by GTS, in view of a better understanding of the structure response to varying flow-induced loading conditions. This objective is pursued using a Discrete Element Method (DEM) model of the flow-barrier system. The calibration of the components models is made by experimental results made under dynamic and quasi-static loadings. Moreover, experimental data of a real flow impact on a structure will be used for the validation of the numerical models under development.

1 INTRODUCTION

Specific protection devices such as flexible debris flow barriers are more and more used to protect infrastructures from different kinds of fast natural gravity driven flows (debris and mud flows, debris flood and debris avalanches) (Villard, 2016). These structures are particularly well adapted to difficult access areas and present reduced costs and installation delays compared to other civil engineering structures. The design methods that have been recently proposed are rather simple and do not consider all the possible situations, in terms of flow velocity and density or surge volume, in particular. There exists a real need for improving the comprehension of the interaction between the flow and the barrier, as this interaction controls the loads that transit through the structure towards the anchors. In this context, this article put a special focus on the development of such specific devices. It investigates the interaction between different debris flows and a specific flexible barrier thanks to numerical modelling. This research is conducted within the frame of an ongoing 4-year long research project entitled PRIDYN (Protection RIsques DYNamiques).

2 MODELING APPROACH

The system model was developed using YADE software, an open source code for discrete element models (DEM). DEM appears relevant and efficient in terms of computation cost as dealing with a discontinuous system (the flexible barrier) when exposed to a dynamic loading induced by a flow containing coarse granular material (the debris flow).

The presented development represents an extension of the work conducted by Albaba (2016) in the sense it aims at improving the realism of both the flow model and the barrier model.

2.1 BARRIER MODELLING

The barrier model was created based on a recently developed DEM model of the GTSs ETAG027 5000kJ ELITE© rockfall fence. This structure consists of an assembly of cables, cable net, and energy dissipating devices. All these components were modelled and the calibration of the model parameters of each component was conducted thanks to experiments carried out in quasi static and dynamic conditions (Olmedo, 2017). A particular attention was in particular paid to the modelling of the interaction between components such as wire-ropes and retaining mesh. The structure response was validated by comparison with real-scale impacts by a projectile.

The debris flow barrier catchment fence being made of the same components, the model was developed considering these previously developed components. Their arrangement was adapted to this specific type of structure, in particular in terms of number and position of energy dissipating devices and cables (Fig. 1). The barrier global geometry was also adapted to the specific case of a torrent bed.

[1] LAMBERT Stéphane, Irstea – UR ETGR, Saint Martin d'Hères, FRANCE, stephane.lambert@irstea.fr

[2] BOURRIER Franck, Irstea – UR EMGR, Saint Martin d'Hères, FRANCE, franck.bourrier@irstea.fr

[3] OLMEDO Ignacio, GTS, Grenoble, FRANCE, iolmedo@gts.fr

[4] ROBIT Philippe, GTS, Grenoble, FRANCE, probit@gts.fr

2.2 FLOW MODELLING

Figure 1: example of debris flow flexible fence and coarse debris flow

The work previously conducted by Albaba et al. (2016) considered a dry granular flow made of large grains. The new development consists in accounting for the presence of the liquid 'matrix', composed of water and fine sediment in suspension, in addition to the solid phase, consisting of the coarse particles. The numerical model will be validated by experimental data obtained from the impact of a real event on a instrumented structure. Indeed, a complete set of sensors are foreseen to acquire data from the structure and the debris. Concerning the structure, force sensors will record the evolution of the efforts on the main cables. A set of high speed cameras will allow to estimate the deflection of the cables and net. Concerning the flow, some parameters such as the flow height and velocity will be monitored and synchronized with the structure data.

3 CONCLUSION

The results of this study will allow characterising the flow loading on the structure based on the flow characteristics and the mesh or structure geometrical and physical parameters.
The results of this numerical model, validated by the experimental results will provide a relevant amount of data to optimize the structures design and their components such as the mesh or the cables distribution. Moreover, this research work might allow establishing the limits of structures in terms of flow retaining capacity.

4 REFERENCES

Albaba A., Lambert S., Kneib, F., Chareyre B. and F. Nicot, 2017. DEM modeling of a flexible barrier impacted by a dry granular flow. Rock Mechanics and Rock Engineering.

Olmedo, I., Robit, P., Bertrand, D. Galandrin, P., Coulibaly, J. and M-A. Chanut, 2017. Extended experimental studies on rockfall flexible fences. Proceedings of Rocexs 2017, Barcelona, Spain

Villard, N., 2016. Rock debris flow mitigation using flexible structures. Proceedings of the 3rd Rock Slope Stability Symposium, RSS2016. Lyon

Numerical investigation of rockfall barrier under realistic on-site impacts

Marie-Aurélie CHANUT[1], Jibril COULIBALY[1], Stéphane LAMBERT[2], François NICOT[2]

Keywords:

Rockfall barriers are efficient and cost-effective protection structures to mitigate hazards in mountainous areas. The design and the use of such structures require a sound understanding of their complex mechanical response under dynamic loading. For that reason, a generic approach for modelling most types of barriers was developed in order to provide a deeper insight into their structural behaviour. In this document, the strengths of the developed tool are taken advantage of to perform numerical simulations of realistic impacts on rockfall barriers. Original insight into barriers on-site mechanical behaviour, as well as their consequences on rockfall management practices, are presented.

1 ROCKFALL BARRIERS MECHANICAL MODELING: A GENERIC APPROACH

A generic model of rockfall barriers was developed in order to provide a common frame of reference for barriers modeling and to harmonize calculation methods. That model ambitions to define a common geometric description and mechanical modeling of all barriers technologies and to build a unified and efficient calculation platform enabling numerical simulation of rockfall barriers dynamic loading.

Barriers are described by their main components: the interception net, the posts, the energy dissipating devices, the cables and the anchors. These components form the common frame of every technology and setup of rockfall barriers. Any rockfall barrier can therefore be described by a particular arrangement of these components.

The dynamic impact calculations are performed using an explicit Discrete Element Method (DEM). DEM models representing the main components, the projectiles and their interactions have been developed. In this purpose, two innovative models for the ring (Coulibaly et al, 2017) and the sliding cable (Coulibaly et al, 2018) were considered for barriers modeling. The models are calibrated against experimental data from characterization tests on individual components which allows simulation of a complete barrier. This approach was validated against full-scale tests on the C2ROP barrier (Olmedo et al, 2017) and simulation results agree with experimental data. The numerical results of the barrier deflection over time as well as tension in cables agree very well with experimental data. The loading duration and timing also match, as well as the peak forces.

It is now possible to use the validated tool to perform exploratory numerical investigation under realistic conditions.

2 SIMULATIONS OF REALISTIC LOADING CASES

In this part, different loading cases are investigated. This approach can be seen as complementary to studies of variations in the kinematics or shape of one incident boulder (Mentani et al, 2016) or of deterioration of the barrier (Luciani et al, 2016). Two different loading cases, corresponding to existing situations encountered on site are performed:

- successive impacts of two boulders with and without removal of the first boulder;
- impact in a preloaded barrier.

2.1 INFLUENCE OF BOULDER REMOVAL ON CONSECUTIVE IMPACTS

In realistic conditions, it is not always possible to know when an impact occurs and to immediately apply maintenance work on the barrier. The barrier must therefore be capable of sustaining an additional impact without any maintenance performed after a first one. In a first simulation, and unlike the ETAG 27 SEL procedure, the second impact happens while the first boulder has not been removed from the net (Figure 1). In a second simulation, removal of the first boulder is performed. The results tend to indicate that the behavior of the barrier (deflection and tension in cables), for energies about the service energy level, is similar if boulder removal is operated or not. This can be explained by two major technological aspects of rockfall barriers: on the one hand, the energy dissipating devices play an active role in controlling the force paths and intensity and on the other hand, rockfall barriers are flexible structures whose geometry adapts to loading. The magnitude of the changes in the deformed geometry due to removal of the first boulder in the net is not influential when compared to the deformed geometry of the net containing the first boulder.

[1] Cerema Centre-Est, 25 avenue François Mitterand, CS 92803, 69674 Bron Cedex, France, marie-aurelie.chanut@cerema.fr, jibril.coulibaly@gmail.fr

[2] IRSTEA - ETNA, Domaine Universitaire 2 rue de la Papeterie, BP 76, F38402 - Saint Martin d'Hères Cedex, France, stephane.lambert@irstea.fr, francois.nicot@irstea.fr

As a result, boulder removal appears to be optional as long as the energy dissipating devices are still in capacity to function properly and when the loss of residual height is small enough so that the interception capacity of the barrier is not significantly reduced.

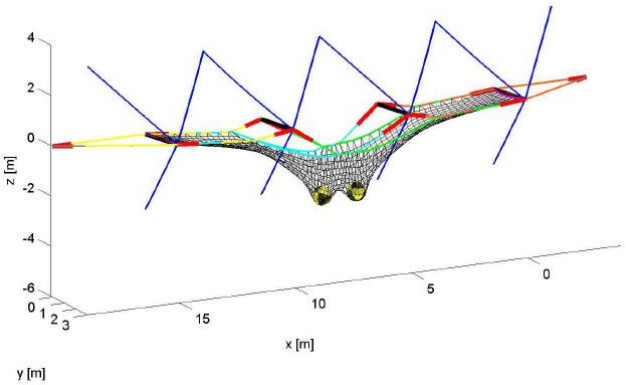

Figure 1: Simulation of successive impacts of two boulders without removal of the first boulder : equilibrium configuration with the two boulders

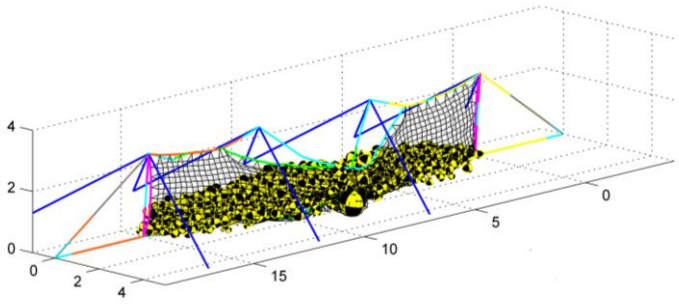

Figure 2: simulation of an impact in a preloaded barrier

2.2 BEHAVIOUR OF A PRELOADED BARRIER

In scree slopes, rubble tends to accumulate in the lower part of the barrier. Clearing of the barrier is therefore regularly requested as part of the maintenance and upkeep of the barriers. In this section, the influence of preloading on the behaviour of the barrier is investigated. The barrier is preloaded with a volume of 10 m^3 of evenly distributed spherical rubble particles before the impact (Figure 2). Simulation results show that the preloading produces a reduction of the barrier height before the impact but does not prevent the barrier from functioning and deforming as usual. Other loading cases (energy level and localization) will be carried out to confirm these observations.

3 CONCLUSION

The two studies showed that the barrier maintains functionality even if a boulder already impacted the structure and has not been removed or if the net is loaded with rubble before the impact. These conclusions may be dependent of the intensity (energy level or pre-loading volume) of the sought configurations and to the technology of the barrier. The capacity of the generic tool to identify the explored mechanical behaviours remains a powerful and interesting feature.

4 REFERENCES

Coulibaly J. B. and Chanut, M-A. and Lambert, S. and Nicot, F. (2017), Non-linear discrete mechanical model of steel rings, *Journal of Engineering Mechanics* (143).

Coulibaly J. B. and Chanut, M-A. and Lambert, S. and Nicot, F. (2018) Sliding cable modeling: An attempt at a unified formulation, *International Journal of Solids and Structures* (130-131).

Mentani A., Govoni L., Gottardi G., Lambert S., Bourrier F., and Toe D..(2016) A new approach to evaluate the effectiveness of rockfall barriers. Procedia Engineering, 158:398 – 403, 2016. *VI Italian Conference of Researchers in Geotechnical Engineering, CNRIG2016 – Geotechnical Engineering in Multidisciplinary Research: from Microscale to Regional Scale*, Bologne (Italie).

Luciani A., Barbero M., Martineli D., and Peila D. (2016) Maintenance and risk management of rockfall protection net fences through numerical study of deterioration. *Natural Hazards and Earth System Sciences*.

Olmedo I. and Robit, P. and Bertrand, D. and Galandrin, C. and Coulibaly, J. B. and Chanut, M-A. (2017) Extended experimental studies on rockfall flexible fences, *RocExs 2017 - 6th Interdisciplinary Workshop on Rockfall Protection.*

An advanced method for designing rockfall fences by surrogate modelling

Loïc DUGELAS[1], Franck BOURRIER[2], Ignacio OLMEDO[3], François NICOT[4]

Keywords: rockfall, fences, design, parametric study, surrogate model, DEM, polynomial chaos expansion,

In order to protect infrastructures against rockfall, flexible fences are widely used, but the complex response to impact remains difficult to predict. A discrete element method (DEM) model of rock impact on a flexible fence has been developed to analyze the response of the structure and identify the prevailing model parameters for a large range of impact configurations. On a perspective of further stochastic analysis and to reduce the computational cost of this model, a surrogate model has been built and used for the aforementioned analysis.

1 INTRODUCTION

The design of rockfall protection fences is currently assessed by fulfilling the European Technical Approval (EOTA, 2012). The barriers are subjected to two full-scale tests. The first test consists of one impact at maximal energy level (MEL), and the other one involves two consecutive impacts at 1/3 of the maximal impact energy level (SEL). The objective of this study is to optimize the structure in the context of the European Technical Approval. In a first stage, the work will focus on the capacity of an existing barrier to fulfill the MEL test only.

The studied barrier is the ELITE® 5000 kJ category A (Figure 22), developed by GTS. It is composed of 3 modules of 11.50m width and 7.00m high.

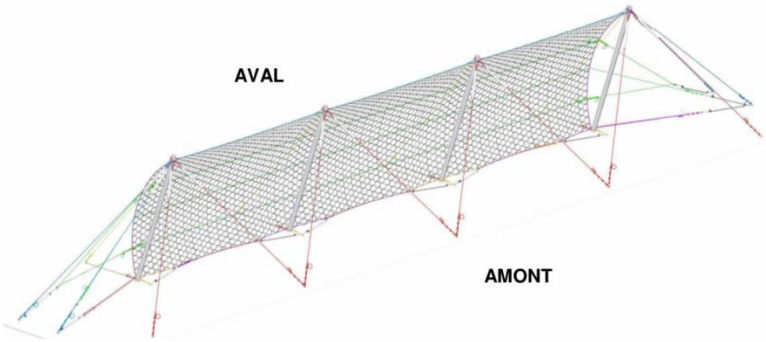

Figure 22 : View of the ELITE® 5000 kJ Cat. A barrier

A DEM model of this structure has been used to build a surrogate model that relates target output parameters to all input parameters of the DEM model. Sensitivity analysis on this surrogate model finally allows determining the prevailing input model parameters.

2 DEM MODEL

The fence model is developed using the YADE-DEM open source code. In a first step, the models of the components of the fence are developed and calibrated separately, using specific experimental tests. The ELITE® net model is based on Bertrand's work (Bertrand et al., 2012): the contacts between the cables are modelled by particles linked by a remote interaction representing the cable. Two types of interactions exist: one for the cables with one curvature, and one for the cables with two curvatures (Figure 23), both calibrated by tensile and punch tests. The supporting cables of the structure are modelled by two deformable cylinders and the connections between the cables and the net are modeled by shackles (Albaba et al., 2017).

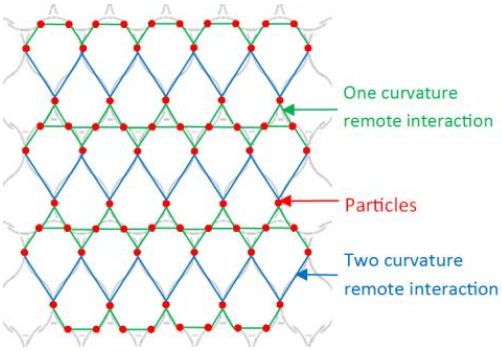

Figure 23 : ELITE® net model

[1] DUGELAS Loïc, Irstea – UR EMGR, Saint Martin d'Hères, FRANCE, loic.dugelas@irstea.fr

[2] BOURRIER Franck, Irstea – UR EMGR, Saint Martin d'Hères, FRANCE, franck.bourrier@irstea.fr

[3] OLMEDO Ignacio, GTS, Grenoble, FRANCE, iolmedo@gts.fr

[4] NICOT François, Irstea – UR ETGR, Saint Martin d'Hères, FRANCE, francois.nicot@irstea.fr

In a second step, the components are assembled to create the complete barrier model. Finally, the comparison with full-scale experimental tests results allows validating the numerical model.

3 SURROGATE MODEL

A surrogate model is a function that approximates the response of the DEM model. It relates target outputs of the DEM model to the input parameters. This function is calibrated from a limited number of simulations obtained from the DEM model for values of the input parameters uniformly sampled in a convenient range.

Ten input parameters have been selected with the following variation ranges (Table 1).

Table 1 : Definition of the input parameters

Variable	Number of inputs	Variation range	Comments
Energy dissipating device trigger force (kN)	4	[50; 200]	There are 12 energy dissipating devices in the structure. These can be clustered to define 4 different classes
Module length (m)	1	$[H_{pot}; 2.5*H_{pot}]$	Where H_{pot} is the posts height. As defined by the ETAG027, we consider that the 3 modules have the same length
Horizontal position of the upper anchorages (m)	2	$[-0.5*L_m; 0.5*L_m]$	Where L_m is the module length. This value is the distance of the anchorage from the center of the module.
Vertical position of the upper anchorages (m)	1	$[0; 2*H_{pot}]$	This value is the vertical distance of the anchorage from the top of the posts
Horizontal position of the lateral anchorages (m)	1	$[0.2*L_m;L_m]$	This value is the horizontal distance of the anchorage from the external post

The selected output parameters are those required for the European Technical Approval: the interception of the rock (checking if the rock is stopped), the residual height of the fence (effective height of the barrier after impact), and the net deflection. Two parameters influencing the cost of the barrier have also been selected. First, the maximum force at the anchorages because its cost of production increases with this force. Second, the elongation of the dissipating devices, this value influencing there type.

In this study, the sparse polynomial chaos expansion method (Blatman et al., 2010) has been used to build the surrogate model. This method is adapted to approximate the expected responses as it can be used with a large number of inputs, and makes it possible to realize sensitivity analysis at low computational cost.

4 CONCLUSION - PERSPECTIVES

In this study, a surrogate model of the response of the ELITE® 5000 kJ (category A) barrier has been developed using a DEM model. This surrogate model will be used for the purpose of parametric studies and sensitivity analyses which allow analyzing the relative effects of the input parameters. Thereby, prevailing parameters will be identified to predict the response of the fence in MEL test conditions. By adjusting these parameters, a configuration is selected to get the most efficient structure.

5 REFERENCES

Albaba, A., Lambert, S., Kneib, F., Chareyre, B., & Nicot, F. (2017). DEM modeling of a flexible barrier impacted by a dry granular flow. *Rock Mechanics and Rock Engineering*.

Bertrand, D., Trad, A., Limam, A., & Silvani, C. (2012). Full-Scale Dynamic Analysis of an Innovative Rockfall Fence Under Impact Using the Discrete Element Method: from the Local Scale to the Structure Scale. *Rock Mechanics Rock Engeneering*, 885-900.

Blatman, G., & Sudret, B. (2010). An Adaptive Algorithm to Build up Sparse Polynomial Chaos Expansions for Stochastic Finite Element Analysis. *Probabilistic Engineering Machanics*.

EOTA (2012 , amended 2013). Guideline for the European Approval of Falling Rock Protection Kits. Brussels.

Comparison of two DEM modeling of flexible rockfall fences under dynamic impact

Loïc DUGELAS[1], Jibril COULIBALY[2], Franck BOURRIER[3], Ignacio OLMEDO[4], Marie-Aurélie CHANUT[5], Stéphane LAMBERT[6], François NICOT[7]

Keywords: rockfall, fences, DEM, models, impact, comparison

Flexible fences are efficient and cost-effective rockfall protection structures, but their complex response to impact remains difficult to predict. Models based on a discrete element method (DEM) of rock impact on a flexible fence are developed for a better understanding of the dynamic response of the structure under impact. Two of these models are introduced and compared in this paper.

1 CONTEXT

Numerical modeling is increasingly used in order to better understand the behavior of flexible rockfall fences. Impact simulations can be used by manufacturers for the design of their structures prior to full-scale tests, or by public authorities before installing the fences. The high number of existing models prompts interests for the realization of a benchmark of the different approaches in order to identify their comparative advantages, limitations and domains of validity. As a first step in pooling together and compare the existing numerical models, the mechanical response of two rockfall fences models independently developed in the context of the French National project C2ROP are compared against a reference structure and experimental data.

2 MODELS

2.1 REFERENCE STRUCTURE

Within the French national project C2ROP, a 300 kJ flexible rockfall fence has been developed. This research prototype results from the collaboration between manufacturers, academic researchers and public authorities and is used as the reference structure in the present study. Several specific tests have been performed on the structural components (ring net, energy dissipating devices) (Olmedo, 2017), as well as instrumented full-scale tests were carried out on the entire structure. A full-scale test with an impact energy of 270 kJ in the ETAG 27 MEL conditions (EOTA, 2012) using a boulder of 750 mm long, a mass of 740 kg and an impact velocity of 27 m/s is used as the reference impact configuration.

2.2 NUMERICAL MODELS

Both models introduced herein are based on a DEM discretization of the individual components. The models are calibrated against identical data from characterization tests on individual components. No back-analysis is performed from the experimental full-scale tests so that differences in the simulation results would only be attributed to the different modeling assumptions. In both models, the anchors are considered as fixed points (boundary conditions) and the energy dissipating devices as two particles linked by a remote interaction. The main differences between the two models lie in the posts, ring net and cable modeling and are summarized in Table 1.

Table 1 : Differences between the models

Component	Model 1	Model 2
Cable / Net link	The cable is modelled by a cylinder which allows a “real” contact. In these conditions it is possible to create the link	Sliding cable model of Coulibaly et al., (2018). Cables are modeled as a set of ordered nodes. Cable/net link is modeled by integrating a sliding node in the set of nodes

[1] DUGELAS Loïc, Irstea – UR EMGR, Saint Martin d’Hères, FRANCE, loic.dugelas@irstea.fr

[2] COULIBALY Jibril, Cerema – Dter-CE, Bron, FRANCE, jibril.coulibaly@cerema.fr

[3] BOURRIER Franck, Irstea – UR EMGR, Saint Martin d’Hères, FRANCE, franck.bourrier@irstea.fr

[4] OLMEDO Ignacio, GTS, Grenoble, FRANCE, iolmedo@gts.fr

[5] CHANUT Marie-Aurélie, Cerema – Dter-CE, Bron, FRANCE, marie-aurelie.chanut@cerema.fr

[6] LAMBERT Stéphane, Irstea – UR ETGR, Saint Martin d’Hères, FRANCE, stephane.lambert@irstea.fr

[7] NICOT François, Irstea – UR ETGR, Saint Martin d’Hères, FRANCE, francois.nicot@irstea.fr

<table>
<tr><th>Component</th><th>Model 1</th><th>Model 2</th></tr>
<tr><td></td><td>between the cable and the net by a shackle (Albaba et al., 2017) (Figure 24).
 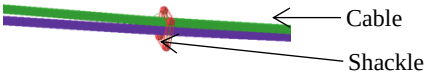

Figure 24 : Link Net/Cable with shackle</td><td>and sliding is obtained by swapping material from one side of the sliding node to the other (Figure 25).
 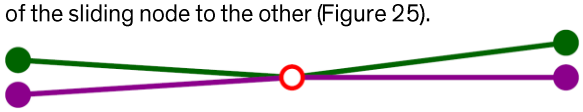
Figure 25 : Sliding model from Coulibaly et al. (2018)</td></tr>
<tr><td>Ring net</td><td>Adaptation of Nicot's 6 contacts rings net model (Nicot et al., 2001) to a 4 contacts rings net. The rings are modelled by a particle located at their center of gravity and the contact between the rings is modelled by a remote interaction (Figure 26). The model is calibrated from an experimental tensile test on a 3x3 rings sample.
 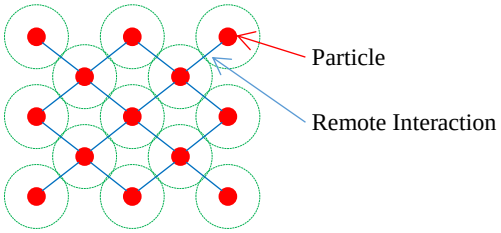

Figure 26 : Adaptation of Nicot's model</td><td>Ring model of Coulibaly et al. (2017). Individual rings are discretized in their 4 contacts points and assembled. The mechanical behavior of a ring is accounted for by 7 specifically defined remote interactions (Figure 27). The model is calibrated from experimental tensile tests on isolated rings.
 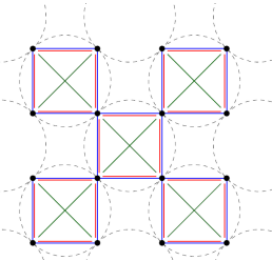
Figure 27 : Ring model from Coulibaly et al. (2017).</td></tr>
<tr><td>Posts</td><td>Elastic beams</td><td>Rigid beams</td></tr>
</table>

3 RESULTS/DISCUSSION

On the structure scale, both models provide similar results on both qualitative and quantitative points of view (Figure 28). The most refined model (model 2) is more suitable for local analysis of the mechanical response. The computation time is also slightly advantageous for model 2, compared to model 1, contrary to the development time. Indeed, the model 1 was built with existing models while for the model 2, new sliding and ring models were developed.

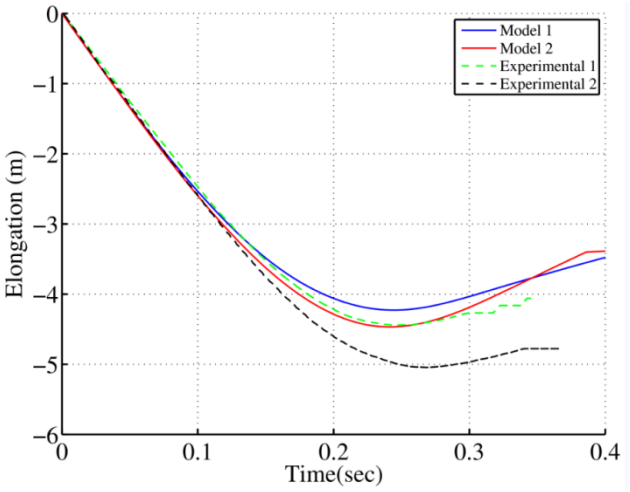

Figure 28 : Elongation of the net versus time for models and experimental tests

4 CONCLUSION

The influence of the differences in the modeling has been illustrated by this exploratory work. The differences observed tend to indicate that the existing numerical models have advantages and limitations that require further investigations. This work is a first step in the realization of a benchmark of the different approaches for the identification their specificities.

5 REFERENCES

Albaba, A., Lambert S., Kneib F., Chareyre B., and Nicot F. (2017). DEM modeling of a flexible barrier impacted by a dry granular flow. Rock Mechanics and Rock Engineering.

Coulibaly, J. B., Chanut M-A., Lambert S., and Nicot F. (2018). Sliding cable modeling: An attempt at a unified formulation. International Journal of Solids and Structures Volume 130-131, pp. 1-10.

Coulibaly, J. B., Chanut M-A., Lambert S., and Nicot F. (2017). Non-linear discrete mechanical model of steel rings. Journal of Engineering Mechanics 143(9).

EOTA (2012), amended 2013. Guideline for the European Approval of Falling Rock Protection Kits, Brussels.

Nicot, F., Cambou B., and Mazzoleni G. (2001). Design of Rockfall Restraining Nets from a Discrete Element Modeling. Rock Mechanics and Rock Engineering, pp. 99-118.

Olmedo, I., Robit P., Bertrand D., Galandrin C., Coulibaly J. B., and Chanut M-A. (2017). Extended experimental studies on rockfall flexible fences. Proceedings of Rocexs 2017, Barcelona, Spain.

The 2016 rock falls sequence at Mont Granier (1933 m a.s.l., Chartreuse massif, France) characterized by seismology and photogrammetry

David AMITRANO[1], Gaëlle LE ROY[1,2], Agnès HELMSTETTER[1], Fabien HOBLEA[3], Ludovic RAVANEL[3], Philippe DELINE[3], Bruno LAILY[4], Mickael LANGLAIS[1], Emmanuel MALET[3]

Keywords: Mont Granier, rock falls, seismology, photogrammetry.

The Mont Granier, well known because of the 1248 major event which is one of the major historical collapse events in Europe, has experienced a sequence of collapses during the winter and spring 2016 with a large media impact. The joint use of seismic signal analysis and relief reconstruction by photogrammetry allowed us to accurately describe chronology, volume and shape of the successive collapses.

1 GEOLOGICAL AND HISTORICAL CONTEXT, AND CHRONOLOGY OF THE 2016 SEQUENCE

The 2016 sequence of collapses took place around the north face of the Mont Granier (1933 m a.s.l., Savoie, France), the one that was affected by the huge event of 1248 (500 × 10^6 m^3) that caused hundreds of fatalities and reshaped entirely the landscape of the northern side of the mountain on a 15 km long area. The north face is a 900-m-high natural geological cross section in Urgonian limestone, Hauterivian marls, Valanginian limestone and Berriasian marls.

The 2016 sequence occurred on two periods. First, on January 9 at 4:57, a single large event (see further) occurred without any visible forerunners on the NW pillar and awaked inhabitants of the municipality of Entremont-le-Vieux. The collapse propagated on the western slope for about 700 m before stopping in the forest without damaging any infrastructure. As no evidence of potential instability was known on that area, no previous topographic data were available.

The second part of the sequence began on April 28th on the NE part of the Mont Granier. This area of the municipality of Chapareillan was known to be often affected by rock falls as revealed by the local name “Ravin du diable” (“Devil’s gully”). From that date onward, a few collapse events of moderate volume (see further) occurred until May 7th at 8:32 when the major event was observed and filmed by several persons thanks to good weather conditions and because a smaller event occurred just 2 minutes before, alerting the inhabitants.

2 SEISMOLOGICAL DETECTION AND CHARACTERIZATION

The two major events (January 9th and May 7th) were recorded and identified by local and regional seismological networks with a magnitude equivalent to M=2.2 and M= 2.0, respectively. As a first estimation, we used the magnitude to determine the volume of each event, applying an empirical relationship based on previously published data (Deparis *et al.*, 2007; Ekström and Stark, 2013). These results were compared with the ones obtained by diachronic photogrammetry (see next paragraph) and showed good reliability.

Using the technic of template matching filtering, *i.e.* measuring the similarity between seismic signals, we succeed in identifying 6 other events that were not identified by usual detection technics based on amplitude. For each of those events we estimated the volume, in the range 200 – 5500 m^3. Moreover, this method provided accurately the occurrence time of each rock fall.

3 RELIEF RECONSTRUCTION AND VOLUME CHARACTERIZATION

In order to determine the geometry of the fallen volumes, we have reconstructed the rock wall topography by photogrammetry before and after the collapses at different steps of the sequence.

[1] Univ. Grenoble Alpes, Univ. Savoie Mont Blanc, CNRS, IRD, IFSTTAR, ISTerre, 38000 Grenoble, France, david.amitrano@univ-grenoble-alpes.fr

[2] Géolithe, Crolles, France

[3] Univ. Grenoble Alpes, Univ. Savoie Mont Blanc, CNRS, EDYTEM, 73000 Chambéry, France

[4] RTM Alpes du Nord, Annecy, France

For the January event, the challenge resulted from the fact that no topographic measurement was performed on this area before the event, as this face did not show any sign of instability. We then called for contributions by an email to our professional networks who responded quickly by sending us several dozens of photos. The second challenge was to use these photos of very uneven quality, with different angles of view and lighting. Recent advances in multi-view photogrammetry allowed us to overcome this difficulty and to build a 3D digital model of the topography before the landslide without specific measurements before. This was, for us, a first experience of collaborative data collection. The post-collapse 3D model was much easier to obtain thanks to the profusion of photos available because of the high media impact of the event. By mapping the difference between 3D reconstructions before and after collapse, we were able to identify and measure the total eroded volume (~ 100 000 m^3). This value fits well with the one obtained with the amplitude of the seismic signal emitted (Tab. 1).

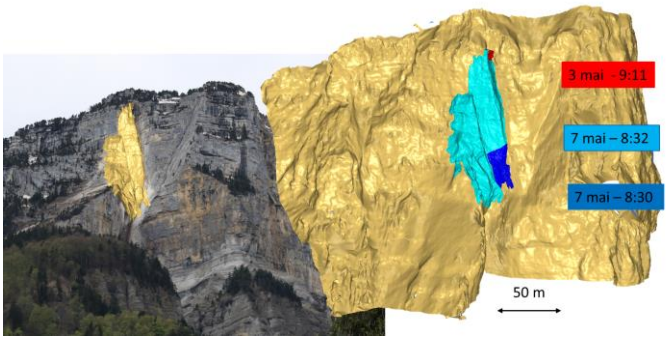

Figure 1: 3D modeling of the eroded volumes on the NE area of the Mont Granier during the 2016 April-May sequence.

Date	Magnitude	Volume (m³) by magnitude	Volume (m³) by photogrammetry
09/01 4:57	2.2	120 000	100 000
28/04 2:54	0.95	1 600	14 000
28/04 3:03	0.97	1 700	
29/04 21:40	1.3	5 500	
30/04 7:47	1.25	4 500	
01/05 4:45	0.63	525	
03/05 9:11	0.51	350	280
07/05 8:30	1.15	3 200	53 000
07/05 8:32	2.04	68 000	

Table 1: Volume of the 2016 Granier rock falls estimated by seismology and photogrammetry.

Concerning the April-May sequence, photos taken by scientists were available before the collapse and campaigns have been performed during (May 3rd, 7th) and after (May 10th, 15th,17th, 20th) the sequence.

This allowed us to accurately determine the eroded volume at different steps of the sequence (Fig. 1) and to compare with the volume estimated by the seismology technic. The results obtained with each technic are well correlated (Tab.1).

Important information may be provided also about the time of occurrence. Intriguingly, the major part of the rock falls occurred by night or in the early morning, that seems to correspond to particular thermal conditions. This should be investigated more in depth in future studies.

4 CONCLUSION

The joined use of seismology and photogrammetry appears to be very helpful for characterizing rock falls. In the particular case of the Mont Granier rock fall sequences, these technics gave accurate information about both the occurrence time, the volume and the shape of the successive rock falls. This stresses the major difference between the 9th January event, which occurred without any forerunner, and the 7th May event, which was preceded by smaller rock falls. The time of occurrence is also of interest and may be helpful for better understanding the role of temperature in the triggering of such events.

5 ACKNOWLEDGEMENTS

The authors warmly thank the municipality of Chapareillan, the Securité Civile, the Parc Naturel de Chartreuse for assistance, and Julien Carcaillet and Arnaud Pêcher for providing aerial photos.

6 REFERENCES

Deparis, J., Jongmans D., Cotton F., Baillet L., Thouvenot F., and Hantz D. (2007), Analysis of rock-fall seismograms in the western Alps, Bull. Seismol. Soc. Am., 98, 1781–1796.

Ekström, G. and Stark, C. P. (2013), Simple scaling of catastrophic landslide dynamics, Science, 339, 1416–1419

Ravanel, L., D. Amitrano, P. Deline, X. Gallach, A. Helmstetter, F. Hobléa, G. Le Roy, E. Ployon, The small rock avalanche of January 9, 2016 from the calcareous NW pillar of the iconic Mont Granier (1933 m a.s.l., French Alps)((poster), Geophysical Research Abstracts, Vol. 18, EGU2016-13535, 2016.

Coupling 3D rockfall propagation to the spatio-temporal frequency for a realistic rockfall hazard mapping

Cécile d'Almeida[1], François Noël[2], Antoine Guerin[3], Michel Jaboyedoff[4], Didier Hantz[5], Marc-Henri Derron[6]

Keywords: rockfall, numerical modelling, failure frequency, propagation simulation, Saint-Eynard

Rockfall hazard is a major threat in mountainous area. To prevent from this natural hazard, it is necessary to estimate where and when a rockfall will occur, its magnitude and where it will propagate. Rockfall hazard is frequently divided into two domains analysed individually: failure hazard and propagation hazard. These hazard analyses are usually performed qualitatively or semi-quantitatively and therefore includes some subjectivity. In the case of extended cliffs, rockfall hazard is carried out in term of diffuse failure hazard: the cliff is assumed to be homogeneous and the rockfall sources are supposed to be uniformly dispatched throughout the cliff surface. Nevertheless, this is a rough approximation. The proposed method aims to perform the whole rockfall hazard analysis, in a quantitative manner, as a single item. This has been achieved by integrating the parameters of the failure analysis (spatial-temporal rockfall frequency, block size distribution and spatial distribution of rockfalls) into the propagation analysis.

1 SPATIO-TEMPORAL FREQUENCY MEASUREMENT

The method is performed on the study site of the Mont Saint-Eynard (Chartreuse massif, France). The site benefits of height years of annual grounded-based lidar monitoring carried out between 2009 and 2017. The erosive dynamic of the cliff is measured with a lidar based method for rockfall detection. The volume distribution of the blocks is estimated from a field measurement.

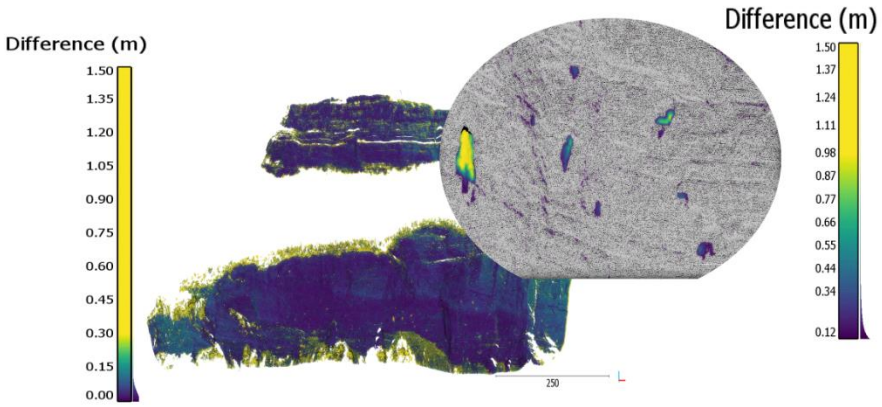

Figure 29: Surface model comparison of the Saint-Eynard cliff

Both the frequency-magnitude distribution of the rockfalls and the volume distribution of the blocks can be modelled with power laws (Barlow et al. 2012; Hantz et al. 2003). Based on the hypothesis of their temporal stability, the fitted power laws are used for diffused hazard assessment of future rockfalls event. Their use provides the failure frequencies of rockfalls of given size, the eroded volume of the cliff and the number of blocks of given size for a period considered.

2 COUPLING APPROACH

With the proposed method, the spatial distribution of the sources is integrated in the propagation analysis. From the rockfall detection, density maps on 3D point cloud of each volume class are produced and are used to weight the 3D spatial distribution of the rockfall sources for the propagation simulation.

[1] D'ALMEIDA Cécile, Risk Analysis Group, Institute of Earth Sciences, University of Lausanne, Lausanne, Switzerland (CH), (d.almeidacecile@gmail.com)

[2] NOËL François, Risk Analysis Group, Institute of Earth Sciences, University of Lausanne, Lausanne, Switzerland (CH), (francois.noel@unil.ch)

[3] GUERIN Antoine, Risk Analysis Group, Institute of Earth Sciences, University of Lausanne, Lausanne, Switzerland (CH), (antoine.guerin@unil.ch)

[4] JABOYEDOFF Michel, Risk Analysis Group, Institute of Earth Sciences, University of Lausanne, Lausanne, Switzerland (CH), (michel.jaboyedoff@unil.ch)

[5] HANTZ Didier, University of Grenoble Alpes, ISTerre, Grenoble, France (FR), (didier.hantz@univ-grenoble-alpes.fr)

[6] DERRON Marc-Henri, Risk Analysis Group, Institute of Earth Sciences, University of Lausanne, Lausanne, Switzerland (CH), (marc-henri.derron@unil.ch)

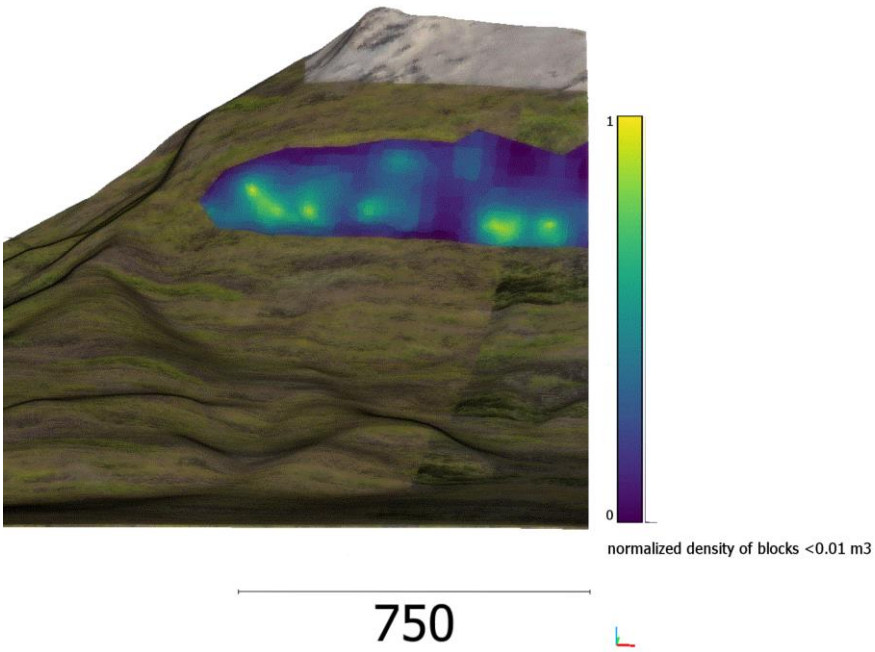

Propagation of distributed blocks are simulated to evaluate their path and stopped distance. Their varying size and spatial distribution are attributed with the block distribution and the density maps. The specific location of the sources is allowed using the Trajecto3D model. The Trajecto3D is a propagation model working on point cloud DEM (Noël et al. 2017). It allows a fine and detailed representation of the terrain and to get rid of the usual bias found on horizontally gridded data.

Figure 2: 3D density map of blocks inferior to 0.01m³ on the southest kilometer of the Saint-Eynard cliff

3 CONCLUSION

Finally, the resulting hazard map not only considers the obtained trajectories, but also considers the inhomogeneous spatial-temporal rockfall frequency and the rockfall and block volume distributions. This would help decision maker in rockfall hazard management by providing accurate hazard map that summarize information of interest.

4 REFERENCES

Barlow, J., Lim, M., Rosser, N., Petley, D., Brain, M., Norman, E. & Geer, M. (2012) Modelling cliff erosion using negative power law scaling of rockfalls, Geomorphology, 139-140, 416-424.

Hantz, D., Vengeon, J-M. & Dussauge-Peisser, C. (2003) An historical and probabilistic approach to rockfall hazard assessment. Natural hazards and Earth System sciences, 3, 693-701.

Noël, F., Cloutier, C. & Turmel, D., Locat J. (2017) Using Point Clouds as Topography Input for 3D Rockfall Modeling, Landslides and Engineered Slopes. Experience, Theory and Practice: Proceedings of the 12th International Symposium on Landslides

Effect of rockfall fragmentation on exposure and subsequent risk analysis

Gerard MATAS[1], Jordi COROMINAS[2], Nieves LANTADA[3]

Keywords: rockfall, fragmentation, Quantitative Risk Analysis, modelling, case study

Rockfalls are frequent natural processes in mountain regions with the potential to produce damage. The quantitative risk analysis (QRA) is an approach increasingly used to assess risk and evaluate the performance of mitigation measures. In case of the fragmentation of the falling rock mass, some of the hypothesis taken in the QRA estimation for rockfalls have to be modified since a single block or rock mass can produce several fragments thus modifying the runout probability, the impact energies and exposure of the elements at risk. In this contribution, we present a procedure to account for the exposure in QRA analysis along linear paths using the fragmental rockfall propagation model RockGIS (Matas et al. 2017). The procedure is applied at the *Monasterio de Piedra*, Spain as part of a QRA.

1 INTEGRATING FRAGMENTATION IN QRA

Risk is estimated as the product of the annual probability of a block reaching a reference location, the spatio-temporal probability of the exposed element and vulnerability of the element for a certain intensity level (Corominas et al. 2014). In case of rockfalls without fragmentation, the runout probability is usually estimated by stochastic computer simulations: some blocks are released from expected sources, then the runout probability at each reference location is computed by dividing total number of blocks reaching the site by total simulated blocks. When considering fragmentation this approach has to be modified since one single rockfall may lead to multiple fragments reaching the location and thus obtaining runout probabilities mathematically higher than one. For the estimation of exposure, fragmentation will also have a significant effect since one single rockfall may produce a number of fragments with divergent trajectories, thus increasing the width of the area affected by the rockfall. Consequently, the probability of any trajectory intersecting the exposed element will increase.

To integrate fragmentation in QRA analysis we have modified the formulation presented by Agliardi et al. (2009). We calculate the probability that a certain number of fragments *f* produced during an event of magnitude *i* could reach the exposed element *j* and then, integrate it for all number of possible fragments reaching the element. Thus, instead of having a single runout probability for each event magnitude we have a probability distribution that a certain number of fragments could reach the element. Equation 1 shows the modified expression to estimate Risk.

$$R = \sum_{j=1}^{J}\sum_{i=1}^{I}\sum_{f=1}^{F} N_i \times P_f\left(S/D\right)_i \times P_f\left(T/S\right)_j \times V_{ijf} \qquad (1)$$

Where: R is the risk due to the occurrence of a rock fall of magnitude (volume) *i* that produces *f* fragments during its propagation on an exposed element *j* located at a reference distance S from the source; N_i is the annual frequency of rockfalls of volume class *i*; $P_f(S|D)_i$ is the probability that *f* fragments generated by the detached rock mass of the size class *i* reach a point located at a distance S from the source; $P_f(T|S)_j$ is the exposure or the probability that an element *j* be in the trajectory of the *f* fragments generated by the rock fall at the distance S, at the timing of the event; V_{ijf} the vulnerability of a exposed element *j* in the case of being impacted by *f* fragments generated by the *i* magnitude block.

Fragmentation modifies the exposure of the elements, since the affected width of the linear structure may increase. Equation 2 shows the expression considered for the exposure (modified from Nicolet et al., 2016).

$$P_f\left(T/S\right) = \frac{f_p \times \left(w_f + l_p\right)}{24 \times 1000 \times v_p} \qquad (2)$$

Where: f_p is the flow of visitors (persons/day); W_f is the width of the rockfall debris front depending on number of impacting fragments *f* computed in the simulation (m); l_p is the width of the person (m) and v_p is the mean velocity of persons (km/h).

[1] MATAS Gerard, Universitat Politècnica de Catalunya-BarcelonaTech, Barcelona, Spain, gerard.matas@upc.edu

[2] COROMINAS Jordi, Universitat Politècnica de Catalunya-BarcelonaTech, Barcelona, Spain, jordi.corominas@upc.edu

[3] LANTADA Nieves, Universitat Politècnica de Catalunya-BarcelonaTech, Barcelona, Spain, nieves.lantada@upc.edu

2 APPLICATION

This methodology has been applied at the *Monasterio de Piedra*, Spain. For this initial estimation just 1m³, 10m³ and 100m³ rockfall events have been considered. Calibration of the model was performed considering historical inventoried events which also allowed to estimate an annual frequency curve to compute N_i. For the trajectory computation of all generated fragments we used the rockfall propagation model RockGIS (Matas et al. 2017) to obtain $P_f(S|D)_i$ from the cumulative probability function shown in Figure 1 and W_f as a proportion of the maximum expected width W_{fmax} depending on number of impacting fragments. Since the exposed elements are visitors we assumed $V_{ijf}=1$ as a conservative hypothesis. To evaluate the effect of account for fragmentation or not, we also carried out simulations without breakage as seen in Figure 2.

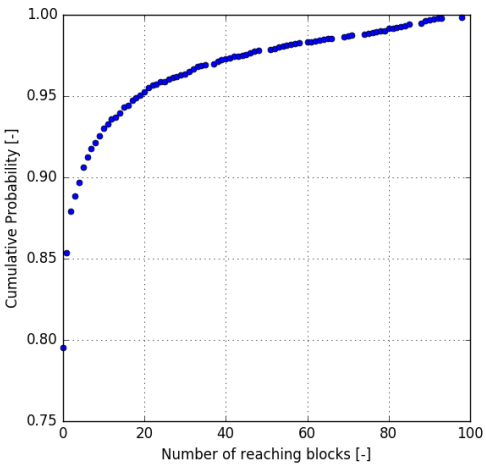

Figure 1: Cumulative probability for each number of reaching fragments

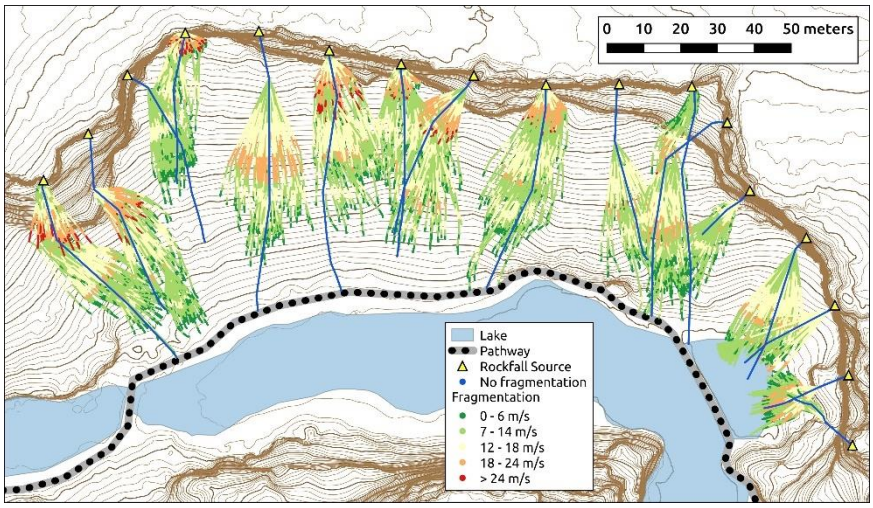

Figure 2: Trajectories with and without considering fragmentation for 10m³ blocks. Just one block released from each source for visualisation purposes.

Risk values obtained with this methodology for rockfall volumes of 1m³, 10m³ and 100m³ are respectively $4.5\cdot10^{-4}$, $1.3\cdot10^{-4}$, $3.52\cdot10^{-5}$ in case of no fragmentation, and $4.35\cdot10^{-5}$, $1.19\cdot10^{-4}$, $1.07\cdot10^{-4}$ when fragmented. This results show that for small-size rockfalls (<1m³), fragmentation reduces risk to the visitors. For rockfall events >100 m³, fragmentation increases the overall risk due to the generation of multiple divergent trajectories and higher exposure of the elements at risk. For 10m³ size rockfall events, the shorter run-out and smaller kinetic energy compensates the increase of width by divergent trajectories.

3 CONCLUSION

The proposed methodology allows the integration of fragmentation effect into QRA in linear paths but is also extensible to non-linear elements. Risk increment or reduction when considering fragmentation is controlled by the relative position of the elements along the slope. The effect of fragmentation in runout and exposure may have opposite effect in the final risk.

4 REFERENCES

Agliardi, F., Crosta, GB., Frattini, P. (2009) Integrating rockfall risk assessment and countermeasure design by 3D modelling techniques. *Nat Hazards Earth Syst Sci* 9:1059–1073

Corominas, J. van Westen, C., Frattini, P., Cascini, L., Malet, J.P., Fotopoulou, S., Catani, F., Van Den Eeckhaut, M., Mavrouli, O, Agliardi, F., Pitilakis, K., Winter, M.G., Pastor, M., Ferlisi, S., Tofani, V., Hervás, J., Smith, J.T. (2014) Recommendations for the quantitative analysis of landslide risk. *Bulletin of Engineering Geology and the Environment*, 73: 209-263

Matas, G., Lantada, N., Corominas, J., Gili, J.A., Ruiz-Carulla, R., Prades, A. (2017) RockGIS: a GIS-based model for the analysis of fragmentation in rockfalls. *Landslides*, 14: 1565–1578

Nicolet, P., Jaboyedoff, M., Cloutier, C., Crosta, G., Lévy, S. (2016). Brief Communication: On direct impact probability of landslides on vehicles. *Natural Hazards and Earth System Sciences* 16, 995-1004

Run-out of rockfall: towards objective assistance in determining the angles of the energy line method

Bastien COLAS[1], Frédéric BERGER[2], David TOE[3]

Keywords: rockfall, run-out, energy line, event database, hazard mapping

In France some works are engaged for 2 last years in order to frame rules & practices for rockfall hazard mapping dedicated for land-use planning at the municipality scale. Works are focused on failure, intensity valuation & run-out of rockfall. This paper presents recent developments on the use of the energy line method to define run-out areas.

1 RUN-OUT APPROACHES

The run-out of rocky elements in a slope depends mainly on the characteristics of the studied slope and unstable rocky elements. Two types of modelizations for the characterization of the run-out of rockfalls are generally used: i) models based on physics, i.e. trajectography (in 2D or 3D) which integrate the mechanical, geotechnical and morphological properties of the blocks and the area of propagation and ii) empirical / statistical models including the so-called energy line model (Heim, 1932). Physical-based models require many input parameters that are rarely routinely measured when performing hazard mapping for land-use planning (PPR in France). The feedback shows that the energy line method has good results (Copons, 2009) and that it is a relevant alternative to physical models.

2 ENERGY LINE MODEL

The method of the energy line is based on a simple and trivial principle: a block can only progress on a slope if it is steep enough. Thus, if the slope is greater than a limiting angle β, it accelerates. If it is less than β, it slows down. Starting from this observation, a block can go from a starting zone A to B, point of intersection of the relief with an imaginary line starting from the starting zone and forming an angle β with the horizontal. This line is called the energy line and the angle β, the angle of the energy line. The difficulty of applying the method lies in the choice of angle values for the expert. Compilations made (Jaboyedoff, 2011), show wide variations of the angles according to the authors. These variations directly inducing the reaching distances, making the justification of the values retained as essential.

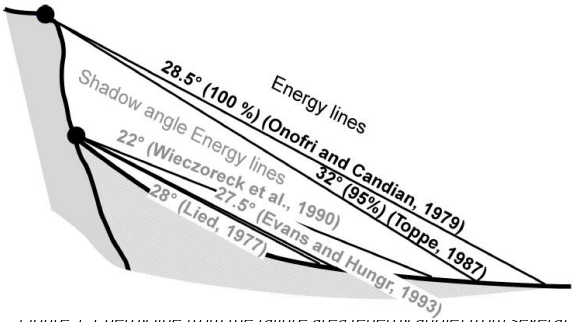

Figure 1: Energy line from the failure area (energy angle) from several authors (Jaboyedoff and Labiouse, 2011)

The aim of this work is to improve, on objective criteria, the decision support in defining the values of angle of the energy line method values. These values characterize the run-out in order to establish the boundaries of areas potentially impacted by falling rocks. We propose the introduction in the energy line method of objective criteria, depending on the morphology, for decision support in the choice of angle values. The analysis is conducted on the basis of feedback from rock events in different geomorphological contexts.

3 ROCKFALL DATABASE

For decision help, an event database of rockfalls was created, laying the foundations of a real observatory "falls of blocks". This database includes: i) a detailed description of slope profiles (morphology, geology, vegetation ...) ii) an identification of the rocky elements involved in landslides (size, volume, shape if possible) iii) the surveys of the zones of starting (breaking) and reaching boulders, in different contexts. This first database was containing 2758 events, of which 2508 are from a Swiss database (Zürcher, 2010) which benefit from specific detailed surveys for the description of the forests stands present along the boulders trajectories. This survey database is integrated in the “rockfall profiles” database under development within the Interreg Alpine Space project “ROCK the ALPS” coordinated by Irstea. These rockfall profiles database currently contains 7039 events profiles coming from Bavaria, France, Italy, Slovenia and Switzerland. Within 2018 data from Austria will be added.

[1] COLAS Bastien, BRGM, Montpellier, France (FR), b.colas@brgm.fr

[2] BERGER Frédéric, IRSTEA, Grenoble, France (FR), frederic.berger@irstea.fr

[3] TOE David, IRSTEA, Grenoble, France (FR), david.toe@irstea.fr

Figure 2: Pictures of Crussol site (Ardèche France). February 2014 rockfall event (© France 3 Region)

4 ENERGY LINE ANGLE – MORPHOLOGY RELATIONSHIP

For all these events, a strong relationship is proposed between slope morphology and observed energy line angle values. Based on this relationship, studies on quantile regressions of observed deposits allow proposing a quantitative approach of the distribution of the potential reaching distances. Finally, depending of the local topographic context, reach angle values to be used for the energy line method can be defined and associated to a probability of the run-out. In most of cases speaking, these values can vary from up to 70° in some particular context of vertical cliff with horizontal reach area (case of quarry for ex.) to 26° for regular slope profile at the foot of the starting area. The confrontation of this approach with sites of past events shows a good coherence with the actual practices.

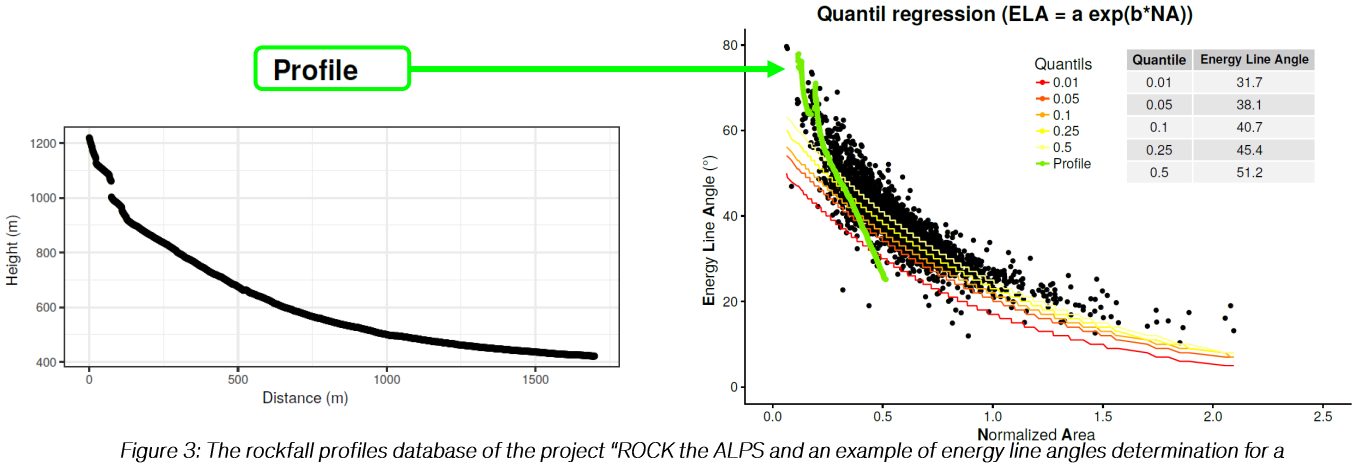

Figure 3: The rockfall profiles database of the project "ROCK the ALPS and an example of energy line angles determination for a profile using a new topographic index and quantile regressions

5 CONCLUSION

This innovative approach, emphasizing the principle of the energy line, enriches the panel of tools available to experts (Jaboyedoff, 2011) for rock hazard mapping and surely opens new perspectives. If the application of these results seems to give a good first-order estimate of runout distances (related to likehood of run-out), how this principle should be included into the panal of tools remains an open question in rockfall engineering.

6 ACKNOWLEDGEMENTS

This work has been initially supported by the Ministry of Ecology (METS, General Directorate for Risk Prevention) through BRGM's public policy support activity for the METS and is currently supported by the European Interreg Alpine-Space program 2014-2020 via the funding of the project ROCK the ALPS (ASP 462)

7 REFERENCES

Copons, R., Vilaplana, J.M., and Linares, R. (2009). Rockfall travel distance analysis by using empirical models (Solà d'Andorra la Vella, Central Pyrenees). *Nat. Hazards Earth Syst. Sci. 9, 2107–2118.*

Heim, A.: Bergsturz und Menschenleben (1932), *Beiblatt zur Vierteljahrsschrift der Naturforschenden Gesellschaft in Zurich, 218 p.*

Jaboyedoff, M., and Labiouse, V. (2011). Technical Note: Preliminary estimation of rockfall runout zones. *Nat. Hazards Earth Syst. Sci. 11, 819–828.*

Zürcher, K., Wiedmer, Y., and Thormann, J.-J. (2010). Weiterentwicklung NaiS-Anforderungsprofil Steinschlag: minimale bewaldete Hang- und kritische Lückenlänge.Wang, H. J., Li, D., & He, X. (2012). Estimation of high conditional quantiles for heavy-tailed distributions. *Journal of the American Statistical Association, 107(500), 1453-1464.*

Multiscale testing of geogrids used for rockfall protection

Christophe NOCITO (corresponding author) [1] **Texinov,** Marie TANKERE [2] Texinov, Patrick JOFFRIN, IFSTTAR [3]; Ignacio OLMEDO, GTS [4]

1 INTRODUCTION

Geogrids and geonets are used since decades as protection against rockfalls. Although meshes on protection structures are traditionally made of cable nets, products made of polymers offer an interesting and revolutionary alternative due to their specific properties: light weight, resistance to weathering and severe climate conditions, flexibility and easy installation. Last but not least, the elastic deformation of synthetic geonets is higher than the deformation allowed by metallic meshes: the energy absorption can therefore be improved by using synthetic geonets or geogrids.
The studies carried out focuses on an accurate characterization of these nets at different scales. These researches aim to improve these components and their adaptation to traditional structures.

2 MULTISCALE TESTING

Due to the particularities of polymeric geogrids in terms of mechanical behavior, it is necessary to carry out reduced scale tests for the analysis of their deformation and resistance. These tests which are done under perfect boundary conditions are used for the characterization and development of new types of grids adapted to the protection structures needs. However, these test conditions differ significantly from those of grids installed on protection devices and impacted by rockfalls. Thus, in order to recreate realistic boundary conditions and to analyze the full mesh behavior, laboratory tests at a greater scale are carried out. So, the combination of these two scale tests allow a full characterization of geogrids under different loading cases.
In particular, tests carried out are:

- Meso scale tests: Tests at reduced scale using a multiaxial dynamometer
- Macro scale tests: Tensile and punch quasi-static tests under realistic boundary conditions and scale (3x3 meter samples)
- Impacts tests on full scale samples, as for metal mesh, following ETAG27 requirements

3 TRI-AXIAL DYNAMOMETER

The triaxial dynamometer has been realized by the company “EMI Develeppement”, based on specifications from Texinov. Hence, the possibility to develop a custom dynamometer allows to obtain a machine that can be adapted and programmed for different test sequences.

The technical characteristics of this machine can be summarized as following:

Velocity : from 0 to 1200 mm/min
Strength : mechanical conception allows maximum strength up to 50 kN for X and Y axis and 30 kN for Z axis.
Linear rails shift : 200 mm (X1, X2, Y1, Y2, Z)
Samples minimum length s: 102×102 mm

The video extensometer is realized through application and CCD camera. The video extensometer is made with the calculation of target shift. Video capture could be linked with each strength / elongation point and time.

[1] NOCITO Christophe, Texinov, La Tour du Pin, France : cnocito@texinov.fr
[2] TANKERE Marie, Texinov, La Tour du Pin, France
[3] JOFFRIN Patrick, IFSTTAR, Bron, France
[4] OLMEDO Ignacio, GTS, Domène, France

Fig.1 – Tri axial dynamometer: X Y and Z axes

4 MESO SCALE TESTS

Two different testing devices are used for caracterising the 3x3 meter samples. A tensile test machine allows loading the grids in 1 axis. The second axis can be blocked and loadings are recorded in the two axis. Moreover, the displacement applied on the loaded side is also measured. The maximal tensile loading is 400kN and the maximal displacement is 150 cm.
The punch tests consist on an orthogonal loading of the mesh at its central location. The punch test device allow fixing the sample at its four sides and the loading apparatus shape can be adapted to the type of grid if necessary. The loading force and displacement evolutions in time are recorded. The maximal loading force is 400kN and the maximal displacement is 220cm.

5 IMPACT TESTS

Tests will mainly focused on:

- Polymer characterisation
- Connection components to support structure
- Dynamical elongation during impact tests
- Residual height after impact

6 CONCLUSION

The full results of the testing will be available during the 1st semester of 2018, the main objective will be to establish the correlation between the different scales, and to qualify new products using the tri axial dynamometer on small samples.

7 ACKNOWLEDGEMENTS

The work described in this paper is supported by the French Ministry of Industry and BPIFrance in the frame of the FUI funding program (PRIDYN project, FUI AAP 21).

8 REFERENCES

Auray G., Tankéré M., Limam A., Robit P.; Mechanical analysis and long-term behaviour of geonets for slope protection. *Proceedings of the JNGG 2012 Conference.*

Bloc Armé© –Landslides passive protective structure

Julien LORENTZ[1], Jean Philippe JARRIN[2], Lucas MEIGNAN[3], Romain LE ROUX MALLOUF[4]

Keywords: Bloc armé©, Concrete blocks, metallic reinforcement, protection structure against gravitational natural risks, emergency kit.

1 CONCEPT PRESENTATION

The Bloc Armé© is composed by 3D prefabricated and adjustable blocks. The blocks are linked by internal, modular and continuous reinforcements (Fig 1). The nature and typologies of the blocks as well as the possibility to design the internal metallic framework allow to adapt the product to different configurations and diverse needs such as retaining wall, reinforced wall or protection against rockfalls or landslides.

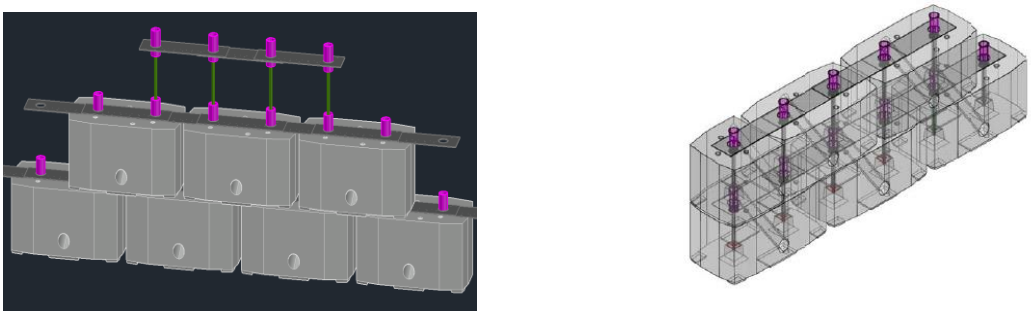

Figure 1: Bloc Armé© : Blocks linked with reinforcements

The *Bloc Armé©* has many advantages:

- It is quick assembled, allowing to limit the risk exposure for the workers.
- The mechanical resistance is more important than a solution composed by an arrangement of blocks without metallic reinforcement. The continuous connection of the metallic framework and the anchorage possibility of the wall ensure a strong resistance to tipping and avoid the risk of block fall on the road (Fig. 2).
- It is easily dismounting thanks to the modular design. The structure can be repaired quickly after important damages and avoid a long road closure.
- The small footprint of 80 cm limits the grading for the set up and leaves more space for the protected structures.

Figure 2: Bloc Armé© solution

The Bloc Armé© solution can be proposed as an emergency kit, temporary protection of work, permanent protection or embankment facing.

[1] LORENTZ Julien, Geolithe Innov, Crolles, France, Julien.lorentz@geolithe.com

[2] JARRIN Jean Philippe, Geolithe, Crolles, France, jp.jarrin@geolithe.com

[3] MEIGNAN Lucas, Geolithe, Crolles, France, lucas.meignan@geolithe.com

[4] LE ROUX MALLOUF Romain, Geolithe, Crolles, France, Romain.lerouxmallouf@geolithe.com

2 BLOC ARMÉ© AS PROTECTIVE STRUCTURE AGAINST LANDSLIDES

The Bloc Armé©, as protective structure against landslides, consists in the implementation of 1,6*0.8*0.8m^3 concrete (C35/C45) blocks. These concrete blocks have 2 vertical holes and foot notches in order to link them together with the metallic framework. The blocks are vertically fixed together using GEWI phi25 steel bars These steel bars are set in the two vertical holes and are linked with a coupler between the different layers of blocks, allowing an easy mounting and dismounting. The blocks are also fixed horizontally by metallic plates. These plates have two holes at each end in order to be inserted between 2 steel tubes themselves embedded in the vertical holes of the concrete blocks. The block can also be anchored to the ground through an oblique hole (Fig 3).

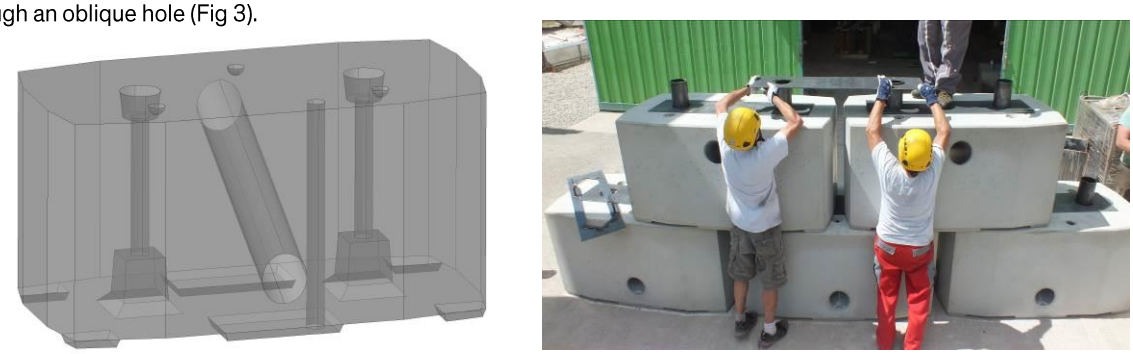

Figure 3: Bloc Armé© : Concrete blocks linked with metallic reinforcements

3 ONE REALISATION WORK WITH BLOC ARME® SOLUTION

The assembling of the blocks has been done very quickly thanks to the easy bloc armé® process. The blocks were lifted with a mobile crane. The implementation was carried out by personnel from the spider nacelle (Fig. 2). Occasional technician interventions with alpine method were necessary for the final adjustment of the position of the blocks. To complete the work, more than 100 blocks have been assembled in few days.

For this case, the stability of the wall is ensured thanks to subhorizontal anchorings. To ensure personnel safety, subhorizontal steel bars have been drilled once all the blocks had been laid and tied together. Inclined holes from downstream face to the upstream face were provided inside each block (Fig. 3). The diameter of the inclined holes has been set to pass the drill bit, which allow to drill with a diameter of 115 mm in accordance with the design (Fig. 4)

Finally, a net fence has been implemented at the top of the structure. This implementation has been facilitated thanks to the connectors of the vertical bars of the wall bloc armé® arranged every 80 cm (Fig. 4).

Figure 4: View of the structure with steel bares and net on the top

4 CONCLUSION

The Bloc Armé© has been installed as landslide passive protective structure. This structure makes it possible to guarantee a greater resistance, thanks to the network of metal reinforcement which ensures a continuity of the structure. In addition, the simplicity of implementation allowed the installation of more than 100 blocks in few days limiting the exposure time of the workers.

This work has showed the interest of bloc armé®. This solution is promising and can be used for other roads in mountain areas. Other cases of application could be envisaged, for example, bloc armé® as emergency kits.

Falling of C40 rock at Livet Gavet

Sébastien PIOT (author)[1], Jerry MAGNIN (author)[2], Didier CALIME (author)[3]

Keywords: Monitoring, sensors, rock fall, real-time

The 11th of September 2016, a 25 000 tons rock felt down in the vicinity of Romanche dam construction site without any casualties.

Prior to the project inception, IMS-RN and SITES teams have been involved to define, implement and operate a real time monitoring system based on sensors dedicated to warn-up in case of imminent hazard.

After a 5 years period of uninterrupted monitoring, the system have recorded an acceleration of the rock displacement predicting an imminent falling. All stakeholders have been warned-up 24 hours before the rock falling, enabling to get the construction site in a safe mode.

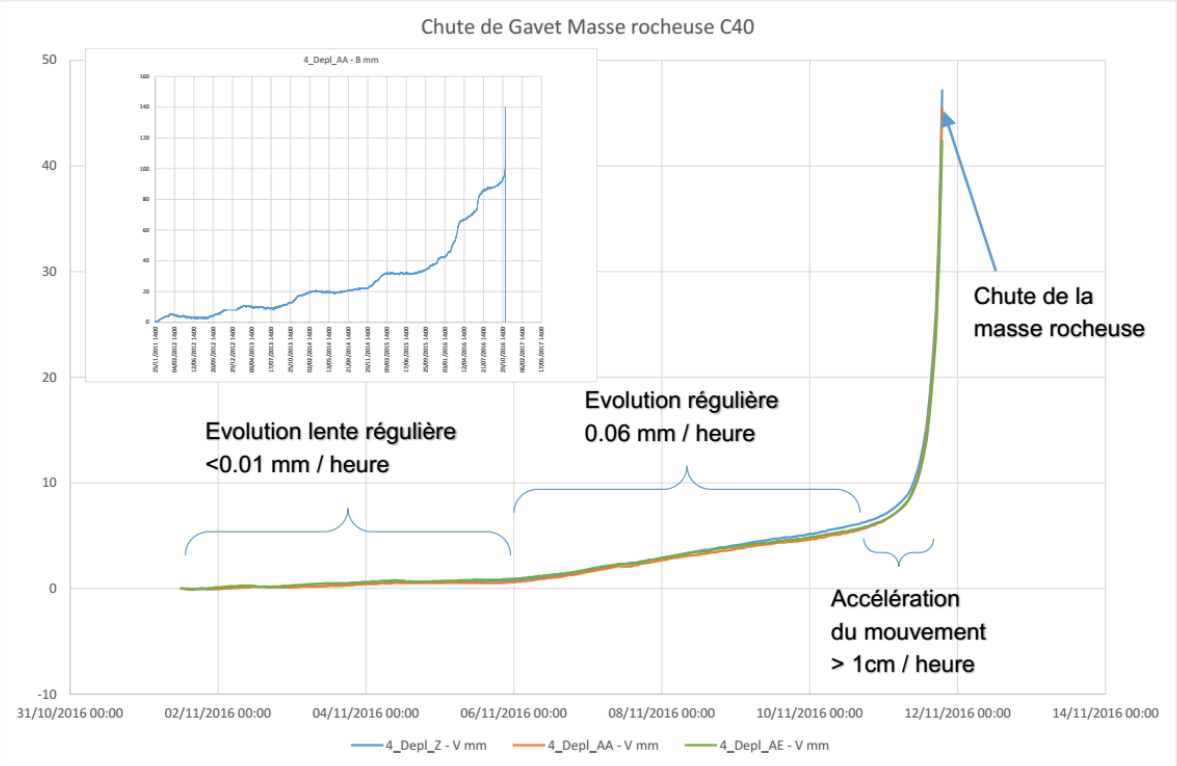

Figure 1: Rock displacement VS time from the monitoring start to the rock falling

[1] PIOT Sébastien, SITES, Lyon, France (FR), sebastien.piot@sites.fr

[2] MAGNIN Jerry, IMS-RN, Grenoble, France (FR), jerry.magnin@imsrn.com

[3] CALIME Didier, SITES, Paris, France (FR), didier.calime@sites.fr

Innovative prefabricated rockfall gallery using a polymer geosynthetic mesh

Joëlle Arnaud[1], Magali Huteau1[2], Philippe Robit[3], Ignacio Olmedo[4], Nicolas Villard[5]

Keywords: prefabricated, rockfall gallery, railway, geosynthetic

Railways in mountain areas, like other communication infrastructures, are especially sensible to rockfall activity. In the French Alps, the major economic implications of perturbations on the train traffic leads to put a particular focus on the rockfall protection of railways. Moreover, during the installation of protection devices uphill, the frequency of rockfall occurrence increases significantly due to the eventual mobilisation of unstable masses by operators. For this and to guaranty the security of the railway and the workers working on, the French national railway company, the SNCF, needed a temporary protection device during the installation of flexible fences to protect the entrance of the Colombiere tunnel at Brison, near Chambery (France). The company GTS proposed a light prefabricated rockfall gallery allowing an efficient installation in reduced time of track-closure. An impact test for the validation of the gallery was carried out on one module.

1 INTRODUCTION

The high-speed train track between Culoz and Modane is an important sector of the French Alps railways as it serves the ski resorts and touristic areas and of the sensitive freight-trains relying with Italy and Switzerland. In the surroundings of Brison, the railway is situated between the Bourget Lake and a limestone cliff. This cliff presents a significant rockfall activity (about 1 litre/week).

For the maintenance tasks of the rockfall detection systems called DCR and to guarantee the secutiry of workers, protection structures such as flexible fences were planned. To reduce the staff exposure and the residual risk of damage during works uphill a temporary protection solution was needed. Considering the emergency and the complexity of such operation, a consortium was created with SNCF, GTS, SAGE INGENIERIE and ENGIENEERISK.

The slope and rockfall trajectography analysis concluded that a 218kg rockfall at an impact velocity of 37m/s event should be considered for the structure dimensioning. Thus an energy level (SEL) of 150kJ was considered. The exposed sections is 60 linear meters long.
Three options were considered (Engineerisk, 2016, SAGE Ingénierie 2016):

- Sandwich structure made of iron, wire mesh and sand bags
- A metallic gallery made of iron sheets
- A gallery made of one high tensile steel wire mesh and a high resistance geosynthetic layer.

Finally, the third option was retained.

2 STRUCTURE DESCRIPTION

The Multi-layer gallery designed, made and installed by GTS was composed of a metallic structure allowing deploying the high tensile wire mesh and the geosynthetic mesh over the first one. This design sought to limit the bullet effect or perforation of the mesh by the low mass/high speed rockfalls (Giacomini, 2011). The geosynthetic allow a progressive loading of the high tensile steel wire mesh. Moreover, energy dissipating devices were installed.
Considering the limited track closure times, the structure was assembled in a safe area and installed in the right position by heavy cranes in four 4 hours' time-slots during the nights. Thus, the structure was composed of 5 independent modules for an easier installation.

The gallery remained operational during the works uphill. Once the works were finished the structure was removed. During this process, one of the modules was tested, in a secured spot away from the rail tracks for development purposes.

[1] ARNAUD Joëlle Irstea – SNCF , FRANCE, joelle.arnaud@reseau.sncf.fr

[2] HUTEAUMagali, Irstea – SNCF, France, magali.huteau@reseau.sncf.fr

[3] ROBIT Philippe, GTS, Grenoble, France probit@gts.fr

[4] OLMEDO Ignacio, GTS, Grenoble, FRANCE, iolmedo@gts.fr

[5] VILLARD Nicolas, GTS, Grenoble, FRANCE, nvillard@gts.fr

Figure 1: The temporary multi-layer rockfall gallery (left) and capture of the impact test (right)

The test was carried out with a 405kg block following the ETAG027 geometry impacting at 27.3 m/S (freefall height of 38m), so impacting at 150kJ. The impact was recorded by a high speed camera at 500fps and complementary cameras. A triaxial accelerometer installed on the bloc allowed recording the bloc acceleration along the impact and to calculate the impact force. The obtained data confirm the progressive loading of the structure, first by the loading of the polymer mesh and then by the complete loading of the high tensile steel wire mesh. The energy dissipating devices were activated during the loading of the steel mesh.

3 CONCLUSION

This innovative multi-layered gallery represents a new possibility for protection of roads and railways. Moreover, this solution presents a reduced installation device. The design principles consisting on using different layers to avoid the bullet effect and the perforation of the steel mesh have been confirmed by the experimental test carried out at 150kJ.

This innovative process has improved the constant interactions between transporters, engineers, the coordinator of safety at work, and civil engineering firms. This project drove us to share technical and scientific information with dynamic team interactions. Communication has helped the team to be involved in the project on all levels from the operational team to the local authorities and the central decision organs of SNCF.

4 REFERENCES

Giacomini, A, Buzzi, O, Hambleton, J (2011) Predicitions of the bullet effect for rockfall barriers: a scaling approach. *Rock mechanics and rock engineering.*

Miali, A, Mihailovitch, F, Chirouze F, Terpereau, JM (2016) Management de la sécurité du système ferroviaire, International Railway Safety Council

SAGE Ingénierie (2016) Etudes des risques de chutes de blocs, Versant de la Colombière, Gières, RP. 7220

Engineerisk (2016) Protection pare-pierres – Falaise de la Colombière – Evaluation de différentes solu-tions au stade préliminaire

Failure mechanisms within unreinforced concrete wall under rockfall impact loading

Marion BOST[1], Ali LIMAM[2], Patrick JOFFRIN[3], Christophe PRUVOST[4]

Keywords: concrete wall, impact, rockfall, failure.

In mountainous areas, unreinforced concrete wall is a commonly used building way for new constructions. Actually this technique offers a suitable strength in case of construction in a slope. In these areas prone to rockfall hazard, the vulnerability of constructions to this hazard has to be considered. Even if numerous studies on the impact strength of concrete wall exist, they addressed either a quite different type of impact loading from rockfall impact (vehicle impact : Miyamoto & King, 1994; projectile impact: Smith & Cusatis, 2016) or a specifically reinforced concrete wall against rockfall (Mougin et al, 2005; Bertrand et al, 2015). To evaluate the strength of unreinforced concrete wall to rockfall impact, an experimental study was performed and some parts of the results are presented in this paper.

1 EXPERIMENTATION

1.1 TESTED UNREINFORCED CONCRETE WALLS

For this experimentation, unreinforced concrete walls were cast in place during a building construction. The walls were 2.5 m long, 2 m wide and 0.2 m thick (Figure 1). Each wall had a PAF® welded mesh panel as skin reinforcement, which is similar to a PAF V® welded mesh panel recommended by the French construction rules (AFNOR, 1993; Perchat, 1997). The concrete compressive strength was of 23.8 MPa ± 3.6MPa and the tensile strength was of 2.9 MPa ± 0.4 MPa.

Figure 1: Example of a tested unreinforced concrete wall

1.2 TEST CONDITIONS

The tests were carried out with the Ifsttar's impact test device (Bost et al, 2011; Figure 2). 12 walls were vertically impacted with 4 manufactured concrete blocks of different weight from 1.05 kN to 10.24 kN. Using reinforced concrete as block material, the block density (circa 2 500 kg/m^3) is equivalent to that of rock (2 700 kg/m^3). Therefore the chosen values for block weights correspond to volumes which are consistent with the real rockfall block sizes. Each block was released at 3 different heights in order to reach 3 different impact velocities. The values were chosen to reproduce the impact energy levels currently quoted in the few existing risk management procedures (VFF/AEAI, 2005; MEDDE, 2014).

All the impacts were located in the middle of the walls. To reproduce the boundary conditions generated by 2 canted walls on an outside wall in a construction, the tested concrete walls were laid on 2 simple supports made of reinforced concrete blocks (Figure 1).

During each test, a tri-axial accelerometer fixed inside the loading block, allows us to monitor its deceleration. The wall deflection was measured dynamically by a wire sensor. All measurements were synchronized.

Figure 2: The Ifsttar's impact test device

2 FIRST OBSERVATIONS AND FAILURE MECHANISMS

For all tests, no damage to the loading blocks was noticed whereas the walls had, depending on the load conditions, at least a weak penetration until a complete rupture. As a conclusion, a rockfall impact on an unreinforced concrete wall generates a hard impact.

The damage observations after impact on each tested wall are summarized in Table 1. According to load characteristics, we observed two failure types, either by punching (Figure 3) or by bending (Figure 4). We can underline that for a same energy level (see tests n° 3 and 12), failure mechanisms can differ. When the velocity increases or the size of the block decreases, the failure

[1] BOST Marion, Univ Lyon – IFSTTAR – GERS - RRO, Bron, FR, marion.bost@ifsttar.fr

[2] LIMAM Ali, Univ Lyon - INSA, FR, ali.limam@insa-lyon.fr

[3] JOFFRIN Patrick, Univ Lyon – IFSTTAR – GERS - RRO, Bron, FR, patrick.joffrin@ifsttar.fr

[4] PRUVOST Christophe, Univ Lyon – IFSTTAR – GERS - RRO, Bron, FR, christophe.pruvost@ifsttar.fr

mechanism changes from bending to punching. These results are consistent with previous studies on reinforced concrete flat slab subjected to localised impact loading (Micallef et al, 2014).

Table 1: Failure type for the 12 tests

Test	Load characteristics				Failure
	Block weight *kg*	Drop height *m*	Impact velocity *m/s*	Impact energy *kJ*	
1	105	5.0	9.9	5.2	Punching
2	105	20.4	20.0	21.0	Punching
3	105	45.9	30.0	47.2	Punching
4	278	2.5	7.0	6.8	Punching
5	278	6.2	11.0	16.9	Punching
6	278	18.4	19.0	50.3	Bending
7	508	0.9	4.1	4.3	Punching
8	508	3.3	8.0	16.2	Bending
9	508	11.5	15.0	57.1	Bending
10	1024	0.5	3.0	4.6	Bending
11	1024	0.9	6.0	18.7	Bending
12	1024	4.7	9.6	47.5	bending

Figure 3: Punching failure (rear face of a wall)

Figure 4: Bending failure

3 CONCLUSION

The impact energy is an inadequate parameter to qualify the vulnerability to rockfall impact of an unreinforced concrete wall. The size of the block or its velocity has to be considered to identify the failure mechanism and prevent damage in the wall design. A complete analysis of the test results with the support of a numerical model is planned in order to understand the conditions for both failure mechanisms and define limit values between them.

4 ACKNOWLEDGEMENTS

This research program is carried out with the support of the Natural Hazard Department of the French Ministry of Ecology.

5 REFERENCES

AFNOR (1993) NF P 18-210 - Travaux de bâtiment – Murs en béton banché – Cahier des clauses techniques.

Bertrand, D., Fassem, F., Delhomme, F., Limam, A. (2015) Reliability analysis of an RC member impacted by a rockfall using a nonlinear SDOF Model. Engineering Structures, 89, p. 93-102.

Bost, M., Loock, S., Luca, L., Rocher-Lacoste, F., Gineys, J., Dubois, L., (2011). A new testing station for rock impact on full-scale structures, Proceedings of the 12th International Congress on Rock Mechanics ISRM 2011, pp. 1165-1168.

MEDDE (2014) Proposition d'une note technique à l'attention des Services Déconcentrés de l'Etat en charge des procédures PPRn. Méthodologie de l'élaboration du volet « aléa rocheux » d'un PPRn. Groupe de travail MEZAP du Ministère de l'Ecologie, du Développement durable et de l'Energie, 49p.

Micallef, K., Sagaseta, J., Fernadez Ruiz, M., Muttoni, A. (2014). Assessing punching shear failure in reinforced concrete flat slabs subjected to lacalised impact loading. Internatinal journal of impact Engineering, vol.71, pp. 17-33.

Miyamoto, A., King, M. W. (1994). Modeling of impact load characteristics for dynamic response analysis of concrete structures. Transactions on the Built environment, vol.8, pp. 71-88.

Mougin, J.-P., Perrotin, P., Mommessina, M., Tonnelo, J., Agbossoua, A. (2005). Rock fall impact on reinforced concrete slab: an experimental approach. International Journal of Impact Engineering, vol. 31, Issue 2, pp. 169-183.

Perchat, J. (1997) Béton armé - Règles BAEL – Ouvrages particuliers. Techniques de l'ingénieur. 38p.

Smith, J., Cusatis, G. (2016) Numerical analysis of projectile penetration and perforation of plain and fiber reinforced concrete slabs. Int. J Numer. Anal. Meth. Geomech.

VFF/AEAI (2005) Recommandations - Protection des objets contre les dangers naturels gravitationnels, chapitre 6 « chutes de pierres », Association des établissements cantonaux d'assurance incendie Edition, 16p.

Study of rebound mechanisms using a Material Point Method (MPM) – Discrete Element Method (DEM) coupling

Fabio Gracia [1], Pascal Villard [2], Vincent Richefeu [3]

Keywords: MPM, DEM, Block Impact, Plasticity, Energy Dissipation

This work deals with the simulation of 2D impacts of rigid blocks on deformable soils. A sensitivity analysis using a coupling between two different numerical approaches was made: Discrete Element Method (DEM) and Material Point Method (MPM); see Cundall & Strack (1979) and Sulsky et al. (1995), respectively. We analyzed the influence of certain initial block parameters such as velocity, angle of incidence, angular velocity, size and shape on the restitution coefficient which is known to be difficult to determine experimentally. Additionally, the soil was modeled as two layers, as a relatively simple approach to real soils, and its effect was also part of the study.

1 NUMERICAL APPROACH

The MPM was chosen since a continuum method allowing large deformations was needed to model the soil. The method achieves the modeling of large deformations because of its hybrid Eulerian (background grid) and Lagrangian (material) description. However, given the continuity of the medium, the rheology of the material has to be given explicitly via constitutive laws, which in this case was Mohr-Coulomb.

Discrete elements were introduced to our in-house MPM software in order to model the rigid behavior of blocks, such as boulders during a rockfall. No dissipation was introduced in the contact laws between the material points and the discrete element. Lastly, computational times were reduced since the object is modeled as a single rigid particle (discrete element).

2 TESTED APPLICATION

The initial setup can be seen in Figure 1. Properties such as velocity, angle of incidence, angular velocity and size were varied individually. A two-layered material was used as a simplified representation of real soil (deformable over rigid), where superficial soils tend to be deformable and soils at depth are usually rigid. The total depth remained the same while varying the depths of each individual layer. A study was made to determine the total depth at which the boundaries had little influence on the result, in this case 5 m. Initially the block shape was chosen to be circular to prevent any variability related to shape. On the second part of the study, a square block was chosen and different initial orientations were taken into account.

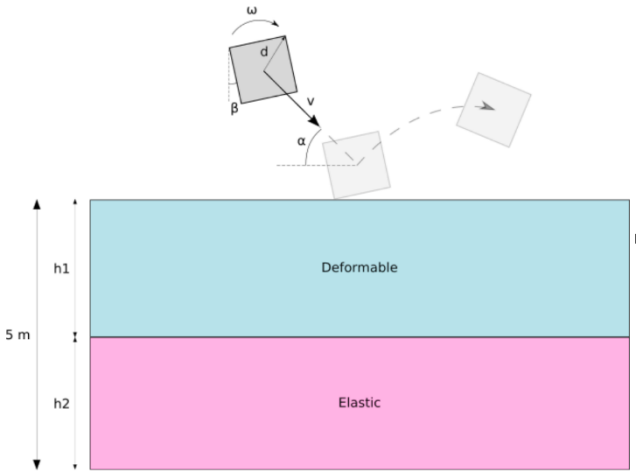

Figure 1: Setup of an impact using a square block

3 MAIN RESULTS

Results were grouped using each of the parameters tested. They were analyzed in terms of restitution coefficients (ratio of energies before to after the impact) (Figure 2). Additionally the energy of the block was broken down into normal, tangential and rotational energy before and after the impact (Figure 2), and the energy dissipation and transformation was analyzed. Finally, to corroborate the results obtained, the plastic zones generated in the soil during the impact were also a part of the study. Figure 3 shows an example of one of the simulations.

Overall variation of each of the four parameters chosen proved to have a large impact in terms of restitution coefficients. As seen in the specific case of the angle of incidence for a circular block (Figure 2), there is a large variability of the energy restored, which ranges between 11% and 80% when moving from a low angle of incidence (15°) to a completely vertical impact.

[1] GRACIA Fabio, IMSRN, Montbonnot F-38330, France and Univ. Grenoble Alpes, CNRS, Grenoble INP, 3SR, 38000Grenoble, France, fabio.gracia@3sr-grenoble.fr
[2] VILLARD Pascal, Univ. Grenoble Alpes, CNRS, Grenoble INP, 3SR, 38000, Grenoble, France, pascal.villard@3sr-grenoble.fr
[3] RICHEFEU Vincent, Univ. Grenoble Alpes, CNRS, Grenoble INP, 3SR, 38000, Grenoble, France, vincent.richefeu@3sr-grenoble.fr

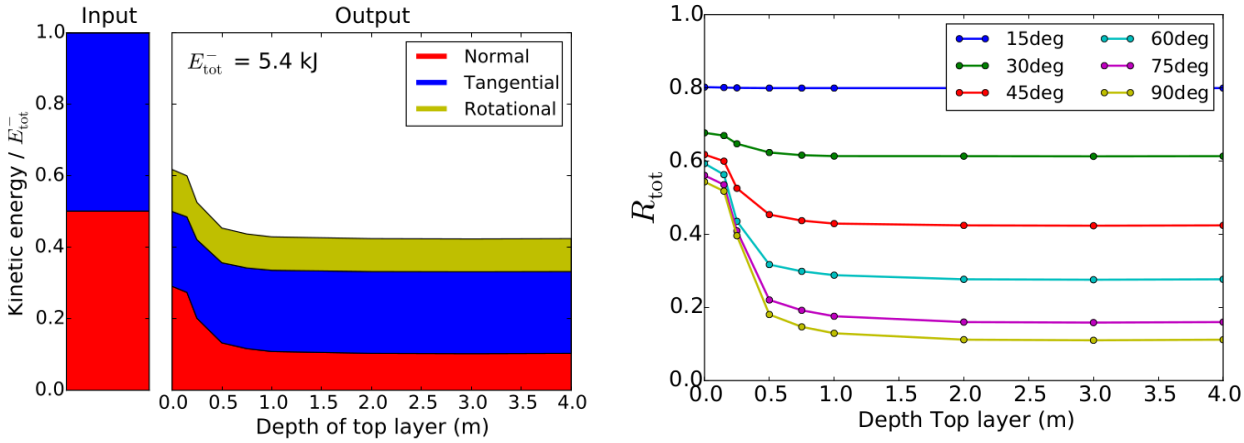

Figure 2: Energy breakdown for an angle of incidence $\alpha = 45°$ (left). Influence of the angle of incidence on the total restitution coefficients (right)

Moreover, the influence of the top layer depth is clearly evident, where its effect is negligible when having a low angle of incidence, and it becomes really important as the angle increases. Lastly, a plateau is reached in all cases which represents the moment at which the top layer depth is sufficiently large making the lower layer have no impact in the energy restored. In the case of the angle of incidence, this plateau is reached at different top layer depths as is depicted in the Figure 2.

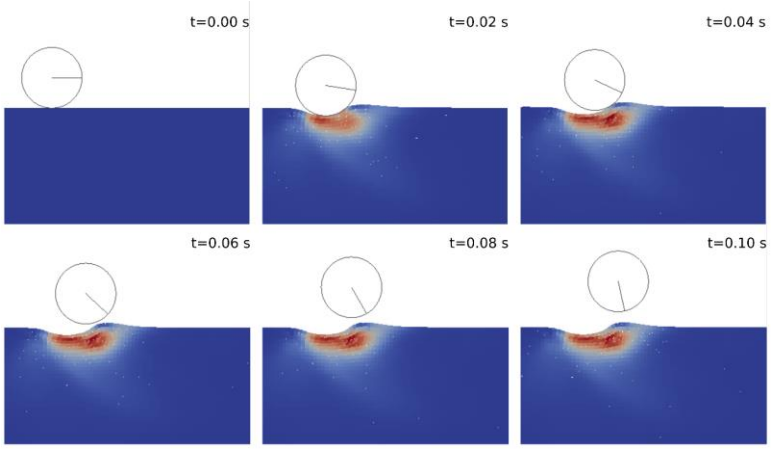

Figure 3: Example of a collision of a circular block and a deformable soil simulated with the DEM/MPM coupled approach. The colors represent the Euclidian norm of the plastic stress tensor

4 CONCLUSION

Different configurations varying block parameters such as velocity, angle of incidence, angular velocity, size and shape were analyzed, while at the same time taking into account depth of the top layer. The results found in the study provided insight into the rebound mechanisms that take place during the impact of a rigid element on a deformable soil. It was shown that the restitution coefficient is very sensitive to changes in each of the parameters, yielding large differences which can be related to soil plastification during the impact. Additionally, the top layer depth was shown to have an important effect on the overall result, at least until a plateau was reached.

5 REFERENCES

Cundall, P.A. & Strack, O.D.L. (1979) A discrete numerical-model for granular assemblies, *Geotechnique 29(1), pp. 47-65.*

Sulsky, D., Zhou, S.-J. & Schreyer, H. (1995) Application of particle-in-cell method to solid mechanics, *Comp. Phys. Comm. 87, pp. 236-252.*

Erosion of the right lateral moraine of the Mer de Glace (France) surveyed by airborne and terrestrial LiDAR

Johan BERTHET[1], Ludovic RAVANEL[2], Antoine GUERIN[3]

Keywords: moraine, glacier retreat, erosion, gullies, LiDAR survey, Mer de Glace.

1 INTRODUCTION

Glacier retreat is the most visible effect of the climate change on high mountain environments, but its consequences are beyond the only ice shrinkage. Large areas are becoming free of ice and surrounding rock/debris slopes are often instable. It is especially the case for Little Ice Age lateral moraines (Ravanel and Lambiel, 2013). Characterizing erosion and evolution of such forms is a key element to understand the future of proglacial rivers and risks associated with deglaciation. For the specific case of the Mer de Glace, goal of research on moraine erosion is also to assess if the subglacial harnessing for hydro-power is sustainable once it will be free of ice.

2 STUDY SITE

The Mer de Glace (Mont Blanc massif) is the largest French glacier with its 31 km² (Gardent *et al.*, 2014). Its tongue has retreated by 700 m during the last 20 years, releasing a 250 m high lateral moraine. Beside this, geomorphic processes in the proglacial area are also deeply affected by the water flow abstraction, due to the subglacial harnessing that works also during flood events (Berthet, 2016). Upper than the glacier front, ice shrinkage reaches 200 m. Thus, the right lateral moraine, in front of the touristic Montenvers rail-way station, is still deeply affected by the retreat of glacier. Out study site extends from the 1996 frontal moraine to 1 km upstream, above the actual tongue.

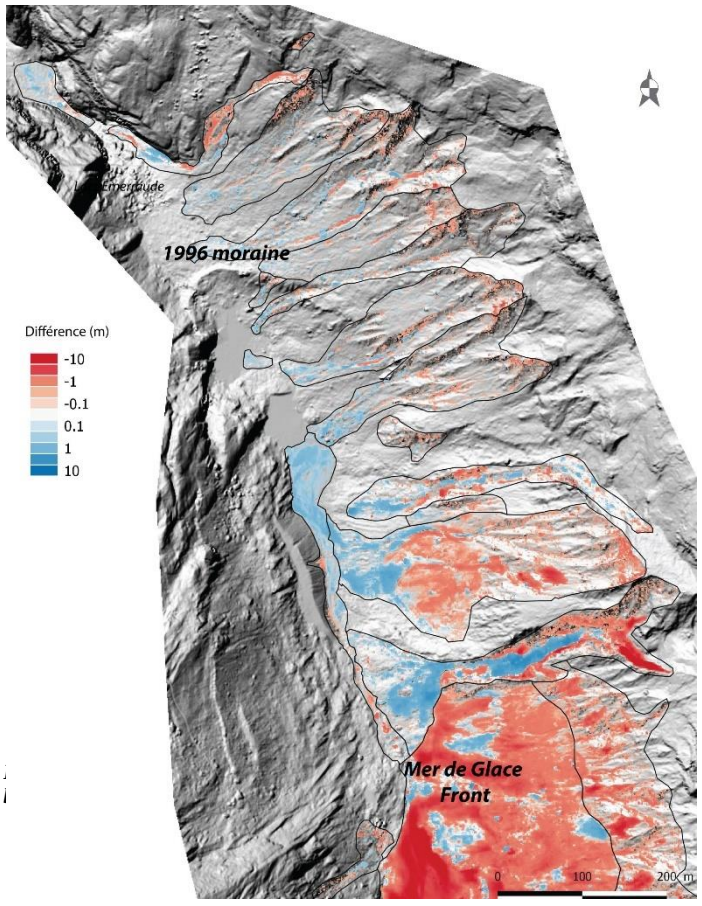

3 METHODOLOGY

We studied the evolution of the lateral moraine and its gullies by combining airborne and terrestrial LiDAR survey (Figure 1; Abellan *et al.*, 2014; Bhardwaj *et al.*, 2016; Ravanel *et al.*, 2012). TLS can be used in several ways in geomorphology, *i.e.* mapping, geometry and monitoring. The main difficulty here was to align the different point clouds. Even concerning data from airborne LiDAR which are directly georeferenced, we had to re-align scans because of systematic errors. Then, volume changes are calculated using comparison of the rasters DEMs.

4 FIRST INSIGHTS

On the upper part of the study area, above the glacier, terrestrial laser scanning campaigns have been carried out once a year between 2011 and 2017. The 6 comparisons of 3D models highlight the lowering of the talus slope at the base of the moraine as the thickness of the glacier decreases, the destabilization of small sections of moraine in the steepest areas, the deepening of some channels, as well as two major destabilizations: the first corresponds to a destabilization that affected the moraine over its entire height on August 28, 2014; the second one corresponds to a very important modification of the main dell in different phases throughout June 2016 (https://youtu.be/AIfRFBcLwhM).

[1] BERTHET Johan, Styx4D, Savoie Technolac, Le Bourget du Lac, France, johan.berthet@styx4d.com

[2] RAVANEL Ludovic, Univ. Grenoble Alpes, Univ. Savoie Mont Blanc, CNRS, EDYTEM, Chambéry, France ludovic.ravanel@univ-smb.fr

[3] GUERIN Antoine, Risk Analysis Group, Institute of Earth Sciences, University of Lausanne, Switzerland, antoine.guerin@unil.ch

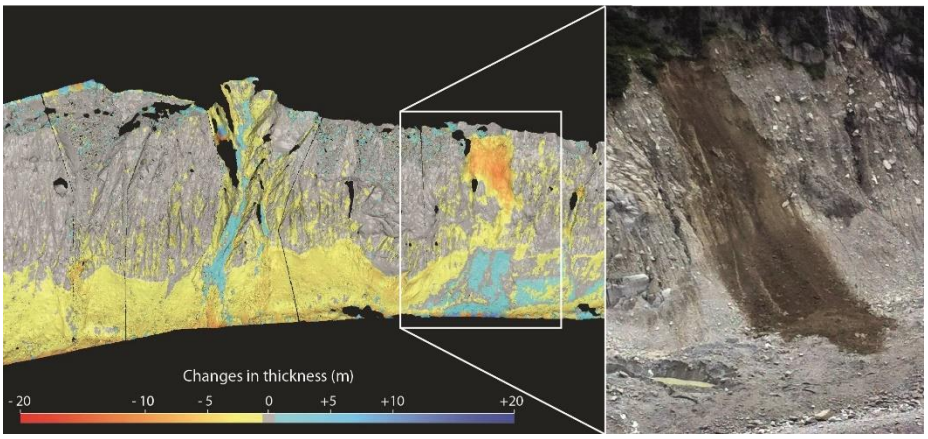

Figure 2: Terrestrial 3D models comparison of the right lateral moraine above the Mer de Glace between October 2013 and 2014. The main event corresponds to the fall of around 25 000 m3 in August 2014.

Our first results thus show that erosion intensity is different upstream and downstream the glacier tongue. It is due to the changing base level controlled by the glacier and the possible presence of ice into the moraine. Dead ice bodies may thus affect the proglacial area while the upper moraine evolution is mainly controlled by the lowering of the glacier associated with intense rainfalls.

5 REFERENCES

Abellan A., Oppikofer T., Jaboyedoff M., Rosser N.J., Lim M., Lato M.J. (2014). Terrestrial laser scanning of rock slope instabilities. Earth Surface Processes and Landforms 39: 80–97.

Gardent, M., Rabatel, A., Dedieu, J. P., Deline, P. (2014). Multitemporal glacier inventory of the French Alps from the late 1960s to the late 2000s. *Global and Planetary Change*, 120: 24–37.

Berthet, J. (2016) *L'évolution géomorphologique des torrents proglaciare de la vallée de Chamonix-Mont Blanc, une approche du couplage sédimentaire du Petit Age Glaciaire au désenglacement récent*. Thèse de Doctorat, Université Grenoble Alpes, 305p.

Bhardwaj A., Sam L., Bhardwaj A., Martín-Torres F.J. (2016). LiDAR remote sensing of the cryosphere: present applications and future prospects. *Remote Sensing of Environment*, 177: 125–143.

Ravanel L., Lambiel C. (2013). Evolution récente de la moraine des Gentianes (2894 m, Valais, Suisse): un cas de réajustement paraglaciaire ? *Environnements Périglaciaires*, 18-19, 8 p.

Ravanel L., Deline P., Lambiel C., Vincent C. (2012). Instability of a highly vulnerable high alpine rock ridge: the lower Arête des Cosmiques (Mont Blanc massif, France). *Geografiska Annaler A*, 95: 51–66.

Lessons learned from Degotalls rock wall monitoring in the Montserrat Massif (Catalonia, NE Spain)

Marc JANERAS[1], Josep A. GILI[2], Marta GUINAU[3], Joan M. VILAPLANA[3], Pere BUXÓ[1], Joan PALAU[1]

Keywords: rockfall, monitoring, instability, precursory displacement, progressive failure

A rockfall risk mitigation plan is currently under development in the Montserrat Massif (Catalonia, NE Spain). The Degotalls cliff is a place where the risk for the main access infrastructures to a highly visited area has been revealed recently. Several tests on monitoring techniques have been carried out to improve the knowledge on precursory displacements as indication of rock block instability.

1 INTRODUCTION

1.1 DEGOTALLS ROCK WALL IN THE MONTSERRAT MASSIF

The Montserrat Massif is located about 50 km North-West of Barcelona in central Catalonia, Spain. This mountain constitutes a Natural Park and hosts a sanctuary and monastery of nearly one thousand years of history. It has become a place of pilgrimage and a popular touristic spot, as well a fabulous place for hiking and climbing. Due to the proximity of the Barcelona conurbation, the number of annual visitors exceeds 3 million on the whole mountain. This massif is formed by thick layers of conglomerate interleaved by siltstone/sandstone from a Late-Eocene fan-delta. It has an overall height difference of 1000 m (from the top at 1236 m.a.s.l.). The staggered slopes are very prone to rock falls due to its structure formed by vertical cliffs of conglomerate alternated with steep slopes of softer ground. In recent years, several rockfall events affected different access infrastructures and facilities, such as the ones that occurred in 2007 and 2008 on the Degotalls rock wall, which involved a total volume of 1200 m^3, fortunately without injuries, but with a great disturbance on the road and rack railway. Those episodes motivated the implementation of a rockfall risk assessment and mitigation plan in the whole massif in order to guarantee an adequate safety level for the population, as well as the visitors. The current challenge for the cultural and natural heritage management consists in widening the perspective all along the cycle of risk mitigation to achieve an optimized response in terms of sustainability (Buxó *et al.*, 2017).

1.2 EXPERIENCES AND LEARNINGS

These last years, rockfall events gave grounds for several learnings, and the knowledge on the rockfall problem in Montserrat has been growing during the risk mitigation works. Many issues are related to those experiences at the Degotalls cliff as explained in Janeras (2017): the exposure and vulnerability in the parking zones; the indirect risk; a comparison between preventive actions versus reactive ones; the complexity of the works on this kind of inaccessible cliffs; the limits of the structural protection; the precursory detachments and displacements (Royan, 2015); the spatial and temporary variability of the hazard; the reinforcement mobilization mechanisms; or the value of the observations for understanding the dynamics.

This communication focuses on the criteria for the instability identification. This signs are expected to become the basis for setting priorities of intervention and/or criteria for warnings. A monitoring strategy is performed in this sense, covering from remote sensing scans to focused surveys. Specifically for the Degotalls wall, the applied monitoring techniques are the terrestrial laser scanner (TLS) from 2007, also a pilot test of terrestrial radar (Gb-InSAR), and more recently, a wireless sensor network (WSN) and total station (TS) surveys (Janeras *et al.*, 2017).

2 PRECURSORY SIGNS OF ROCKFALL

2.1 SUCCESSIVE DETACHMENTS AND PROGRESSIVE FAILURE

The sequence of rockfalls detached from the Degotalls wall is described in Figure 1. This sequence and some additional field observations lead us to conclude that the events were part of a progressive failure increasing in size. A partial rockfall can be identified as a precursory sign of further detachments if the rupture mechanism persists, but other signs in terms of rupture propagation, as presented below, are needed to conclude the proximity of the next one.

[1] Institut Cartogràfic i Geològic de Catalunya (ICGC), ES-08038 Barcelona, marc.janeras@icgc.cat

[2] Universitat Politècnica de Catalunya (UPC), ES-08034 Barcelona

[3] Universitat de Barcelona (UB), ES-08028 Barcelona

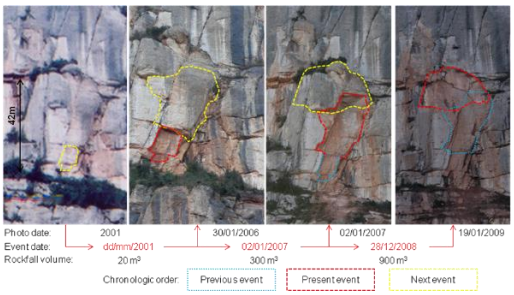

Figure 1: Rockfall sequence on the Degotalls wall, interpreted as progressive failure causing partial detachments.

2.2 SEQUENCED ROCKFALL AND RELATED DISPLACEMENTS

The rockfall activity and small displacements of blocks were detected by comparing the sequence of TLS surveys (Royan, 2015). After a small rockfall in 2011 (block A), which source was identified in the Degotalls wall by TLS, an adjacent block (B) has been moving with cumulative displacement (Figure 2). The last 58 days before block B fell down in 15th February 2018 were recorded by a crackmeter installed on a wireless sensor network (WSN). A perfect correlation between slight precipitation and sudden displacements is observed (Figure 2), and for the last 5 hours block B undergoes creep behaviour leading to collapse.

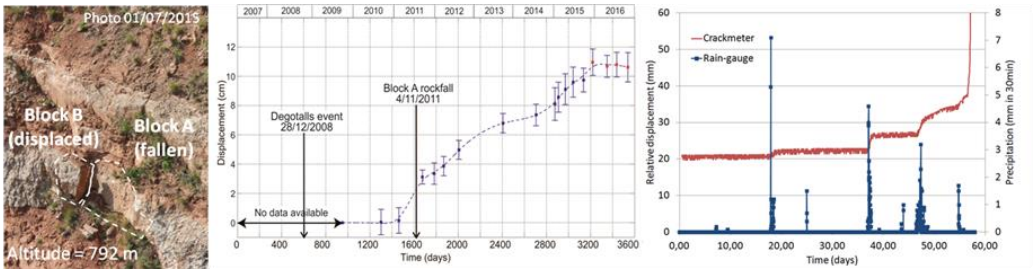

Figure 2: Displacement of block B after the detachment of the adjacent one (block A), according to TLS measurements since 2009, and WSN measurements for the last 58 days.

2.3 ROCK BLOCK DISPLACEMENT COUPLED WITH REINFORCEMENT LOADING

With the same technique of the previous case, the movement of a large block is being monitored, showing an oscillatory behaviour limited by the stabilizing steel wire net (Figure 3). At present, this displacement is recorded with crackmeters and the response of the wire net with a load cell. These sensors are connected to a WSN as described in (Janeras *et al.*, 2016). In parallel, prisms have been fixed on the block and the surrounding massif to cross-check the measurements done with total station (TS), like those previously tested in La Cadireta rock needle (Janeras *et al.*, 2017). As a drawback, the reflector prisms for TS disturb the TLS scans at some extent.

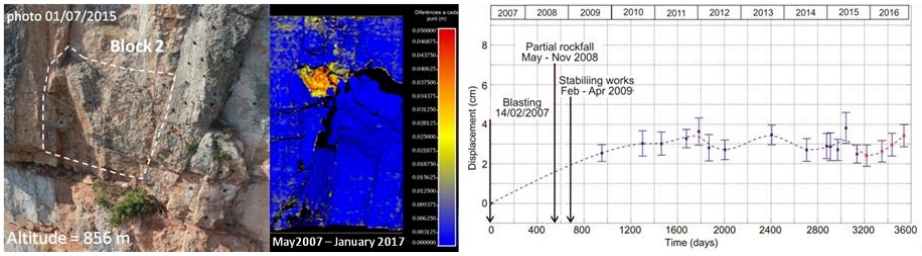

Figure 3: Displacement measurement of block 2 with TLS during 10 years.

3 CONCLUSION

The monitoring techniques used in Degotalls wall (TLS, Gb-InSAR, WSN and TS) provide data for the instability identification which will be modelled from now on. The knowledge improvement in rock instability processes is expected to be conclusive in the near future for the design of warning systems and the prioritization of intervention.

4 REFERENCES

Buxó, P., Janeras, M., Domènech, G., Pons, J., Prat, E., López, F. (2017) Development of a Rockfall Risk Mitigation Plan in the Montserrat Massif (Central Catalonia, Spain). In: Mikoš M., Casagli N., Yin Y., Sassa K. (Eds.) *Advancing Culture of Living with Landslides*. WLF 2017, Ljubljana. Springer, pp 677-684, DOI:10.1007/978-3-319-53485-5_78.

Janeras, M., Jara, J.A., López, F., Marcè, A., Carbonell, T., Elvira, A. (2016) Development of a wireless sensor network for rock mass deformation monitoring in the Montserrat Massif. In: *3rd RSS International Symposium on Rock Slope Stability*, Lyon, pp 131-132.

Janeras, M. (2017) ¿Qué nos enseña la pared de Degotalls en Montserrat sobre los desprendimientos de roca? In: *Proceedings of the IX Simposio Nacional sobre Taludes y Laderas Inestables*. Santander, June 2017. CIMNE, ISBN:978-84-946909-5-2, pp 917-929.

Janeras, M., Jara, J.A., Royán, M.J., Vilaplana, J.M., Aguasca, A., Fàbregas, X., Gili, J.A., Buxó, P. (2017) Multi-technique approach to rockfall monitoring in the Montserrat massif (Catalonia, NE Spain). *Engineering Geology*, 219, pp 4–20, DOI:10.1016/j.enggeo.2016.12.010.

Royán, M.J. (2015) *Caracterización y predicción de desprendimientos de rocas mediante LiDAR terrestre*. PhD Thesis, Vilaplana J.M. (Adv.) Universitat de Barcelona.
[http://diposit.ub.edu/dspace/bitstream/2445/68667/1/MJRC_TESIS.pdf]

Extended experimental analysis of friction energy dissipating device aging

Consortium of task R.2 "Experiments on aged protection devices" of C2ROP French National Project[12]

Keywords: rockfall, protection, aging, energy dissipating device, experiments

Since decades, protection devices such as flexible fences have been installed to protect people and infrastructures against rockfalls. Most of the devices installed in the 80's or 90's are still operational. A specific working group of the French national project C2ROP focuses on the characterization of such devices and in particular the evolution of their performances in time. Being one of the most important components of flexible fences, this study has focused on the energy dissipating devices. Thus, a dysfunction of one of these elements would significantly disturb the behavior of the whole structure in case of impact.
Exhaustive analyzes of key components such as the energy dissipating devices in degraded conditions have been carried out. In particular, 11 devices exposed during more than 20 years in mountainous conditions have been collected to be tested. Tests consisted in quasi-static and dynamic tensile tests. Those tests permitted to characterize the devices behaviors, to identify their trigger values and the maximal tensile strengths reached.

1 EXPERIMENTAL CAMPAIGN: TENSILE TESTS OF AGED AND NEW DEVICES

The experiment on aged flexible fences has been focused on the characterization of the mechanical response of the frictional energy dissipating devices (Castanon-Jano 2016). This kind of dissipating devices is the most representative of the older protection infrastructure. More recent and innovative types of dissipating devices have been developed more recently and are not included in this analysis (Trad 2011).

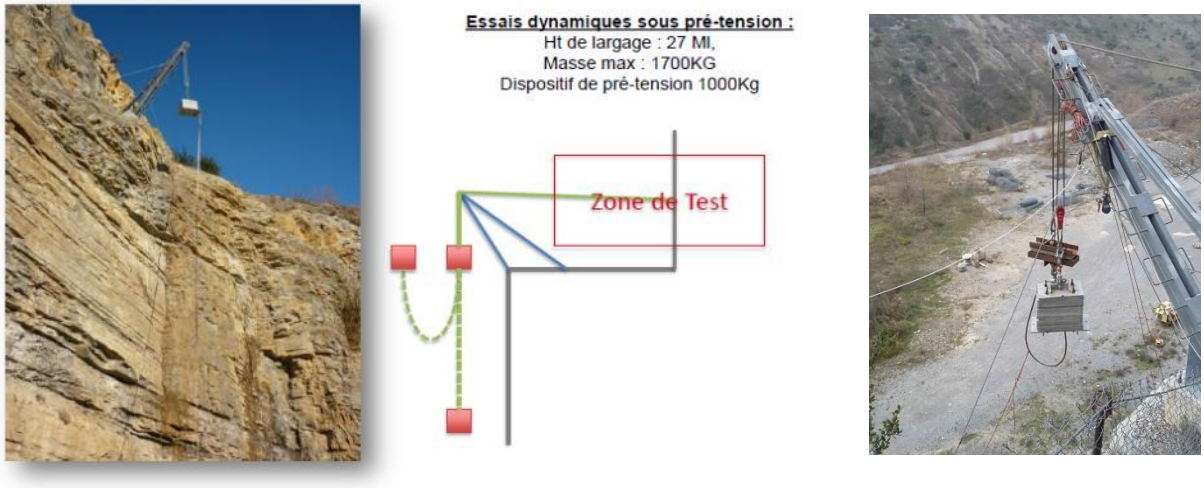

Figure 1: Dynamic tests experimental device

Eleven devices have been collected from a dismantled flexible fence installed more than 20 years ago. These devices, have not suffered any impact or particular loading. The technical description of the devices provided by the fabricant indicates a triggering force of 120 kN and an energy dissipation of 100 kJ per meter of elongation of the device.

[1] OLMEDO Ignacio, GTS, iolmedo@gts.fr
[1] HUTEAUMagali, Irstea – SNCF, France, magali.huteau@reseau.sncf.fr
[1] MULLER Nicolas, CD Savoie, nicolas.muller@savoie.fr
[1] LE-BIDAN Valentin, CD Isère, valentin.le-bidan@isere.fr
[1] CHANUT Marie-Aurélie, CEREMA, Marie-Aurelie.Chanut@cerema.fr
[1] COUILIBALY Jibril, CEREMA,
[1] GALANDRIN Clément, CAN, cgalandrin@can.fr
[1] VERDET Mathieu, CAN, mverdet@can.fr

The experiments consisted in tensile tests in quasi static (QS) and dynamic conditions. New and aged devices were tested in parallel and results compared. The QS tests were carried out at a loading velocity of 2 mm/s. The devices were tested until an elongation of 1,30m. The maximal loading force and the displacements were recorded by a displacement sensor and a force cell.

Concerning the dynamic tensile tests, the experiments were carried out using a free-fall test device (Fig.1). A defined mass is released on free-fall before being retained by a steel rope attached to the tested energy dissipating device. Thus, a dynamic loading is applied to the latter at an established impact energy. Two configurations were considered for the same impact energy (Impact A: 1700 kg at 10 m/s; Impact B: 525 kg at 18 m/s). Three impacts of each were carried out for the aged dissipators and 5 for the new ones. For these experiments, two high speed cameras were used to follow the elongation of the device and to record the free-fall trajectory of the impact mass. Moreover, a force cell was installed to record the loading forces. Both cameras and force cell were synchronized by an optical flash system.

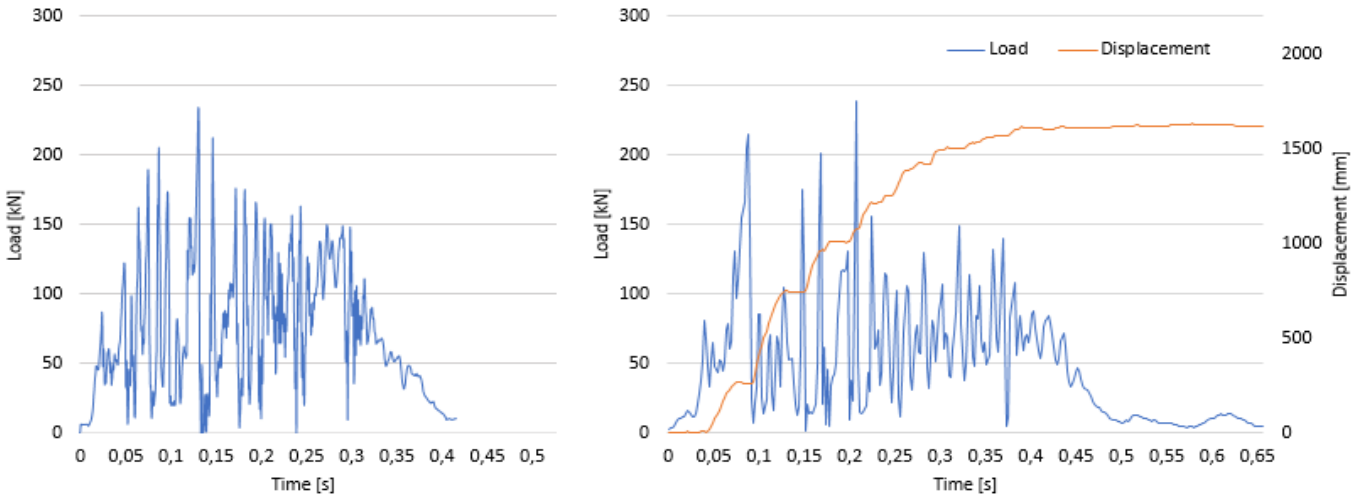

Figure 2: Force evolutions in time for a dynamic test on aged (left) and new (right) device

2 RESULTS

The results of the QS test on the aged devices show a trigger force around 80 kN and a progressive diminution of the force value during the elongation of the device. These results present a good repeatability of the force-displacement curves.
Under dynamic loading conditions (Fig.2), the behavior of these aged components presented a much less satisfactory behavior. Compared to the QS tests, the trigger force is slightly lower and around 72 kN in average. However, after the triggering of the device, the apparition of high force peaks can be observed. These peaks, which can reach 270 kN, present a relevant duration in time, about 30 ms. Globally, the same behavior was observed for the new devices, in particular the high force peaks and the trigger forces.

3 CONCLUSION

These experimental studies show the limits of this widely used energy dissipating device technology. The apparition of extremely high force peaks with a significant duration in time represents a significant threat to the stability and durability of anchors and foundations of the structures. Moreover, it has been shown that the behavior of the tested devices is not significantly modified by their aging.

4 REFERENCES

Castanon-Jano, L, Blanco-Fernandez, E, Castro-Fresno, D, Ballester-Munoz, F (2016) Energy dissipating devices in falling rock protection barriers. *Rock mechanics and rock engineering.*

Trad A(2011). Analyse du Comportement et Modélisation de Structures Souples de Protection: le cas des Ecrans de Filets Pare-Pierres sous Sollicitations Statique et Dynamique. PhD thesis, *Institut National des Sciences Appliquees de Lyon*

Automatic monitoring of landslide displacements using total station

Simon DEFORTIS[1], Mathieu LE BRETON[1,2], Quentin BARBIER[1], Lucas MEIGNAN[1], Fabrice GUYOTON[1], Romain LE ROUX-MALLOUF[1], Jean-Marc VERDIER[1], Gilles DELABELLE[3], Romain GAUCHER[4]

Keywords: landslide displacement, monitoring, velocity, automatic survey, total station

Landslides are characterized by surface movements with (1) velocity ranging from millimetres to meters and (2) a right of way from meters to tens of kilometres. Detecting the deformation timing and kinematic is a key point in the understanding of the physical causes and to warn possible hazards. Different systems are used to monitor the deformation including differential GPS, optical laser, lidar, radar interferometers (Gili et al., (2000), Abellàn et al., (2009), Herrera et al., (2009), Travelletti et al., (2012)). In this study, we use an automatic survey using total stations to (1) monitor the landslide velocity and kinematic and (2) set up a warning system to close the road, in case of a significant slip which could reach the foothill road.

1 STUDY SITE

The Pas de l'Ours landslide is situated in the Queyras valley in France, on the right bank of the Guil, between Aiguilles and Abries cities (Fig. 1).

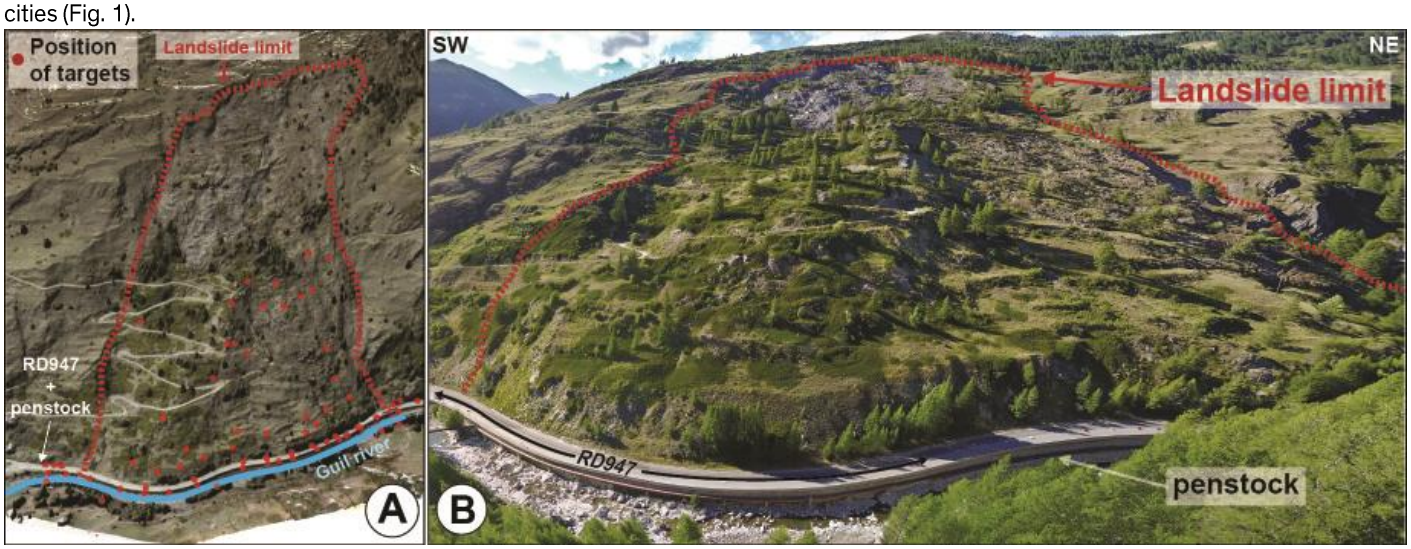

Figure 30. Context views of the Pas du L'Ours Landslide. A. 3D view of the landslide. Red dotted line is the landslide limit. B. Drone aerial photography of the landslide. Red dotted line is the landslide limit.

It's one of the largest active slow-moving landslides in the Alps with a width of about 500 m and a high of 400 m and a volume estimated at 15 million cubic meters. The landslides affects the RD947. This road is built in the foothill on excavated soil raised above the Guil River by support structure (Fig. 1). Several issues are concerned by the Pas de l'Ours landslide including the road itself which is the single access to the ski stations of Abries and Ristolas, a penstock or the downstream towns in case of rapid flood caused by breach of a landslide dam. This landslide is monitored since the beginning of 2017 with several facilities such as radar interferometry, GPS, topographic survey, inclinometer measurements (Bornemann et al., 2016, Bornemann et al., 2017, Provost et al., 2017). Since September 2017, the Géolithe Company were assigned to set up an automatic survey of the landslide composed by two total stations (distance measuring systems) and 75 targets located on the road and the landslide (Fig. 2).

2 MATERIAL AND METHOD – AUTOMATIC MEASUREMENT DEVICES

The device is composed by 75 targets including 8 reference targets allowing post-treatment corrections. The targets are laid out on the lower part of the landslide between the RD947 at 1480 m to 1640 m of elevation. The two total stations are placed on the opposite hillside and scan the targets with 15-to-45-min frequency.

[1] Géolithe, Crolles, France, corresponding author: romain.lerouxmallouf@geolithe.fr

[2] Institut des Sciences de la Terre, Université Grenoble Alpes, CNRS, Grenoble, France

[3] Département des Hautes-Alpes

[4] Direction interdépartementale des routes méditerranée

3 PRELIMINARY RESULTS – MORPHOLOGY AND KINEMATIC OF THE LANDSLIDE

Combine to manual measurement from spring 2017, the automatic measurement (set up in september 2017) monitored two distinct phases of the landslide including (1) a slipping phase (27/04/2017 to 10/07/2017) and (2) remission phase (10/10/2017 to 20/12/2017). This dataset allow us to make assumptions on the landslide kinematic.

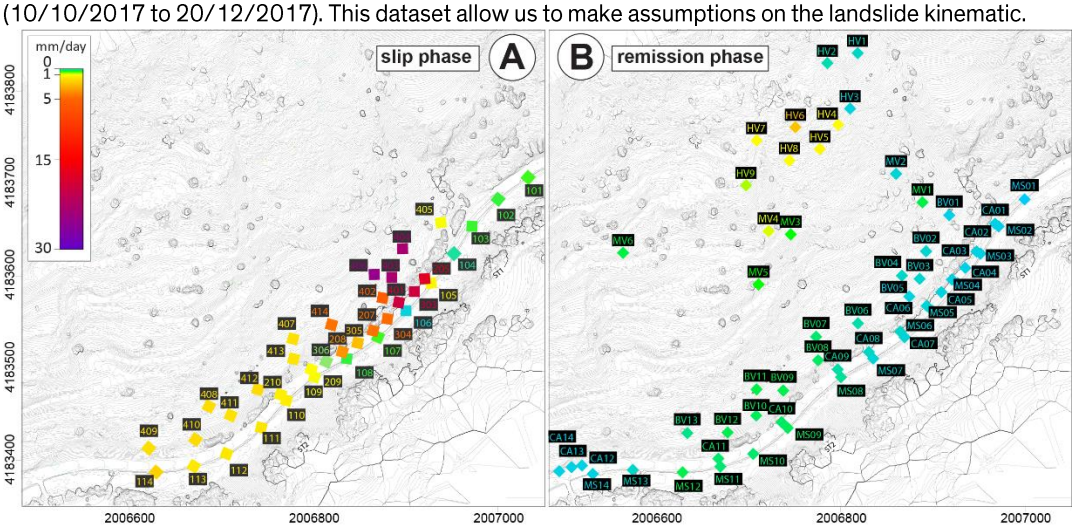

Figure 2. Average landslide velocities during slip and remission phases. A. Average velocities during the slip phase of the landslide between the 27/04/2017 and 10/07/2017. B. Average velocities during the remission phase between the 10/10/2017 and

The landslide morphology displays two distinct compartments (west and east).

1. The east part is characterized by rough steep topography without vegetation
2. The west part displays a smoother topography with a vegetal cover.

This lateral variation is clearly visible in the kinematic measurements through a velocity difference during the two phases (remission and slip) between the two compartment feet. The slip phase is characterized by large landslide feet displacement as shown by the figure 2a. This displacement is larger along the east side than the west side. Conversely, during the remission phase, the landslide feet is locked while the automatic measurements show surface displacements (targets HV4 to HV9 in figure 2B).

This lateral variation is associated with a retaining wall built on the landslide east feet, below the road (Fig. 1). The wall is reinforced by horizontal anchored to the ground and is considered as undeformed as shown by the really low values of the targets 103 to 108 (less than 1 mm/day) during the slip phase.

4 CONCLUSION

The automatic monitoring of the Pas de l'Ours landslide by an automatic monitoring allows us to better constrain the kinematic of the deformation. Our results show that (1) the landslide can be divided in two distinct part characterized by two different deformation mechanism and (2) the landslide have average displacement rates that can exceed 30 mm per day. Associated with the data acquisition system, we set up a warning system to close the road based on daily velocity threshold to ensure the safety of the road users.

REFERENCES

Abellán, A., Jaboyedoff, M., Oppikofer, T., Vilaplana, J. M., (2009) "Detection of millimetric deformation using a terrestrial laser scanner: experiment and application to a rockfall event," *Nat Hazards Earth Syst Sci*, vol. 9, no. 2, pp. 365–372.

Bornemann, P., Jean-Philippe, M., André, S., Anne, P., & Julien, T. (2016, April). Terrestrial laser scanning point clouds time series for the monitoring of slope movements: displacement measurement using image correlation and 3D feature tracking. In *EGU General Assembly Conference Abstracts* (Vol. 18, p. 13050).

Bornemann, P., Kromer, R., Malet, J.-P., Puissant, A., Travelletti, J., Diot, P., (2017) Automated Terrestrial Laser Scanning for deformation monitoring on a fast moving landslide in Aiguilles (Hautes-Alpes, France), *Journées Aléas Gravitaires, Besançon, France.*

Gili, J. A. , Corominas, J. , Rius, J. , (2000) "Using Global Positioning System techniques in landslide monitoring," *Eng. Geol.*, vol. 55, no. 3, pp. 167–192.

Herrera, G. , Fernández-Merodo, J. A., Mulas, J., Pastor, M., Luzi, G., Monserrat, O., (2009), "A landslide forecasting model using ground based SAR data: The Portalet case study," *Eng. Geol.*, vol. 105, no. 3–4, pp. 220–230.

Provost, F., Bornemann, P., Faustin, E., Malet, J-P., Hibert, C., Puissant, A., Fleck, M., Ferhat, G., Diot, P., Ségel, V., (2017) Multi-method monitoring of the large and rapidly developping Pas de l'Ours landslide - Queyras, France *Journées Aléas Gravitaires, Besançon, France.*

Travelletti J., *et al.*, "Correlation of multi-temporal ground-based optical images for landslide monitoring: Application, potential and limitations," *ISPRS J. Photogramm. Remote Sens.*, vol. 70, pp. 39–55, Jun. 2012.

Evolution of quarry exploitation plan as a suitable countermeasure against rock instability phenomena

Federico VAGNON (corresponding author)[1], Anna Maria FERRERO[1], Marina PIRULLI[2], Claudio SCAVIA[2]

Keywords: rockfall, rock avalanche, numerical modelling, quarry exploitation

The identification of potential rock instability phenomena, the estimation of their magnitude and the prediction of their possible runout are fundamental aspects in quarry exploitation plans to guarantee the safe activities of workforce. In some cases, the wise management of the quarry exploitation plan can represent a useful means for facing and reducing the hazard generated by rock instability phenomena. In the present work, combined surveys and different numerical approaches have been used to examine the stability conditions of the rock slope that overlooks a dolomite quarry, in the Eastern Italian Alps. The results will be used to design the future quarry exploitation plan.

1 SITE LOCATION AND GEOLOGICAL OVERWIEV

The case study is located in the Valdastico municipality, in Vicenza province, close to the border with Trentino Alto Adige region (Figure 1a). Here, an ancient landslide deposit, named "La Marogna" (Figure 1b), generated after the 1117 Verona earthquake (Zampieri and Adami, 2013), is exploited from some decades for the production of calcareous materials. A steep cliff, named "La Gioia" (Figure 1b), overlooks the Marogna deposit in the upper part of the quarry concession. This rock face is susceptible to rock fall and rock avalanche phenomena, which can involve volumes from hundreds to thousands of m^3. Thus, the present study was divided into two main steps: firstly, the quantification of the possible unstable volumes that can detach from the La Gioia rock face. Secondly, on the basis of the previous geo-mechanical characterization, the definition of the possible collapse scenarios and consequently the evolution of the exploitation plan to reduce the hazard of the area.

Figure 1: Location (a) and photograph of the study area (b)

2 ROCK MASS GEOMECHANICAL CHARACTERIZATION

Traditional and non-contact geomechanical surveys were performed for identifying the main discontinuity sets that characterize La Gioia rock face. 89 (traditional survey) and 863 (non-contact survey based on semi-automatic analysis of laser scanner data) planes were acquired and statistically analysed using Dips code (Rocscience Inc.). Three main discontinuity sets were identified crossing data of the two above mentioned survey approaches, showing a good agreement between the results (Table 1). The spacing belonging to the three identified discontinuity sets (1: KS, 2: K1 and 3: K2) were measured and the potential block volumes (V_b) were estimated as follows:

$$V_b = \frac{S_1 S_2 S_3}{sin\gamma_{12} sin\gamma_{23} sin\gamma_{13}} \qquad (1)$$

where S_1, S_2 and S_3 are the spacing of the three discontinuity sets and γ_{12} is the angle between the poles of system 1 and 2 (and analogously γ_{23} and γ_{13}). Considering the data listed in Table 1, the block volumes vary between 11 and 331 m^3. Starting from these results, a Monte Carlo simulation was performed for evaluating the frequency distribution of the block volume. The characteristic block volume was assumed as the 90% of the cumulative frequency and equals to 75 m^3. Even if, during the traditional survey, rock prisms characterized by volume greater than 300 m^3 were also identified as possible unstable masses. Further analyses in terms of potential rock avalanche, using the conservative hypothesis of planar sliding, evidenced the possible collapse of sectors of the "La Gioia" rock face with an estimated maximum volume of about 60000 m^3. This volume was estimated after parametric analyses varying the distance of tension cracks from the scarp, seismic coefficient and the inclination of sliding surface.

[1] VAGNON Federico, University of Torino, Turin, Italy, fvagnon@unito.it

[1] FERRERO Anna Maria, University of Torino, Turin, Italy, anna.ferrero@unito.it

[2] PIRULLI Marina, Politecnico di Torino, Turin, Itali, marina.pirulli@polito.it

[2] SCAVIA Claudio, Politecnico di Torino, Turin, Itali, claudio.scavia@polito.it

Table 1: Mean orientation, spacing range and angle range between each discontinuity set.

Discontinuity sets	Mean orientation [°]		Spacing range, S [m]
	Traditional	Non-contact	
KS	319/17	347/49	0.7 - 7.2
K1	164/75	345/86	0.2 - 6.5
K2	83/82	276/89	0.4 - 3.4
	Angle range, γ [°]		
KS-K1	37 - 57		
K1-K2	59 - 79		
K2-KS	67 - 87		

3 PROPAGATION ANALYSIS

3.1 ROCKFALL

The bidimensional lumped mass code, RocFall (Rocscience Inc.), was used for performing numerical simulations in order to define the hazard map of the quarry area (Figure 2a). Five significant sections were chosen and 5000 blocks, with characteristics block volume of 75m^3, were considered for each simulation. The restitution coefficients were selected on the basis of scientific literature and coherently with deposit characteristics.
The simulations highlighted that only the upper part of the deposit could be affected by rockfall phenomena.

3.2 ROCK AVALANCHE NUMERICAL SIMULATION

As stated above, the collapse of rock sectors of about 60000 m^3 cannot be excluded. The simulation of this possible runout scenario was performed under the following hypotheses: i) the simultaneous collapse of the whole unstable volume, ii) the simulation of the rock avalanche as a flow-like process, iii) the use of two rheological laws (frictional and Voellmy).
The RASH3D code (Pirulli, 2005) was used for performing the numerical simulations. Since no laboratory tests or back analyses were available for this site, the rheological parameter values were chosen in the range of values suggested by Hungr and Evans (1996) for cases with analogous slope characteristics.
In Figure 2b, the forecasted runout scenarios considering the most conservative cases for each rheological law is presented. Compared to the rockfall scenarios, the hazardous area generated by the 60000 m^3 rock avalanche affects the whole quarry. However, in terms of depositional height, the maximum simulated thickness does not exceed 5m. The results coming from both the numerical simulations suggest changing the exploitation plan of the quarry: in particular, the design and realization of a quarry yard, progressively larger, for reducing and stopping the dynamics of rock avalanche.

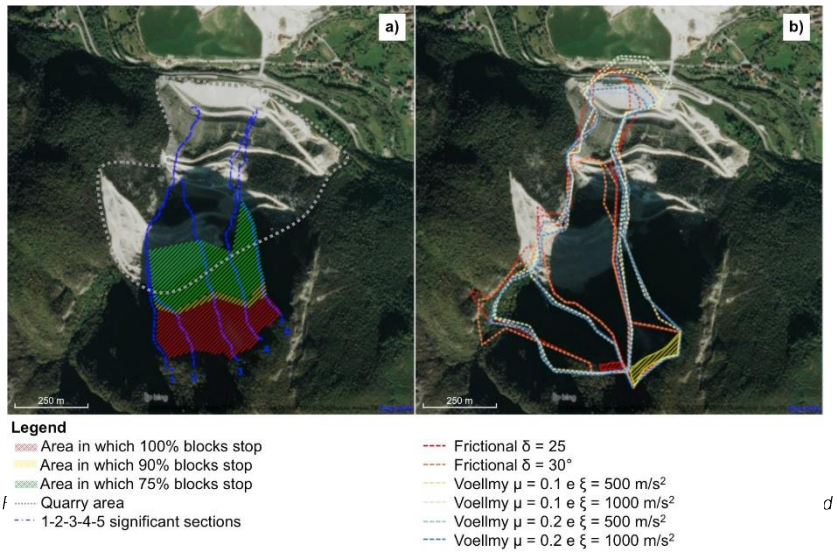

4 CONCLUSION

In this study the overall stability of "La Gioia" rock face has been evaluated, combining different methods and approaches. The geomechanical characterization has highlighted that the cliff could be subjected to rockfall process involving rock blocks with maximum volume of 300 m^3 and/or rock avalanche phenomena with maximum magnitude of 60000 m^3. A correct management of the quarry exploitation, based on the hazard scenarios resulting from carried out numerical analyses, could face and reduce the travel distances of unstable blocks and increase the safety conditions into the quarry area. In particular, the excavation of quarry yards, surrounded by debris levees and correctly designed (both in width and height) could represent a good solution for controlling and stopping the whole mobilized volume.

5 REFERENCES

Hungr, O. and Evans, S. G. (1996) Rock avalanche runout prediction using a dynamic model. *Landslides*, 233–238.

Pirulli, M. (2005) Numerical modelling of landslide runout, a continuum mechanics approach. *PhD Dissertation, Politecnico di Torino*, Italia.

Zampieri, D. and Adami, S. (2013) Influence of the geological structure on a rockslide in northeastern Italy. *It. J. Eng. Geol. Environm., Book Series* (6), 507-512.

A new method of dating rockfalls in the Mont Blanc massif using reflectance spectroscopy

Xavi GALLACH[1,2], Julien Carcaillet[2], Philip Deline[1], Ludovic Ravanel[1], Yves Perrette[1], Christophe Ogier[2], Dominique Lafon[3]

Keywords: rockfalls, Mont Blanc massif, Cosmogenic Nuclide dating, climate change, reflectance spectroscopy

1 INTRODUCTION

Rockfalls and rock avalanches are active processes in the Mont Blanc massif, with infrastructure and alpinists at risk. Thanks to a network of observers (hut keepers, mountain guides, alpinists) set up in 2007 current rockfalls are well surveyed and documented (Ravanel and Deline 2013). Rockfall frequency has been studied over the past 150 years by comparison of historical photographs (Ravanel and Deline 2008), showing that it strongly increased during the three last decades, likely due to permafrost degradation caused by the climate change. In order to understand the possible relationship between rockfall frequency and the warmest periods of the Lateglacial and the Holocene, we study the morphodynamics of some selected high-elevated (>3000 m a.s.l.) rockwalls of the massif on a long timescale.

2 MAIN TEXT

Since rockfall deposits in glacial areas are evacuated by the glaciers, our study focuses on the rockfall scars. ^{10}Be TCN dating of a rockwall surface gives us the rock surface exposure age, interpreted as a rockfall age. Here we present a dating dataset of 80 samples carried out between 2006 and 2016 at nine high-elevated rockwalls in the Mont Blanc massif (Figure 1). The resulting ages vary from present (0.04 ± 0.02 ka) to far beyond the Last Glacial Maximum (*c.* 100 ka). Three clusters of exposure ages are correlated to i) the Holocene Warm Period, ii) the Roman Warm Period, and iii) the Little Ice Age and post-LIA. Ages of this last one are generally related to small rockfall volumes (< 15000 m^3), considered as the normal erosion. A 4th cluster at 4.2-5.0 ka is not associated with any evident global climate period.

Furthermore, a relationship between the colour of the Mont Blanc granite and its exposure age has been established: fresh rock surface is light grey (e.g. in recent rockfall scars) whereas weathered rock surface is in the range grey to orange/red: the redder a rock surface, the older its age (Böhlert et al, 2008). Reflectance spectroscopy is used to quantify the granite surface colour. We explored the spectral data in order to find an index to measure the rock weathering evolution along time, thus allowing to date the rock surface exposure age using reflectance spectroscopy: the GReen Infrared GRanite Index (GRIGRI), based on the Remote Sensing-used GRVI Vegetation Index. GRIGRI uses the ratio between Green (530 nm) and Photographic Infrared (770 nm) reflectance to obtain the index, directly related to the granite exposure age (R= 0.863; Figure 2). The GRIGRI method has been tested for 8 samples where TCN dating failed, and for two samples where ^{10}Be exposure age are considered outliers. The resulting ages, according to the geomorphology of the scars and their surroundings, are plausible

3 CONCLUSION

TCN dating enabled to understand the rockfall frequency of the MBM over a large timescale. Dating complements historical evidence such as photograph datasets and present-day observations and surveys. The data presented here is probably the biggest dataset that explores the relationship between Holocene rockfall episodes and climate. We demonstrate that a significant part of the occurred rockfalls correlate well with climate variability. A new method of dating surface exposure age of the MBM using spectral data is presented here. We aim to develop surface exposure dating using photographic RGB coordinates, thus to obtain a tool allowing to launch a large scale surface dating campaign.

4 REFERENCES

Böhlert R, Gruber S, Egli M, Maisch M, Brandová D, Haeberli W, Ivy-Ochs S, Christl M, Kubik P.W, Deline P (2008) Comparison of exposure ages and spectral properties of rock surfaces in steep, high alpine rock walls of Aiguille du Midi. *Proceedings of the 9th International Conference on Permafrost*, Institute of Northern Engineering – University of Alaska Fairbanks 143–148.

Ravanel L, Deline P (2008) La face ouest des Drus (massif du Mont-Blanc) : évolution de l'instabilité d'une paroi rocheuse dans la haute montagne alpine depuis la fin du Petit Age Glaciaire. *Géomorphologie: relief, processus, environnement* 4:261–272.

[1] Univ. Grenoble Alpes, Univ. Savoie Mont Blanc, CNRS, EDYTEM, 73000 Chambéry, France
xavi.gallach@univ-savoie.fr

[2] Univ. Grenoble Alpes, Univ. Savoie Mont Blanc, CNRS, IRD, IFSTTAR, ISTerre, 38000 Grenoble, France

[3] IMT Mines Alès. 30100 Alès, France

Ravanel L, Deline P (2013) A network of observers in the Mont Blanc massif to study rockfalls in high alpine rockwalls. *Geografia Fisica e Dinamica Quaternaria* 36:151-158. doi 10.4461/GFDQ.2013.36.12

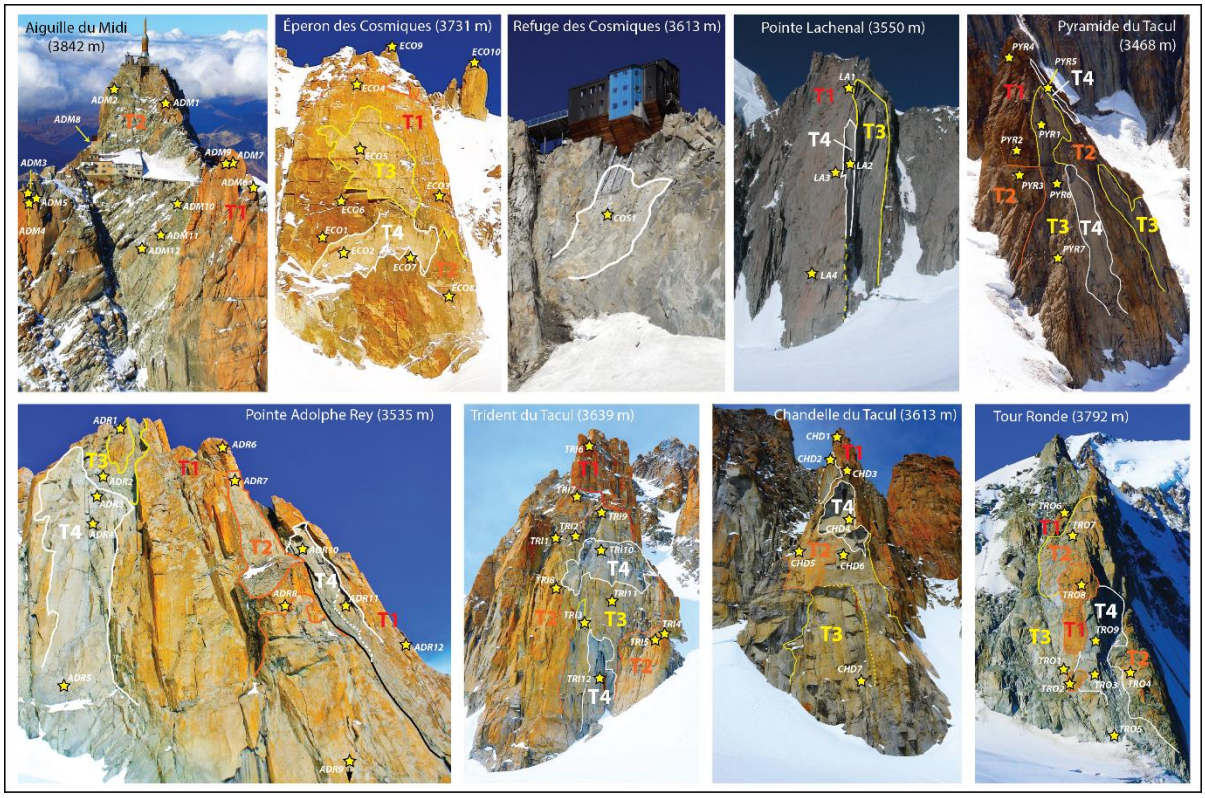

Figure 1. Sampling sites in the Glacier du Géant basin.

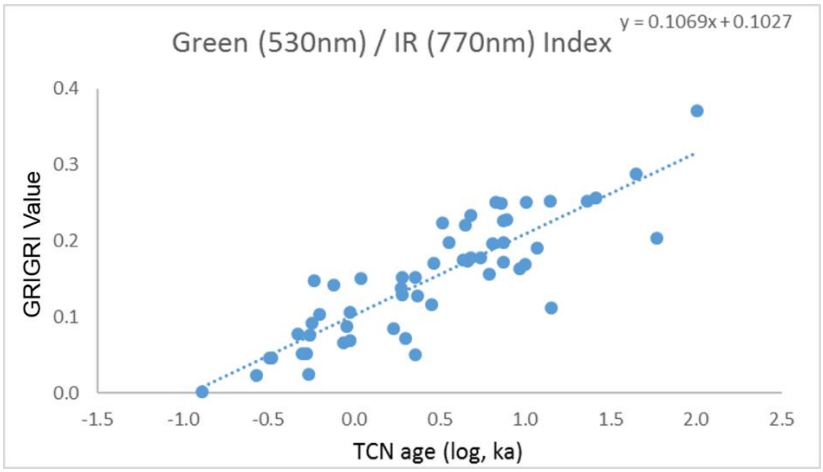

Figure 2. Colour-age relationship established using the GRIGRI method. Age is il log, ka.

Robust sub-mm displacement measurements with interferometric radar technology applied to early warning systems

Lorenz MEIER[1], Richard STEINACHER[2], Susanne WAHLEN[3]

Keywords: radar, rockfall, monitoring, early warning system, surface deformation

The successful operation of a warning or alarm system monitoring natural hazards requires robust and reliable measurement technology. Radar functions day and night, and is almost unaffected by weather conditions, such as fog or dust. We have successfully applied various radar instruments for slope monitoring, slope failure prediction, and detection of rockfall and debris flows in real-time. The application of Ground-Based Interferometric Synthetic Aperture Radar (GB-InSAR), Doppler and gauge radars allows to detect a full range of geophysical displacements, from slow sub-mm movements to several metres a second. We present the warning and alarm setup applied on Pizzo Cengalo/Bondo (Switzerland) to detect both the failure of the large rock avalanche as well as debris flow events, with emphasis on our novel analysis feature for long-term monitoring of small-scale displacements by GB-InSAR (few millimetres per month or less).

1 METHODS

In slope stability monitoring, we apply three types of radar according to hazard requirements. GB-InSAR is widely used to monitor slower processes, such as landslides and rock or glacier motion, over an extended period of time with the objective of forecasting an imminent collapse or break-off event (Montserrat et al, 2012; Nolesini et al, 2013). GB-InSAR is capable of measuring surface displacements as small as millimetres mm or even less. On the other hand, Doppler radar is applied to detect fast moving objects, such as falling rocks, in real-time for automatic road closure or evacuation (Meier et al, 2017). The rockfall radar application focusses on the reliable and fast detection and tracking of single rocks and boulders with alarm option on the detection of an event. The third radar application is the real-time detection of debris flows with gauge radar as alarm system for downstream dwellings or transport infrastructure.

2 MONITORING AT PIZZO CENGALO / BONDO

The debris flow resulting from the large rockfall at Pizzo Cengalo on 23 August 2017 triggered our debris flow alarm system at Bondasca river, and automatically closed several road sections in Bondo notifying the authorities. The gauge radar station was installed in 2013 with additional cameras and three trigger lines. However, unstable rock material remained on Pizzo Cengalo and further rockfalls as well as debris flow events were (and still are) likely. Subsequently, we extended the measurement setup at Bondasca valley and the alarm options at the clean-up sites in and around Bondo. We installed a GB-InSAR on 2120 m.a.s.l for continuous monitoring of Pizzo Cengalo's northeast face. The autonomous operation of the radar, a camera and the data

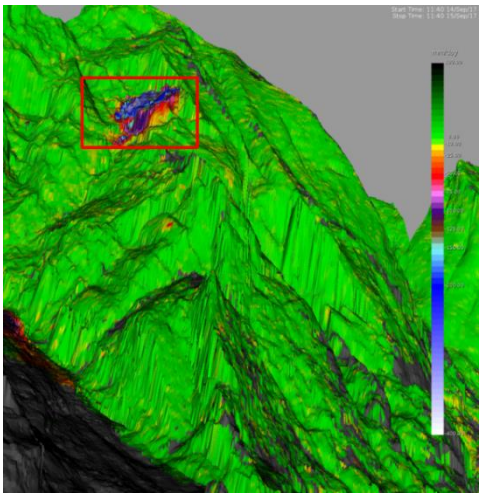

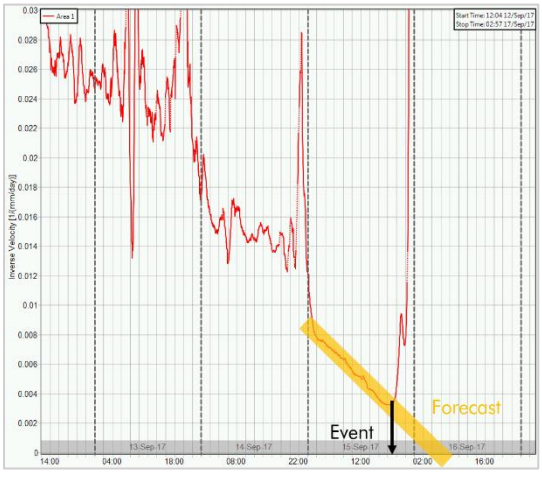

Figure 1 (left): Radar image of 15 Sept 2017 generated with GB-InSAR; the image clearly shows the accelerated rock area in the north eastern face of Pizzo Cengalo.

Figure 2 (right): Plotting the inverse velocity (1/v) of the accelerated areas against time is used to forecast time of failure. Linear extrapolation indicated breakoff in the early morning hours of 16 September 2017. However, experience has shown that collapse usually occurs slightly before as it was also the case here.

[1] MEIER Lorenz, GEOPRAEVENT AG, Zurich, Switzerland (CHE), lorenz.meier@geopraevent.ch

[2] STEINACHER Richard, GEOPRAEVENT AG, Zurich, Switzerland (CHE), richard.steinacher@geopraevent.ch

[3] WAHLEN Susanne, GEOPRAEVENT AG, Zurich, Switzerland (CHE), susanne.wahlen@geopraevent.ch

transmission infrastructure present challenges in themselves when considering the harsh winter conditions at this location and lack of electricity and mobile phone coverage.

The gauge radar station functions as alarm system to immediately close transport corridors in the main valley; and is situated 1000 m below the GB-InSAR station which acts as warning system for future rock slope failures. The GB-InSAR detects sub-mm surface deformations and identifies accelerated areas within the rock face (figure 1). The principal rock slope failure usually occurs after a phase of acceleration and an inverse velocity analysis of the measured displacements allows the time of failure to be predicted (Sättele et al. 2016). Figure 2 shows the radar forecast with inverse velocity analysis for the rock slope failure event on Pizzo Cengalo on 15 September 2017.

3 CHALLENGING LONG-TERM MEASUREMENTS

Surface deformations prior to slope failure typically show velocities on the scale of several centimetres to metres per day. These relatively large and quick displacements are rapidly captured by GB-InSAR and can trigger warnings within hours or less. However, the automatic detection of small-scale displacements in the range of only few millimetres per month or less is challenging. Conventional data analysis is currently not capable of detecting such displacements.

Hence, we added additional data processing steps to identify small-scale, steady slope movements over the long term. We chose 10, 30 and 90 days as analysis interval for long-term surface deformation. The developed algorithm uses thousands of measurements from the continuously operating radar and illustrates the calculated deformation periodically on a digital terrain model (Figure 3). With this novel methodology we are able to include GB-InSAR into an automated warning system detecting millimetre deformations on clean rock faces over many months even in though weather conditions.

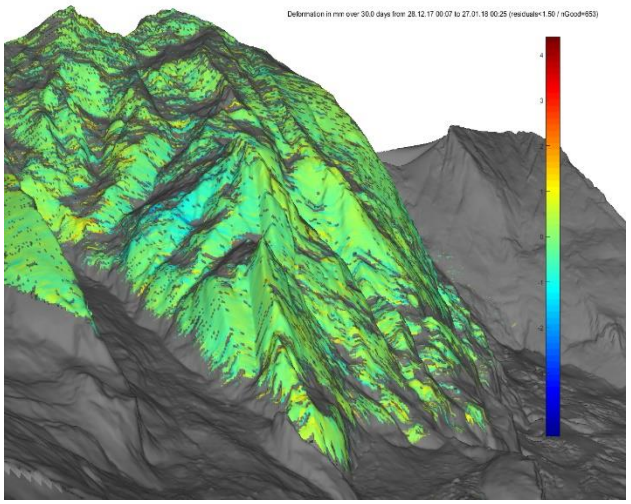

Figure 3: Deformation in mm over 30 days. This image was retrieved from more than 650 measurements in the time period of 30 days.

4 CONCLUSIONS

The application of GB-InSAR for slope stability monitoring allows to successfully measure surface deformations ranging from sub-mm to several metres in time scales of a few minutes to several months, probably even years. Multiple events have demonstrated the practical application of GB-InSAR for detecting accelerations in rock slope and glacier displacements, and hence the precursors of imminent slope failure. Inverse velocity analysis has further proved successful in forecasting the time of failure within a time frame of 24 hours and on several occasions less than 24 hours. In terms of long-term monitoring, additional data processing steps were developed that enable the detection of small but steady deformations that would otherwise become lost in random noise.

5 REFERENCES

Monserrat, O., Corsetto, M., Luzzi, G. (2012) A review of ground-based SAR interferometry for deformation measurement, *ISPRS Journal of Photogrammetry and Remote Sensing*, Vol. 93, pp. 40-48

Nolesini, T., Di Traglia, F., Del Ventisette, C., Morett, S., Casagli, N. (2013) Deformations and slope instability on Stromboli volcano: Integration of GBINSAR data and analog modelling, *Geomorphology*, Vol. 180-181, pp. 242-254

Meier, L., Jacqumart, M., Wahlen, S., Blattmann, B. (2017) Real-time rockfall detection with Doppler radars, *Conference Proceedings of RocExs 2017, 6th Interdisciplinary Workshop on Rockfall Protection*, Barcelona, Spain

Sättele, M., Krautblatter, M., Bründl, M. et al. (2016) Forecasting Rock Slope Failure: How reliable and effective are warning systems? *Landslides* (2016) 13: 737.

Bioengineering in rockfall mitigation : innovative high-energy barriers anchored on trees (case study)

Nicolas VILLARD[1], Ignacio OLMEDO[1], Franck BOURRIER[2], Laurent MUQUET[3], Bernard ALMERAS[4]

Keywords: forest; trees; rockfall; barriers; CE / ETAG 027 label

1 BACKGROUND

Forests have been managed against geohazards in mountainous areas since 1850, especially for erosion and avalanche control. More recently, latest developments such as rockfall trajectography, impact modelling on trees and dendrometric analysis offer alternates regarding assessment methods and mitigation strategy.

If wooden materials have already been preferred for installing "active" defence in sensitive areas (snow barriers for instance), the use of trees for "passive" structures is still very limited.

However many protective structures in the Alps such as rockfall barriers have to be installed on vegetated slopes, sometimes in a protected environment. Then installation works could generate nuisance (deforestation, helicopter…) where impacts should be limited. That's why early test have been conducted for low energy fences (~100 kJ) in order to explore the capacity of rockfall nets anchored on trees (Olmedo et al., 2016). This approach try to adapt the structure to the field, rather than the opposite.

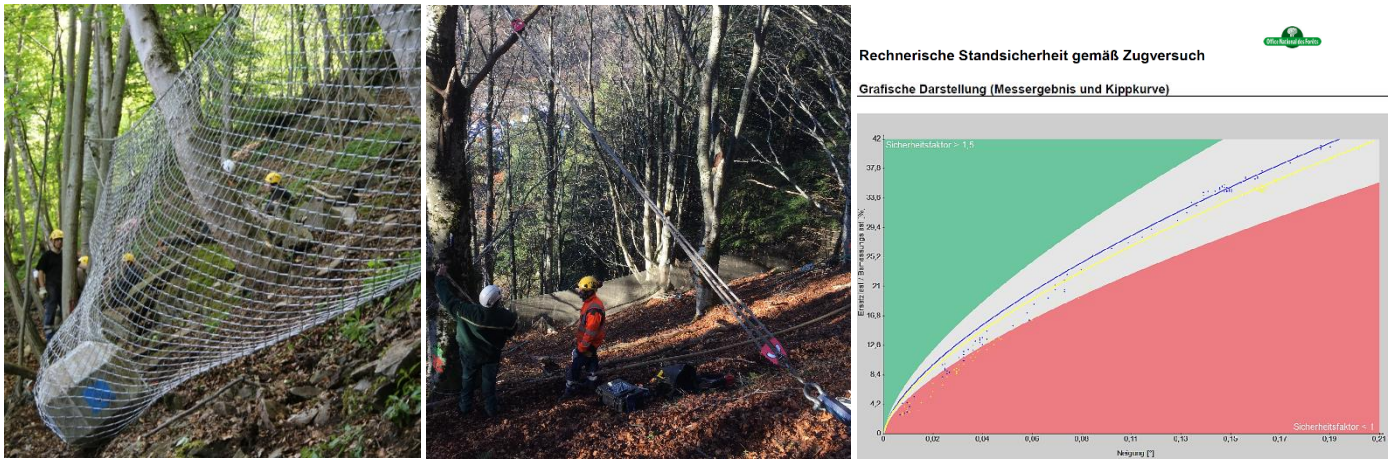

Figure 1 : full scale test at 100 kJ (GTS / IRSTEA) ; flexion test and mechanical expertise ; stability abaqus loading / deformation (ONF)

2 PRINCIPLES AND OBJECTIVES

Previous developments have often been conducted within a research or qualitative approach. However the interest of public clients invites to conduct new experimental operations with more guaranties according to procurement, contracting and normative background, especially with sensitive issues to be protected.

A recent project in the Massif Central (Muquet et al., 2017) allowed to apply with quantitative bioengineering. A first permanent high energy rockfall catch fence (3000 kJ) has been installed in a forest with huge trees (spruces, beeches…). The customised and patented design is as closed as possible to certified structure (Bost et al., 2015) in order to maximise guaranties (CE) and in the same time minimise impacts on a sensitive environment (nature reserve).

The design follows key steps below, by order of priority :

1. Use trees at least for supporting the weight of rockfall nets and components (instead of posts)
2. Refer to ETAG succeed tests, with broken posts (boulder stopped even with cut tree)

[1] **VILLARD Nicolas,** OLMEDO Ignacio, **NGE Group (GTS), Lyon FR, nvillard@gts.fr**

[2] BOURRIER Franck, IRSTEA, Grenoble FR

[3] MUQUET Laurent, ARIAS MONTAGNE, Grenoble FR

[4] ALMERAS Bernard, ONF, Clermont-Ferrand FR

3. Use some trees on the upstream side for anchoring the barrier (if possible according to expertise below)
4. Dissipate energy using tree deformation (is possible, ultimate option according to R&D results, not used)

3 DESIGN & EXPERTISE

A feasibility and implantation study should be validated by a dedicated forestry expertise (ONF, 2013) : site exposure, wind, sanitary, arboreal, mechanical…

Then full scale mechanical tests are conducted through a patented process:

- Flexion tests (at about 2 tons) on selected trees (root system, mechanical resistance…)
- Traction destructive tests (at about 40 tons) on representative trees used as anchors (figure 1)

Finally, the process is comparable to preliminary / control tests on passive anchors in geotechnical engineering. The incremental methods could be used in conservative way and allows to adapt to the forest quality and expertise results.

4 CONSTRUCTIVE OPTIONS

Some details during installation illustrate the expertise fully required, for instance:

- In order to support catch nets and dissipation devices, it is recommended to drill the trunks with respect to living materials (forestry methods), and then to install dedicated components able to follow the growth of the tree while supporting efforts from ETAG tests (figure 2).
- Moreover during installation works, a strong procedure should be established to bring all materials by helicopter through a dense and thick forest with minimal pruning (electric hook over the canopy).

Figure 2 : mechanical analysis (i.e response to wind) for drilling procedure ; example on selected trees (GTS / ONF)

5 CONCLUSION

Last developments in rockfall mitigation methods and bioengineering allow the use of lived trees for the design of high energy passive protection structures according to strong standards. A specific expertise is required for forestry assessment, full scale tests and installation, associated to a customized approach essential to take into account site effects that could appear as unusual sizing parameters (wind, forest quality…).
However these skills allow new alternates for rockfall mitigation, reducing the fooprint of these structures in a sensitive environment and improving the global resilience of our infrastructures thanks to forest.

6 AKNOWLEDGMENTS & REFERENCES

Olmedo et al. (2016) Tree-anchored rockfall fences: experimental and numerical studies. *RSS 2016, Lyon.*

Muquet L. et al. (2017) DCE d'appel d'offres de la commune du Mont-Dore (63). *Rapport d'étude G2 ARIAS*

Bost M. et al. (2015) Recommendation for rockfall barriers. *Information meme CEREMA*

ONF (2013) Perçage de supports dans les arbres et diagnostic approfondis. *Guides méthodologique.*

On the interest of reduced models for the design of soft rockfall barriers

R. Boulaud[1], C.Douthe[2]

Keywords: DEM, flexible fence, structural design, surrogate model

Soft rockfall barriers exhibit strong non-linearities (large deformation, plasticity and contact), their modelling is therefore a challenging issue. Considerable effort has been done in the last decade to this end and it has lead to very convincing results [1,2,3,4]. To support this modelling effort, experiments have been conducted in the framework of the National Project C2ROP. The structure studied consists in a 15m long three modules barrier with a capacity of 300 kJ. Several loading tests are conducted: quasi-static and dynamics, in service conditions (SEL) and maximal conditions (MEL). Their comparison and analysis are used to better understand the behaviour of these structures under impact and to identify key aspect of their modelling.

1 LEARNING FROM EXPERIMENTS

Typical results of the experimental tests are:

- the position of the block and its acceleration given by digital image correlation and an accelerometer,
- the stress level in the cables given by load cells mounted on the cables,
- the movement of characteristic points on side cables given by digital image correlation (see figure 1 for locations).

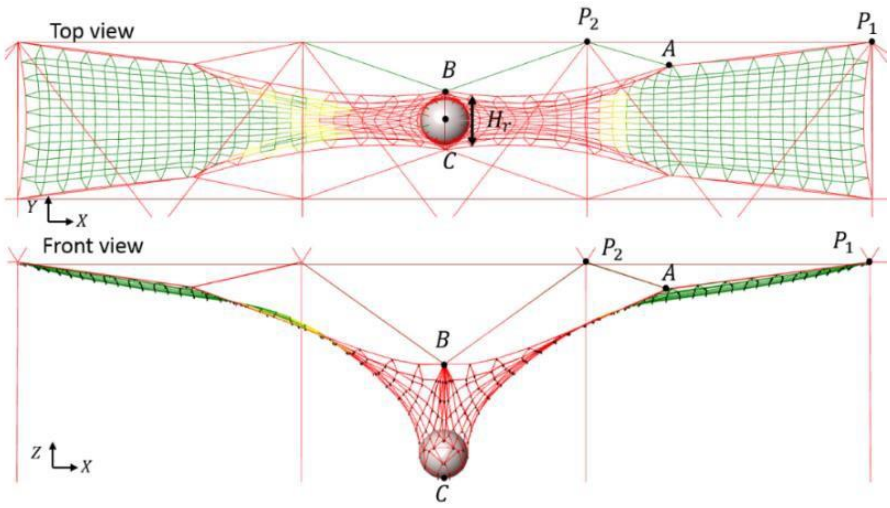

Figure 1: Distribution of internal forces in the structure for a vertical displacement of 3.75m

From these measures, one can deduce that there are two distinct phases in the loading of the barrier:

- first the barrier deforms globally at very low stress level: the ASM4 net simultaneously extends in the transverse direction and slides in the longitudinal direction, while contact points of the side cables converge toward the plane of symmetry: almost no energy is dissipated;
- then the geometry of the net remains almost constant, only the brakes extend and dissipate the kinetic energy of the block.

In the first phase, the deformation of the fence is pure rearrangement of the structure so that it is able to resist the load. This phase involves no forces so that it is independent of dynamic issues and could be described by a quasi-static model. In the second phase, considering that the mass of the block represents 85-90% of the total mass of the system and that the geometry of the net is almost constant, one should be able to describe the dynamic response of the structure by a reduced model of the supporting structures.

[1] BOULAUD Romain, Laboratoire Navier, UMR8205 Ecole des Ponts ParisTech IFSTTAR CNRS, Champs sur Marne, FRANCE, romain.boulaud@ifsttar.fr

[2] DOUTHE Cyril, Laboratoire Navier, UMR8205 Ecole des Ponts ParisTech IFSTTAR CNRS, Champs sur Marne, FRANCE,cyril.douthe@ifsttar.fr

2 DEVELOPMENT AND VALIDATION OF REDUCED MODELS

Based on the previous observations of the experiments, this paper proposes thus to investigate in what extend the dynamic behaviour of a rockfall barrier can be described by a combination of a quasi-static model of the whole barrier and a dynamic reduced model of the supporting structure (see for example the 5 ddls model of figure 2). It questions the accuracy of the proposed methodology for the prediction of main characteristics of the barrier behaviour (maximal force in the cables, dissipated energy inthe brake, residual height, etc.). It also emphasises the problem of parameters identification. Finally, it concludes on the interest of such approach for the design of rockfall barriers and its complementarity with existing numerical approaches more targeted at barriers justification.

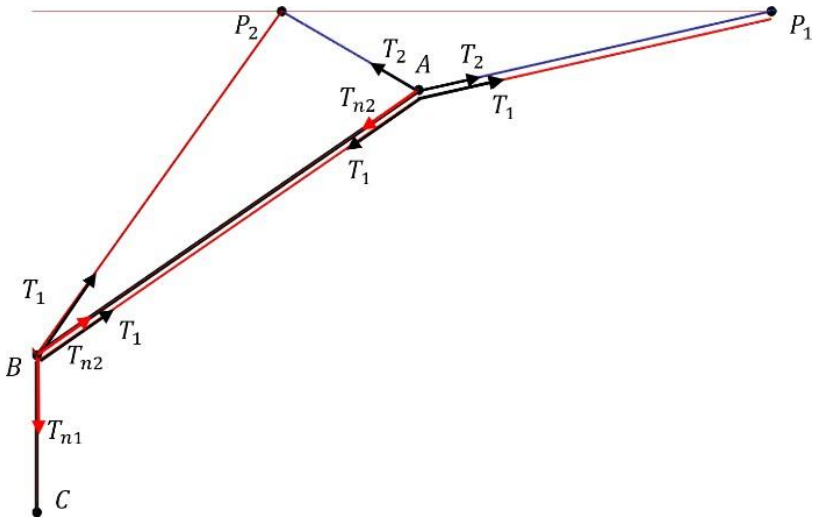

Figure 2: Reduced model of the supporting structure used for dynamic simulations

3 REFERENCES

VOLKWEIN A.: NUMERISCHE SIMULATION VON FLEXIBLEN STEINSCHLAGSCHUTZSYSTEMEN. THESE DE DOCTORAT, ECOLE POLYTECHNIQUE FEDERALE DE ZURICH, 2004.

TRAD A.: ANALYSE DU COMPORTEMENT ET MODELISATION DE STRUCTURES SOUPLES DE PROTECTION : LE CAS DES ECRANS DE FILETS PARE-BLOCS SOUS SOLLICITATIONS STATIQUES ET DYNAMIQUES. THESE DE DOCTORAT, INSA LYON, 2011.

GHOUSSOUB L., ANALYSE DE QUELQUES ELEMENTS DU COMPORTEMENT DES ECRANS DE FILETS PARE-BLOCS, THESE DE DOCTORAT, UNIVERSITE PARIS EST, 2014

COULIBALY J., MODELISATION NUMERIQUE DISCRETE DU COMPORTEMENT MECANIQUE SOUS IMPACT DES STRUCTURES D'ECRANS DE FILETS PARE-PIERRES, THESE DE DOCTORAT, UNIVERSITE GRENOBLE ALPES, 2017

Scale effect on roughness estimation by non-contact survey

Maria MIGLIAZZA[1], Anna Maria FERRERO[2], Gessica UMILI[3]

Keywords: discontinuity, roughness, scale effect, photogrammetric survey

The stability conditions of rock slope are strongly affected by the presence of discontinuity sets in terms both of their orientation and shear resistance. The latter one is generally estimated by means of laboratory shearing tests on specimens containing a discontinuity or by the evaluation of local surface roughness measured with easy instruments (Barton's profilometer). The study shown below deals with the roughness estimation of rocky natural surfaces carried out with non-contact survey at different scales: the on-site block scale and the laboratory specimens scale. At the laboratory scale the results are compared to that got by the back-analysis of shearing tests.

1 NON-CONTACT SURVEY

A quantitative assessment of roughness requires a Digital Surface Model (DSM) representing in the most accurate and detailed way the surface of the joint to be analyzed. The authors chose to obtain the DSM by means of a photogrammetric survey.
A 20 mm lens mounted on a digital camera Nikon D7000 was used for acquiring four images of the block; Agisoft PhotoScan was then run to produce a mesh representing the block surface. The mesh is constituted by 3D points evenly scattered on the surface, with a density of about 1 pt/mm^2 on the block surface (Figure 1 – left side) and of about 5 pt/mm^2 on the specimen surfaces (Figure 1 – right side).
Laboratory CNL shear tests have been carried out on three specimens obtained cutting blocks containing discontinuity picked up at the slope toe. Each specimen has been subjected to 5 shearing cycles. All the coupled discontinuity surfaces have been subjected to a photogrammetric survey before the test, after the first cycle and at the end of five cycles. Each DSM has been obtained following the same procedure used for in situ survey. In this case eight images of each surface have been taken by placing the specimens always in the same position using a mask having suitable markers to scale the model and define the reference system.
Surfer code (Golden Software Inc.) was used to convert the scattered clouds of point into regular x-y grid, in which the z coordinates are obtained from z values of the original mesh with a nearest neighbor interpolation algorithm. A grid with several constant spacing along the x and y directions was obtained: the x and y–profiles of the grid have been analyzed with the aim to compute the geometrical descriptor of the surface roughness.

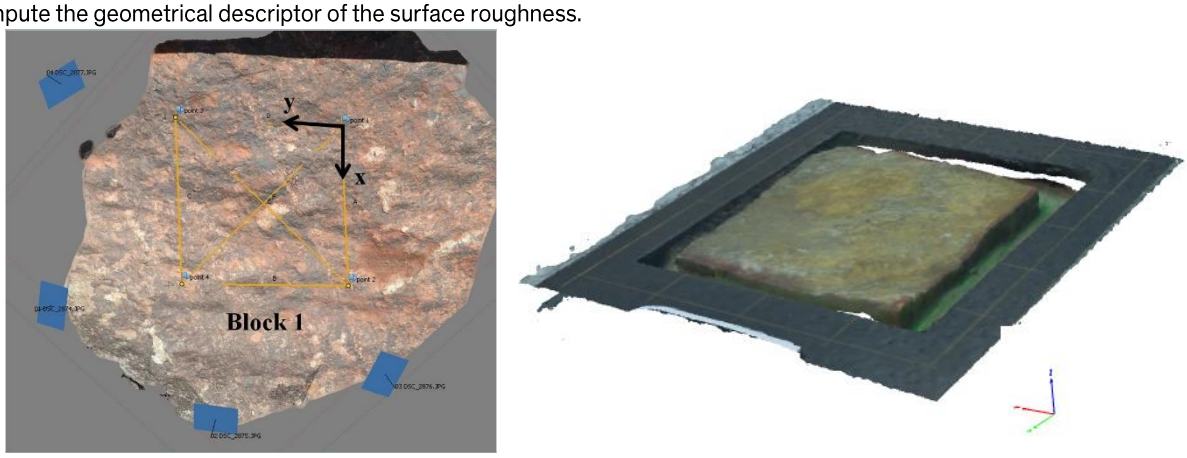

Figure 1: left) mesh of the in situ block (left) and laboratory specimen (right) surfaces and reference systems.

2 ROUGHNESS ESTIMATION

Many statistical descriptors based on the geometry of rock joints profiles have been developed to quantitatively determine joint roughness. Root mean square of the first derivative (Z_2) method (Myers, 1962)

$$Z_2 = \left(\frac{1}{L}\sum_{i=1}^{N-1}\frac{(y_{i+1}-y_i)^2}{x_{i+1}-x_i}\right)^{1/2} \quad (1)$$

[1] MIGLIAZZA Maria, Politecnico di Torino, Torino, IT, maria.migliazza@polito.it
[2] FERRERO Anna Maria, University of Turin, Turin, IT, anna.ferrero@unito.it
[3] UMILI Gessica, University of Turin, Turin, IT, gessica.umili@unito.it

Maximum apparent asperity inclination (θ^*_{max}) method for 2D and 3D analysis (Tatone and Grasselli, 2010)

$$L_{\theta*} = L_0\left(\frac{\theta^*_{max}-\theta^*}{\theta^*_{max}}\right)^C \text{ and } A_{\theta*} = A_0\left(\frac{\theta^*_{max}-\theta^*}{\theta^*_{max}}\right)^C \quad (2)$$

where L_0 and A_0 are the normalized length and normalized area corresponding to $\theta^* = 0°$, respectively, θ^*_{max} is the inclination of steepest segment or facet; and C is a dimensionless fitting parameter, calculated via a non-linear least-squares regression analysis, that characterizes the shape of the cumulative distribution (Grasselli et al., 2002). Many authors proposed correlations for deriving JRC from the above mentioned geometrical descriptors. The most commonly used are listed below:

$$JRC = 32.2 + 32.47 \cdot Log_{10}(Z_2) \quad \text{(Tse and Cruden, 1979)} \quad (3)$$

$$JRC = 55.03(Z_2)^{0.74} - 6.10 \text{ (for 1.0 mm sampling interval)} \quad \text{(Tatone and Grasselli, 2010)} \quad (4)$$

$$JRC = 2.40\left(\frac{\theta^*_{max}}{[C+1]_{2D}}\right)^{0.85} - 4.42 \text{ (for 1.0 mm sampling interval)} \quad \text{(Tatone and Grasselli, 2010)} \quad (5)$$

A complete review of all the proposed empirical formulations can be found in Li and Zhang (2015).

3 CONCLUSION

From the results of the laboratory shear test it possible to get a unique value of JRC by the back-analysis of the peak stress conditions, On the contrary the non-contact discontinuity survey and the following surface geometrical analysis allowed to obtain a series of information: discontinuity roughness estimation at different scale (in situ blocks and laboratory specimens), along different directions, roughness distribution and anisotropy along the surface.

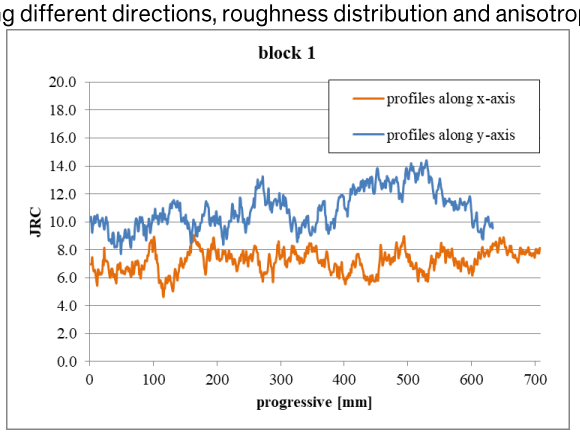

Figure xx: JRC calculated with eq. 5 along the profiles in the two considered directions

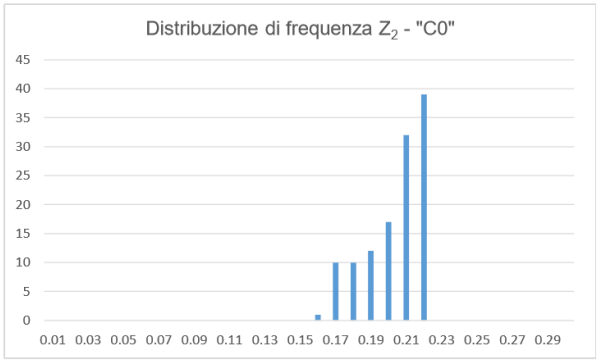

Table xx: Mean values of JRC calculated following equations 3, 4 and 5 along the two considered directions

Table 1: Layout of the proceedings

		Mean JRC		
	Direction	Eq. 3	Eq. 4	Eq 5
Blocks	X	7.7	9.2	7.2
	Y	10.7	11.8	10.9
Specimens	Shearing	9.5	9.6	9.4
	Back-analysis	8.1		
	Profilometer	6-8		

4 REFERENCES

Myers N.O. (1962) - Characteristics of surface roughness. Wear. 5: 182-189

Tatone B.S.A. & Grasselli G. (2010) - A new 2D discontinuity roughness parameter and its correlation with JRC. International Journal of Rock Mechanics and Mining Sciences, 47 (8): 1391-1400

Tse R. & Cruden D.M. (1979) - Estimating joint roughness coefficients. International Journal of Rock Mechanics and Mining Sciences & Geomechanics Abstracts, 16 (5): 303-307

Yang Z.Y., Lo S.C., Di C.C. (2001) – Reassessing the Joint Roughness Coefficient (JRC) Estimation Using Z2. Rock Mech. Rock Eng., 34 (3): 243-251